Design and Synthesis of Novel Lanthanide Complexes for Luminescent Devices

By

Mark Jones

A Thesis submitted to the University of Wales in accordance with the requirements for the degree of Doctor of Philosophy in the Faculty of Science, Department of Chemistry, University of Wales, Cardiff.

July 2005

UMI Number: U488157

All rights reserved

INFORMATION TO ALL USERS
The quality of this reproduction is dependent upon the quality of the copy submitted.

In the unlikely event that the author did not send a complete manuscript
and there are missing pages, these will be noted. Also, if material had to be removed,
a note will indicate the deletion.

UMI U488157
Published by ProQuest LLC 2013. Copyright in the Dissertation held by the Author.
Microform Edition © ProQuest LLC.
All rights reserved. This work is protected against
unauthorized copying under Title 17, United States Code.

ProQuest LLC
789 East Eisenhower Parkway
P.O. Box 1346
Ann Arbor, MI 48106-1346

Acknowledgements

I must first thank Dr. Angelo J. Amoroso for his ideas and guidance throughout the last three years of my research.

I would like to thank the persons who carried out the crystallography described in this thesis, Simon Coles and Dr. Li Ling Ooi. Thanks also to the EPSRC National Crystallography and Mass Spectrometry Service Centres at Southampton and Swansea, respectively. I would also like to thank Drs. Simon Aldridge (I enjoyed those vivas really) and Ian Fallis for numerous discussions and use of their chemicals and equipment. Thanks also to the technical staff Gaz, Robin, Jobo, Sham, Alan, Rob, and Ricky for keeping the department running and for providing me with much entertainment.

A big thanks goes to everyone in Labs 1.124 and 1.125 past and present for (nearly) always sharing a laugh with me. It has been a pleasure working with these people who include Bres, Debs, Graham, Dave, Miles, Rob, Rich, Claire, Steve, Becky, Andrea, Strato, Anne, Ruth, Neha, Mini, Tim, Tom and Bunn.

I would like to thank Mum, Dad, Phil and BB for supporting me through the highs and lows of all my studies, without their love and help I'm sure I would not be where I am today.

Lastly, I would like to thank Cerys for her immeasurable love and support over the past three years. Cerys has helped me through the best and worst times with her limitless energy, enthusiasm and shared love for life.

Contents

Chapter 5 – Experimental

Appendix One

Notes

The following abbreviations were used in the text:

Terpy	2,2':6',2''-terpyridine
TerpyO	2,2':6',2''-terpyridine-1-mono oxide
$TerpyO_2$	2,2':6',2''-terpyridine-1,1'-bis oxide
$TerpyO_3$	2,2':6',2''-terpyridine-1,1',1''-tri oxide
PhTerpy	4'-phenyl-2,2':6',2''-terpyridine
$PhTerpyO_2$	4'-phenyl-2,2':6',2''-terpyridine 1,1''-bisoxide
$PhTerpyO_3$	4'-phenyl-2,2':6',2''-terpyridine 1,1',1''-trioxide
$PhTerpyCN_2$	4'-phenyl-2,2':6',2''-terpyridine-6,6''-dicarbonitrile
$PhTerpyCN_2O$	4'-phenyl-2,2':6',2''-terpyridine-6,6''- dicarbonitrile-1'-mono oxide
$PhTerpyAcid_2$	4'-phenyl-2,2':6',2''-terpyridine-6,6''-dicarboxylic acid
$PhTerpyA_2O_3$	4'-phenyl-2,2':6',2''-terpyridine-6,6''-dicarboxylic acid 1,1',1''-trioxide
$PhTerpyAmide_2$	N,N'-(di-*tert*-butyl)-4'-phenyl-2,2':6',2''-terpyridine-6,6''-dicarboxamide
PhQuater	4',4''-bisphenyl-2,2':6',2'':6'',2'''-quaterpyridine
4-^{is}Pr-PhQuater	4',4''-(4-isopropyphenyl)-2,2':6',2'':6'',2'''-quaterpyridine
$PhQuaterO_2$	4',4''-bisphenyl-2,2':6',2'':6'',2'''-quaterpyridine-1,1'''-bisoxide
4-^{is}Pr-$PhQuaterO_2$	4',4''-(4-isopropyphenyl)-2,2':6',2'':6'',2'''-quaterpyridine-1,1'''-bisoxide
$PhQuaterO_4$	4',4''-bisphenyl-2,2':6',2'':6'',2'''-quaterpyridine-

	1,1':1'',1'''-quateroxide
4-^{is}Pr-PhQuaterCN$_2$	4',4''-(4-isopropyphenyl)-2,2':6',2'':6'',2'''-quaterpyridine-6,6'''-dicarbonitrile
4-^{is}Pr-PhQuaterAcid$_2$	4',4''-(4-isopropyphenyl)-2,2':6',2'':6'',2'''-quaterpyridine-6,6'''-dicarboxylic acid
4-^{is}Pr-PhQuaterAmide$_2$	N,N'-(di-*tert*-butyl)-4',4''-(4-isopropyphenyl)-2,2':6',2'':6'',2'''-quaterpyridine-6,6'''-dicarboxamide
4-^{is}Pr-PhQuinque	4',4'''-(4-isopropyphenyl)-2,2':6',2'':6'',2''':6''',2''''-quinquepyridine
4-^{is}Pr-PhQuinqueO$_2$	4',4'''-(4-isopropyphenyl)-2,2':6',2'':6'',2''':6''',2''''-quinquepyridine-1,1''''-bisoxide
4-^{is}Pr-PhQuinqueCN$_2$	4',4'''-(4-isopropyphenyl)-2,2':6',2'':6'',2''':6''',2''''-quinquepyridine-6,6''''-dicarbonitrile
4-^{is}Pr-PhQuinqueAcid$_2$	4',4'''-(4-isopropyphenyl)-2,2':6',2'':6'',2''':6''',2''''-quinquepyridine-6,6''''-dicarboxylic acid
4-^{is}Pr-PhQuinqueAmide$_2$	N,N'-(di-*tert*-butyl)-4',4'''-(4-isopropyphenyl)-2,2':6',2'':6'',2''':6''',2''''-quinquepyridine-6,6''''-dicarboxamide
Å	Angstrom
cm^{-1}	Reciprocal centimeters
d	Doublet
dd	Double doublet
δ	NMR chemical shift
EI	Electron ionisation
ES	Electrospray

ε	Absorption coefficient
g	Grams
IR	Infrared
HBr	Potassium bromide
λ	Wavelength
m	Multiplet (NMR), medium (IR)
MS	Mass spectrometry
m/z	Mass/charge ratio
v	Stretching mode
NMR	Nuclear magnetic resonance
ppm	Parts per million
q	Quartet
s	Singlet (NMR), strong(IR)
sh	Shoulder
t	Triplet
UV	Ultraviolet
w	Weak

Abstract

The design of complexes of lanthanide ions with an encapsulating ligand is currently an important theme in the field of luminescence based assays because it offers the possibility to obtain stable luminescent compounds which offer better sensitivity and specificity than traditional methods such as radioactive labelling.

Along this theme, europium and terbium complexes of a series of ter- and quaterpyridine-N-oxide ligands have been prepared and structurally characterised by crystallographic studies. The solid-state structures reveal some interesting topologies of the ligands due to the flexibility introduced to the coordination sphere by the N-oxide donors. Europium and terbium complexes were also prepared for a series of quinquepyridine-N-oxides. Luminescence studies of the N-oxide complexes in acetonitrile show typical europium and terbium emission spectra, dominated by the $^5D_0 \rightarrow {}^7F_2$ and $^5D_4 \rightarrow {}^7F_5$ transitions respectively. No simple trend was revealed in the relative quantum yields, with [Eu(4',4''-bisphenyl-2,2':6',2'':6'',2'''-quaterpyridine-1,1':1'',1'''-quateroxide)$_2$][ClO_4]$_3$ having the most intense luminescence. Decomplexation of the non-oxidised ligand complexes was observed at low solution concentrations in the luminescence spectra and so strong lanthanide-binding groups were introduced to the 6 positions of the external pyridine rings of the ter-, quater- and quinquepyridine ligands to improve complex stability.

Lanthanide-binding groups introduced were hard, anionic carboxylate groups and also, the more organic solvent soluble, *tert*-butyl amide groups. Europium and terbium complexes of the series of ter-, quater- and quinquepyridine carboxylic acid and *tert*-butyl amide ligands were prepared and the ligands shown to be capable of sensitising the trivalent lanthanide europium and terbium ions. Luminescence studies revealed an increased binding strength of the ter-, quater- and quinquepyridine carboxylic acid ligands with no decomplexation at low solution concentrations being observed. From the relative quantum yields [Eu(4'-phenyl-2,2':6',2''-terpyridine-6,6''-dicarboxylic acid)(H_2O)$_2$][ClO_4]$_2$ was determined to have the most intense luminescence. Also, a trend of the carboxylic acid ligands being more suitable for Eu(III) sensitisation and the *tert*-butyl ligands being more suitable for Tb(III) sensitisation was revealed.

Chapter 1

Introduction

1.1 Introduction

Over the past 12 years there has been a resurgence of interest in the coordination chemistry of the lanthanides and the rare earth elements. Whereas 20 years ago activity was focused on the use of complexes of Eu, Pr and Yb as NMR shift reagents, interest now centres on the application of lanthanide complexes in luminescence research and the *in vivo* application of related paramagnetic gadolinium complexes as contrast agents in magnetic resonance imaging.[1] This renewal of interest may be related to an enhanced appreciation of the rich functionality of the ground and excited states of lanthanide complexes.

The use of lanthanide complexes as luminescent labels for analyses in biological media has also overtaken interest in the development of solid-state phosphors (in television screens) and lasers (e.g. yttrium aluminium garnet (YAG) lasers). The immunological methods for the determination of biological materials are far superior to almost all other methods as far as sensitivity and specificity are concerned. They are used particularly for the clinical investigation of compounds that are in very low concentrations and for which chemical methods are not sufficiently specific.

The immunological method based on the use of luminescent labels is called fluoroimmunassay.[2] Fluoroimmunassays provide an important alternative to radioimmunoassays, which is still the most widely used technique, even though it presents some drawbacks related to radioactivity. This technique is widely used in the detection and quantification of important biological molecules with typical systems

comprising of a targeting group and a reporter group. The targeting group is designed to recognise selectively and bind strongly to the molecule of interest and the reporter group incorporates a radioisotope to allow detection at low levels. Luminescence can potentially provide a cheaper, equally sensitive detection method where the hazardous problems of handling and disposing of radiolabelled substances can be avoided.

Luminescent labels are not limited to application in immunological assays. They can be envisaged to target smaller molecules such as peptides and nucleic acid strands. In such cases the luminescent label may provide further advantages as the binding of the analyte may cause a direct effect on the luminescence, for example a triggering or quenching or the luminescence or a shift in the emission or excitation wavelength maxima. Luminescent compounds may also be used as 'tags' to monitor molecules or ions within cells.

Any luminescent label application designed for biological media faces the problem of background fluorescence leading to decreased sensitivity. Any biological sample will contain a large number of fluorescent compounds such as the aromatic amino acids tyrosine and trytophan. Scattered light and Raman bands are further potential problems, especially where the Stokes shift is small.

The lanthanides provide a solution to this problem but in turn provide their own set of problems, which shall be discussed.

The research discussed herein lies in the design and synthesis of novel lanthanide complexes and the study of the influence of various ligand substituents on

their luminescence properties. These studies will be applied to influence the design and synthesis of specific immunological assay and 'tag' species.

1.2 Introduction to Lanthanides [3]

The lanthanides or rare earth metals lie between lanthanum and hafnium. They range from cerium to lutetium and all the lanthanides have a $6s^2 4f^n$ configuration. Lanthanum ($5d^1 6s^2$), scandium ($3d^1 4s^2$) and yttrium ($4d^1 5s^2$) have differing electronic configurations but due to their similar properties to the lanthanides are generally included in the classification of lanthanides.

The chemistry of the lanthanides is dominated by the +3 oxidation state. One of the principle reasons for this is due to ionisation energies. The fourth ionisation energy, I_4 [the energy associated with the process $Ln^{3+}(g) \rightarrow Ln^{4+}(g) + e^-(g)$] is greater than the sum of the first three ionisation energies. The extra energy required to remove the fourth electron is so great that in most cases it cannot be recovered through chemical bond formation, and thus the +4 oxidation state is largely inaccessible. The less stable +2 oxidation state is also rare but can be found and examples of these less stable states are encountered when oxidation or reduction of the trivalent state leads to a stable electronic configuration.

Five lanthanides show tetravalent chemistry. For neodymium and dysprosium this is confined to solid-state fluoride complexes, while praseodymium and terbium also form the tetrafluoride and dioxide. Cerium shows the most extensive Ln^{4+} chemistry with a variety of tetravalent compounds and salts known. The Ce^{4+} is

chemically accessible due to the high energy of the 4*f* orbitals at the start of the lanthanide series, such that they are not sufficiently stable in Ce^{3+} to prevent the loss of another electron.

The +2 oxidation state is typically stabilised by oxide and fluoride compounds. Europium and ytterbium are examples of the +2 state where this oxidation state leads to a half-filled *f* shell (f^7) for Eu and a filled *f* shell (f^{14}) for Yb.

One of the most characteristic properties of the lanthanides is the lanthanide contraction, which refers to the reduction in the lanthanide metal and Ln^{3+} radii with increasing atomic number. These contractions arise from the poor ability of *f* electrons to screen the other valence electrons from the nuclear charge, which leads to a steady contraction of the ionic radius of the ions across the period.

The *f* electron configuration of the lanthanides has little effect with regards to geometry. To an incoming ligand, lanthanide ions have the appearance of a noble gas atom, except with a positive charge (typically +3). This is because the 4*f* orbitals which contain the valence electrons do not extend out far enough to interact to any great degree with ligand orbitals. The complexes thus formed are held together largely by electrostatic interactions - ionic bonding. Lanthanides can therefore be thought of as hard Lewis acids and will prefer to coordinate to hard bases such as F^- and H_2O. The strength of their ionic bonding will depend on the charge density on the ion. The f elements are large but due to the common oxidation state of +3 they still have a high charge density, this coupled with the lanthanide contraction means as we cross the 4f series charge densities and ionic bond strength increases.

Geometry is therefore governed more by steric effects dictated by the size of the ionic radius of the metal ion. Coordination numbers for the lanthanides can range from 6 to 12 as a consequence of the large size of the lanthanide ions but more typical numbers are 8, 9 and 10. There is little or no "directionality" in the Ln^{3+}- ligand interactions so that primary coordination numbers and coordination geometries are determined almost entirely by ligand characteristics (conformational properties and the number, sizes and charged nature of donor groups).

The luminescence of the lanthanides is the foremost property we are interested in as discussed. Under favourable conditions many of the lanthanide (III) ions are able to exhibit long-lived luminescence following excitation into higher electronic states. This phenomenon is often observed in the solid state, where there is often little competition from other non-radiative deactivation sources. The energy level diagram for the lanthanide ions in aqueous solutions is given in Fig. 1.1. The luminescence properties can be discussed as being in the following groups: Group1: Lanthanide ions that luminesce strongly in the visible wavelength region (Sm^{3+}, Eu^{3+}, Tb^{3+} and Dy^{3+}); Group 2: Lanthanide ions that exhibit weak luminescence in the visible part of the spectrum (Pr^{3+}, Ho^{3+} and Tm^{3+}); Group 3: Lanthanide ions that emit in the NIR (Pr^{3+}, Nd^{3+}, Dy^{3+}, Er^{3+} and Yb^{3+}).[4] The group we are primarily concerned with is group 1 and shall be discussed in the next section.

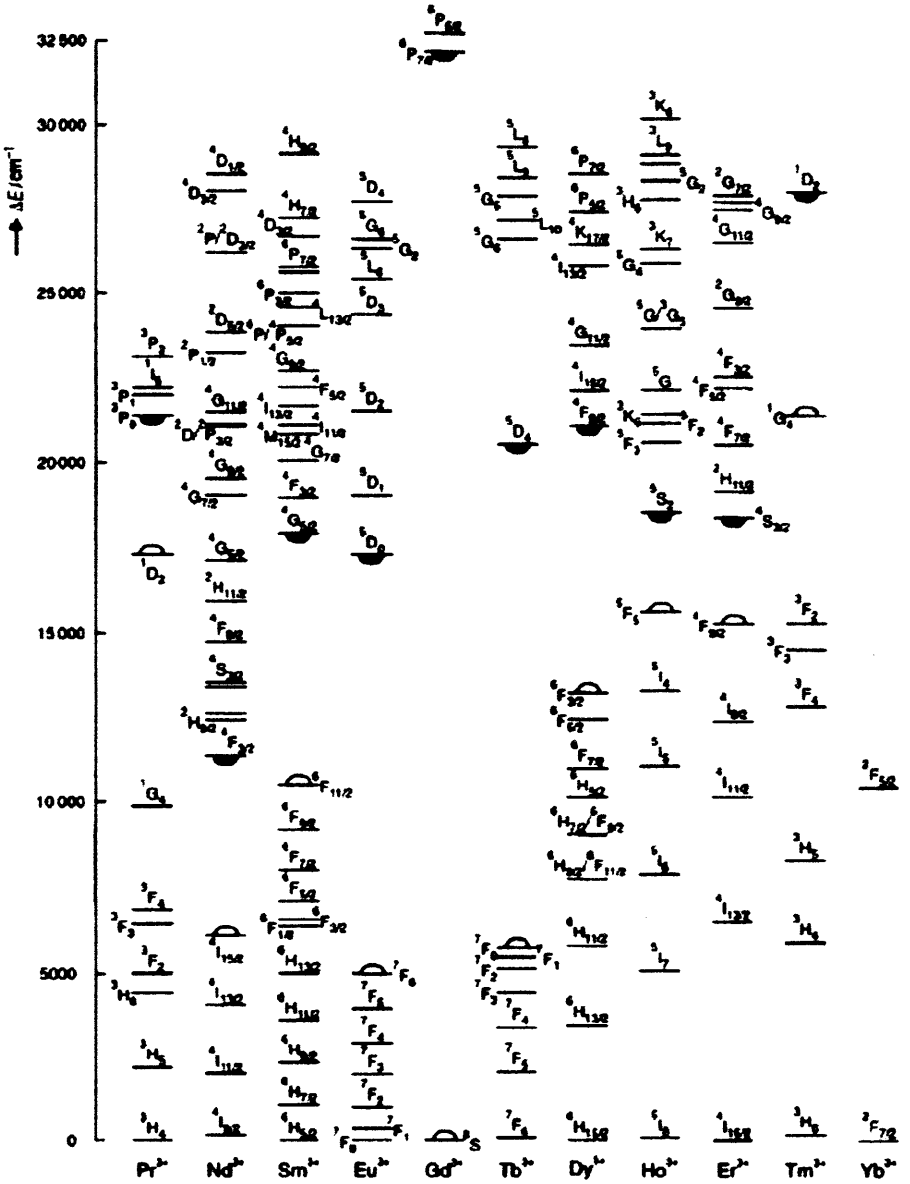

Fig.1.1: Energy level diagram for the lanthanides ions in aqueous solution.[5] Black semi-circles represent the lowest luminescence level. The white semi-circles represent the highest level of the ground state.

1.3 Luminescence of the Lanthanides

The attraction of the lanthanides lies in the fact that long-lived luminescence may be observed under ambient conditions. Eu(III), Tb(III) and Sm(III) ions exhibit excellent luminescent properties making them suitable probes or labels for chemical and biological applications[6]. Their emission spectra display bands that are very narrow and are insensitive to environmental changes; the wavelengths do not shift more than $\pm 2cm^{-1}$ on changing conditions such as temperature or the co-ordination site. Also the use of sensitised emission gives rise to a large stokes shift such that there is unlikely to be any overlap of the emission bands with strong absorbance bands.

Lanthanide ions, however, have two problems. They have very weak absorption bands with molar absorption coefficients usually $< 1\ dm^{-3}mol^{-1}cm^{-1}$.[7] This is due to the fact that the transitions occurring involve the same f^n configuration which are parity (Laporte) forbidden. The second problem relates to deactivation of the metal emissive states by vibrational energy transfer. The effect arises through an energy transfer process from the metal excited state to the O-H stretching vibrations of coordinated or closely diffusing water molecules. [8] Unfortunately, the lanthanides are strong coordinators of strong bases such as solvent water molecules.

In order to enhance the absorption of the metal ions the lanthanides are usually chelated with ligands that have much broader and more intense absorption bands. In chelated lanthanide systems the intense luminescence may be obtained by the "antenna effect" [6] (see Fig.1.2), which is defined as a light conversion process via an

absorption-energy transfer-emission sequence involving distinct absorbing (ligand, light collector) and emitting (metal ion) components. Intense luminescence emission depends upon three quantities:

1) the intensity of the ligand absorption
2) the efficiency of the ligand –to-metal energy transfer
3) the efficiency of the metal luminescence

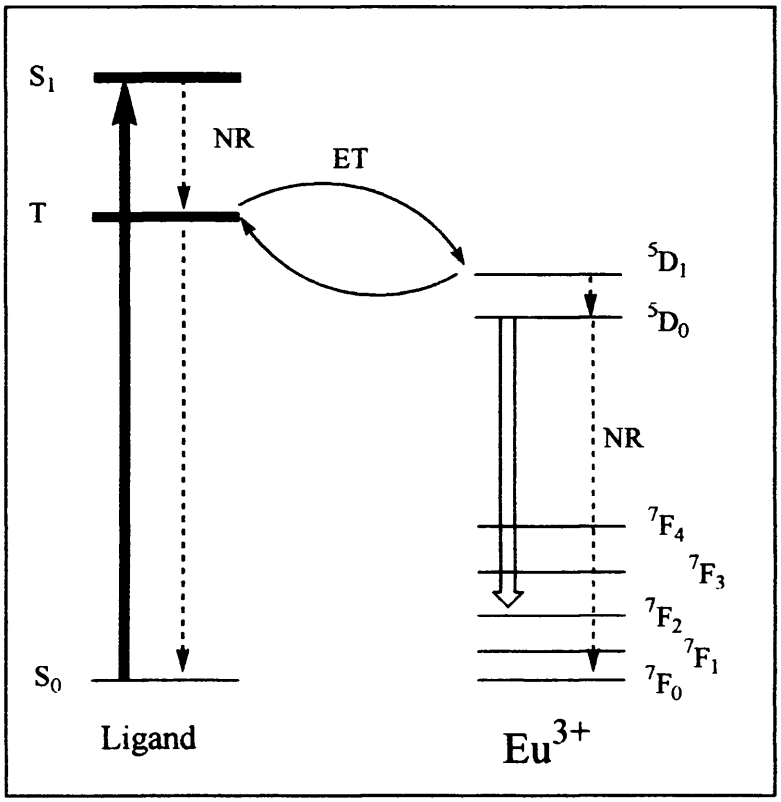

Fig.1.2: The "antenna effect" illustrated with Eu(III)

Therefore the ligand must have a high molar extinction coefficient and be able to efficiently transfer energy to the lanthanide ion. For an efficient transfer of energy from the ligand triplet state to the Ln excited metal state, a matching of the energy levels is required, preferably with the donor triplet being slightly lower in energy than the metal excited state in order to ensure the forward process is exothermic. Also, a

problem can occur if the energy gap is too small. Under such circumstances, thermally activated back energy transfer can arise from the excited state of the metal to the triplet state of the antenna, which may subsequently be deactivated by the usual pathways. Such a process will clearly lead to a reduction in both the intensity of emission and the effect will be more significant at higher temperature.[9]

The third problem described above is also overcome by the use of this "antenna" ligand. The ligand can be designed so as to sufficiently shield the metal centre from solvent molecules, in particular water, which will provide a non-radiative deactivation for the excited metal through vibrational modes.

Some common examples of ligands that have been used to chelate lanthanides for luminescent species include cryptates[10-12], Bipy cryptates[13], N-oxide cryptates[14], β-diketonates[15], polypyridyls (which include Bipyridine and terpyridine[16]) and a host of structural analogues of the described systems including crown ether calixarenes [17].

Another advantage of using 'antenna' chelates to complex the lanthanides is that the use of just one ligand can produce many different wavelengths by changing the complexed metal, although it is unlikely each metal will emit with the same efficiency. As shown in Fig. 1, the different groups of metal ions can emit in different regions of the spectrum so the 'antenna' ligand can be tuned by use of different lanthanides.

The work described in this study is primarily interested in the visible wavelength emission of Eu(III) and Tb(III). The lowest-energy multiplets associated with the $4f^6$ electronic configuration of Eu^{3+} and the $4f^8$ electronic configuration of Tb^{3+} are shown in Fig.1.3.

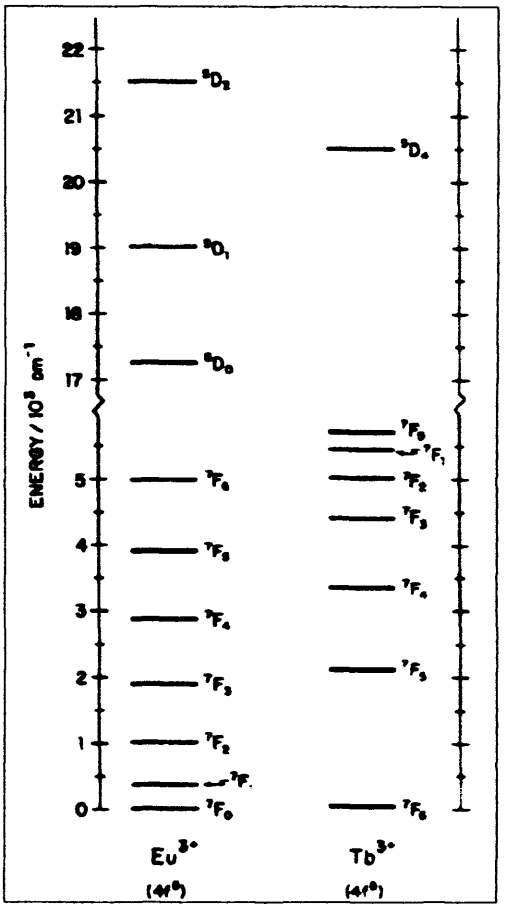

Fig.1.3: The energy levels of Eu^{3+} and Tb^{3+}.

For Europium (III) complexes in aqueous solution, all emission emanates from the nondegenerate $^5D_0$ level when excitation is at υ>17300cm^{-1}. Therefore the ligand triplet state needs to lie in this region for an efficient energy transfer mechanism. The strongest emissions emanate from the $^5D_0 \rightarrow {}^7F_1$ and $^5D_0 \rightarrow {}^7F_2$ transitions, and $^5D_0 \rightarrow {}^7F_4$ transitions are usually observed to have moderately strong intensities. The remaining $^5D_0 \rightarrow {}^7F_J$ transitions are generally either very weak or unobservable.

The line like emissions result from predominately electric dipole character, although magnetic dipole radiation is often jointly responsible (if J=0, ±1 except 0→0).[18] For the free ion of Eu(III) electric dipole transitions are forbidden as they are between states of the same f^n configuration. Therefore the observed emissions must be explained in terms of interactions by the ligand field. The ligand field mixes in higher energy states of opposite parity by removing the centre of symmetry of the Eu(III) ion. The 4*f* orbitals are well shielded from ligand interactions by the intervening $5s^25p^6$ octet, so the extent to which the degeneracy is removed depends upon both the strength and symmetry of the ligand field. The intensities of the $^5D_0 \rightarrow {}^7F_1$ and $^7F_2$ transitions are very sensitive to the nature of the ligand environment. The $^5D_0 \rightarrow {}^7F_1$ generally shows strong magnetic dipole character and the $^5D_0 \rightarrow {}^7F_2$ shows hypersensitivity to the ligand environment.[19] The small splittings of the Eu(III) emission that are shown from the ligand field interaction are useful in establishing by a group theoretical method, the local site symmetry of the metal ion in the complex if spectra may be obtained with sufficient resolution.[18]

For Eu(III) complexes in nonaqueous solutions it is also possible to observe emissions from the $^5D_1$ and $^5D_2$ levels when excitation is at $\upsilon > 21\ 500 cm^{-1}$. However, these are not typical expected, in accordance with Kasha's rule.

A typical emission spectra of a Eu(III) complex and the determination of its symmetry can be demonstrated by discussion of a sample relevant to this study, $[Eu(terpy)_3][ClO_4]_3$. Figure 1.4 shows the observed luminescence spectra of the $[Eu(terpy)_3][ClO_4]_3$ complex reported by Hart *et al.*[20]. All intense transitions

originate at the $^5D_0$ level and terminate at ^7F_J levels. The $^5D_0 \rightarrow {}^7F_1$, $^7F_2$, $^7F_4$ transitions are intense and well resolved. The remaining transition $^5D_0 \rightarrow {}^7F_0$ is notably absent.

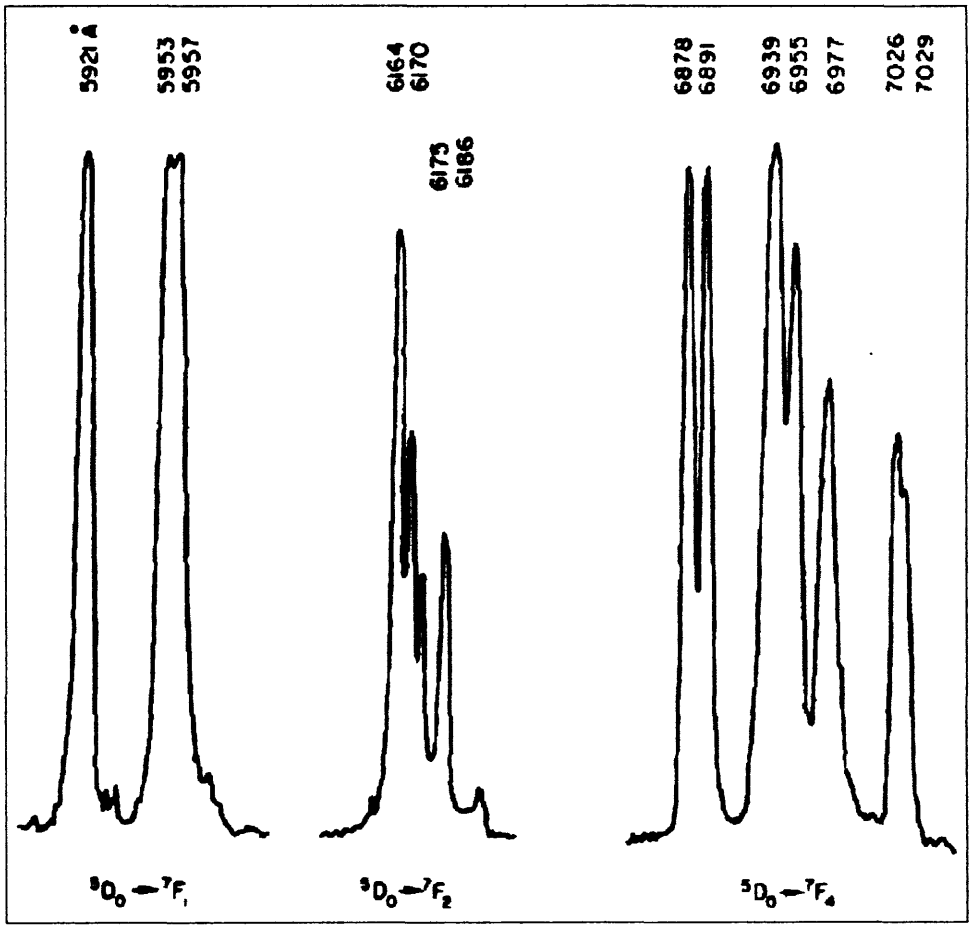

Fig. 1.4: The strong transitions in the fluorescence spectrum of $[Eu(terpy)_3][ClO_4]_3$.

From their analysis of D_3 symmetry requisites[18], the crystal field splitting and allowed transitions are described in Table 1.1. Both magnetic dipole and electric dipole transitions A_2 or E. The spectrum therefore is in accord with a slight low-symmetry perturbation of a basic D_3 symmetry, probably due to a distortion of the terpyridine co-ordination sphere.

$^5D_0 \rightarrow$	Stark-split Component in D_3	Transitions Allowed to	Assignments (Å)
$^7F_4$	$2A_1 + A_2 + 3E$	$A_2 + 3E$	7029, 7026 (E) 6977 (A_2) 6955, 6939 (E) 6891, 6878 (E)
$^7F_3$	$A_1 + 2A_2 + 2E$	$2A_2 + 2E$	Transitions very weak; Singlet only at 6499
$^7F_2$	$A_1 + 2E$	2E	6186, 6175 (E) 6170, 6164 (E)
$^7F_1$	$A_2 + E$	$A_2 + E$	5921 (A_2) 5957, 5953 (E)
$^7F_0$	A_1	none	Transitions absent

Table 1.1: The crystal field splitting and allowed transitions for $[Eu(terpy)_3][ClO_4]_3$.

For terbium (III) complexes in aqueous solutions all emission emanates from the $^5D_4$ level when excitation is at υ>20 400cm^{-1}. Therefore the ligand triplet state needs to lie in this region for an efficient energy transfer mechanism. The most intense emission is observed for the $^5D_4 \rightarrow {}^7F_5$ transition occurring at ~544nm. The $^5D_4 \rightarrow {}^7F_{0,1,}$ emissions are always weak and the observed intensities of the remaining transitions fall in the order $^5D_4 \rightarrow {}^7F_6 > {}^7F_4 > {}^7F_3 > {}^7F_2$. Tb(III) is not as useful as Eu(III) for probing the symmetry of its complexes since it only exhibits moderate sensitivity (not hypersensitivity) to ligand environment.

1.4 Ligand Design and Previous Work

Commercial kits for fluoroimmunoassays presently make use of Eu^{3+} chelates. The well-known DELFIA (dissociation-enhancement lanthanide fluoroimmunoassay) method involves two steps in which two different europium chelates are used.[21] The first step uses, for example, an EDTA chelate that makes sure that the Eu^{3+} ion is strongly bound to the immunoreactive component. The EDTA chelate is then dissociated at low pH and the Eu^{3+} ion is complexed by the second chelating ligand, usually a β-diketonate, inside a protective micelle to give the luminescent complex.

A different approach to fluoroimmunoassay is available, which is more promising and the one that is ultimately the aim in this research project. It is based on the use of complexes of lanthanides that both shield the metal ion and luminesce strongly. The design of complexes, which are simultaneously stable and luminescent, makes possible a one step procedure.

There are three general approaches to the synthesis of these one-step chelates that incorporate the sensitiser directly into the shield: acyclic systems and macrocyclic and macropolycyclic systems. These ligands must be designed to fulfil the criteria as previously discussed. In summary:

- The ligand must be stable with respect to metal ion dissociation. Since the applications in mind are concerned with the detection of molecules at low concentrations, it is clearly essential that metal dissociation at high dilution is negligible, otherwise quantitative measurements will not be possible. To be able to bind strongly the ligand must possess donor atoms that satisfy the demands of a hard,

polarising lanthanide ion. Thus, among neutral donors, more polarisable amine nitrogens are preferred to ether oxygens and obviously hard anionic groups such as carboxylates, phosphonates and phosphinates are attractive binders.

- The ligand requires broad, intense absorption bands with high molar absorption coefficients and needs to be able to transfer energy efficiently in the ligand-to-metal energy transfer.
- The ligand needs to shield the metal ion from incoming solvent molecules to prevent a loss of energy through radiationless deactivation.
- Long excitation wavelengths are required in order to avoid background luminescence from biological substrates that lead to decreased sensitivity. Compounds such as tyrosine and tryptophan will exhibit substantial and variable levels of background fluorescence. Biological samples usually absorb strongly below about 330nm.
- Solubility in aqueous media at biological pH.
- Long luminescence lifetimes and a high quantum yield are required.

1.4.1 Complexes of Shielding Luminescent Ligands

The synthesis of thermally stable and highly luminescent chelate labels has long been a challenge for numerous research groups including John Toner, Jean M. Lehn, Gilberto F. De Sä, V. Balzani, D. Parker, Takkalo, Bünzli and Piguet to name but a few. Their work has covered such chelates as cryptates, Bipy cryptates, N-oxide cryptates, β-diketonates, polypyridyls and a host of structural analogues of the described systems. The most luminescent complexes of the lanthanide(III) ions are those formed with certain β-diketone ligands. However, the majority of these neither

have sufficient water solubility nor stability in aqueous solution. Similarly, the other chelate labels developed so far do show promising properties but do not possess satisfactory properties regarding their luminescence intensity, thermodynamic and kinetic stability, photostability and suitability as immunolabels.

1.4.2 Macrocyclic and Macropolycyclic Systems

Some of the earlier work of interest to this research is that of Lehns and co-workers. Their initial examination of encapsulating chelates such as cryptates, Bipy cryptates and N-oxide cryptates for the enhancement of luminescent properties of the lanthanides with the proposition that these complexes could be used as light-conversion molecular devices (LCMD) is one of the reasons for the recent resurgence of N-oxide coordination chemistry. Initially Lehn reported macrocyclic ligands and cryptands based on the strongly absorbing bipyridine as suitable targets for the coordination of Eu(III). The ligands were identified due to their properties of light absorption and energy transfer from the ligand to the metal (the 'antenna effect') and the binding of the metal in a cavity in such a fashion as to shield the metal from solvent molecules. The Eu(III) complex of the macrobicyclic tris(bipyridine) ligand[22] (see Fig 1.5. Ligand **1**) showed intense absorption bands in the UV region due to $\pi \rightarrow \pi^*$ transitions in the bpy units.[23] An energy transfer process from the ligand to the metal was taking place but rather low values of the emission quantum yield were obtained ($\phi_{H_2O}^{300K}$ =0.02). This seemed to indicate that the energy transfer was not taking place efficiently. It was determined from comparisons of the lifetimes and quantum yields in H_2O and D_2O solutions that non-radiative deactivations via O-

H vibrations were occuring. It was estimated that ~2.5 water molecules were co-ordinated to the metal ion.

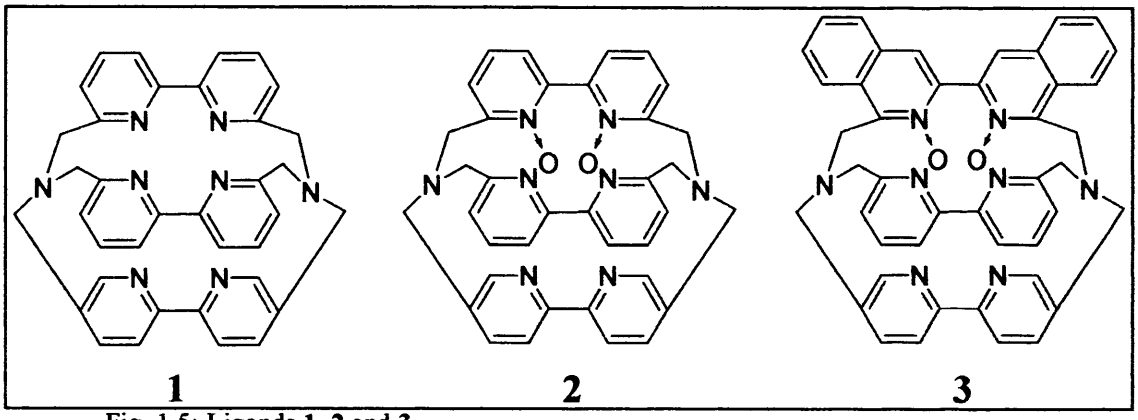

Fig. 1.5: Ligands **1**, **2** and **3**.

In an attempt to increase both the shielding of the enclosed ion and the yield of intramolecular energy transfer ligands **2** and **3** were synthesised.[24] The absorption spectra of the Eu(III) complexes showed the same bands as the parent cryptates containing only bip and biq units and shoulders on the red side of the lowest energy bands due to $bpyO_2$- and $biqO_2$- localised ligand excited states. The molar absorption coefficients at the maximum were lower than the corresponding cryptate without N-oxide groups. Although the molar absorption coefficients were lower, much higher values of the emission quantum yield were obtained over the parent non-oxidised cryptand ([Eu**2**]: $\phi_{H_2O}^{300K}$=0.15, [Eu**3**]: $\phi_{H_2O}^{300K}$=0.20). The shielding ability of these ligands is also far superior to that of the ligand in the [Eu**1**] complex as confirmed by the lifetime values in H_2O and D_2O with [Eu**2**] and [Eu**3**] having 1.4 and 1.1 water molecules co-ordinated to the metal ion respectively. These higher quantum yields can be explained by both the greater shielding capabilities of the ligands **2** and **3** and an increase in the efficiency of population of the lowest $^3\pi\pi^*$ level (see Fig.1.6),

which in turn leads to more efficient energy transfer from the ligand to the metal centre.

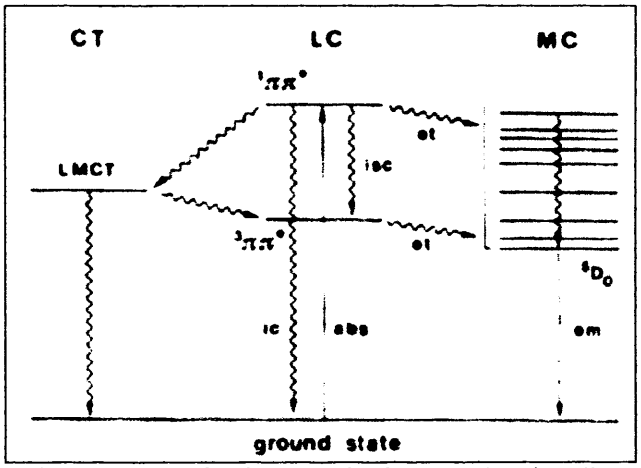

Fig.1.6: Diagram of energy transfer in Eu(III) chelates showing ligand to metal charge transfer (LMCT), ligand centred transitions (LC) and metal centred transitions (MC).

Lehn's work went on to utilise the 2,2'-bipyridine chromophoric group as a building block to synthesise the branched macrocyclic ligands **4a**, **4b**[25], **5**[26]. In most cases these ligands shielded the metal ion against interaction with solvent molecules more efficiently than the cryptands.

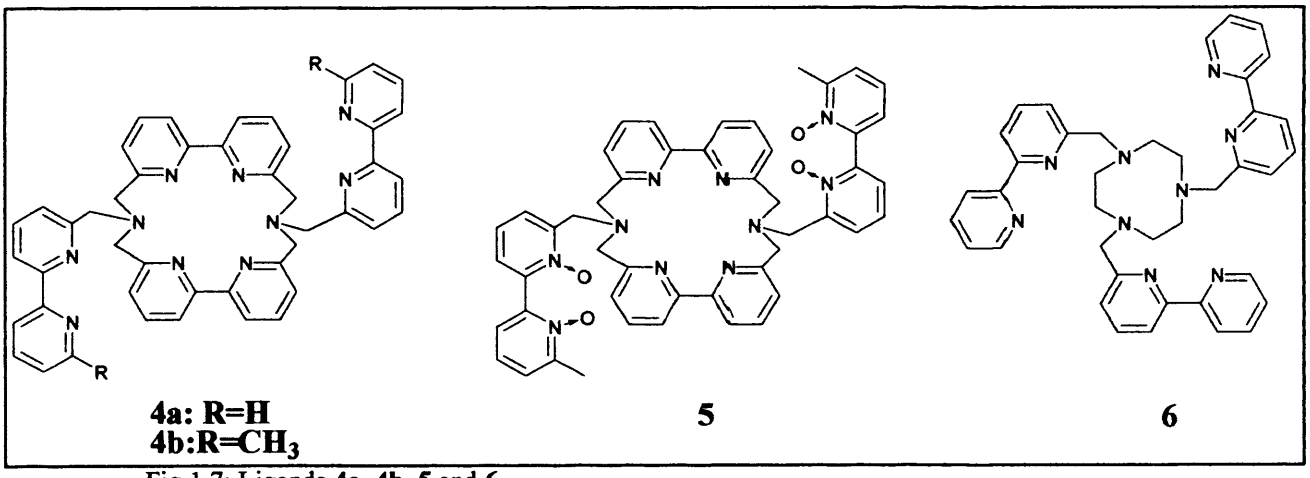

Fig.1.7: Ligands **4a**, **4b**, **5** and **6**.

The Eu^{3+} complex of **4a** gave a resulting quantum yield of 0.1 in H_2O at 300K whilst **4b** gave a much smaller quantum yield of 0.01 in H_2O at 300K. This was

attributed to a reduced efficiency of ligand-to-metal energy transfer due to the presence of the methyl groups. The presence of the methyl groups also appeared to reduce stability of the complex. Whilst in methanol, a weaker complexing solvent than water, the complex was stable, in water the complex was unstable, presumably because the methyl groups prevent a close approach of the branched bpy units to the metal ion, thus allowing the water molecules to compete for ion complexation.

Following the approach described for cryptand ligands, N-oxide groups were introduced to the branched bipy units giving the ligand **5**. In contrast to ligand **4b**, ligand **5** showed remarkable stability in water, most likely due to the N-oxide being able to overcome the steric hindrance of the methyl groups and even approach the Eu^{3+} ion better than the bpy nitrogens of **4b**. Analogously to the effect of introducing N-oxide groups to the cryptand **1** the quantum yield of [Eu**5**] showed an increase to 0.015 in water.

At a similar time, the macrocyclic bpy-branched triazacyclononane **6**[27] was synthesised by Balzani and co-workers. For both Eu^{3+} and Tb^{3+} complexes, lifetime experiments showed the complexes to be coordinating no water molecules to the metal ions. The Tb^{3+} complex showed promising photophysical properties with a quantum yield of $\phi_{H_2O}^{300K}$ =0.37 and lifetime of $\tau_{H_2O}^{300K}$ =1.5ms. For the Eu^{3+} complex the superior shielding capability was let down by the poor photophysical properties of the complex. The short lifetimes ($\tau_{H_2O}^{300K}$ =0.5ms) and low quantum yields ($\phi_{H_2O}^{300K}$ =0.05) were associated with the presence of low-lying LMCT levels involving the aliphatic nitrogens.

A number of research groups have examined the luminescence properties of lanthanide complexes of calixarenes[28] with the calix[4]arenes receiving the most attention. Encapsulation of the Eu^{3+} and Tb^{3+} ions in the p-t-butylcalix[4]arene tetra acetamide ligand **7** by Sabbatini and co-workers[29] has led to relatively stable, water soluble complexes, which show interesting luminescence properties. The ligand exists in a fixed 'cone' conformation in both the free and complexed states and the X-ray crystal structure of its KSCN complex shows that the cation is encapsulated in a polar environment of eight oxygen atoms (four ester and four amide) which form a square anti-prism.[30] Sabbatini showed that the Eu^{3+} and Tb^{3+} complexes of **7** had only one water molecule coordinated to the metal ion and that the complexes were soluble in polar solvents.

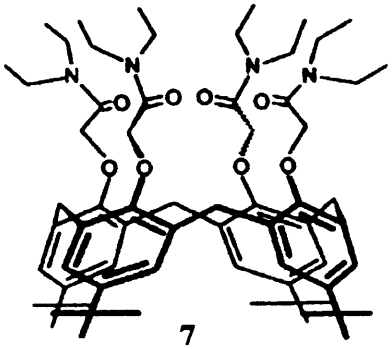

7

Fig.1.8: Ligand 7

The absorption spectrum of the free ligand and the excitation spectrum of the Tb^{3+} complex of **7** in methanol are given in Fig.1.9. The two bands at ~270nm and ~280nm correspond to transitions in the aromatic groups of the ligand. The analogy between both spectra shows that energy transfer from the ligand to the encapsulated metal is taking place. The excitation spectrum of the Eu^{3+} complex is similar to that of the Tb^{3+} but much weaker. The measured quantum yields and lifetimes of the complexes are quite differing. The Tb^{3+} complex shows a high luminescence

quantum yield ($\phi_{H_2O}^{300K}$ =0.2) and a long luminescence lifetime ($\tau_{H_2O}^{300K}$ =1.5ms), whereas the Eu^{3+} complex shows a very low quantum yield ($\phi_{H_2O}^{300K}$ =2.0x10^{-4}) and a relatively short lifetime ($\tau_{H_2O}^{300K}$ =0.65ms). The strong luminescence for the Tb^{3+} complex can be explained by i) an efficient ligand-to-metal energy transfer (the triplet excited state of the ligand lies at about 4000cm^{-1} above the $^5D_4$ Tb^{3+} emitting state) and ii) effective shielding capabilities of the chelate, whereas the weak luminescence of the Eu^{3+} complex can be ascribed to the presence of a ligand-to-metal charge transfer state (observed as a shoulder at ~300nm in the absorption spectrum) which may be efficiently deactivating the singlet excited state of the ligand and the $^5D_0$ emitting state of the metal ion in the ground state.

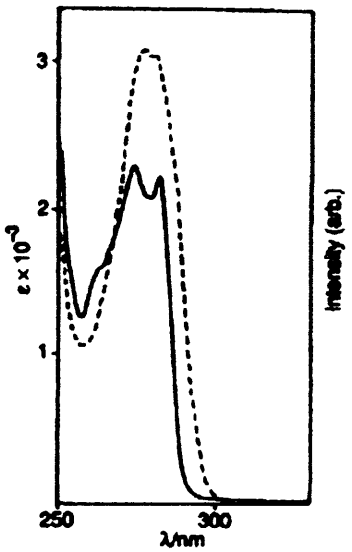

Fig.1.9: Absorption spectrum of 7 (-----) and excitation spectrum of $[Tb\subset 7]^{3+}$ (——) in methanol.

Some related calix[4]arenes have been synthesised in which two or four of the amide groups are replaced by bipyridine groups.

Similarly, the work of Sato and Shinkai [31] on analogous aryl ketone-appended calixarenes has shown that by adjustment of the calix[4]arenes attached sensitiser the excitation of any lanthanide ion to obtain various kinds of colour emission can be possible. They found that calix[4]arene-triacetamide derivatives are thermally stable ligands that can retain lanthanide ions in the ionic cavity. Thus, by introducing an energetically suitable sensitiser via the ketone linkage to the residual OH group, an efficient ligand-to-metal energy transfer should be obtainable. They successfully attached a phenyl and biphenylyl-carbonyl unit to the residual linker and Fig.1.10 shows the observed energy levels from their measurements.

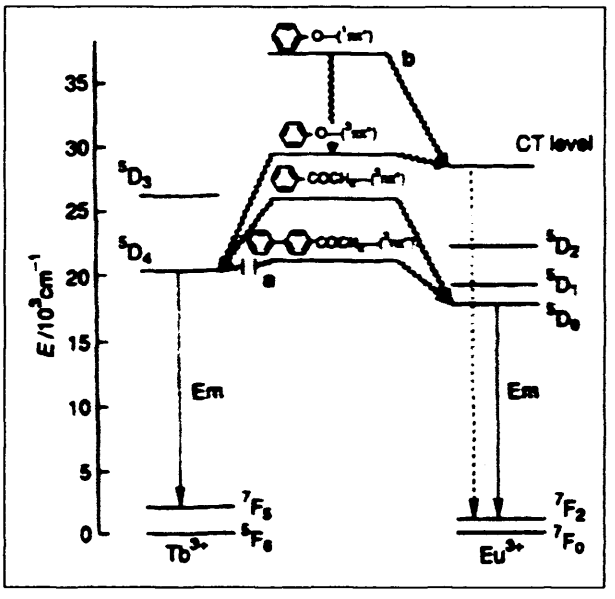

Fig.1.10: Energy-transfer diagram for Sato and Shinkai's Calix[4]arene systems. Energy transfer to the Tb^{3+} ion levels from the triplet energy levels of the biphenylylcarbonyl cannot occur (see mark **a** in the figure). As the C=O to Eu^{3+} charge-transfer band deactivates the excited-state of the phenol units to the ground state one cannot transfer the energy to the Eu^{3+} ion levels from the excited energy levels of the phenol units (see mark **b** in the figure).

The measured quantum yields for the 25-Phenacyloxy-26,27,28-(trispiperidinocarbonylmethoxy)-calix[4]arene complexes were found to be: Eu^{3+}

complex, ϕ_{MeCN}^{300K}=0.06 and Tb^{3+} complex, ϕ_{MeCN}^{300K}=0.27. The measured quantum yields for the 25-(4-Phenyl)Phenacyloxy-26,27,28-(trispiperidinocarbonylmethoxy)-calix[4]arene complexes were found to be: Eu^{3+} complex, ϕ_{MeCN}^{300K}=0.017 and Tb^{3+} complex, ϕ_{MeCN}^{300K}=0.015. The lower quantum yields for the biphenylyl-carbonyl calix[4]arene are explained in Fig.1.10 where the energy levels are a poor match, whereas the phenyl unit gives higher quantum yields due to a better matching of the energy levels.

Although the attempt to produce a highly luminescent Eu^{3+} complex of a calix[4]arene system, which had been limited to the Tb^{3+} ion, was not as successful as Sato and Shinkai had hoped, their concept had proven that the sensitiser can be adjusted to adapt to the lanthanide ion required.

The final area to be briefly discussed concerning macrocylic lanthanide complexes is that of tetra-N-functionalised 1,4,7,10-tetraazacyclododecane based macrocycles. A variety have been produced with the pendant groups ranging from amides to carboxylic acids to phenolic.[32a & b] The research groups of David Parker, Jean-Claude Bünzli and Stephen Faulkner are amongst many groups working in this area[32b] whose research mainly concentrates on varying the length and nature of the pendant arms with particular focus on lanthanide complexes of specific lanthanide derivatives. Parker has two excellent reviews extensively covering this topic highlighting the complexation chemistry of lanthanide ions in aqueous solution.[32c] One such ligand to be synthesised by Parker *et al* is the ligand shown in Fig.1.11.[32d] The Eu(III) and Tb(III) complexes of the ligand were found to have 1.16 and 1.2

lanthanide-bound water molecules and for both complexes the overall quantum yields for metal-based emission are low ($<10^{-3}$, following excitation at 250nm).

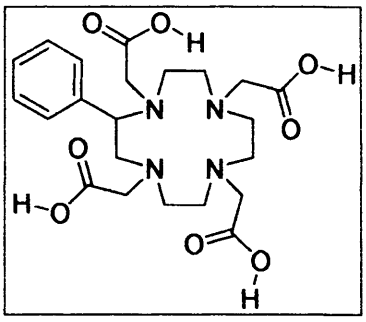

Fig.1.11: One of the [12]aneN$_4$ ligands ligand synthesised and investigated by D. Parker

Lehn had shown that heteroaromatic N-oxides are much more powerful binding ligands for lanthanide ions, due to the hard Lewis base-Lewis acid strong interactions, when compared to initial N-heterocycles, and at the same time showed they can be more efficient sensitisers for lanthanide emission. Numerous groups have since been researching in this area and these findings have been applied in this study, which shall be discussed in subsequent sections. Balzani had also shown the promising binding and shielding capabilities of the triazacyclononane **6** and excellent quantum yields values for its Tb^{3+} complexes.

1.4.3 Acyclic Ligands

An alternative route to highly luminescent materials is the use of acyclic ligands and is the one used in this research project. They have the advantage of being simpler to synthesise than devices based on complexes involving macrobicyclic cryptates but lack the stability advantage of the macrocyclic effect. The acyclic chelating agents commonly used for the sensitisation of Eu(III) and Tb(III) ions are β-diketonates, multidentate phenol, 4-amino-2-hydroxybenzoic acid, 7-amino-4-methylquinoline-2(1H)-one, pyridine, bipyridine, terpyridine and their structural analogues as polyamine-polycarboxylates.

In 1989 a patent by Toner[33] described various classes of heterocyclic and aromatic nitrogen-containing compounds such as quinquepyridines, quaterpyridines, terpyridines and phenanphrolines that had the requisite triplet levels to be effective lanthanide sensitisers. Following the success of this study, numerous groups have worked in this area with the inclusion of Mukkala and co-workers.[34,35 and 37] They have been interested in designing acyclic heterobiaryl systems possessing polycarboxylic functions.

Mukkala and co-workers studies initially focused on identifying ligands containing six-membered N-heteroaromatic rings that could be employed as efficient 'antennas'.[34] From the twelve ligands they synthesised and complexed with Eu(III) and Tb(III) ions they, like Toner, identified the chromophoric units 2,2'-bipyridine and 2,2':6',2''-terpyridines as potential probe alternatives in luminescence assays.[34 and 35] These two chromophores pose a problem, as although they are very suitable

energy-absorbing and energy-transferring units they requires additional chelating groups to form stable lanthanide complexes. In order to increase stability of the complexes Mukkala's group utilise two (methylenenitrilo)bis(acetic acid) groups in suitable positions. The addition of these different chelating groups creates a problem of their own, however, in which they affect the luminescent properties of the ligand. To gain more information on the effect of the addition of different chelating groups Mukkala synthesised 20 different 2,2'-bipyridine derivatives chelated with Eu(III) and Tb(III) ions. The parent chelate was ligand **8** (which was first synthesised by Ohm and Vögtle[36] but which was not studied at the time for its luminescent properties) and different groups were substituted at the bipyridine moiety. The different substituents are given in Table 1.2 along with their relative luminescence yields (log R).

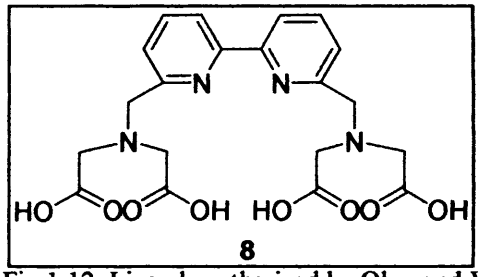

8

Fig.1.12: Ligand synthesised by Ohm and Vögtle.

Substitution at the Bipyridine Moiety	Eu^{3+} Log R	Tb^{3+} Log R
Unsubstituted	5.5	5.27
4,4'-dimethyl	5.61	5.51
4-nitro	4.12	2.94
4,4'-dinitro	4.14	Too weak
4-ethoxy	5.33	5.31
4,4'-diethoxy	5.11	5.13
4-bromo	5.36	5.12
4,4'-dibromo	5.31	5.02
5-bromo	4.16	4.50
3,3'-bis(ethoxycarbonyl)	4.31	Too weak
4,4'-dicarboxy	4.42	3.54
3,3'-bis(benzoyloxy)	5.36	2.83
4,4'-diphenyl	5.52	5.18
4,4'-bis(4-methoxyphenyl)	5.57	4.84
4,4'-bis(fur-2-yl)	5.32	2.10
4,4'-distyryl	2.95	2.63
N,N-dioxide	4.72	3.74
4-amino	4.42	4.62
3,3'-dicarboxy	4.90	2.23
3,3'-dihydroxy	3.91	Too weak

Table 1.2: The relative luminescence yields (log R) of the different substituents attached to the bipyridine ligand **8**. (Log R relative to uncomplexed Eu(III), Log R= 4.4).

From their analysis Mukkala found that nearly all of the complexes had one water molecule coordinated to the Eu^{3+} ion, with the exception of the 3,3'-dihydroxy substituted complex which was shown to coordinate two water molecules to the Eu^{3+} ion and the N,N-dioxide which they could not calculate due to the fact that there were

either two different chelates existing in the solution or there were two alternative energy-releasing processes.

As can be seen, the best relative luminescence yields, R, for the Eu^{3+} and Tb^{3+} complexes are obtained with the 4,4'-dimethyl derivative and so it would seem that electron-donating substituents (e.g. Me and Ph) seem to enhance R, and the electron-withdrawing substituents (e.g. NO_2 and COOH) lower it, although there is no straight correlation.

In a similar fashion Mukkala and co-workers went on to report the synthesis of 20 different 2,2':6',2''-terpyridine derivatives with (methylenenitrilo)bis(acetic acid) groups as the stable complex forming moieties and applied them to protein labelling.[37] The different ligands synthesised included the ligands **9**, **10**, **11** and **12**.

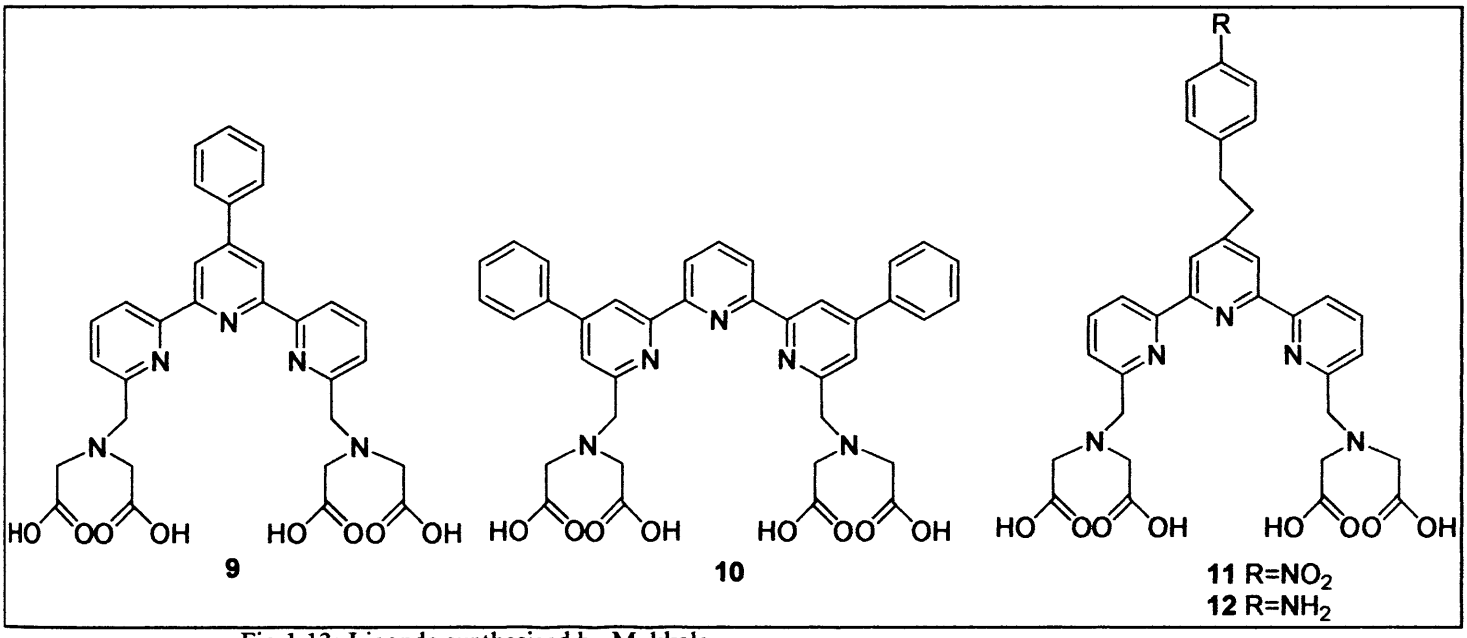

Fig.1.13: Ligands synthesised by Mukkala.

These ligands were shown to be excellent shielders of the metal ion core from decay time experiments and it was estimated that ~0.3 water molecules were co-ordinated to the metal ions. The parent compound **9** showed relatively high

luminescence intensities for both Eu^{3+} and Tb^{3+} (Eu^{3+}: $\varepsilon.\Phi$=1970, Tb^{3+}: $\varepsilon.\Phi$=1900) and ligand **10** nearly doubled the relative luminescence of the Eu^{3+} complex ($\varepsilon.\Phi$=3900). Conversely, it decreased the relative luminescence of the Tb^{3+} complex ($\varepsilon.\Phi$=1500). Ligands **11** and **12** gave even worse relative luminescence intensities for both Eu^{3+} and Tb^{3+} (**11** Eu^{3+}: $\varepsilon.\Phi$=580, Tb^{3+}: $\varepsilon.\Phi$=32; **12** Eu^{3+}: $\varepsilon.\Phi$=220, Tb^{3+}: $\varepsilon.\Phi$=53) seeming to indicate that the substituents in the aromatic part caused lowering of the ligand triplet state causing an energy leakage back to the ligand triplet state. Further coupling of these ligands to proteins gave varied results. The Eu^{3+} chelates coupled to proteins gave luminescence intensities almost identical to the parent complexes, whereas Tb^{3+} chelates coupled to proteins behaved unpredictably with regard to decay times and luminescence intensities.

Mukkala and co-workers had shown that these ligands are strong candidates for luminescent devices and with this study proven that it is quite possible to develop acyclic ligands that could be applied as luminescent labels. The presence of carboxylic groups had led to an enhancement of the overall stability of their complexes and they had also shown that careful consideration must be taken with ligand development as even small adjustments can give quite unpredictable results.

De Sá and co-workers have also been interested in the use of acyclic ligands and have followed Lehns theme of incorporating N-oxides to the chromophoric unit. They synthesised the mixed ternary complex tris(3-aminopyrazine-2-carboxylato)(2,2'-bipyridine)europium(III) and its bpy N-oxide.[38] Similarly to Lehns results the bpy N-oxide improved the photophysical properties giving higher

quantum yields (N-oxide Φ_{DMSO}=0.360, parent complex Φ_{DMSO}=0.261) and longer lifetimes (N-oxide $\tau_{DMSO}/10^{-6}$s=1580, parent complex $\tau_{DMSO}/10^{-6}$s=1500).

Numerous other research groups including Bünzli and Piguet, Bing Yan, M. Pietraszkiewicz, P.G. Sammes and J. Yuan have carried out similar research utilising oligopyridine ligands, each with varying degrees of success.

Bünzli and Piguet's research has centred on adjustments of the LMCT state by variation of such ligands as **13** (mbzimpy) and have observed dramatic changes to their quantum yields.[39] They also went on to study 4-alkylated 2,2':6',2''-terpyridines to try to further the understanding of the factors influencing the sensitisation of lanthanide luminescence.[40]

J. Yuan and co-workers synthesised and studied the luminescence properties of thienyl-substituted terpyridine analogues (**14**).[41] They found that the thienyl substituent favourably enhanced the luminescent properties of Eu^{3+} complexes but oppositely decreased the luminescent properties of Tb^{3+} complexes. The thienyl substituent was also expected to be able to have an amino-reactive group attached for biomolecular labelling purposes.

The work of Sammes and Cooper utilised the 2,2':6',2''-terpyridyl chelating group similarly to Mukkala *et al* and also incorporated an isothiocyanate group for biological labelling.[42] They proved its usefulness in time resolved fluorescence studies and for delayed fluorescence resonance energy transfer (DEFRET).

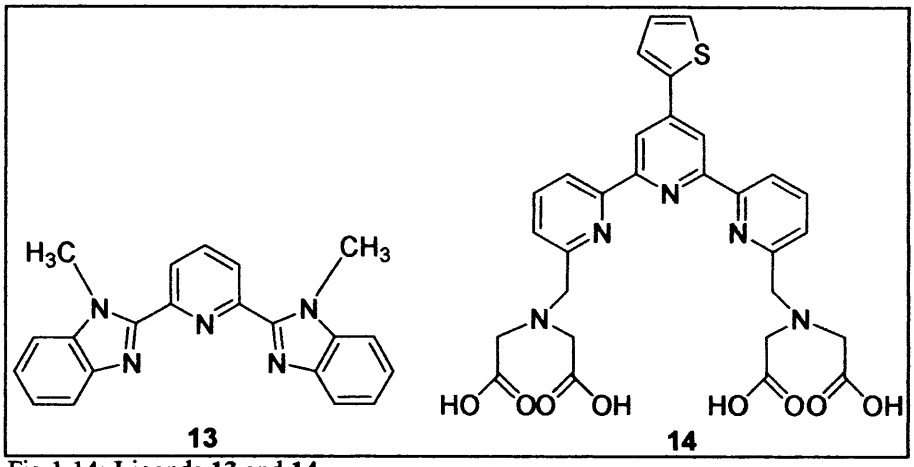

Fig.1.14: Ligands **13** and **14**.

The β-diketonates are the last area to be discussed in this introduction and have attracted much attention as luminescent devices since Weisman first noticed that a variety of Eu(III) β-diketonate complexes exhibited a line-like emission characteristic of the europium(III) ion.[43] Many of these complexes have shown potential application as laser materials and luminescent labels. At least several groups are researching in this area and includes the group of de Sá and co-workers

One of de Sá and co-workers most interesting β-diketonates synthesised has been the highly luminescent, mixed ligand complex tris(4,4,4-trifluoro-1-phenyl-1,3-butanedionate)(1,10-phenanthroline-N-oxide)europium(III) ($Eu(btfa)_3PhenNO$).[44] The emission spectrum is shown in Fig.1.15. The ligand was determined to have a solid-state quantum yield of 66% at 300K. The substitution of water molecules with the 1,10-phenanthroline-N-oxide greatly enhanced the quantum yield. This was ascribed to the N-oxide providing more efficient ligand–to-metal energy transfer and removal of the less efficient non-radiative $^5D_0$ relaxation processes.

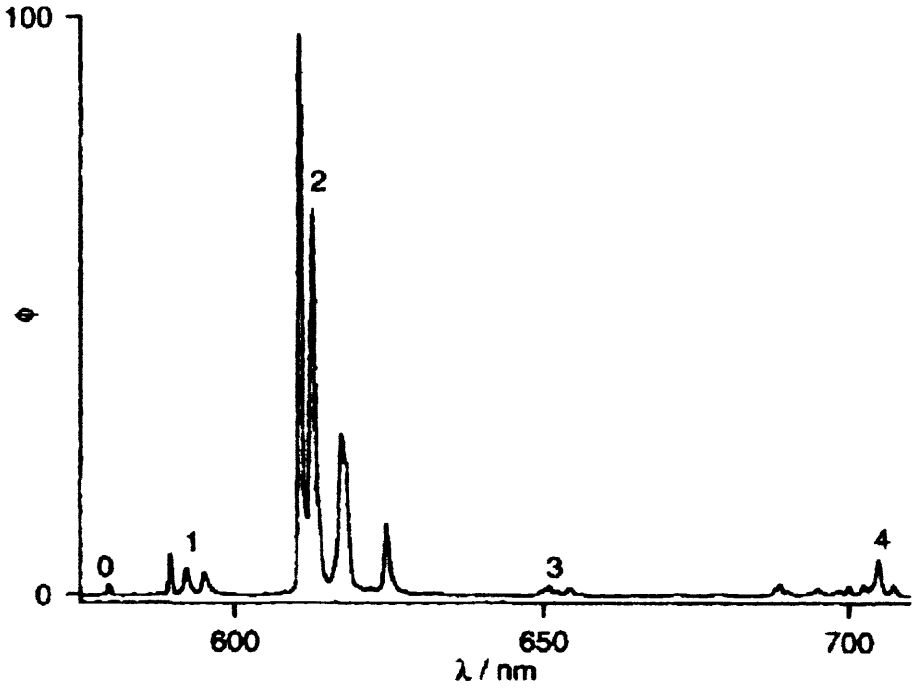

Fig.1.15: Emission spectrum of $[Eu(btfa)_3PhenNO]$ at 4.2K, upon ligand excitation (370nm). The labels refer to the *J* values of the final level of the emission transition $^5D_0 \rightarrow {}^7F_J$.

To try to improve upon this impressive β-diketonate complex de Sá and co-workers synthesised the mixed ligand complex $Eu(bzac)_3L$ (bzac=1-phenyl-1,3-butanedionate, L= water, 1,10-phenanthroline [phen] or 1,10-phenanthroline-NO [phenNO]).[45] The β-diketone bzac was chosen for its chemical similarity to the ligand 4,4,4-trifluoro-1-phenyl-1,3-butandionate. The luminescence spectra of the complexes consisted of the Eu^{3+} emission lines only and were essentially the same at room temperature and at 77K, apart from intensity differences. The measured quantum yields and lifetimes are described in Table 1.3.

Complex	Φ_{300K} (%)	T_{300K} (ms)
$Eu(bzac)_3.2H_2O$	5	0.300
$Eu(bzac)_3.phen$	8	0.410
$Eu(bzac)_3.phenNO$	27	0.855
$Eu(btfa)_3.phenNO$	66	0.670

Table 1.3: Measured Quantum yields upon ligand excitation (375nm) and lifetimes.

Once again the results concur with Lehns findings of increased luminescence quantum yield with the inclusion of N-oxides in the ligand framework. It is believed that the phenNO decreases the non-radiative $^5D_0$ relaxation rates and the increase in lifetimes is consistent with the suggestion. The quantum yield of the $Eu(btfa)_3.phenNO$ was not improved upon and this was attributed the presence of the electron-donor $-CH_3$ group in bzac and the electron withdrawing group $-CF_3$ group in btfa.

The group of Yanagida and co-workers made the first observation of photosensitised luminescence of Nd^{3+} in organic solutions with the use of β-diketone ligands.[46] Nd^{3+} containing systems have been one of the most popular luminescent materials for application in laser systems but very little was known about Nd^{3+} solution photophysical properties. Yanagida and co-workers synthesised the complex **15** with the deuterated molecule possessing low vibrational C-F and C-D bonds and a pentafluorophenyl group as a chromophore. The group observed a very strong emission in deuterated methanol when excited at the ligand excitation wavelength of 359nm, although they had not measured any quantum yields or lifetimes at the time.

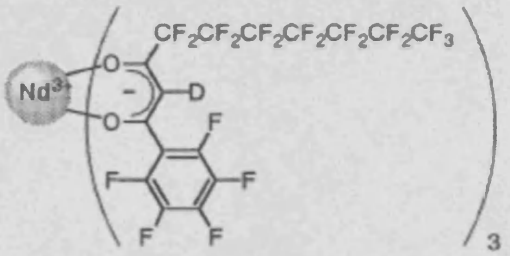

Fig.1.16: Complex **15**

Similarly, the group of Serra and co-workers synthesised and characterised photophysically a solid Tm^{3+} luminescent organic complex for the first time by use of the β-diketonate sensitiser 3-phenyl-2,4-pentanedionate (ppa).[47] The complex synthesised was $Tm(ppa)_3$ and by analysis it was found that two water molecules were coordinated to the Tm^{3+} ion. Serra and co-workers also did not carry out quantum yield and lifetimes measurements but reported strong emission intensity.

As can be seen from this discussion of macrocyclic, macropolycyclic and acyclic ligands, it is very difficult to predict ligand behaviour in lanthanide sensitisation. Obviously, research in this field needs to be further investigated and the findings taken into account in future ligand chelate design. De Sá and Donegá have shown a good appreciation of this by synthesising the mixed ligand complex tris(4,4,4-trifluoro-1-phenyl-1,3-butanedionate)(1,10-phenanthroline-N-oxide)europium(III).[12] By drawing upon Lehns study of N-oxides and various other groups work on 1,10-phenanthroline and β-diketonates the synthesised complex showed a remarkable solid-state luminescence quantum yield of 66% at 300K.

1.5 Quantum Yields

Knowing the quantum yield of a lanthanide complex is one of the most important methods for determining the competence of its luminescence capabilities and for determining how efficient 'antenna' ligands are at the ligand-to-metal energy transfer. Quantum yields are defined as the ratio of photons absorbed to photons emitted through luminescence. In other words the quantum yield gives the probability of the excited state being deactivated by luminescence rather than by another, non-radiative mechanism.[48]

The photophysical model that accounts for the sensitisation pathway in luminescent complexes is illustrated in Fig.1.17 (Using Eu^{3+} as an example).[49] The overall luminescence quantum yield (Φ) of complexes upon excitation of the chromophore can be determined by the efficiency of the sensitisation ($\Phi_{S\rightarrow Ln}$) and by the quantum yield (Φ_{Ln}) of the lanthanide luminescence step (eqn. (1.1)).[50]

$$\Phi = \Phi_{S\rightarrow Ln} \cdot \Phi_{Ln} \qquad (1.1)$$

Φ can be readily measured but the separate contributions of $\Phi_{S\rightarrow Ln}$ and Φ_{Ln} are usually not that easily accessible. Knowledge of these two is useful for the optimisation of luminescent lanthanide complexes, as it specifies the efficiency of the individual steps leading to the photosensitised luminescence of organolanthanide complexes.

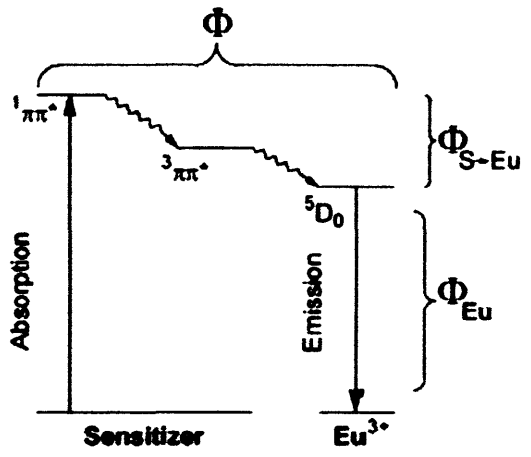

Fig.1.17: Energy transfer mechanism for the sensitised emission of Europium(III) with the related quantum yields. Solely depicted is the main luminescent level of Eu^{3+}.

The method used to measure relative quantum yields in this study is similar to the one used by Verhoeven *et al.*[50] It involves measuring the unknown sample against a sample of known quantum yield at equal-absorbing excitation wavelengths and by using Eqn.(1.2).

$$\Phi_u = \frac{n_u^2 I_u A_{ref}}{n_{ref}^2 A_u I_{ref}} \Phi_{ref} \qquad (1.2)$$

In which n_u, I_u and A_u are the refractive index, the area of the corrected emission spectrum and the absorbance at the excitation wavelength, respectively, for the sample of which the quantum yield is unknown. n_{ref}, I_{ref} and A_{ref} are the same observables for the reference sample. Φ_{ref} is the quantum yield of the reference sample.

Also, by use of this study,[50] Φ_{Eu} can be calculated for Eu^{3+} complexes and therefore the value for $\Phi_{S\rightarrow Eu}$ can be derived. Φ_{Eu} can be evaluated on the basis of the

corrected emission spectra, the observed lifetimes (τ) and by using Eqs. (1.3) and (1.4).

$$\Phi = \tau / \tau_R \tag{1.3}$$

$$1/\tau_R = A_{MD} \cdot n^3 \cdot \left(I_{\sum Fj} / I_{\sum F1}\right) \tag{1.4}$$

Where τ_R is the pure radiative lifetime, A_{MD} the spontaneous emission probability of the $^5D_0 \rightarrow {}^7F_1$ transition (A_{MD}=14.65 s^{-1} [50]), *n* the refractive index of the solvent and $\left(I_{\sum Fj} / I_{\sum F1}\right)$ the total area of the corrected Eu(III) emission spectrum to the area of the $^5D_0 \rightarrow {}^7F_1$ transition.

1.6 Determination of the Number of Water Molecules

As established, the knowledge of the number of water molecules coordinated to the lanthanide ion is of paramount importance. For most metal ions and their complexes in solution, the determination of the number of water molecules, *q*, occupying the first coordination sphere of the metal ion is difficult or impossible. However, for luminescent tripositive lanthanide ions, most notably Eu^{3+} and Tb^{3+}, a convenient method is available. The recently published correlation proposed by Horrocks[51] is a simple method in which the experimental lifetimes of lanthanide complexes at 295K in H_2O and D_2O solutions (and more recently MeOH and MeOD solutions) can be used to deduce *q*. Horrocks and Sudnick[52 and 53] utilised and

calibrated the fact that OH oscillators of coordinated water molecules provide non-radiative pathways for deexcitation of the emissive state of certain lanthanide ions, whereas, OD oscillators of coordinated D_2O are inefficient at accomplishing this deexcitation. By measuring various decay rates of a series of crystalline solids containing Eu^{3+} complexes and later by refinement of their correlation the equation given in (1.5) was derived.

$$q = A[\tau_{H_2O}^{-1} - \tau_{D_2O}^{-1} - K_{XH}] \tag{1.5}$$

$$K_{XH} = \alpha + \beta n_{OH} + \gamma n_{NH} + \delta n_{O=CNH} \tag{1.6}$$

Where the constant A was determined to be 1.11 (water molecules·ms) and n_{OH} is the number of alcoholic O-H oscillators in the first coordination sphere of Eu^{3+}, n_{NH} is the number of amine N-H oscillators in the first coordination sphere of Eu^{3+}, and $n_{O=CNH}$ is the number of amide N-H oscillators in which the amide carboxylic oxygen is in the first coordination sphere of Eu^{3+}. The respective contributions of these X-H oscillators to the deexcitation of the $^5D_0$ state of Eu^{3+} are β=0.44ms^{-1}, γ=0.99 ms^{-1} and δ=0.075 ms^{-1}. The value α is the quenching of excited state Eu^{3+} by second coordination sphere molecules and has been calculated as 0.31. The estimated error in the resulting q value is ±0.1 water molecules.

The equation, (1.5), is not only useful for predicting the q values of Eu^{3+} complexes that exist in a single form in solution, but it also provides insight into the equilibrium among Eu^{3+} complexes that exist in more than one conformation in

solution. By use of other experimental data such as luminescence spectra and lifetime measurements, accurate numbers of q can help determine the equilibrium among these Eu^{3+} complexes.[51]

An alternative method for the determination of the number of inner-sphere water molecules coordinated to lanthanide(III) ions has been reported by Peters *et al.*[54] The modified procedure involves the measurement of Dy(III)-induced ^{17}O NMR water shifts (d.i.s.) as a function of the concentration of the complex in question.

It had previously been observed that for paramagnetic lanthanide(III) ions the contact contribution to the Ln(III)-induced shift of a Ln(III)-bound ^{17}O nucleus is almost independent of the nature of any coordinated ligands. Therefore, the Ln(III)-induced ^{17}O shifts can be utilised to establish the coordination sites of the ligand and to determine the stoichiometry of the complex. For Dy(III) as the lanthanide, the induced ^{17}O shift is dominated by the contact shift (usually>85%) and so a separation of the contact and pseudo-contact contributions is not needed resulting in a simple procedure which can be utilised.

By measuring the d.i.s. of the lanthanide complexes in deionised water containing 20% D_2O and assuming that the d.i.s. of a water ^{17}O nucleus is independent of the nature and of the stoichiometry of the complex, the experimental induced shift of a $Dy(ligand)_n(H_2O)_q$ can be given by equation (1.7).

$$d.i.s. = q\Delta[Dy(ligand)_n(H_2O)_q]/[H_2O] \qquad (1.7)$$

Where Δ is the shift of a ^{17}O nucleus bound in the complex and q is the number of coordinated water molecules. The value of $\Delta/[H_2O]$ for a coordinated water molecule has been calculated experimentally as –40ppm dm^3mol^{-1}.

The d.i.s. measurements are performed over the range of 15mmol dm^{-3} to at least 100mmol dm^{-3}, therefore $[H_2O]$ is approximately constant, and a plot of the d.i.s. *versus* $[Dy(ligand)_n(H_2O)_q]$ should give a straight line with slope $q\Delta/[H_2O]$, if q is independent of the concentrations of the complex.. Therefore, using the value for $\Delta/[H_2O]$, equation (1.7) and the slopes of the plots of d.i.s. *versus* the concentration of the complex, the water coordination number (q) can be calculated. These measurements require not more than one minute of spectrometer time due to the extremely fast relaxation times of ^{17}O (acquisition times of only 0.2 seconds required).

The number of coordination sites available is a subject of some controversy and hydration numbers of eight and nine have been proposed [55]. The coordination number utilised by Peters *et al* is nine following on from the studies carried out by Brücher *et al*[56] which have shown that the hydration number of Lu(III) increases upon dilution up to values ≥9. Therefore assuming a constant coordination number for Dy(III) of nine, there are (9-q) coordination positions left for the organic ligand.

1.7 References

1) D. Parker, *Chem. Br.*, (1994), 833.

2) E. Soini and I. Hemmilä, *Clin. Chem.*, **25**, (1979), 353.

3) N. Kaltsoyannis and P. Scott, The *f* elements, Oxford Chemistry Primers.

4) D. N. Reinhoudt, *J. Chem. Soc. Perkin Trans.*, **2**, (1998), 2141.

5) G. Stein, E. Würzberg, *J. Chem. Phys.*, **62**, (1975), 208.

6) Lehn, J. M, *Coord. Chem. Rev.*, **123**, (1993), 201.

7) N. Kaltsoyannis, P. Scott, *The F elements*, Oxford Chemistry Primers 76.

8) J.L. Kropp and M.W. Windsor, *J. Chem. Phys.*, **45**, (1966), 761.

9) D. Parker and J. A. G. Williams, *J. Chem. Soc., Dalton Trans.*, (1996), 3613.

10) N. Sabbatini, S. Dellonte, M. Ciano, A. Bonazzi, and V. Balzani, *Chem. Phys. Lett.*, **107**, (1984), 212.

11) G.Blasse, M. Buys and N. Sabbatini, *Chem. Phys. Lett.*, **124**, (1986), 538.

12) N. Sabbatini, S. Dellonte and G.Blasse, *Chem. Phys. Lett.*, **129**, (1986), 541.

13) J. C. Rodriguez-Ubis, B. Alpha, D. Plancheral and J. M. Lehn, *Helv. Chim. Acta.*, **67**, (1984), 2264.

14) J. M. Lehn and C. O. Roth, *Helv. Chim. Acta.*, **74**, (1991), 572.

15) Mello Donegá, S.A. Junior and G.A. de Sá, *Chem. Comm.*, (1996), 1199.

16) Mukkala, V.M. Helenius, M. Hemmila, I. Kankare, J. Takalo, *Helv. Chim. Acta.*, **76**, (1993), 1361.

17) Jiang, J. Higasiyama, N. Machida, K. Adachi, *Coord. Chem. Rev.*, **170**, (1998), 1.

18) J.H. Forsberg, *Coord. Chem. Rev.*, **10**, (1973), 195.

19) Richardson, *Chem. Rev.*, **82**, (1982), 541.

20) D.A.Durham, G.H. Frost, F.A. Hart, *J. Inorg. Nucl. Chem.* **31**, (1969), 833.

21) I. Hemmilä, S. Dakuba, V. Mukkala, H. Siitari, T. Lövgren, *Anal. Biochem*, **137**, (1984), 335.

22) J. C. Rodriguez-Ubis, B. Alpha, D. Plancharel and J. M. Lehn, *Helv. Chim Acta.*, **67**, (1984), 2264.

23) B. Alpha, R. Ballardini, V. Balzani, J. –M. Lehn, S. Perathoner, N. Sabbatini, *Photochem. Photobiol.*, **52**, (1990), 299.

24) J.M. Lehn, Christine O. Roth, *Helv. Chim Acta.*, **74**, (1991), 572. L. Prodi, M. Maestri, V. Balzani, J.M. Lehn, C. Roth, *Chem. Phys. Lett.*, 180, (1991), 45.

25) R. Ziessel and J. M. Lehn, *Helv. Chim Acta.*, **73**, (1990), 1149.

26) C. O. Paul-Roth, J. M. Lehn, J. Guilhem, C. Pascard, *Helv. Chim Acta.*, **78**, (1995), 1895.

27) L. Prodi, M. Maestri, R. Ziessel and V. Balzani, *Inorg. Chem.*, **30**, (1991), 3798.

28) Coord. Chem. Rev., **123**, (1993), 201.

29) N. Sabbatini, M. Guardigli, A. Mecati, V. Balzani, R. Ungaro, E. Ghidini, A. Casnati and A. Pochini, *J. Chem. Soc., Chem. Commun.*, (1990), 878.

30) G. Calestani, F. Ugozzoli, A. Arduini, E. Ghidini and R. Ungaro, *J. Chem. Soc., Chem. Commun.*, (1985), 344; A. Arduini, E. Ghidini, A. Pochini, R. Ungaro, G. D. Andreetti, G. Calestani and F. Ugozzoli, *J. Inclusion Phenom.*, **6**, (1988), 119.

31) N. Sato and S. Shinkai, *J. Chem. Soc., Perkin Trans.*, **2**, (1993), 621.

32) a) U. Brunner, M. Neuburger, M. Zehnder, T. A. Kaden, *Supramolecular Chemistry*, **2**, (1993), 103. b) G. Zucchi, R. Scopelliti, J.-C. G. Bünzli, *J. Chem. Soc., Dalton Trans.*, (2001), 1975. c) D. Parker, G. J. A. Williams, *J. Chem. Soc., Dalton Trans.*, (1996), 3613; D. Parker, R. S. Dickins, H. Puschmann, C. Crossland, J. A. K. Howard, *Chem. Rev.*, **102**, (2002), 1977. d) C. D. Edlin, S. Faulkner, D. Parker, M. P. Wilkinson, *Chem. Commun.*, (1996), 1249.

33) J. Toner, United States Patent, 4,859,777, 1989.

34) V-M. Mukkala, C. Sund, M. Kwiatkowski, P. Pasanen, M. Högberg, J. J. Kankare, H. Takalo, *Helv. Chim. Acta*, **75**, (1992), 1621.

35) V-M. Mukkala, J. J. Kankare, *Helv. Chim. Acta*, **75**, (1992), 1578; V-M. Mukkala, M. Kwiatkowski, J. J. Kankare, H. Takalo, *Helv. Chim. Acta*, **76**, (1993), 893.

36) C. Ohm, F. Vögtle, *Chem. Ber.*, **118**, (1985), 22.

37) V-M. Mukkala, M. Helenius, I. Hemmilä, J. Kankare, H. Takalo, *Helv. Chim. Acta*, **76**, (1993), 1361.

38) G. de Sá, W. M. Azevedo, A. S. L. Gomes, *J. Chem. Research (S)*, 1994, 234.

39) S. Petoud, J. C. G. Bünzli, T. Glanzman, C. Piguet, Q. Xiang, R.P. Thummel, *J. Luminesc.*, **82**, (1999), 69.

40) H-R. Mürner, E. Chassat, R. P. Thummel, J-C. G. Bünzli, *J. Chem. Soc., Dalton Trans.*, (2000), 2809.

41) J. Yuan, M. Tan, G. Wang, *J. Luminesc.*, **106**, 2, (2004), 91.

42) M. E. Cooper, P. G. Sammes, *J. Chem. Soc., Perkin Trans.*, **2**, (2000), 1695.

43) S. I. Weissman, *J. Chem. Phys.*, **10**, (1942), 214.

44) C. Donegá, S. A. Junior, G. F. de Sá, *Chem. Commun.*, (1996), 1199.

45) S. Alves Junior, F. V. de Almeida, G. F. de Sá, C. de Mello Donegá, *J. Lumin.*, **72/74**, (1997), 478.

46) M. Iwamuro, Y. Hasegawa, Y. Wada, K. Murakoshi, T. Kitamura, N. Nakashima, T. Yamanaka, S. Yanagida, *Chem. Lett.*, (1997), 1067.

47) O. A. Serra, E. J. Nassar, P. S. Calefi, I. L. V. Rosa, *J. Alloys Compounds*, **275/277**, (1998), 838.

48) A Guide to recording Fluorescence Quantum Yields, JobinYvon.

49) J-M Couchet, J. Azma, P. Tisns, C. Picard, *Inorg. Chem. Commun.*, **6**, (2003), 978.

50) M. H. V. Werts, R. T. F. Jukes, J. W. Verhoeven, *Phys. Chem. Chem. Phys.*, **4**, (2002), 1542.

51) R. M. Supkowski, W. D. Horrocks Jr., *Inorg. Chim. Acta*, **340**, (2002), 44.

52) W. D. Horrocks Jr., D. R. Sudnick, *Acc. Chem. Res.*, **14**, (1981), 384.

53) S. T. Frey, W. D. Horrocks Jr., *Inorg. Chem. Acta.*, **229**, (1995), 383.

54) M. C. Alpoim, A. M. Urbano, C. F. G. C. Geraldes, J. A. Peters, *J. Chem. Soc. Dalton. Trans.*, 1992, 463.

55) C. Cossy, A. E. Merbach, *Pure Appl. Chem.*, **60**, (1988), 1785.

56) E. Brücher, J. Glaser, I. Grenthe, I. Puigdomènech, *Inorg. Chim. Acta.*, **109**, (1985), 111.

Chapter 2

Oligopyridine N-Oxide Lanthanide Complexes

2.1 Introduction

As discussed, our interests lie in utilising lanthanide(III) sensitisers that are incorporated directly into the shielding moiety. To fulfil the list of requirements for effective luminescence and stability the choice of ligand remains a crucial point and molecules containing aromatic moieties have been shown in chapter 1 to be effective sensitisers of Ln(III) ions. The groups of Toner, Mathis and Hemmilä have employed derivatives such as bipyridine, terpyridine and phenanthroline as chelating sensitisers possessing good absorption coefficients that can funnel energy via triplet energy transfer to the metal ion. In an effort to bring further understanding to the relationship between the ligand structure and the efficiency of the energy transfer process and, also, to identify suitable synthons for the design of elaborate compartmental ligands, we have concentrated our attention on the oligopyridines bipyridine, terpyridine, quaterpyridine and quinquepyridine.

In earlier work, our research group commenced an investigation into Lehn's findings of an expected increase in quantum efficiency with the inclusion of N-oxides to lanthanide sensitising ligands. The oligopyridine ligands shown in Fig.2.1 were synthesised with the focus of the study at the time being on transition group metal complexations.[1] Only the terpyridine N-oxide ligands **2**, **3** and **4** were investigated with Eu(III) and structural properties were determined along with some preliminary luminescent data. In continuation of the work and to investigate the applicability of Lehn's findings, the Eu(III) and Tb(III) complexes were synthesised for the ligands shown along with the precursor non-N-oxide ligands to allow comparison of any increase in quantum yield. Relative quantum yields were determined and a

comparison carried out across the series to determine an order of sensitiser efficiencies.

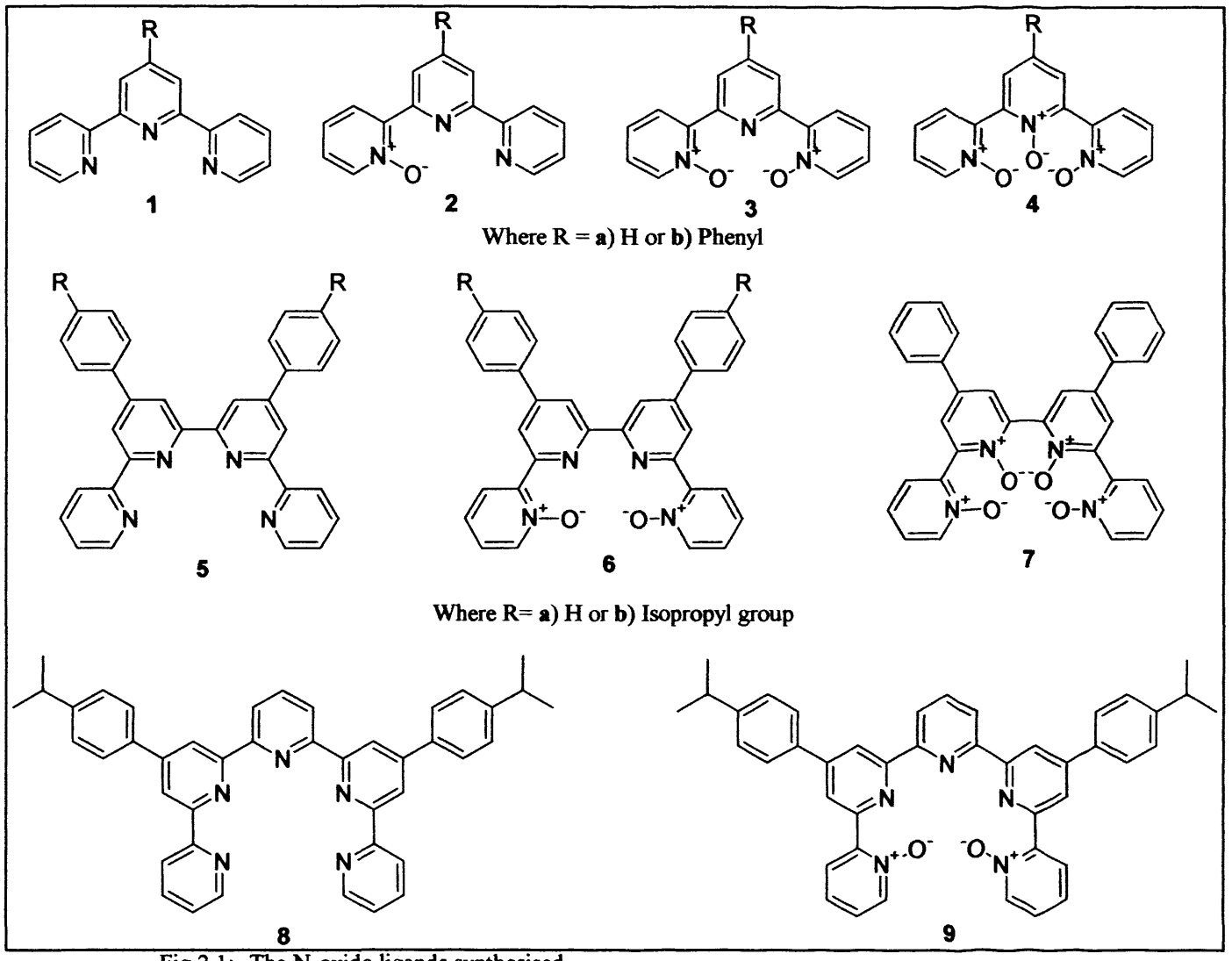

Fig.2.1: The N-oxide ligands synthesised

2.2 The Synthesis of Oligopyridines

The methods of synthesis of terpyridine, quaterpyridine and quinquepyridine are thoroughly researched and shall only be briefly discussed. An excellent review has been written by Kröhnke[2] specifying the various approaches to the synthesis of oligopyridines, with the methods utilised in this study described therein. The principles of the method adopted involve the conversion of methyl ketones into substituted pyridines, which was first reported in 1961.[3] Using the synthesis of 4',4''-(bisphenyl)-2,2':6',2'':6'',2'''quaterpyridine as an example, the methyl ketone, **10**, is reacted with iodine and pyridine to give the pyridinium salt, **11**. The salt is then reacted with unsaturated ketone, **12**, to give the 1,5-diketone via a Michael addition. The 1,5-diketone undergoes ring closure on treatment with ammonium acetate to give the desired oligopyridine, **5** (See Fig.2.2). One of the main advantages of this method is the 'one pot' nature of the reaction meaning numerous separate reactions are not required to produce the final product. By use of the unsaturated ketones **14** and **15**, which can be synthesised quite easily, terpyridine and quinquepyridine can be obtained (See Fig.2.3).

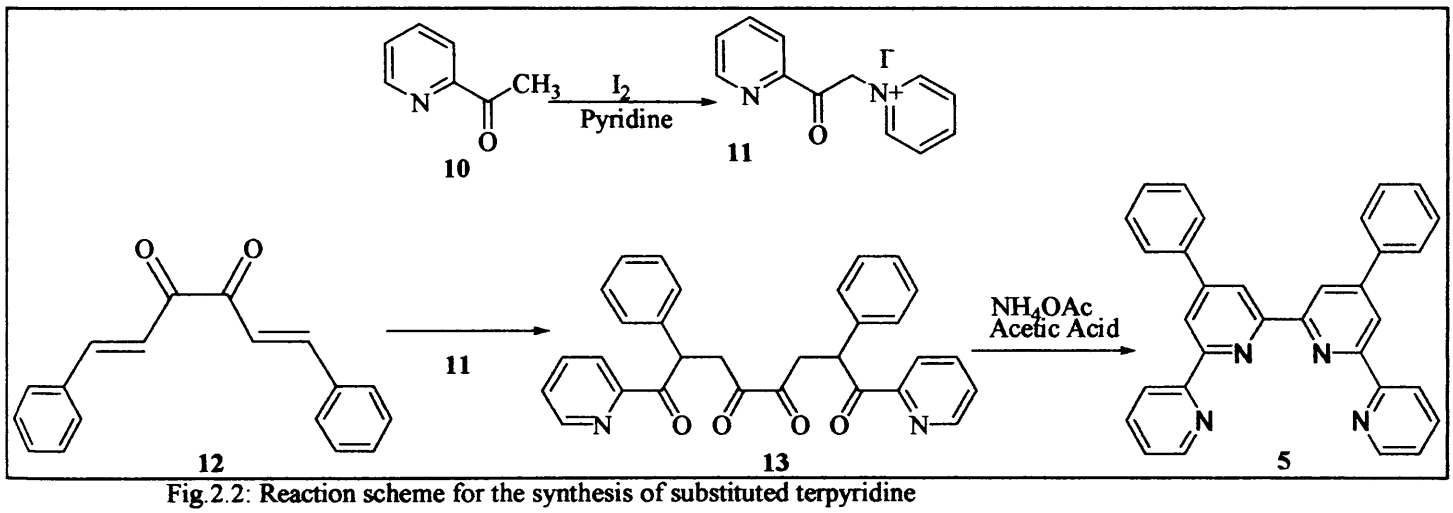

Fig.2.2: Reaction scheme for the synthesis of substituted terpyridine

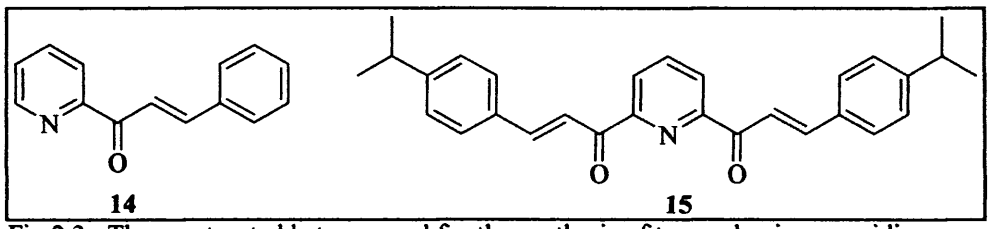

Fig.2.3: The unsaturated ketones used for the synthesis of ter- and quinquepyridine

The synthesis of 4'-phenyl-2,2':6',2''-terpyridine using the Kröhnke method has recently been made obsolete by a new more versatile method developed by Raston *et al.*[4] They have devised a solventless scheme that produces 4'-phenyl-2,2':6',2''-terpyridine via a sequential aldol and Michael addition reaction (see Fig.2.4). This method has made a dramatic improvement in the yield (>60%) and allows access to a range of compounds not accessible using the conventional Kröhnke method involving organic solvents. The clean nature of the conditions means a simpler reaction to carry out with an easier purification method (usually re-crystallisation).

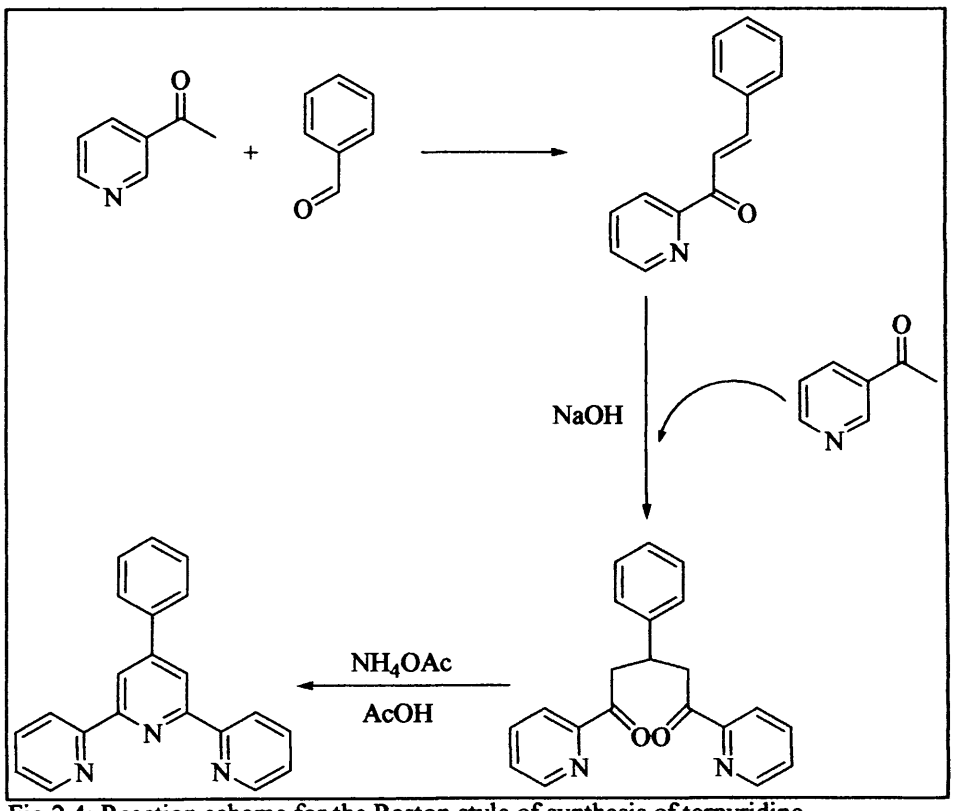

Fig.2.4: Reaction scheme for the Raston style of synthesis of terpyridine

The synthesis of unsubstituted terpyridine, however, requires a different method. Jameson and Guise[5] have described a two step procedure based on a variation of the Potts stratergy.[6] By synthesis of a 1,5-enedione, which is accompanied by the loss of dimethyl amine, ring closure yields terpyridine (see Fig.2.5). Unfortunately, it is a time-consuming difficult procedure, but the most efficient that is available.

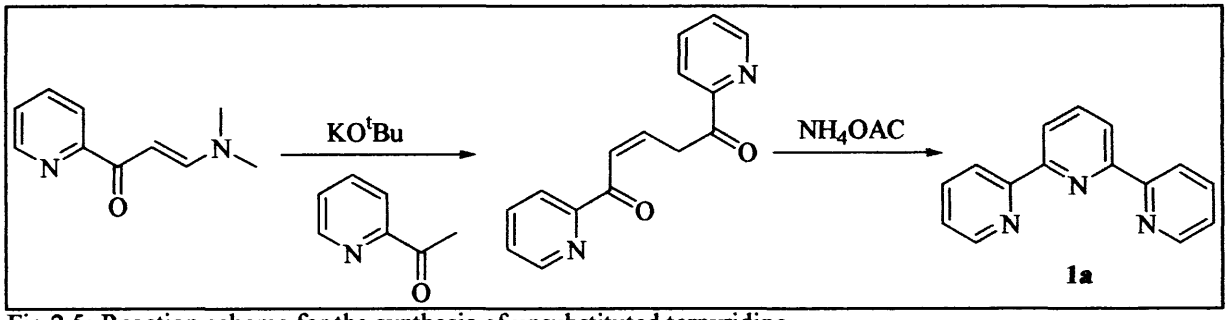

Fig.2.5: Reaction scheme for the synthesis of unsubstituted terpyridine

2.3 N-Oxides

The introduction of N-oxides to chelating lanthanide ligands has been shown to increase quantum yields and to produce longer lifetimes.[7] These findings have been ascribed to more efficient ligand-to-metal energy-transfers and to less efficient non-radiative relaxation processes, perhaps contributed to by the closer approach allowed to the coordinated lanthanide(III) ions by the N-oxide.[8] The N-oxides have also been shown to improve the shielding capability of chelating ligands, with the O sites blocking the face of macrobicyclic structures, thereby preventing the approach of water molecules to the metal ion.[9]

When designing ligands that utilise N-oxides as donors the ring substituents must be taken into account. The N-oxides as donors can be "tuned" to be harder or softer by altering the substituents on the ring, in which, the oxygen 2π electrons interact directly with the ring meaning that the extent of the interaction will depend on the substituents present on the ring. Electron withdrawing groups in the ortho and para positions in the ring enhance the N-O double bond character whilst electron donating substituents favour the single bond character.[10] Because of this the N-oxides can usually be identified by their characteristic N-O stretches at the 1250cm^{-1} region in I.R. spectroscopy. Also to be noted, the N-O bond lies in the same plane as the aromatic ring, due to the lone pair of the pyridyl ring lying in an sp^2 orbital.

There are numerous methods available in the literature for the preparation of N-oxides in heterocyclic chemistry. The large numbers of methods available reflects the important role that N-oxides play in organic synthesis and in applications outside

of those specified in this study. N-oxides have been applied to catalytic systems,[11] supramolecular systems,[12] pharmaceutical applications[13] and to organometallic systems.[14] The oxidation of pyridine to its N-oxide is usually perceived as a straight forward chemical transformation and is most often accomplished using a peracid, such as peracetic acid, mcpba or magnesium monoperphalate[15] and more recently $HOF.CH_3CN$ complex.[16] The peracid can also be generated *in situ* by use of 30-90% H_2O_2, but, although H_2O_2 is a readily available, cheap oxidising agent, dilute H_2O_2 is a weak oxidiser. For the production of N-oxides in electron poor pyridine ligand systems the presence of a catalyst is required.[17] The use of strongly oxidising 90% H_2O_2 also provides its own set of problems relating to the use of hazardous distilled peroxides and its use has been made redundant by an alternative safer, more practical method using trifluoroacetic acid and hydrogen peroxide-urea complex (UHP),[18] which can also oxidise difficult, electron poor pyridines to their N-oxide.

The pyridines being oxidised in this study are large chelating systems that generally have no other sites within the system that are readily oxidised, a factor that can be a problem in other ligand systems containing additional donors that may be readily oxidised. By use of methods that can be generalised into selective and non-selective oxidation methods, various N-oxide chelates can be selectively synthesised. The use of large, sterically hindered oxidising agents such as mcpba has allowed the selective oxidation of the oligopyridines used in this study whilst the use of non-selective methods, such as UHP complex and trifluoroacetic acid, results in the exhaustive oxidation of the oligopyridines.

2.4 N-Oxides of 2,2':6',2''-Terpyridine

Terpyridine tris-oxide was first synthesised by Case in 1962 via a non-selective method involving the generation of peroxyacetic acid *in situ* by the addition of excess H_2O_2 (30 vol.) to glacial acetic acid.[19] By refluxing the mixture for 18 hours the tris-oxide can be obtained in 88% yield with a simple purification method of precipitating the ligand from solution by the addition of excess acetone. This method continues to be applied today due to its inexpensive and simple methodology but has the drawback of lacking any means to perform selective oxidations. The methodology can also be applied to derivatives of terpyridine, which have been functionalised in the 4' position with a phenyl group.

The selective strategy for the synthesis of terpyridine mono and bis oxides is based upon the steric preferences of the oxidising agent. By utilising a bulky oxidant such as mcpba, the two peripheral pyridyl rings are preferentially oxidised first.[20] The use of a 2:1 stoichiometric amount of mcpba in DCM at ambient temperature after stirring overnight will yield the bis-oxide in 78% yield whilst a 1:1 stoichiometric amount leads to the mono-oxide in a 28% yield. A simple washing process with acetone can then purify the products. A side product of the 1:1 stoichiometric reaction is a small amount of the bis-oxide, which can be separated from the mono-oxide product by column chromatography on alumina. Use of an excess amount of mcpba will continue to yield the bis-oxide; the steric hindrance of the mcpba prohibits the complete oxidation of the ligand to give the tris oxide.

The reaction scheme for the preparation of the terpyridines is shown in Fig.2.6.

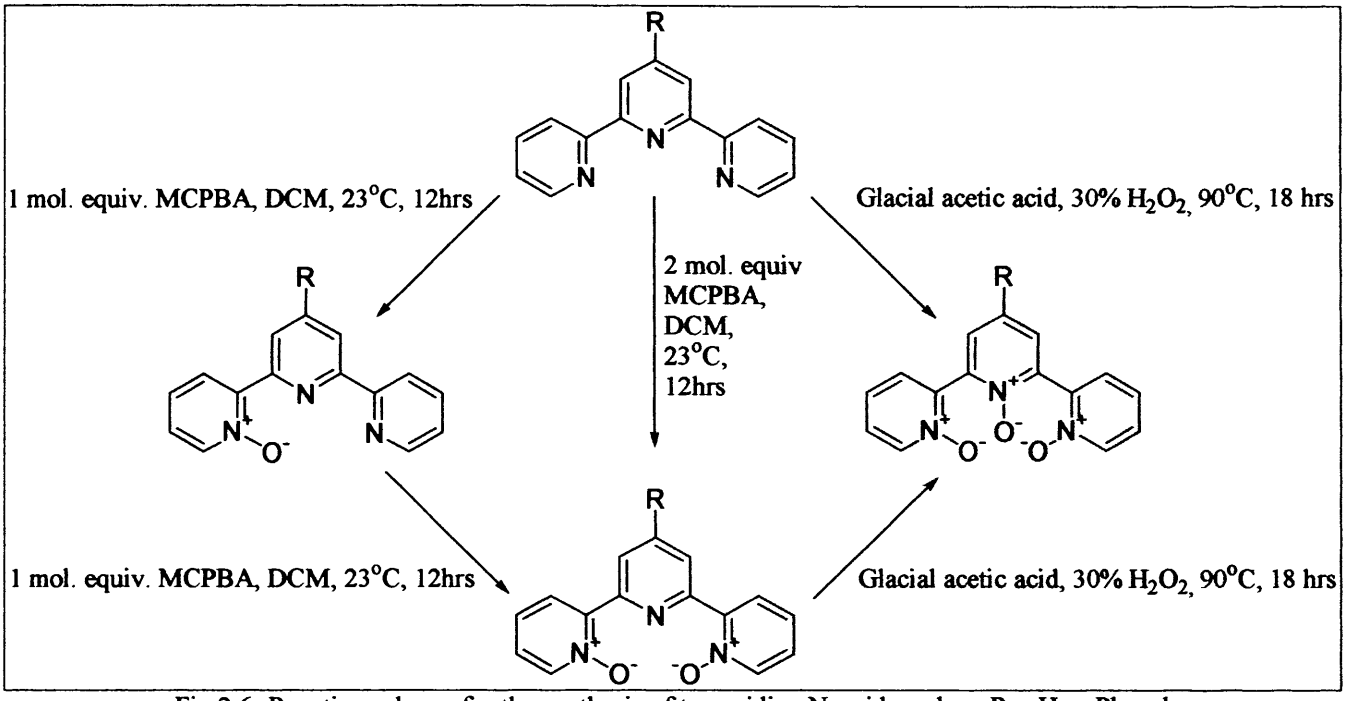

Fig.2.6: Reaction scheme for the synthesis of terpyridine N-oxides where R = H or Phenyl

The I.R. spectra for the three ligands reveal characteristic stretches appearing at 1261, 1235 and 1207cm^{-1} for the mono-oxide, 1259, 1227 and 1211cm^{-1} for the bis-oxide and 1273 and 1247cm^{-1} for the tris N-oxide. The mass spectra show the respective parent ions along with subsequent fragmentation products due to a loss of 1, 2 and 3 oxygen atoms dependent on the N-oxide. The ^{1}H-NMR has been extensively discussed by both Thummel[2] and our research group in previous work,[1] so only the main points of interest shall be discussed here. The ^{1}H-NMR shifts in aprotic solvent show significant chemical shifts when compared to the un-oxidised parent terpyridine ligand. These shifts can be explained by reviewing the canonical forms exhibited by N-oxides (See Fig.2.7).

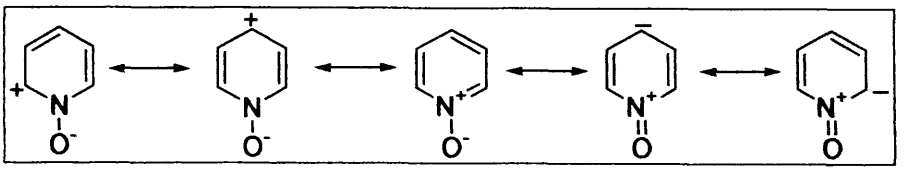

Fig.2.7: The canonical forms of pyridine N-oxide

Dependant on the functionalities present on the ring, there is a tendency for the protons in the ortho and para positions to undergo shifts to a lower frequency than those observed in the parent heterocyclic ring. The meta positions may also undergo a similar shift but to a lesser extent, or may even be observed to undergo shifts to higher frequencies.

The observed chemical shifts of the three N-oxides synthesised and the parent terpyridine ligand are given in Tables 2.1 and 2.2. By reviewing the data large differences between the shifts of the H3 and H3' protons may be noted, which provides a useful method of characterisation.

Compound	H3	H4	H5	H6	H3'	H4'
Terpyridine (**1a**)	8.58	7.82	7.30	8.65	8.41	7.93
Terpyridine-bis-oxide (**3a**)	8.20	7.35	7.35	8.35	8.94	7.98
Terpyridine-tris-oxide (**4a**)	7.67	7.28	7.28	8.27	7.72	7.37

Table 2.1: Chemical shifts for proton resonances of the terpyridines in ppm ($CDCl_3$)

Compound	H3	H4	H5	H6	H3'	H4'	H5'	H3''	H4''	H5''	H6''
Terpyridine-mono-oxide (**2a**)	8.34	7.32	7.32	8.34	9.00	7.95	8.47	8.47	7.81	7.32	8.68

Table 2.2: Chemical shifts for proton resonances of the terpyridine-mono-oxide in ppm ($CDCl_3$)

For the bis-oxide, a shift of ~0.5 ppm to a higher frequency of H3' can be observed. This shift is explained by the proximity of the N-O bond on the adjacent ring to the H3' proton. In solution the ligand will be in a transoid conformation so that H3' will be close enough in space to the δ^- oxygen of the N-O function to cause deshielding of the H3' proton. This shift is not observed in the tris-oxide due to the steric hindrance and electronic effects of the polar N-oxide groups of the ligand which do not allow the oxygen atom and the H3' proton to come within close proximity.

This proximity effect of the N-oxide on the H3' proton can be highlighted by the mono-oxide. In the mono-oxide, H3' undergoes a deviation of 0.53 ppm to a higher energy whist H5', which has no adjacent N-oxides, only moves by 0.01 ppm.

2.5 N-Oxides of 4',4''-diphenyl-2,2':6',2'':6'',2'''-Quaterpyridine

The synthesis of quaterpyridine-tetra-N-oxide requires a more potent non-selective methodology than that used for the terpyridines. Use of 30% H_2O_2 and glacial acetic acid yields a reaction mixture of unreacted quaterpyridine and oxidised products that prove hard to separate. Therefore, the trifluoroperoxyacetic acid procedure using UHP and trifluoroacetic acid was applied. The procedure typically involves the formation of trifluoroperoxy acid, formed by the dropwise addition of trifluoroacetic anhydride to a stirring solution of the urea adduct at 0°C. Stirring is continued at 0°C for 30 minutes to ensure formation of the peroxy acid and after this time the quaterpyridine is added and the mixture heated to 50°C. Yields for this reaction lie in the range of 35-45%.

Similar to the terpyridines, the addition of two stoichiometric equivalents of mcpba in DCM to quaterpyridine allows the synthesis of the bis-oxide in 96% yield. Interestingly though, the mono- and tris-N-oxides cannot be obtained by use this selective method with the reaction products containing a mixture of un-reacted quaterpyridine and its bis-oxide.

The reaction scheme for these reactions is shown in Fig. 2.8.

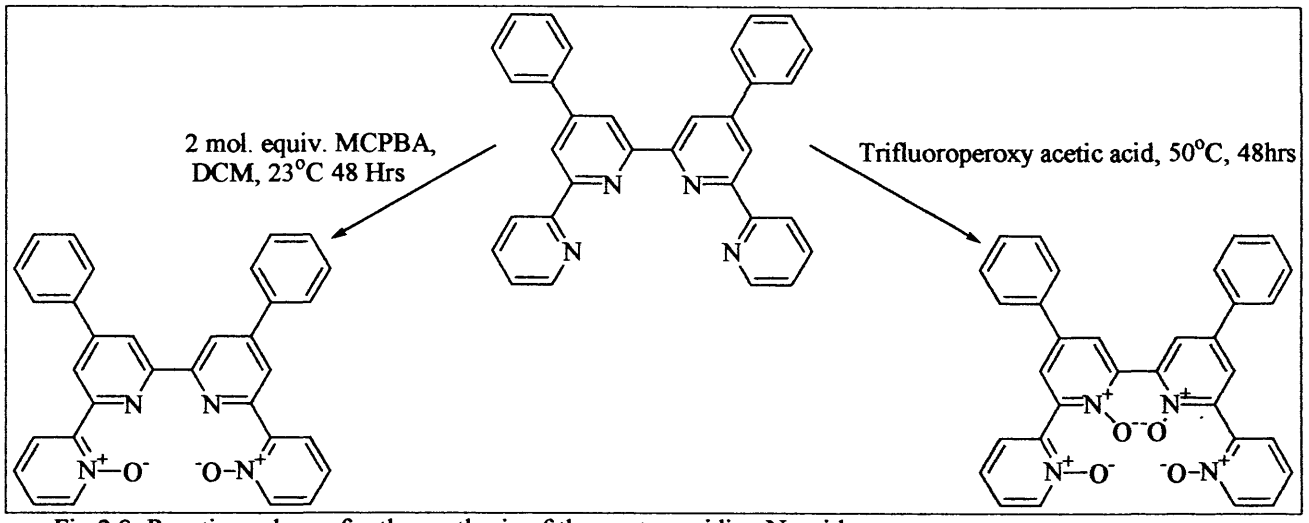

Fig.2.8: Reaction scheme for the synthesis of the quaterpyridine N-oxides

Analogously to the terpyridines, the quaterpyridine N-oxides show characteristic IR and MS trends. The characteristic stretches occur at 1277, 1255 and 1223cm^{-1} in the bis-oxide and 1261 and 1230cm^{-1} for the tetra-oxide. The mass spectra reveal the parent ions with fragmentation products due to the loss of the respective amount of oxygen. The ^{1}H-NMRs in $CDCl_3$ (see table 3) show the same characteristics as those found for the terpyridines with the distinctive shifts in protons H3' and H5' present.

Compound	H3	H4	H5	H6	H3'	H_O	H_M	H_P	H5'
PhQuater (**5a**)	8.69	7.90	7.34	8.69	8.89	7.90	7.51	7.45	8.74
PhQuaterO_2 (**6a**)	8.35-8.30	7.45-7.39	7.26	8.35-8.30	9.23	7.79	7.48-7.39	7.48-7.39	8.75
PhQuaterO_4 (**7a**)	7.69	7.34-7.39	7.26	8.29	8.05	7.59	7.34-7.39	7.34-7.39	7.90

Table 2.3: Chemical shifts for proton resonances of the quaterpyridines in ppm ($CDCl_3$)

2.6 N-Oxides of 4',4'''-(4-isopropyphenyl)-2,2':6',2'':6'',2''':6''',2'''':6'''',2''''-Quinquepyridine

Attempted synthesis of the penta-N-oxide has to date been unsuccessful. By use of extended reaction times and more forcing reaction conditions using the trifluoracetic acid methodology the desired N-oxide product has not been obtained. The more potent oxidation method using FOH/CH_3CN could be attempted but specialist equipment for the use of fluorine gas would be required.[21]

The bis-N-oxide can be synthesised, analogously to the ter- and quarterpyridines, by use of a 2:1 stoichiometric equivalents of mcpba at room temperature to give the product in 42% yield (see Fig.2.9). Similarly to quarterpyridine, the selective mcpba methodology is unable to produce mono-, tris- or tetra N-oxides.

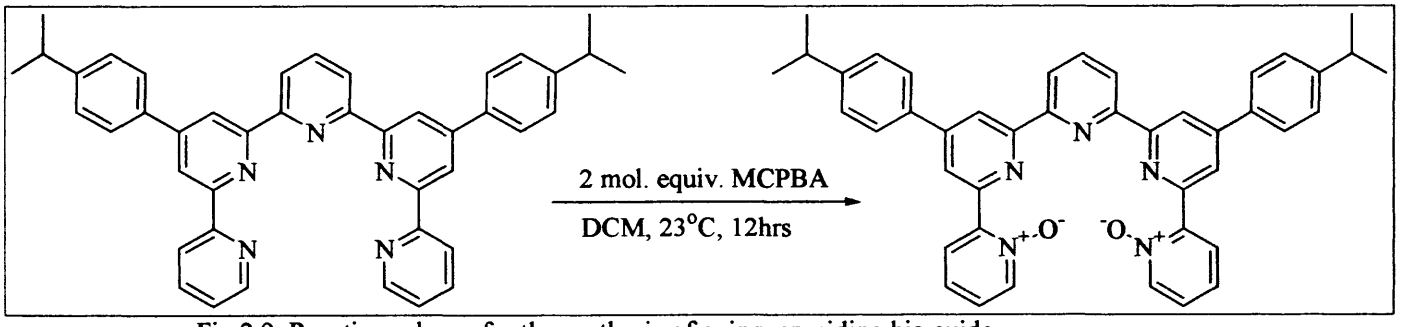

Fig.2.9: Reaction scheme for the synthesis of quinquepyridine-bis-oxide

The IR spectrum of the bis-oxide shows the characteristic stretches at 1281, 1271 and 1230cm^{-1} and the mass spectrum shows the parent ion along with the fragmentation ions due to the loss of one and two oxygens. The ^{1}H-NMR, as expected, revealed the same defining properties as that of the ter- and quarter-N-

oxides with the H3' proton undergoing the proximity effect caused by the N-oxide in the N1 position (see table 2.4).

Compound	H3	H4	H5	H6	H3'	H_O	H_M	H5'	H3''	H4''	H_{iso}	H_{CH3}
4-^{iS}Pr-PhQuinque (**8**)	8.69	7.86	7.31	8.95	8.69	7.86	7.36	8.69	8.62	8.01	2.96	1.28
4-^{iS}Pr-PhQuinqueO_2 (**9**)	8.54	7.27	7.40	8.34	8.94	7.79	7.35	9.26	8.40	7.95	2.95	1.26

Table 2.4: Chemical shifts for proton resonances of the quinquepyridines in ppm ($CDCl_3$)

2.7 Europium and Terbium Terpyridine N-Oxide Complexes

The Europium (III) and Terbium (III) complexes obtained and discussed here illustrate changes in the co-ordination preferences of the ligands and also their effect on their luminescent properties. The steric strain of the ligands with an increasing number of N-oxide donors shall be illustrated by observation of the solid state structures of the complexes.

$[M(terpyO)_3][ClO_4]_3$ and $[M(PhterpyO)_3][ClO_4]_3$ (where M= Eu or Tb)

The complexes were synthesised by the addition of either Eu(III) or Tb(III) perchlorate in the minimum amount of ethanol to a three-fold excess of the ligand also in the minimum amount of ethanol at room temperature. The white complex precipitates out shortly after the addition of the lanthanide perchlorate in a 60-80% yield and is filtered and dried. IR spectra of the four complexes are very similar, showing the presence of absorption bands characteristic of the pyridine moiety ($\nu_{C=C}$ and $\nu_{C=N}$ around 1598 and 1575cm^{-1}). The perchlorate counter ion is observed as a very strong broad band at 1087cm^{-1} and the co-ordination of the metal centre is indicated to be via the N-O oxygen atom. The N-O absorption is observed at 1261, 1235 and 1207cm^{-1} in the terpyO free ligand but once complexed a weakening of the N-O bond is apparent with a shift of the peaks to 1235 and 1216cm^{-1} with one of the peaks not being observed. A similar observation is made with the PhterpyO ligand. The ^{1}H-NMR spectrum of the $[Eu(terpyO)_3][ClO_4]_3$ complex in CD_3CN displays 33 peaks between 13 and –11 ppm and the data is consistent with the solid state structure suggesting that the solution structure is very similar to the solid state structure. The

^{1}H-NMR spectrum of the $[Tb(terpyO)_3][ClO_4]_3$ complex was unable to be obtained due to the paramagnetic broadening caused by the Tb(III) ion. The FAB^+/MS mass spectrum (NOBA matrix) of all complexes yields the parent ions for the complexes and suitable fragmentation patterns. Both NMR and MS data unambiguously point to the presence of a single species in solution, with a 1:3 metal:ligand stoichiometry.

$[M(terpyO_2)_3][ClO_4]_3$ and $[M(PhterpyO_2)_3][ClO_4]_3$ (where M=Eu or Tb)

Similar to the mono-oxide, the complexes were synthesised by the addition of either Eu(III) or Tb(III) perchlorate in the minimum amount of ethanol to a three-fold excess of the ligand also in the minimum amount of ethanol at room temperature. The white complex precipitates out shortly after the addition of the lanthanide perchlorate in a 67-69% yield and is filtered and dried. IR spectra of the four complexes are very similar, showing the presence of absorption bands characteristic of the pyridine moiety ($\nu_{C=C}$ and $\nu_{C=N}$ around 1595 and 1575cm^{-1}). The perchlorate counter ion is observed as a very strong broad band at 1090cm^{-1} and the co-ordination of the metal centre is indicated to be via the N-O oxygen atom. The N-O absorption is observed at 1259, 1227 and 1211cm^{-1} in the $terpyO_2$ free ligand but once complexed a weakening of the N-O bond is apparent with a shift of the peaks to 1276, 1230 and 1215cm^{-1}. A similar observation is made with the PhterpyO ligand. The ^{1}H-NMR spectrum of the $[Eu(terpyO_2)_3][ClO_4]_3$ complex in CD_3CN displays 6 peaks between 10 and 5.5 ppm, inconsistent with the solid state structure data. If the complex was in a distorted monocapped square antiprism geometry in solution, non-equivalency of the protons would lead to thirty-three peaks being observed in the ^{1}H-NMR. This would suggest that the solution structure undergoes some fluxtionality of the geometry allowing the

tricapped trigonal prism geometry to be adopted and so only six peaks are observed in the ^{1}H-NMR. The FAB$^+$/MS mass spectrum (NOBA matrix) of all complexes yields the parent ions for the complexes and suitable fragmentation patterns. Both NMR and MS data point to the presence of a single species in solution or two with very fast interconversion rate, with a 1:3 metal:ligand stoichiometry.

$[Eu(terpyO_3)_3][ClO_4]_3$ and $[Eu(PhterpyO_3)_3][ClO_4]_3$

The tris-oxide ligand forms a fine suspension in ethanol due to its decreased solubility but the complexes were still synthesised by the addition of either Eu(III) or Tb(III) perchlorate in the minimum amount of ethanol to a three-fold excess of the ligand also in the minimum amount of ethanol at room temperature. The mixture was left to stir for longer than the mono- and bis-oxide with the white complex forming after stirring for 1 hour in a 96% yield. The Tb complex of the $terpyO_3$ complex has not yet been successfully synthesised despite numerous repeated attempts using longer reaction times and more vigorous conditions. IR spectra of the two europium complexes are very similar, showing the presence of absorption bands characteristic of the pyridine moiety ($\nu_{C=C}$ and $\nu_{C=N}$ around 1595 and 1575cm^{-1}). The perchlorate counter ion is observed as a very strong broad band at 1090cm^{-1} and the co-ordination of the metal centre is once again indicated to be via the N-O oxygen atom but with an interesting anomaly. The N-O absorption is observed at 1273 and 1247cm^{-1} in the $terpyO_3$ free ligand but once complexed three peaks can be observed at 1278(s), 1233(s) and 1211(m) cm^{-1}. The strong band at 1278cm-1 which is observed to be quite weak in the mono- and bis-oxides can perhaps be attributed to the fact the complex is eight co-ordinate whilst the other complexes are nine co-ordinate. The

uncoordinated N-O pendant arm is not weakened from being co-ordinated so gives this stronger absorption. A similar observation is made with the PhterpyO ligand. The ^{1}H-NMR spectrum of the $[Eu(terpyO_3)_3][ClO_4]_3$ complex in CD_3CN displays very broad peaks (0.5-1 ppm wide) between 10 to 0 ppm. The reasons for this are unclear, perhaps due to the fluxional processes involving the pendant donor or it may be due to a mixture of species in solution. The FAB^+/MS mass spectrum (NOBA matrix) of all complexes yield the parent ions for the complexes and suitable fragmentation patterns.

2.7.1 Crystal Structures of Eu(III) terpyridine N-oxides

Single crystals of the three Eu(III) terpy N-oxide complexes have previously been obtained by our research group.[1 and 22] The structural points of interest relevant to this study shall be discussed, however the structure of $Eu(terpyO_2)_3$ was originally described as having a tricapped trigonal prism geometry which was misinterpreted at the time and shall be rectified now.

Crystals of the three complexes were obtained by the diffusion of ether into an acetonitrile solution of the complex. The increasing number of N-oxide donors creates an increasing steric demand of the ligands and becomes apparent upon viewing the data. The bis- and mono-oxides are nine co-ordinate whilst the tris-oxide is eight coordinate.

The crystal structure for $[Eu(terpyO)_3][ClO_4]_3$ is shown in Fig.2.10. It is best described as a tricapped trigonal prism with the average bond length of the Eu-O bond being 2.3315Å and the Eu-N bonds varying from 2.580(2) to 2.691(2)Å. The structure is similar to the crystal structure of $[Eu(terpy)_3][ClO_4]_3$ which also has an approximate tricapped trigonal prism geometry but the Eu-N bond lengths do not have as pronounced a deviation, varying from 2.57-2.62Å. This difference is attributed to the steric influences induced by the mono-oxide ligand. The N-oxide bond is twisted out of plane with respect to the adjacent pyridyl which increases the volume of the mono-oxide system taken around the metal. This increased volume has the effect of forcing some of the donor atoms away from the metal centre slightly.

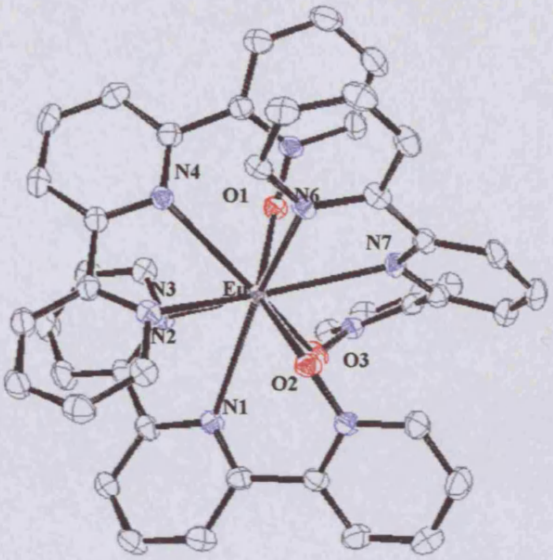

Fig.2.10: Crystal structure of $[Eu(terpyO)_3][ClO_4]_3$

The crystal structure of $[Eu(terpyO_2)_3][ClO_4]_3$ is shown in Fig.2.11 with selected bond lengths and angles given in Table 2.5. Unlike the mono-oxide, the complex contains a distorted monocapped square antiprism of donor atoms. The Eu-O bond lengths are similar to that of the mono-oxide complex but the Eu-N bond lengths are longer than those observed for the mono-oxide (average 2.752(8)Å). The co-ordination geometry resembles that of the closely related tricapped trigonal prism, however, the large O2-Eu-O4 bond angles (~110°) force O2 and O4 apart, breaking an edge of what would otherwise be the trigonal prism leading to the formation of a monocapped square antiprism.

Examples of other N_3O_6 donor set europium complexes are described by Piguet and Bunzli with the co-ordination of lanthanide ions with pyridine-2,6-diamide ligands[23] and related podands with the three pyridine diamide groups linked via a central tren moiety.[24] The characterised complexes were found to have pseudo-

tricapped trigonal prismatic geometries and it is clear from looking at the literature that the tricapped trigonal prism is the typical geometry adopted when three tri-dentate ligands are co-ordinated to a lanthanide but this variation represents only a minor distortion of this geometry and perhaps reflects the increasing steric demands of the bis-oxide.

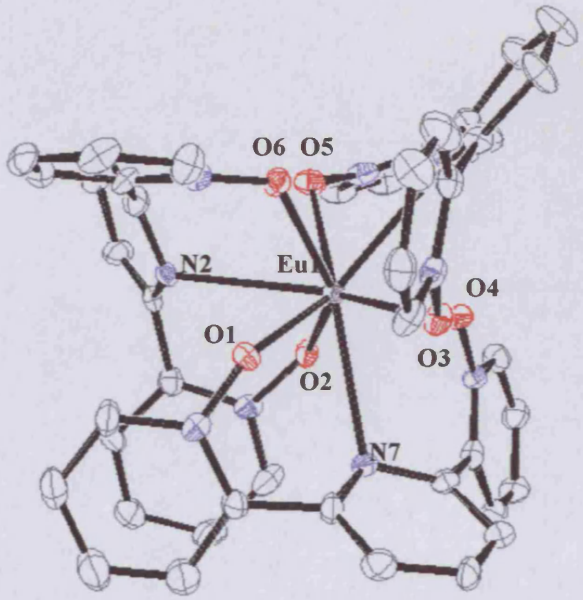

Fig.2.11: Crystal structure of $[Eu(terpyO_2)_3][ClO_4]_3$

Table 2.5: Selected bond lengths (Å) and bond angles (°).

Eu(1)-O(1)	2.353(5)	Eu(1)-N(2)	2.792(6)
Eu(1)-O(2)	2.362(6)	Eu(1)-N(5)	2.769(6)
Eu(1)-O(3)	2.354(6)	Eu(1)-N(7)	3.168(7)
Eu(1)-O(4)	2.385(6)	Eu(1)-N(8)	1.341(9)
Eu(1)-O(5)	2.346(6)	Eu(1)-N(9)	1.313(9)
Eu(1)-O(6)	2.340(5)		
O(1)-N(1)	1.328(9)	O(4)-N(6)	1.330(9)
O(2)-N(3)	1.327(10)	O(5)-N(7)	1.341(9)
O(3)-N(4)	1.324(8)	O(6)-N(7)	1.313(9)
O(6)-Eu(1)-O(5)	132.1(2)	O(4)-Eu(1)-N(7)	155.03(17)
O(6)-Eu(1)-O(1)	90.5(2)	O(1)-Eu(1)-N(5)	138.7 (2)
O(5)-Eu(1)-O(1)	72.6(2)	O(2)-Eu(1)-N(5)	70.73(19)
O(6)-Eu(1)-O(3)	73.3(2)	O(3)-Eu(1)-N(5)	73.0(2)
O(5)-Eu(1)-O(3)	87.9(2)	O(4)-Eu(1)-N(5)	69.73(19)
O(1)-Eu(1)-O(3)	135.4(2)	O(5)-Eu(1)-N(5)	147.8(2)
O(6)-Eu(1)-O(2)	131.28(18)	O(6)-Eu(1)-N(5)	67.47(19)
O(5)-Eu(1)-O(2)	78.8(2)	N(8)-Eu(1)-N(5)	124.78(19)
O(2)-Eu(1)-O(2)	138.13(18)	O(5)-Eu(1)-N(2)	69.8(2)
O(3)-Eu(1)-O(2)	71.5(19)	O(2)-Eu(1)-N(2)	72.56(19)
O(6)-Eu(1)-O(4)	77.5(2)	O(3)-Eu(1)-N(2)	137.7(2)
O(5)-Eu(1)-O(4)	132.91(19)	O(2)-Eu(1)-N(2)	69.19(19)

O(1)-Eu(1)-O(4)	71.65(19)	O(4)-Eu(1)-N(2)	71.0(2)
O(3)-Eu(1)-O(4)	139.16(18)	O(4)-Eu(1)-N(2)	147.6(2)
O(2)-Eu(1)-O(4)	110.1(2)	N(5)-Eu(1)-N(2)	107.4(2)
O(6)-Eu(1)-N(8)	65.9(2)	N(8)-Eu(1)-N(2)	127.8(2)
O(5)-Eu(1)-N(8)	66.2(2)	O(1)-Eu(1)-N(9)	68.53(19)
O(1)-Eu(1)-N(8)	68.7(2)	O(2)-Eu(1)-N(9)	152.96(18)
O(3)-Eu(1)-N(8)	66.7(2)	O(3)-Eu(1)-N(9)	91.22(19)
O(2)-Eu(1)-N(8)	125.3(2)	O(4)-Eu(1)-N(9)	69.5(2)
O(4)-Eu(1)-N(8)	124.6(2)	O(5)-Eu(1)-N(9)	122.4(2)
O(6)-Eu(1)-N(7)	121.8(2)	O(6)-Eu(1)-N(9)	22.06(18)
O(5)-Eu(1)-N(7)	22.41(18)	N(5)-Eu(1)-N(9)	84.59(19)
O(1)-Eu(1)-N(7)	91.18(19)	N(2)-Eu(1)-N(9)	131.1(2)
O(3)-Eu(1)-N(7)	65.62(18)	N(8)-Eu(1)-N(9)	60.9(2)
O(2)-Eu(1)-N(7)	70.57(19)		

The crystal structure for $[Eu(terpyO_3)_3][ClO_4]_3$ is shown in Fig.2.12. The structure is 8 co-ordinate with one pendant pyridine-N-oxide donor. The structure was assigned to be between cubic and square anti-prismatic with no obvious geometry able to be assigned. The Eu-O and Eu-N bonds are comparable to those already observed although the Eu-O lengths show a greater variance compared to the previous two structures. This reduced co-ordination number highlights the increasing steric hindrance felt with the increasing numbers of N-oxide donors. The role this plays in the stability of the complex is highlighted in the luminescence studies discussed later in the chapter.

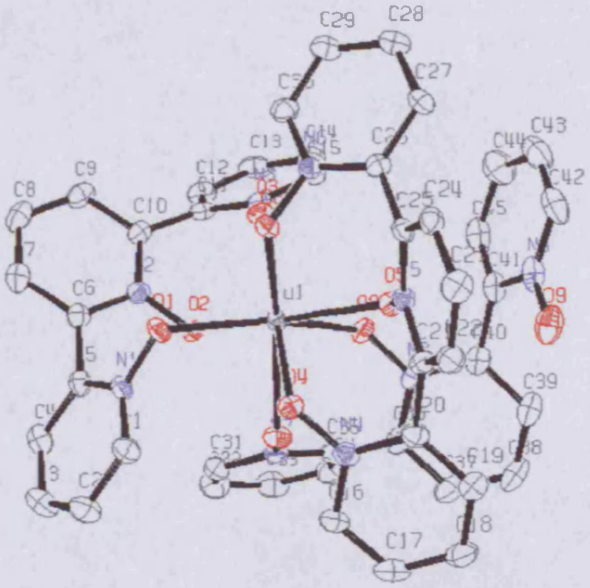

Fig.2.12: Crystal structure of $[Eu(terpyO_3)_3][ClO_4]_3$

2.7.2 Crystal Structures of Tb(III) terpyridine N-oxides

Single crystals of the mono- and bis-oxide Tb complexes were obtained by the diffusion of ether into an acetonitrile solution of the complex. The results of the X-ray data show analogous structures to the Eu(III)terpyridine N-oxides with both containing the nine co-ordinate metal centre and the increasing steric demand with increasing number of N-oxide donors in evidence.

$[Tb(terpyO)_3][ClO_4]_3$

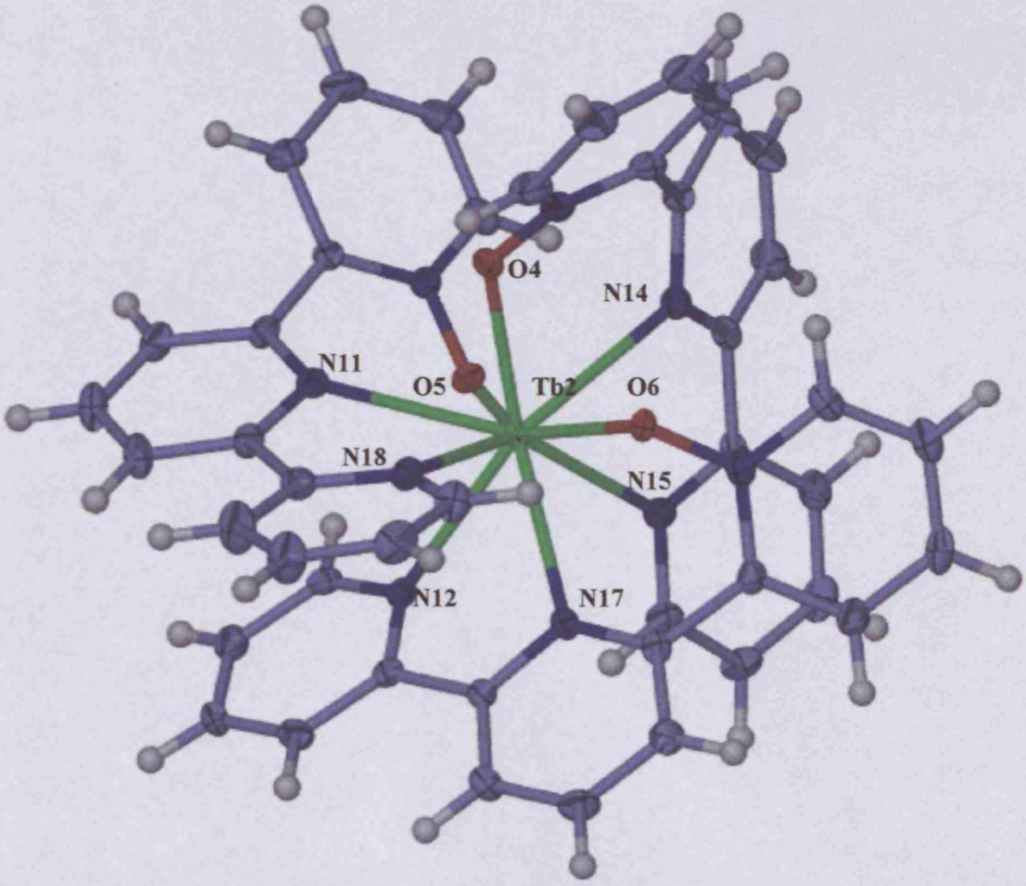

Fig.2.13: Crystal structure of $[Tb(terpyO)_3][ClO_4]_3$

The $[Tb(terpyO)_3][ClO_4]_3$ complex crystallised in the triclinic P-1 space group and similarly to its Eu counterpart the complex adopts the nine co-ordinate tricapped trigonal prism coordination geometry. The unit cell is isostructural to the Eu(III) mono-oxide complex having two independent molecules present in the unit cell (see fig.2.14). The geometry can clearly be seen when only the metal core and coordinated heteroatoms are visible (see Fig.2.15).

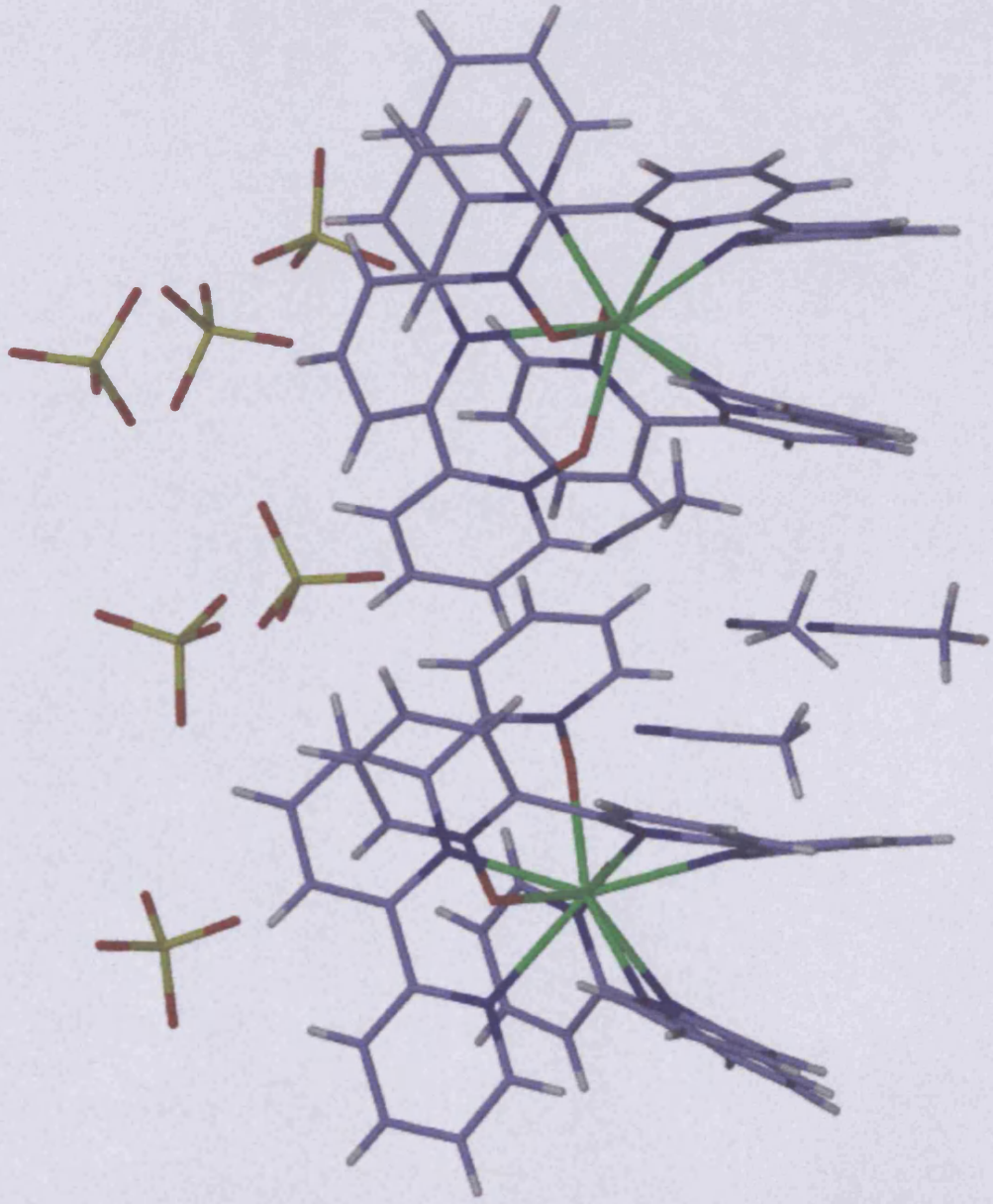

Fig.2.14: Unit cell of the $[Tb(terpyO)_3][ClO_4]_3$ complex

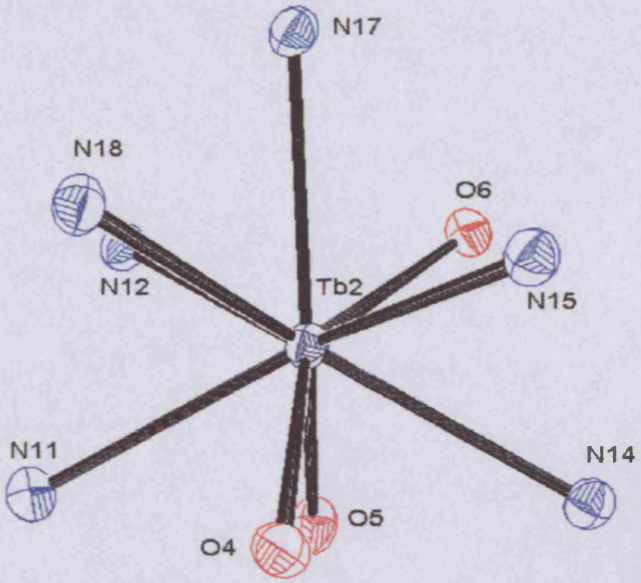

Fig.2.15: Ortep plot of the co-ordinated heteroatoms and metal core of the $[Tb(terpyO)_3][ClO_4]_3$ complex

Table 2.6: Selected bond lengths (Å) and bond angles (°).

O(1)-Tb(1)	2.313(3)	O(4)-Tb(2)	2.295(3)
O(2)-Tb(1)	2.278(3)	O(5)-Tb(2)	2.283(3)
O(3)-Tb(1)	2.321(3)	O(6)-Tb(2)	2.348(3)
N(2)-Tb(1)	2.589(4)	N(11)-Tb(2)	2.638(4)
N(3)-Tb(1)	2.598(4)	N(12)-Tb(2)	2.568(4)
N(5)-Tb(1)	2.691(4)	N(14)-Tb(2)	2.673(4)
N(6)-Tb(1)	2.589(4)	N(15)-Tb(2)	2.581(4)
N(8)-Tb(1)	2.622(4)	N(17)-Tb(2)	2.615(4)
N(9)-Tb(1)	2.564(4)	N(18)-Tb(2)	2.595(4)
N(1)-O(1)	1.344(5)	N(10)-O(4)	1.343(5)
N(4)-O(2)	1.335(5)	N(13)-O(5)	1.327(5)
N(7)-O(3)	1.339(5)	N(16)-O(6)	1.330(5)
O(2)-Tb(1)-O(1)	80.48(11)	O(5)-Tb(2)-O(4)	91.53(11)
O(2)-Tb(1)-O(3)	87.43(11)	O(5)-Tb(2)-O(6)	80.95(11)
O(1)-Tb(1)-O(3)	147.07(11)	O(4)-Tb(2)-O(6)	145.77(11)
O(2)-Tb(1)-N(9)	80.94(12)	O(5)-Tb(2)-N(12)	78.14(11)
O(1)-Tb(1)-N(9)	75.91(11)	O(4)-Tb(2)-N(12)	132.53(11)
O(3)-Tb(1)-N(9)	132.37(11)	O(6)-Tb(2)-N(12)	78.75(11)
O(2)-Tb(1)-N(2)	142.05(12)	O(5)-Tb(2)-N(15)	131.97(11)
O(1)-Tb(1)-N(2)	68.95(11)	O(4)-Tb(2)-N(15)	73.15(11)
O(3)-Tb(1)-N(2)	130.30(11)	O(6)-Tb(2)-N(15)	87.22(11)
N(9)-Tb(1)-N(2)	70.46(11)	N(12)-Tb(2)-N(15)	144.40(11)
O(2)-Tb(1)-N(6)	131.08(11)	O(5)-Tb(2)-N(18)	138.15(11)
O(1)-Tb(1)-N(6)	91.37(11)	O(4)-Tb(2)-N(18)	76.88(11)
O(3)-Tb(1)-N(6)	73.78(11)	O(6)-Tb(2)-N(18)	129.35(11)
N(9)-Tb(1)-N(6)	143.65(11)	N(12)-Tb(2)-N(18)	80.80(12)
N(2)-Tb(1)-N(6)	73.19(11)	N(15)-Tb(2)-N(18)	83.35(12)
O(2)-Tb(1)-N(3)	136.98(11)	O(5)-Tb(2)-N(17)	139.14(12)
O(1)-Tb(1)-N(3)	130.65(11)	O(4)-Tb(2)-N(17)	128.99(11)
O(3)-Tb(1)-N(3)	77.59(11)	O(6)-Tb(2)-N(17)	68.13(11)
N(9)-Tb(1)-N(3)	80.21(12)	N(12)-Tb(2)-N(17)	70.35(11)
N(2)-Tb(1)-N(3)	62.50(11)	N(15)-Tb(2)-N(17)	74.06(11)
N(6)-Tb(1)-N(3)	83.10(11)	N(18)-Tb(2)-N(17)	61.41(12)
O(2)-Tb(1)-N(8)	67.75(11)	O(5)-Tb(2)-N(11)	68.06(11)
O(1)-Tb(1)-N(8)	130.73(11)	O(4)-Tb(2)-N(11)	69.86(11)
O(3)-Tb(1)-N(8)	69.78(11)	O(6)-Tb(2)-N(11)	134.50(11)
N(9)-Tb(1)-N(8)	63.03(11)	N(12)-Tb(2)-N(11)	63.26(12)
N(2)-Tb(1)-N(8)	116.73(11)	N(15)-Tb(2)-N(11)	138.28(11)
N(6)-Tb(1)-N(8)	137.89(11)	N(18)-Tb(2)-N(11)	70.20(11)

N(3)-Tb(1)-N(8)	69.23(11)	N(17)-Tb(2)-N(11)	116.45(11)
O(2)-Tb(1)-N(5)	68.53(11)	O(5)-Tb(2)-N(14)	68.84(11)
O(1)-Tb(1)-N(5)	72.70(11)	O(4)-Tb(2)-N(14)	74.18(11)
O(3)-Tb(1)-N(5)	74.36(11)	O(6)-Tb(2)-N(14)	71.95(11)
N(9)-Tb(1)-N(5)	139.02(11)	N(12)-Tb(2)-N(14)	138.47(11)
N(2)-Tb(1)-N(5)	119.71(11)	N(15)-Tb(2)-N(14)	63.23(11)
N(6)-Tb(1)-N(5)	63.03(11)	N(18)-Tb(2)-N(14)	140.72(11)
N(3)-Tb(1)-N(5)	140.71(11)	N(17)-Tb(2)-N(14)	121.75(11)
N(8)-Tb(1)-N(5)	123.55(11)	N(11)-Tb(2)-N(14)	121.80(11)

The Tb-O bond lengths are in the expected range of 2.283(3) to 2.348(3)Å with the Tb-N bond lengths experiencing a variation ranging from 2.568(4) to 2.673(4)Å. These observations are analogous to the Eu(III) mono-oxide complex already discussed reinforcing the evidence for the conformational strain introduced by the N-oxides. When considering the positioning of the three tridentate ligands to give the tricapped trigonal prism, two possibilities exist, similar to the $[Eu(terpyO)_3][ClO_4]_3$ complex (see Fig.2.16). In both possibilities, the central nitrogen donor of the ligand always provides the capping donor of the polyhedron. The arrangement can then be either in the most symmetrical manner with the ligands arranged with all three oxygen donors on one triangular face and all three nitrogen donors on the other triangular face (Fig.2.16a) or alternatively, the ligands may be arranged so that two oxygen donors are in one face and one oxygen in the other. The second arrangement, in fact, leads to two enantiomers (Fig.2.16b and 2.16c). Both isomers are observed in the crystal structure of $[Tb(terpyO)_3][ClO_4]_3$.

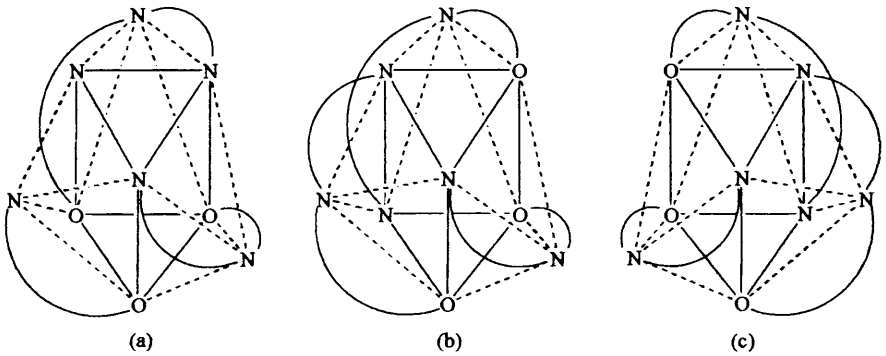

Fig.2.16: Possible arrangements of the three unsymmetrical tridentate ligands coordinating in a meridonal fashion.

$[Tb(terpyO_2)_3][ClO_4]_3$

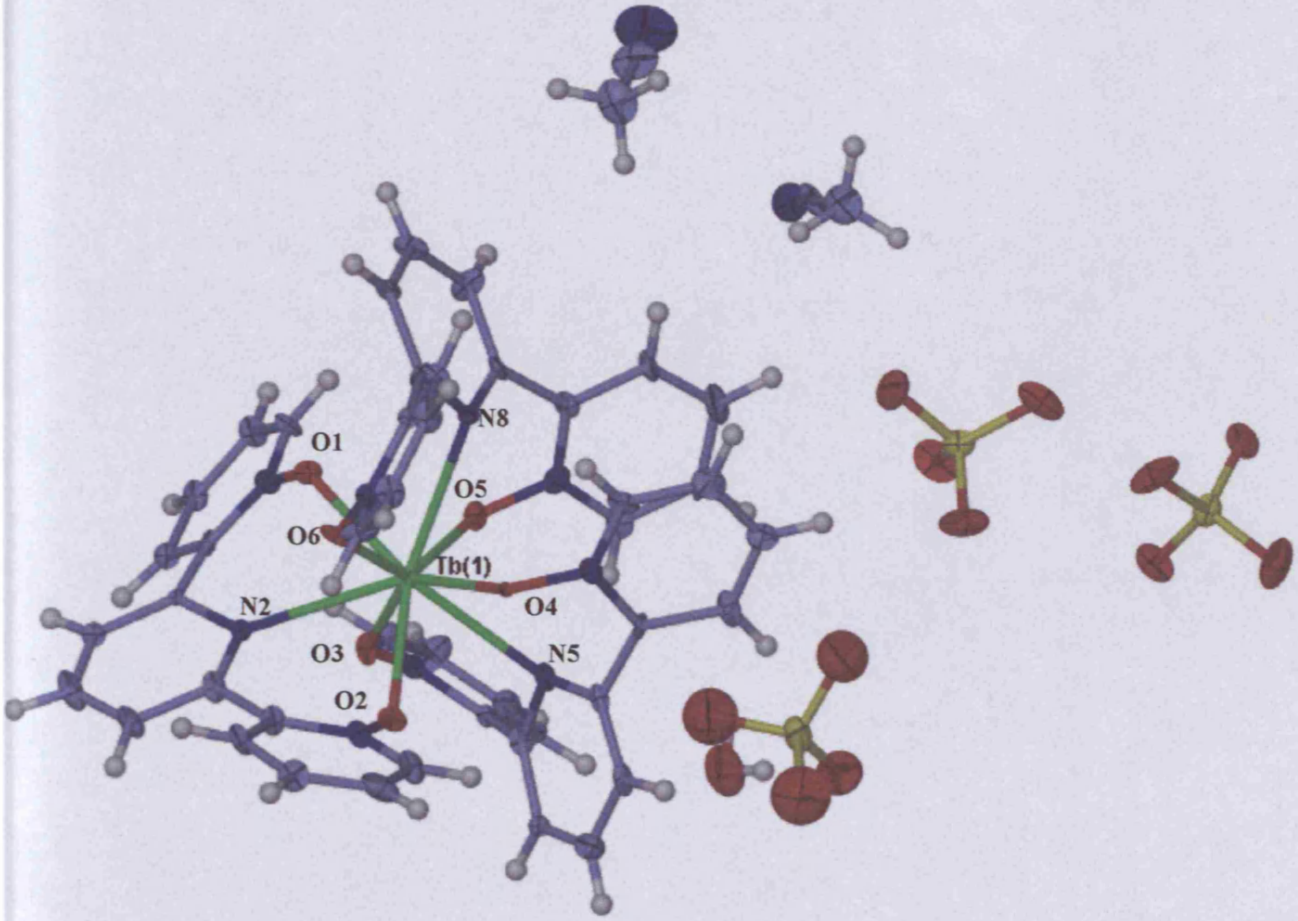

Fig.2.17: Crystal structure of $[Tb(terpyO_2)_3][ClO_4]_3$

The $[Tb(terpyO_2)_3][ClO_4]_3$ complex crystallised in the monoclinic C2/c space group and similar to its Eu(III) counterpart the complex adopts a distorted monocapped square antiprism geometry (see Fig.2.18). The Tb-N bond lengths are longer than those for the mono-oxide (average 2.746Å) and the Tb-O bond lengths are similar in length. These observations are analogous to the Eu(III) bis-oxide complex already discussed, once again exhibiting the increased steric strain induced by the N-oxides, forcing the geometry from the commonly occurring trigonal tricapped prism to the distorted monocapped square antiprism geometry.

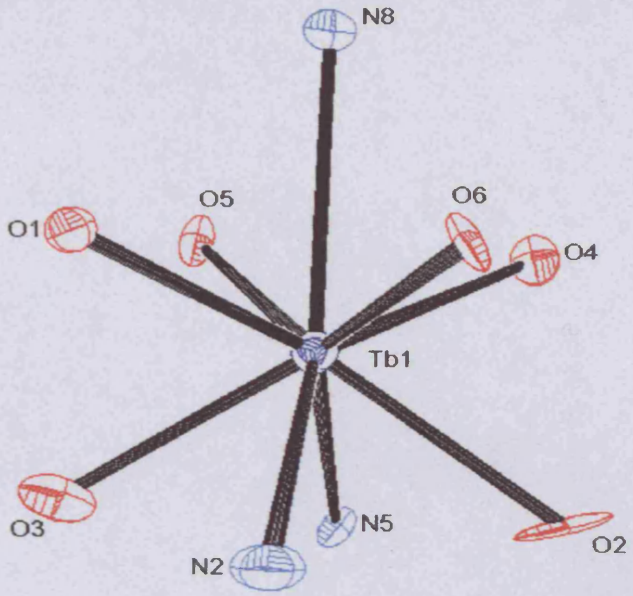

Fig.2.18: Ortep plot of the co-ordinated heteroatoms and metal core of the $[Tb(terpyO_2)_3][ClO_4]_3$ complex

Table 2.7: Selected bond lengths (Å) and bond angles (°).

O(1)-Tb(1)	2.336(13)	N(2)-Tb(1)	2.751(17)
O(2)-Tb(1)	2.345(13)	N(5)-Tb(1)	2.786(14)
O(3)-Tb(1)	2.318(14)	N(8)-Tb(1)	2.702(14)
O(4)-Tb(1)	2.353(14)		
O(5)-Tb(1)	2.328(13)		
O(6)-Tb(1)	2.313(13)		
N(1)-O(1)	1.30(2)	N(6)-O(4)	1.324(19)
N(3)-O(2)	1.352(18)	N(7)-O(5)	1.35(2)
N(4)-O(3)	1.38(2)	N(28)-O(6)	1.344(19)
O(6)-Tb(1)-O(3)	130.6(5)	O(1)-Tb(1)-N(8)	67.2(4)
O(6)-Tb(1)-O(5)	132.8(5)	O(2)-Tb(1)-N(8)	125.5(5)
O(3)-Tb(1)-O(5)	79.1(5)	O(4)-Tb(1)-N(8)	68.1(4)
O(6)-Tb(1)-O(1)	74.5(5)	O(6)-Tb(1)-N(2)	66.6(5)
O(3)-Tb(1)-O(1)	70.3(5)	O(3)-Tb(1)-N(2)	70.9(5)
O(5)-Tb(1)-O(1)	87.5(4)	O(5)-Tb(1)-N(2)	148.4(5)
O(6)-Tb(1)-O(2)	77.7(5)	O(1)-Tb(1)-N(2)	73.5(5)
O(3)-Tb(1)-O(2)	109.5(5)	O(2)-Tb(1)-N(2)	69.2(5)
O(5)-Tb(1)-O(2)	132.5(5)	O(4)-Tb(1)-N(2)	137.9(5)
O(1)-Tb(1)-O(2)	139.9(5)	N(8)-Tb(1)-N(2)	125.0(5)
O(6)-Tb(1)-O(4)	89.8(4)	O(6)-Tb(1)-N(5)	147.4(4)
O(3)-Tb(1)-O(4)	139.5(5)	O(3)-Tb(1)-N(5)	70.0(5)
O(5)-Tb(1)-O(4)	72.9(5)	O(5)-Tb(1)-N(5)	69.0(4)
O(1)-Tb(1)-O(4)	135.2(5)	O(1)-Tb(1)-N(5)	136.8(5)
O(2)-Tb(1)-O(4)	72.0(5)	O(2)-Tb(1)-N(5)	70.8(4)
O(6)-Tb(1)-N(8)	66.8(5)	O(4)-Tb(1)-N(5)	72.9(4)
O(3)-Tb(1)-N(8)	125.0(5)	N(8)-Tb(1)-N(5)	126.8(4)
O(5)-Tb(1)-N(8)	66.0(5)	N(2)-Tb(1)-N(5)	108.2(4)

2.8 Europium and Terbium Quaterpyridine Oxide Complexes

The only publication to date describing the coordination of lanthanides to quaterpyridine is a patent held by Toner and co-workers.[1] Toner recommended ligands such as 2,2':6',2'':6'',2'''quaterpyridine-6,6'''-dicarboxylic acid in the patent as suitable lanthanide sensors but detailed analysis of the complexes were not carried out and crystal structures of the complexes were not obtained. There is an obvious lack of research into the coordination and luminescent capabilities of lanthanide quaterpyridine complexes, which is investigated here. The Europium (III) and Terbium (III) complexes obtained and discussed here illustrate the co-ordination capabilities of the ligands.

$[M(4\text{-}^{is}Pr\text{-}Phquaterpyridine)_2(H_2O)][ClO_4]_3$ (where M= Eu or Tb)

The complexes were synthesised by the addition of either Eu(III) or Tb(III) perchlorate in the minimum amount of ethanol to a two-fold excess of the ligand also in the minimum amount of ethanol at room temperature. The white complex formed shortly after the addition of the lanthanide perchlorate and the complex was isolated by filtration with the yield determined to be 52% yield. The solid state structure (see Fig. 2.19) reveals a co-ordinated water which plays an important role in the geometry adopted by the complex. IR spectra of the two complexes complexes are very similar, showing the presence of absorption bands characteristic of the pyridine moiety ($\nu_{C=C}$ and $\nu_{C=N}$ around 1607 and 1574cm^{-1}). These absorptions have shifted from 1582 and 1535 cm-1 in the free ligand indicating a strengthening of the bonds in the aromatic ring. This is caused by co-ordination of the Eu(III) or Tb(III) ion via the nitrogens on

the pyridine rings. The perchlorate counter ion is observed as a very strong broad band at 1091cm^{-1}. The ^{1}H-NMR spectrum of the [Eu(4-^{is}Pr-Phquaterpyridine)$_2$(H_2O)][ClO_4]$_3$ complex in CD_3CN displays nine peaks (H_o and H_m being observed as a multiplet) with correct integrals for the proposed 2:1 ligand:metal structure suggesting that the two ligands are not only equivalent, but each ligand only has a two fold symmetry axis. The spectrum indicates coordination of the paramagnetic Eu(III) ion to the ligand due to the downfield shifts of all of the cavity surrounding protons, which appear in the range 5.49 to 3.45ppm. The external isopropyl groups feel no effect from the Eu(III) ion and appear at chemical shifts similar to that of the uncoordinated ligand. A water peak is also present at 2.58ppm and appears as a very sharp singlet. The ES/MS spectra do not give a straightforward parent ion peak or correlation of the fragmentations. Two peaks which do not originate from the matrix, appear at 1256 and 1320 m/z with correct isotope patterns for europium and at 1259 and 1319 m/z with correct isotope patterns for the terbium complex. The parent ion excluding perchlorates and water should appear at 1243m/z for Eu and 1250m/z for Tb. Peaks also appear at 547m/z representing fragmentation to give [ligand+H]$^+$.

[Eu(4-^{is}Pr-PhquaterpyridineO$_2$)$_2$][ClO_4]$_3$

The complex was synthesised by the addition of Eu(III) perchlorate in the minimum amount of ethanol to a two-fold excess of the ligand also in the minimum amount of ethanol at room temperature. The white complex precipitates out shortly after the addition of the lanthanide perchlorate, filtered, and was found to be in a 95% yield. Similarly to the non-oxidised complexes, the absorption bands characteristic

of the pyridine moiety ($\nu_{C=C}$ and $\nu_{C=N}$) are shifted to 1605 and 1548cm^{-1} indicating co-ordination via the nitrogens on the pyridine rings. The co-ordination of the metal centre is also indicated to be via the N-O oxygen atoms. The N-O absorptions are observed at 1277(s), 1255(w) and 1223(s) cm^{-1} in the free ligand but once complexed a weakening of the N-O bond is apparent with either a shift or weakening of the intensity of the peaks to 1278(w) and 1238(s)cm^{-1}. Once again the ES/MS spectra does not give a straightforward parent ion peak or correlation of the fragmentations. The parent ion $[M\text{-}ClO_4]^+$ should appear at 1339m/z. Peaks at m/z 989 (corresponding to LEu(NOBA Acid)+2EtOH) and 1011 (corresponding to LEu(NOBAOH)+$(ClO_4)_2$+H_2O) are present with correct Eu isotope patterns. Peaks also appear at 495m/z representing fragmentation to give $[ligand+H]^+$.

$[Eu(4\text{-}^{is}Pr\text{-}PhquaterpyridineO_4)_2][ClO_4]_3$

The complex was synthesised in an analogous fashion as described above in 60% yield. Similarly to the non-oxidised complexes the absorption bands characteristic of the pyridine moiety ($\nu_{C=C}$ and $\nu_{C=N}$) are shifted but to a greater amount to 1626 and 1569cm^{-1}. The co-ordination of the metal centre is indicated to be via the N-O oxygen atoms. The N-O absorption is observed at 1261(vs) and 1230(s) cm^{-1} in the free ligand but once complexed a weakening of the N-O bond is apparent with a shift and weakening of the intensity of the peaks to 1281(w), 1239(s) and 1223(s)cm^{-1}. Once again the ES/MS spectra does not give a straightforward parent ion peak or correlation of the fragmentations. Two peaks appear at 1419 (corresponding to M-(ClO_4)+O^-) and 1425 (corresponding to M-EtOH-2O^-) m/z whereas the parent ion should appear at 1502m/z. Peaks also appear at 527m/z representing fragmentation of the complex to $[ligand+H]^+$.

2.8.1 Crystal Structures of the Quartepyridine N-oxides

The crystal structure of $[Eu(4\text{-}^{is}Pr\text{-}PhenylQuaterpyridine)_2(H_2O)][ClO_4]_2$ has been obtained by the diffusion of ether into an acetonitrile solution of the complex. The crystal structures of Gd(III) quaterpyridine tetra-oxide and Tb(III)quaterpyridine bis-oxide have also previously been obtained by this research group[1] and shall be discussed due to their relevance to the study. The trend that has been observed for the terpyridine lanthanide complexes of the less N-oxide donors present, the higher the coordination number of the complex can also be seen here with the quaterpyridine complex being nine coordinate and the bis and tetra N-oxide complexes being eight coordinate.

$[Eu(4\text{-}^{is}Pr\text{-}PhenylQuaterpyridine)_2\ (H_2O)][ClO_4]_3$

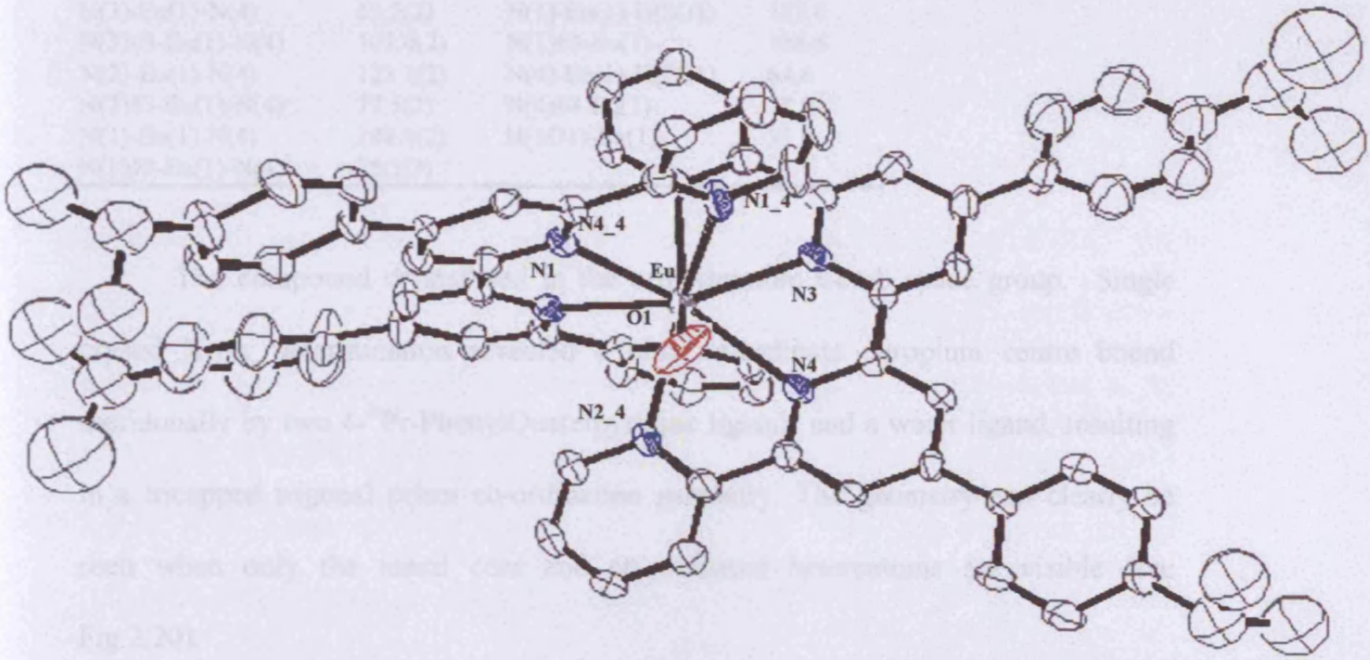

Fig.2.19: Crystal structure of $[Eu(4\text{-}^{is}Pr\text{-}PhenylQuaterpyridine)_2(H_2O)][ClO_4]_2$

Table 2.8: Selected bond lengths (Å) and bond angles (°).

N(1)-Eu(1)	2.588(7)	Eu(1)-N(3)#3	2.512(7)
N(2)-Eu(1)	2.529(7)	Eu(1)-N(2)#3	2.529(7)
N(3)-Eu(1)	2.512(7)	Eu(1)-N(1)#3	2.588(7)
N(4)-Eu(1)	2.609(8)	Eu(1)-N(4)#3	2.609(8)
O(1)-Eu(1)	2.477(11)	Eu(1)-H(1O1)	1.9659
Eu(1)-H(2O1)	2.4728		
O(1)-Eu(1)-N(3)	73.11(17)	O(1)-Eu(1)-N(4)#3	67.18(19
O(1)-Eu(1)-N(3)#3	73.11(17)	N(3)-Eu(1)-N(4)#3	103.0(2)
N(3)-Eu(1)-N(3)#3	146.2(3)	N(3)#3-Eu(1)-N(4)#3	63.2(2)
O(1)-Eu(1)-N(2)	115.13(17)	N(2)-Eu(1)-N(4)#3	77.5(2)
N(3)-Eu(1)-N(2)	64.1(2)	N(2)#3-Eu(1)-N(4)#3	123.1(2)
N(3)#3-Eu(1)-N(2)	133.1(2)	N(1)-Eu(1)-N(4)#3	75.3(3)
O(1)-Eu(1)-N(2)#3	115.13(17)	N(1)#3-Eu(1)-N(4)#3	148.9(2)
N(3)-Eu(1)-N(2)#3	133.1(2)	N(4)-Eu(1)-N(4)#3	134.4(4)
N(3)#3-Eu(1)-N(2)#3	64.1(2)	O(1)-Eu(1)-H(1O1)	18.2
N(2)-Eu(1)-N(2)#3	129.7(3)	N(3)-Eu(1)-H(1O1)	56.2
O(1)-Eu(1)-N(1)	141.08(17)	N(3)#3-Eu(1)-	90.2
N(3)-Eu(1)-N(1)	127.3(2)	N(2)-Eu(1)-H(1O1)	108.0
N(3)#3-Eu(1)-N(1)	81.1(2)	N(2)#3-Eu(1)-	119.8
N(2)-Eu(1)-N(1)	64.3(2)	N(1)-Eu(1)-H(1O1)	155.4
N(2)#3-Eu(1)-N(1)	76.9(2)	N(1)#3-Eu(1)-	124.6
O(1)-Eu(1)-N(1)#3	141.08(17)	N(4)-Eu(1)-H(1O1)	55.5
N(3)-Eu(1)-N(1)#3	81.1(2)	N(4)#3-Eu(1)-	80.2
N(3)#3-Eu(1)-N(1)#3	127.3(2)	O(1)-Eu(1)-H(2O1)	19.9
N(2)-Eu(1)-N(1)#3	76.9(2)	N(3)-Eu(1)-H(2O1)	89.7
N(2)#3-Eu(1)-N(1)#3	64.3(2)	N(3)#3-Eu(1)-	57.2
N(1)-Eu(1)-N(1)#3	77.8(3)	N(2)-Eu(1)-H(2O1)	134.1
O(1)-Eu(1)-N(4)	67.18(19)	N(2)#3-Eu(1)-	95.9
N(3)-Eu(1)-N(4)	63.2(2)	N(1)-Eu(1)-H(2O1)	135.5
N(3)#3-Eu(1)-N(4)	103.0(2)	N(1)#3-Eu(1)-	138.6
N(2)-Eu(1)-N(4)	123.1(2)	N(4)-Eu(1)-H(2O1)	64.6
N(2)#3-Eu(1)-N(4)	77.5(2)	N(4)#3-Eu(1)-	72.5
N(1)-Eu(1)-N(4)	148.9(2)	H(1O1)-Eu(1)-	33.6
N(1)#3-Eu(1)-N(4)	75.3(3)		

The compound crystallised in the orthorhombic Ccmb space group. Single crystal X-ray determination revealed a nine co-ordinate europium centre bound meridonally by two 4-^{is}Pr-PhenylQuaterpyridine ligands and a water ligand, resulting in a tricapped trigonal prism co-ordination geometry. The geometry can clearly be seen when only the metal core and co-ordinated heteroatoms are visible (see Fig.2.20).

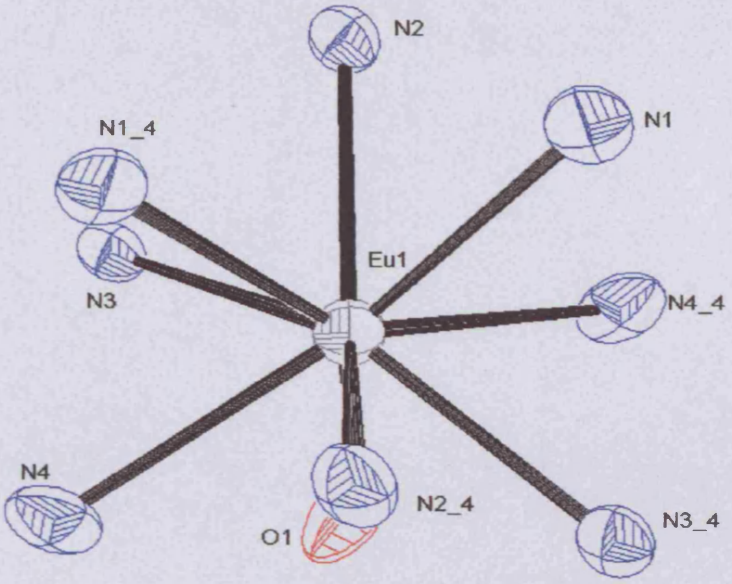

Fig.2.20: Ortep plot of the co-ordinated heteroatoms and metal core of the [Eu(4-^{is}Pr-PhenylQuaterpyridine)$_2$(H_2O)][ClO_4]$_2$ complex

A point of interest is the unexpected co-ordination of a water molecule to the Eu(III) centre. As opposed to the anticipated 8 co-ordinate complex this extra donor atom allows the formation of the commonly occurring nine co-ordinate tricapped trigonal prism geometry. The occupation of the ninth coordination site by an O-donor water molecule has been observed before by M. D. Ward and co-workers[25]. Crystal structures of dihydrobis[3-(2-pyridyl)pyrazolyl]borate coordinated to Eu(III) and Tb(III) showed the presence of DMF, nitrate or water completing the coordination sphere. Typical bond lengths of the coordinated water, Tb-O, were found to be 2.353(5)Å, with DMF having similar bond lengths coordinated to europium, Eu-O 2.360(5) Å. These observed bond lengths are shorter than those observed for the [Eu(4-^{is}Pr-PhenylQuaterpyridine)$_2$(H_2O)][ClO_4]$_2$ complex (Eu-O 2.477(11)Å). The structure is similar to the crystal structure of [Eu(terpy)$_3$][ClO_4]$_3$ and the Eu(III) and Tb(III) complexes of terpyridine-mono-oxide, which also have an approximate tricapped trigonal prism geometry. The Eu-O bond (2.477(11)Å) is longer than those

of the N-oxides (~2.340Å) whilst the Eu-N bonds are generally shorter (2.512-2.609Å opposed to 2.600-2.655Å of $[Eu(TerpyO)_3][ClO_4]_3$).

Structures of the bis and tetra N-oxide Quaterpyridines

The structures of [Tb(4',4''-diphenyl-2,2':6',2'':6'',2'''-quaterpyridine-1,1'''-bisoxide)$_2$][(ClO_4)]$_3$ and [Gd(4',4''-diphenyl-2,2':6',2'':6'',2'''-quaterpyridine-1,1',1'',1'''-tetraoxide)$_2$][(ClO_4)]$_3$ are shown in Figs.2.21 and 2.22 respectively. Once again, the introduction of the N-oxides greatly affects the co-ordination geometry in comparison to the non-oxidised quaterpyridine, with both structures being eight coordinate. The bis-oxide has an approximate dodecahedral geometry whilst the tetra-oxide has an almost cubic geometry. The bis–oxides greatest limiting factor in its co-ordination mode is that it forms a central bipyridine fragment with a small bite angle and if both N atoms are to bind to the metal centre then the ligand must adopt an almost planar conformation. The tetra-oxide is quite similar to terpyridine tris-oxide with the steric hindrance causing a cubic geometry to be adopted. Unlike the terpyridine tris-oxide though, there are no pendant N-oxide arms due to the increased ligand size allowing the coordination of all four N-oxides per ligand. The Gd-O bond lengths are similar to those observed for europium complexes of pyridine-N-oxides[26 and 27] and are also similar to the europium terpyridine N-oxides (average 2.380(4)Å). The terbium complex has slightly shorter Tb-O bonds with respect to the gadolinium species (average 2.282(5)Å) but the Tb-N bonds are much longer (average 2.539(4)Å) being similar to the $[Eu(terpyO)_3][(ClO_4)]_3$ complex (2.57-2.62Å).

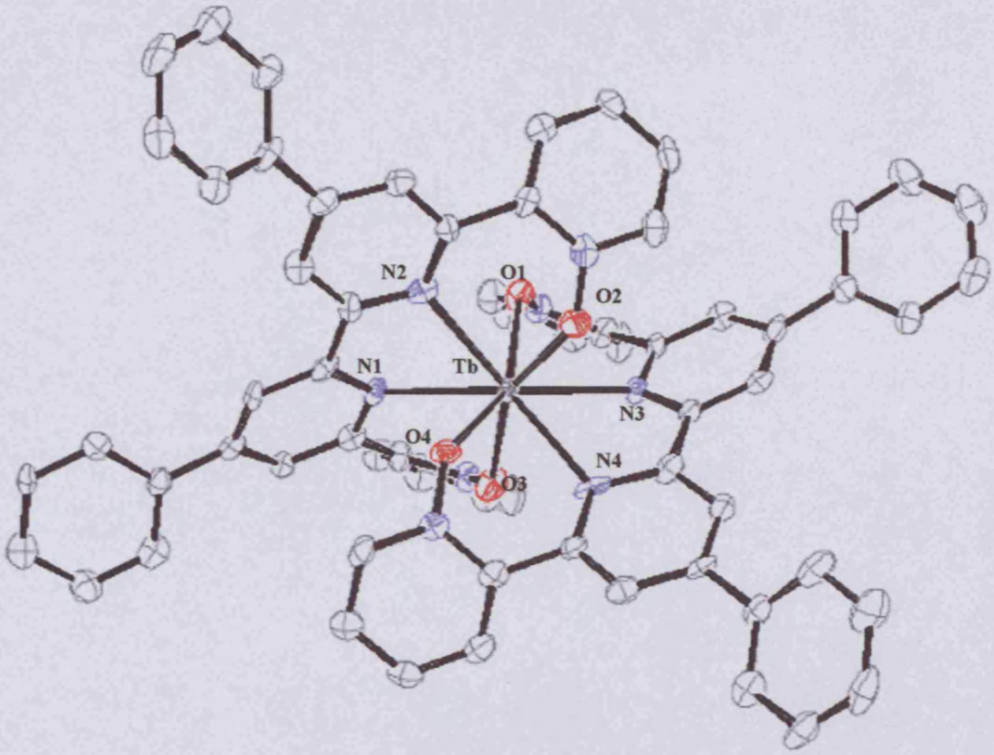

Fig.2.21: Structure of [Tb(4',4''-diphenyl-2,2':6',2'':6'',2'''-quaterpyridine-1,1'''-bisoxide)$_2$][(ClO_4)]$_3$

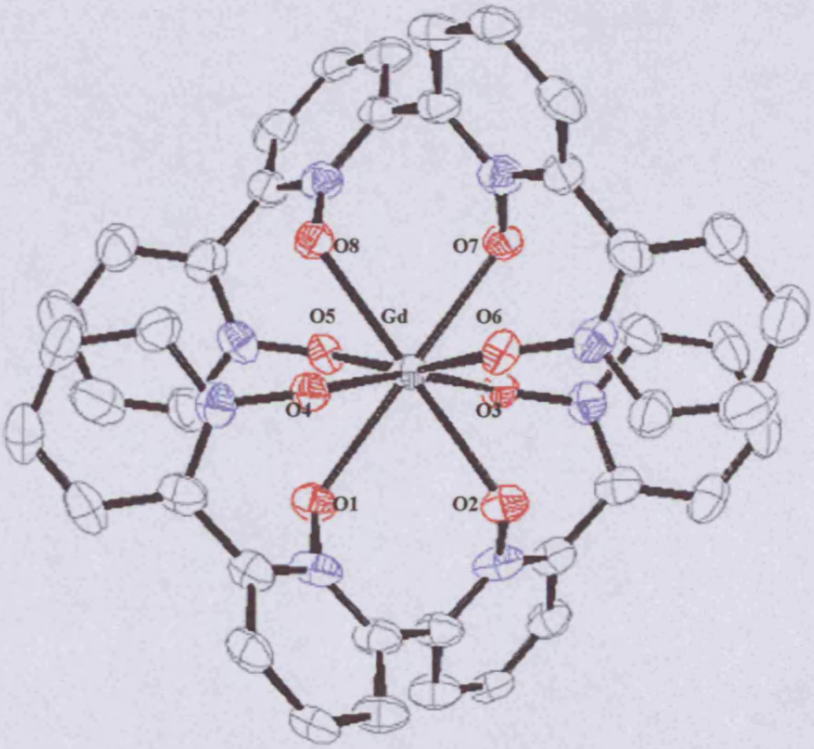

Fig.2.22: Structure of [Gd(4',4''-diphenyl-2,2':6',2'':6'',2'''-quaterpyridine-1,1',1'',1'''-tetraoxide)$_2$][(ClO_4)]$_3$

2.9 Europium and Terbium Quinquepyridine N-Oxide Complexes

Similar to the quaterpyridines, the only publication to date describing the coordination of lanthanides to quinquepyridine is a patent by Toner and co-workers[28]. Coordination of quinquepyridine to transition metals has been previously reported[29] and shall be discussed further in the next chapter. The Europium (III) and Terbium (III) complexes were obtained for the quinquepyridine ligands described. Solid-state structures have not been obtained for the complexes as of yet but the luminescence properties were investigated.

$[M(4\text{-}^{is}Pr\text{-}PhQuinquepyridine)_2][ClO_4]_3$ (where M= Eu and Tb)

The complexes were synthesised by the addition of either Eu(III) or Tb(III) perchlorate in the minimum amount of acetonitrile to a two-fold excess of the ligand as a suspension in the minimum amount of acetonitrile at room temperature. A yellow solution forms shortly after the addition of the lanthanide perchlorate and the addition of diethyl ether precipitates out the complex in a 47% yield. IR spectra of the two complexes are very similar, showing the presence of absorption bands characteristic of the pyridine moiety ($\nu_{C=C}$ and $\nu_{C=N}$ around 1607(s) and 1572(m) cm^{-1}). The perchlorate counter ion is observed as a very strong broad band at 1086cm^{-1}. However, the ES mass spectra of the complexes do not yield the parent ions. The Eu(III) complex reveals clusters at 892 and 932 m/z containing Eu whilst the parent ion theoretically should appear at 1397 m/z. The cluster at 932m/z suggests a $[LEu_2]$ species from the isotope pattern but is not a perfect match (should appear at 925 m/z theoretically) and the peaks at m/z 892 have a good isotope pattern for a one europium species. The Tb(III) complex

reveals clusters at 900 and 940 m/z containing Tb whilst the parent ion should appear at 1404m/z for the 2:1 complex. The cluster at m/z 900 has the isotope pattern for a two terbium species whilst the peaks at m/z 940 have an isotope pattern matching a one terbium species, the reverse of the europium complex.

$[M(4\text{-}^{\dot{n}}Pr\text{-}PhQuinquepyridineO_2)_2][ClO_4]_3$ (where M= Eu and Tb)

The complexes were synthesised in the same manner as the non-oxidised quinquepyridine. IR spectra of the two complexes are very similar, showing the presence of absorption bands characteristic of the pyridine moiety ($\nu_{C=C}$ and $\nu_{C=N}$ around 1604(s) and 1574(m)cm^{-1}) through which it appears co-ordination takes place ($\nu_{C=C}$ and $\nu_{C=N}$ in the free ligand appear around 1610(w) and 1580(s)cm^{-1} with differing intensities). The co-ordination of the metal centre is also indicated to be via the N-O oxygen atoms. The N-O absorption is observed at 1281(w), 1271(m) and 1230(w) cm^{-1} in the free ligand but once complexed a weakening of the N-O bond is apparent with either a shift or weakening of the intensity of the peaks to 1244(m) and 1222(w) cm^{-1}. The perchlorate counter ion is observed as a very strong broad band at 1088cm^{-1}. Similarly to the non-oxidised quinquepyridine complexes, the ES mass spectra of the complexes do not yield any obvious ions like the parent ions. The Eu(III) complex reveals clusters at 920, 936, 988 and 1006 m/z containing Eu whilst the parent ion theoretically should appear at 1461 m/z. A cluster at 656 indicates the fragmented $[ligand+H]^+$. The Tb(III) complex reveals Tb containing clusters at m/z 944 (corresponding to $TbL+ClO_4+MeOH$) and 1012 (corresponding to $LTb+2(ClO_4)$). The parent ion should appear at 1750m/z for the 2:1 complex.

2.10 Luminescence Studies

The luminescence emission spectra of the complexes synthesised and discussed in this chapter were measured along with their UV-Vis absorbance spectra where possible. No luminescence has been observed in aqueous solution for any of the complexes. The emission spectra were generally measured by using acetonitrile solutions of the complexes that were diluted such that all samples had an absorbency of 1 $mol^{-1}dm^{-3}cm^{-1}$ at the excitation wavelength. However, as shall be discussed, some of the complexes only show lanthanide emission in concentrated solution samples. Therefore, concentrated solutions had to be run. Where ligand luminescence was observed in the lanthanide complex emission spectra, the emission spectra of the ligands were also carried out to verify this. Initially, the individual spectra shall be discussed and compared and then a comparison of the relative luminescence intensities shall be discussed.

In all of the Eu(III) complexes, the $^5D_0 \rightarrow {}^7F_2$ emission dominates the emission spectra indicating that the Eu(III) ion is in a non-centrosymmetric ligand field which allows not only magnetic-dipole but also electric-dipole transitions.[30] The $^5D_0 \rightarrow {}^7F_2/{}^5D_0 \rightarrow {}^7F_1$ ratios (η) range from 37.6 to 8.19. Increases in the value of η have been suggested to be indicative of increasing covalency and have previously been shown to correlate with an increasing donor ability of the ligand.[31] It shall be seen that all of the spectra exhibit differing spectral properties with regards to the number of lines, line splitting and intensities, which can all be used to help provide information of the symmetry and structural nature of the Eu(III) co-ordination site.

However, due to the spectral resolution limitations of the equipment used, detailed analysis is limited and so relative luminescent properties shall be focused upon.

The emission spectra are typical of Eu(III) and Tb(III) complexes and exact wavelengths, along with emission intensities of the Eu(III) complexes are reported in table 2.8 and Figs.2.23-2.42 with the Tb(III) complexes reported in table 2.9 and Figs.2.24-2.43.

Complex	$^5D_0 \rightarrow {}^7F_0$	$^5D_0 \rightarrow {}^7F_1$	$^5D_0 \rightarrow {}^7F_2$	$^5D_0 \rightarrow {}^7F_3$	$^5D_0 \rightarrow {}^7F_4$
$Eu(Terpy)_3^{3+}$ [33]	-	592(1.0)	616(2.5)	-	687(0.89)
		593	617		689
		595	618		697
					702
$Eu(TerpyO)_3^{3+}$	580(0.1)	590(1.0)	612(6.25)	-	680(4.0)
			614		690
$Eu(TerpyO_2)_3^{3+}$	-	590(1.0)	612(16.7)	-	700(0.91)
$Eu(TerpyO_3)_3^{3+}$	-	590 (1.0)	612(9.09)	660(0.1)	700(0.16)
$Eu(4\text{-}^{is}Pr\text{-}PhQuater)_2^{3+}$	578(0.08)	592(1.0)	615(5.58)	651(0.12)	686(2.47)
		598	621		694
					700
$Eu(PhQuaterO_2)_2^{3+}$	-	594(1.0)	618(10.75)	665(0.42)	686(2.16)
					695
$Eu(PhQuaterO_4)_2^{3+}$	-	590(1.0)	611(37.6)	626(1.22)	692(1.39)
$Eu(4\text{-}^{is}Pr\text{-}PhQuinque)_2^{3+}$	-	-	-	-	-
$Eu(4\text{-}^{is}Pr\text{-}PhQuinqueO_2)_2^{3+}$	578(0.1)	593(1.0)	615(4.5)	-	690(3.96)
	591				696

Table 2.8: Peak positions and relative intensities in the emission spectra of the Eu(III) complexes (nm).

Complex	$^5D_4 \rightarrow {}^7F_6$	$^5D_4 \rightarrow {}^7F_5$	$^5D_4 \rightarrow {}^7F_4$	$^5D_4 \rightarrow {}^7F_3$	$^5D_4 \rightarrow {}^7F_2$	$^5D_4 \rightarrow {}^7F_1$	$^5D_4 \rightarrow {}^7F_0$
$Tb(Terpy)_3^{3+}$	491	543	583	623	-	-	-
	(1.0)	(1.75)	(0.43)	(0.14)			
$Tb(TerpyO)_3^{3+}$	491	543	583	622	-	-	-
	(1.0)	(2.1)	(0.67)	(0.5)			
$Tb(TerpyO_2)_3^{3+}$	-	-	-	-	-	-	-
$Tb(4\text{-}^{is}Pr\text{-}PhQuater)_2^{3+}$	491	543	583	622	649	670	678
	(1.0)	(1.75)	(0.62)	(0.25)	(0.04)	(0.014)	(0.013)
$Tb(4\text{-}^{is}Pr\text{-}PhQuinque)_2^{3+}$	491	543	596	621	-	-	-
	(1.0)	(2.15)	(0.72)	(0.38)			
$Tb(4\text{-}^{is}Pr\text{-}PhQuinqueO_2)_2^{3+}$	490	544	584	622	-	-	-
	(1.0)	(1.7)	(0.55)	(0.16)			

Table 2.9: Peak positions and relative intensities in the emission spectra of the Tb(III) complexes (nm).

2.10.1 The Luminescence Properties of $[Eu(terpyO)_3][ClO_4]_3$

The absorbance spectra for the terpy N-oxides had been obtained previously by our research group.[1] The spectrum recorded in acetonitrile at room temperature shows a broad band at 310nm (ε = 20 400 $M^{-1}cm^{-1}$). With irradiation experiments it was found that after irradiation at approximately 366nm for 0, 5, 30 and 45 minutes a slight broadening in the absorption spectrum occurs (See Fig.2.23). This was a trend increasingly followed by the bis- and tris-N-oxide complexes. A possible explanation for these observations is a photochemical change to the N-oxide moiety when irradiated at 366nm.

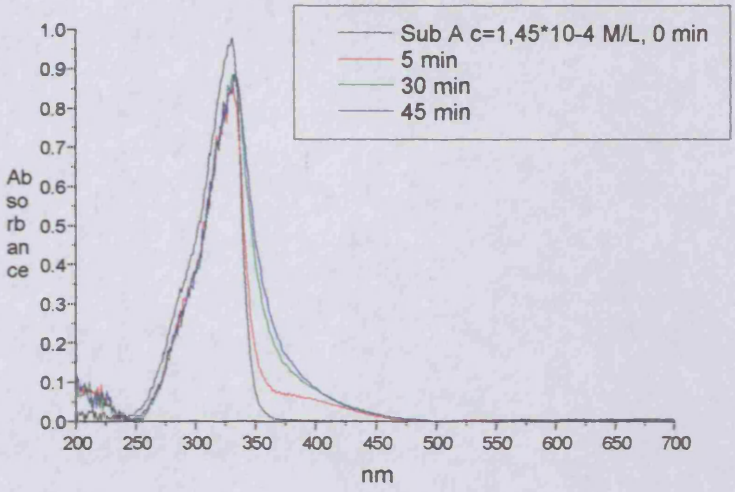

Fig.2.23: Influence of irradiation (366 nm) of $[Eu(terpyO)_3][ClO_4]_3$ on absorption spectra

The emission spectrum was obtained in acetonitrile at a concentration of 45µmol (see Fig.2.24).

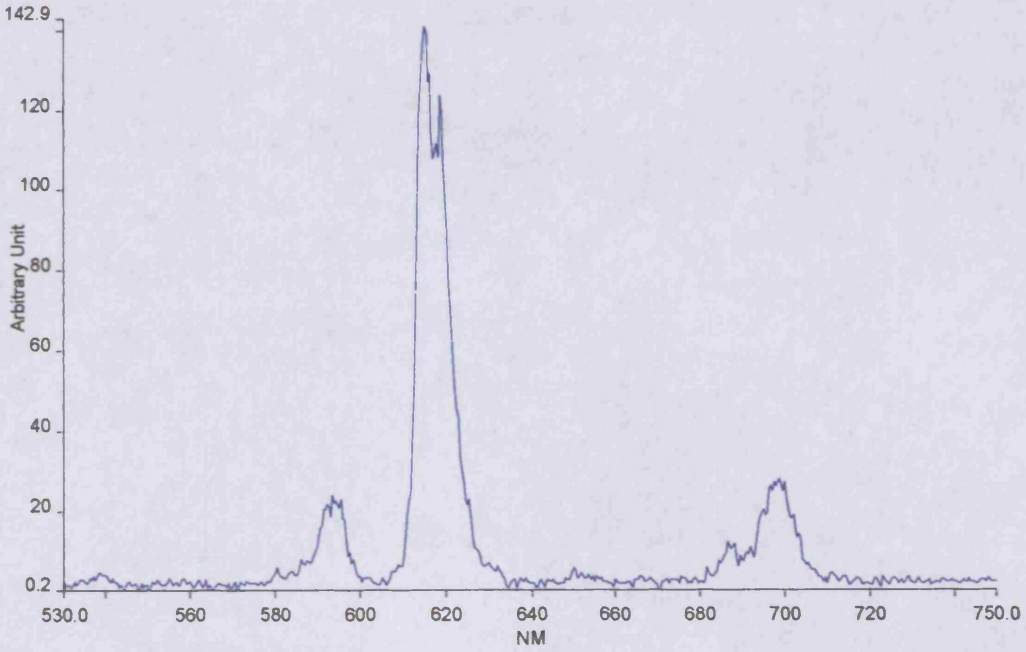

Fig.2.24: The emission spectrum of $[Eu(terpyO)_3][ClO_4]_3$ (λ_{exc} = 310nm, λ_{emis} = 617nm).

The complex exhibits less splitting than the parent $[Eu(terpy)_3][ClO_4]_3$ complex which was assigned a slight low-symmetry perturbation of a basic D_3

symmetry from its luminescence spectrum.[33] Therefore, it can be predicted that the mono-oxide complex has a higher symmetry than D_3 in solution. The relative integrated areas of the $^5D_0 \rightarrow {}^7F_J$ transitions are 0.1, 1.0, 6.25 and 4.0 for J=0, 1, 2 and 4 respectively. The complex has a higher η value (6.25) than that of the parent $[Eu(terpy)_3][ClO_4]_3$ complex (η = 2.5). $[Eu(terpy)_3][ClO_4]_3$ is known to exhibit a concentration effect, in which, at low concentrations the complex exhibits a large amount of ligand intensity as a result of decomplexation.[34] This is not observed in the terpyO complex and we propose the increased donor property of the terpyO ligand increases the chemical stability of the complex in solution.

2.10.2 The Luminescence Properties of $[Eu(terpyO_2)_3][ClO_4]_3$

Similar to the mono-oxide, the absorbance spectrum[1] had been obtained in acetonitrile with a broad peak evident at 296nm (ε = 29 200 $M^{-1}cm^{-1}$)(see fig.2.25). The shoulder in the spectrum continues to grow as the length of time of irradiation increases. Notably, the shoulder is far more pronounced at 15 minutes than the mono-oxide implying that the rate of reaction for the bis-oxide is much greater than that of the mono-oxide.

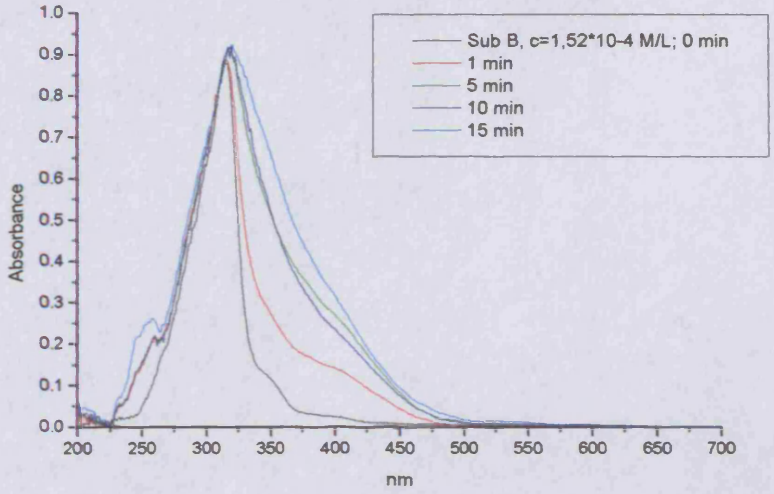

Fig.2.25: Influence of irradiation (366 nm) of $[Eu(terpyO_2)_3][ClO_4]_3$ on absorption spectra

The emission spectrum was obtained in acetonitrile at a concentration of 75µmol (see Fig.2.26).

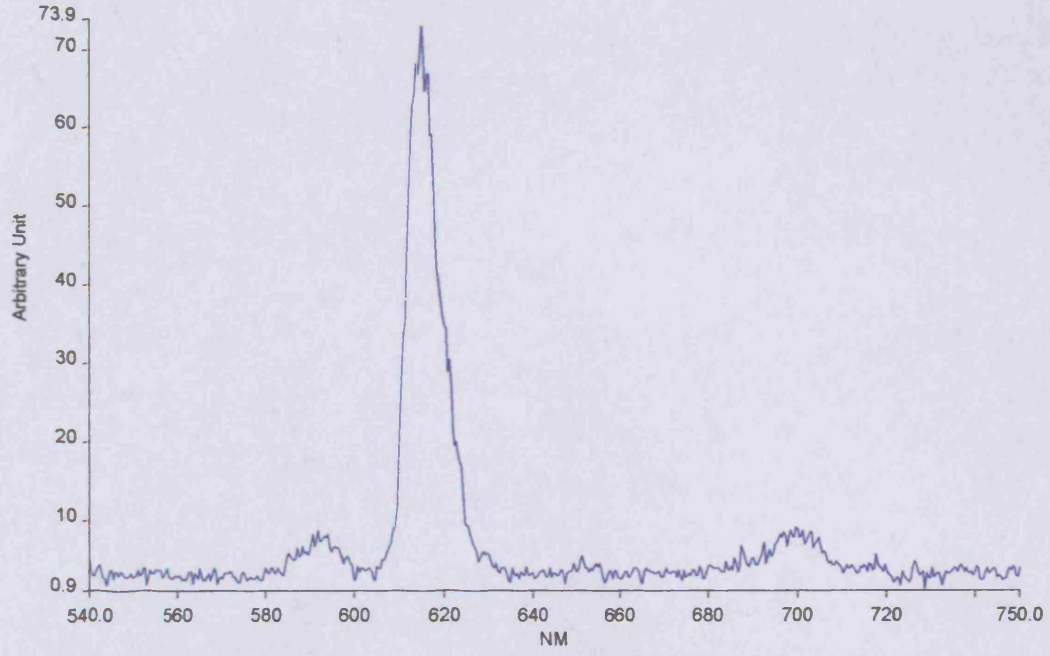

Fig.2.26: The emission spectrum of $[Eu(terpyO_2)_3][ClO_4]_3$ (λ_{exc} = 310nm, λ_{emis} = 617nm).

Notably there is less splitting of the peaks than the mono-oxide which implies a more symmetrical structure in solution. The relative integrated areas of the $^5D_0 \rightarrow {}^7F_J$ transitions are 1.0, 16.7 and 0.91 for J=1, 2 and 4 respectively. The complex exhibits the second highest value of η in the series with an η value of 16.7 and also does not exhibit decomplexation at low concentrations like the $[Eu(terpy)_3][ClO_4]_3$ complex.

2.10.3 The Luminescence Properties of $[Eu(terpyO_3)_3][ClO_4]_3$

The absorbance spectrum[1] shows a broad peak at 283nm (ε = 13 256 $M^{-1}cm^{-1}$) (see fig.2.27). Irradiation experiments yield results similar to that of the bis-oxide, in particular broadening of the peak to longer and shorter wavelengths.

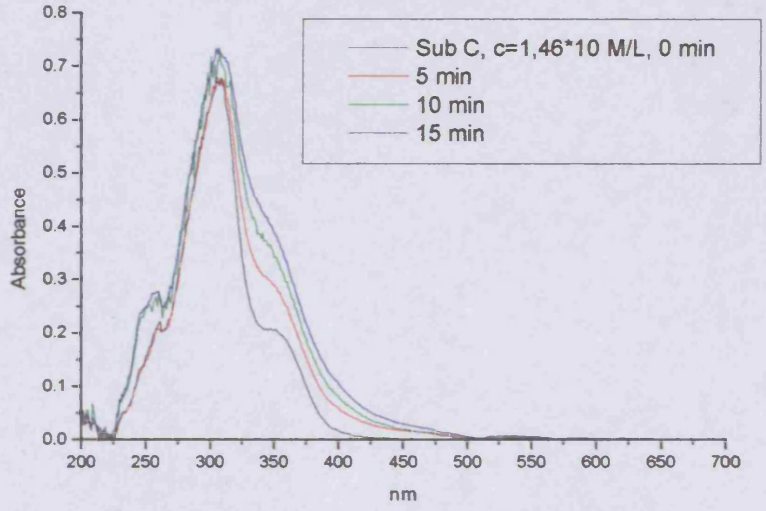

Fig.2.27: Influence of irradiation (366 nm) of $[Eu(terpyO_3)_3][ClO_4]_3$ on absorption spectra

The emission spectrum was obtained in acetonitrile at a concentration of 290μmol (see Fig.2.28).

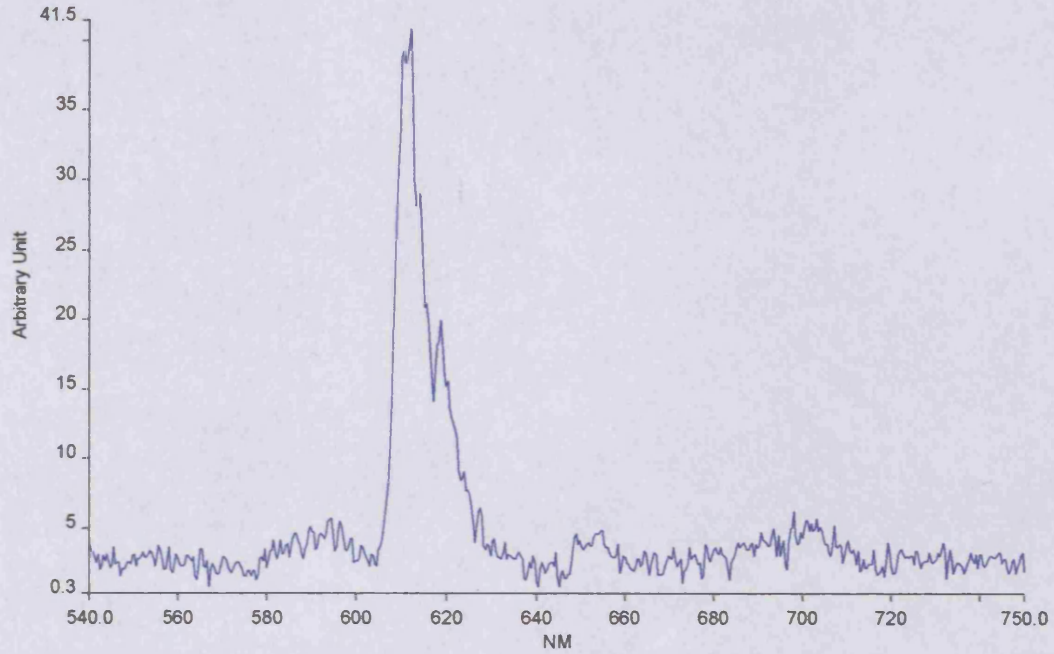

Fig.2.28: The emission spectrum of $[Eu(terpyO_3)_3][ClO_4]_3$ (λ_{exc} = 310nm, λ_{emis} = 617nm).

The emission spectrum is similar to that of the bis-oxide species, in that there is less splitting of the peaks than in the spectrum of the mono-oxide. The relative integrated areas of the $^5D_0 \rightarrow {}^7F_J$ transitions are 1.0, 9.09, 0.1 and 0.16 for J=1, 2, 3 and 4 respectively. The complex exhibits a lower value of η (9.09) compared to the bis-oxide but higher than the mono-oxide. It does not exhibit de-complexation at low concentrations.

It is interesting to note that previous solid state luminescence studies had suggested the geometry of the tris-oxide species to be a tricapped trigonal prism.[31] While it may be the case that the species may have different geometries in solution, the crystallographic data has shown that it is fact a distorted cubic structure in the solid state and highlights the difficulty in trying to assign geometries from luminescent data.

2.10.4 The Luminescence Properties of $[Tb(terpyO)_3][ClO_4]_3$

The absorbance spectrum in acetonitrile at room temperature shows three broad peaks at 230nm (ε = 62 240 $M^{-1}cm^{-1}$), 276nm (ε = 28 140 $M^{-1}cm^{-1}$) and 312nm (ε = 22 657 $M^{-1}cm^{-1}$) attributed to $\pi \rightarrow \pi^*$ transitions on the pyridine rings (see Fig.2.29). The absorption at 312nm has lowered 20nm in comparison to the $[Tb(terpy)_3][ClO_4]_3$ complex which has absorptions at 204nm (ε = 69 404 $M^{-1}cm^{-1}$) 234nm(ε = 41 860 $M^{-1}cm^{-1}$), 286nm (ε = 27 718 $M^{-1}cm^{-1}$), and 332nm (ε = 23 872 $M^{-1}cm^{-1}$). This lowering in absorption wavelength and intensity is indicative of a lowering of the triplet energy of the ligand making it more suitable for Eu(III) than the Tb(III) ion.

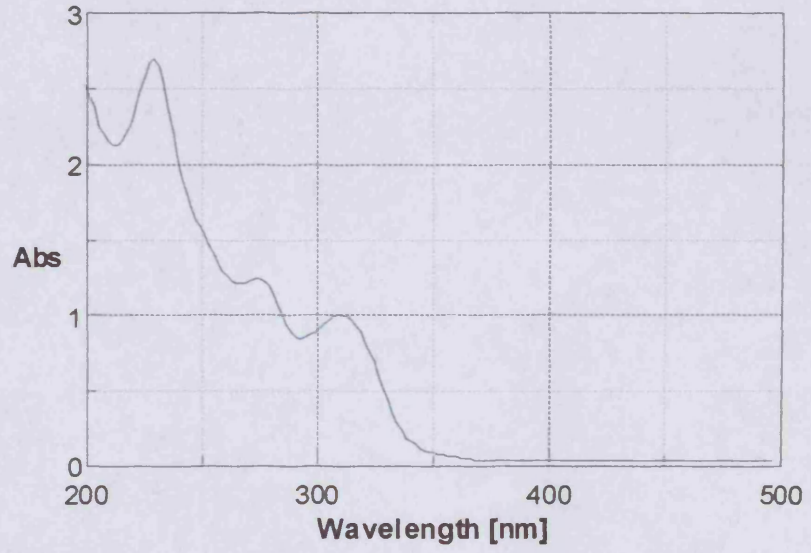

Fig.2.29: The absorbance spectrum of $[Tb(terpyO)_3][ClO_4]_3$

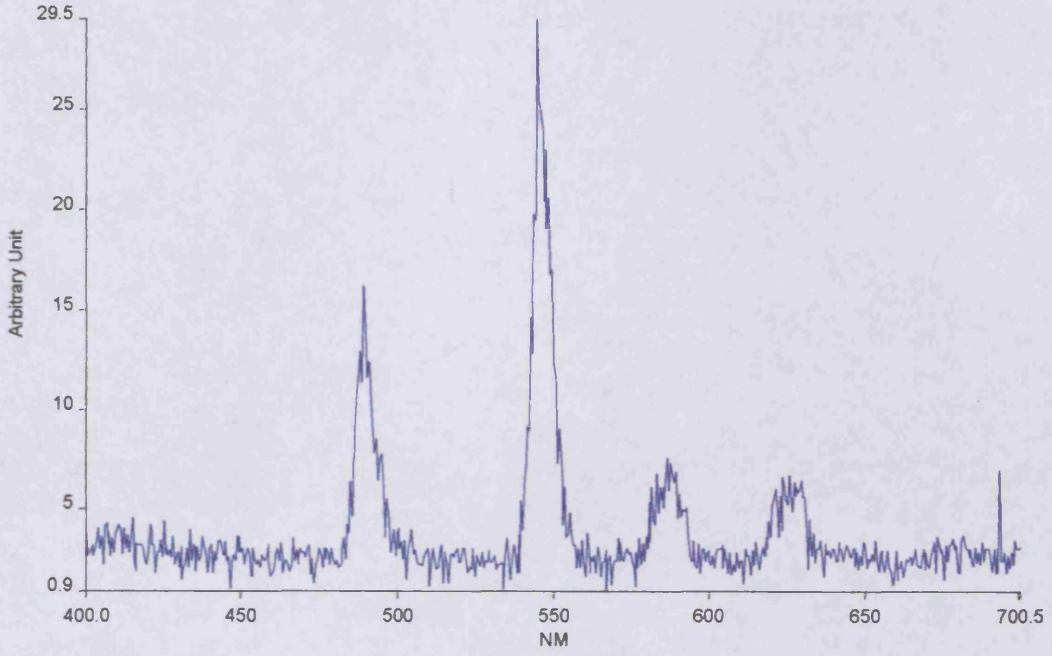

Fig.2.30: The emission spectrum of $[Tb(terpyO)_3][ClO_4]_3$ (λ_{exc} = 314nm, λ_{emis} = 544nm).

The emission spectrum showed four sharp bands, typical of Tb(III) emission. The relative integrated areas of the $^5D_4 \rightarrow {}^7F_J$ transitions are 1.0, 2.1, 0.67 and 0.5 for J=6, 5, 4 and 3 respectively.

2.10.5 The Luminescence Properties of $[Tb(terpyO_2)_3][ClO_4]_3$

The absorbance spectrum in acetonitrile at room temperature shows an intense broad peak at 230nm (ε = 66 340 $M^{-1}cm^{-1}$), with shoulders at 270nm (ε = 33 966 $M^{-1}cm^{-1}$) and 300nm (ε = 20 965 $M^{-1}cm^{-1}$) attributed to $\pi \rightarrow \pi^*$ transitions on the pyridine rings (see Fig. 2.31). This complex shows a further 12nm lowering of the highest wavelength absorption compared to $[Tb(terpyO)_3][ClO_4]_3$ suggesting a further lowering of the triplet energy. This further drop of the triplet energy makes the complex even less suitable for Tb(III) than Eu(III) compared to $[Tb(terpyO)_3][ClO_4]_3$ and is perhaps reflected in the luminescence spectra.

CARDIFF UNIVERSITY PRIFYSGOL CAERDYDD

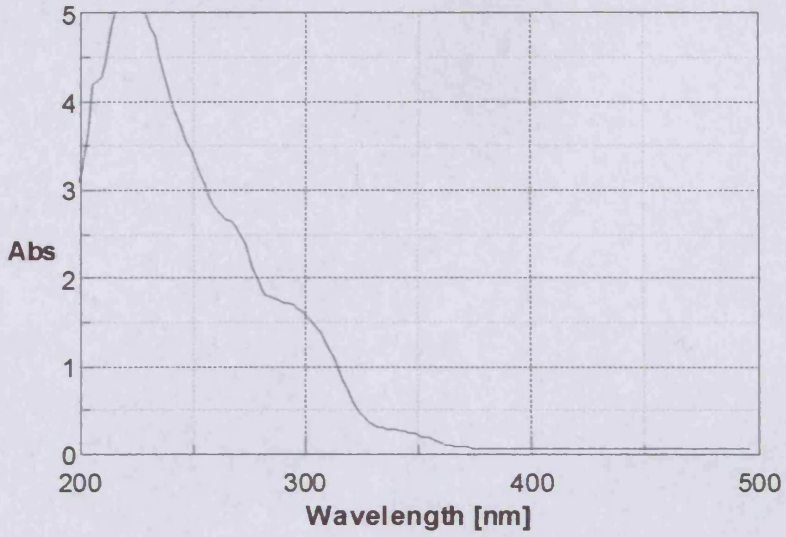

Fig.2.31: The absorbance spectrum of $[Tb(terpyO_2)_3][ClO_4]_3$

The emission spectrum show neither Tb(III) emission nor ligand emission (see Fig. 2.32). The reasons for the absence of any ligand emission remain unclear but due to the presence of Eu(III) emission for the Eu(III) analogue the lack of Tb(III) emission could be attributed to a lowering of the triplet levels of the ligand meaning a mismatching to the excited metal state of the Tb(III) ion such that the energy-transfer process does not occur.

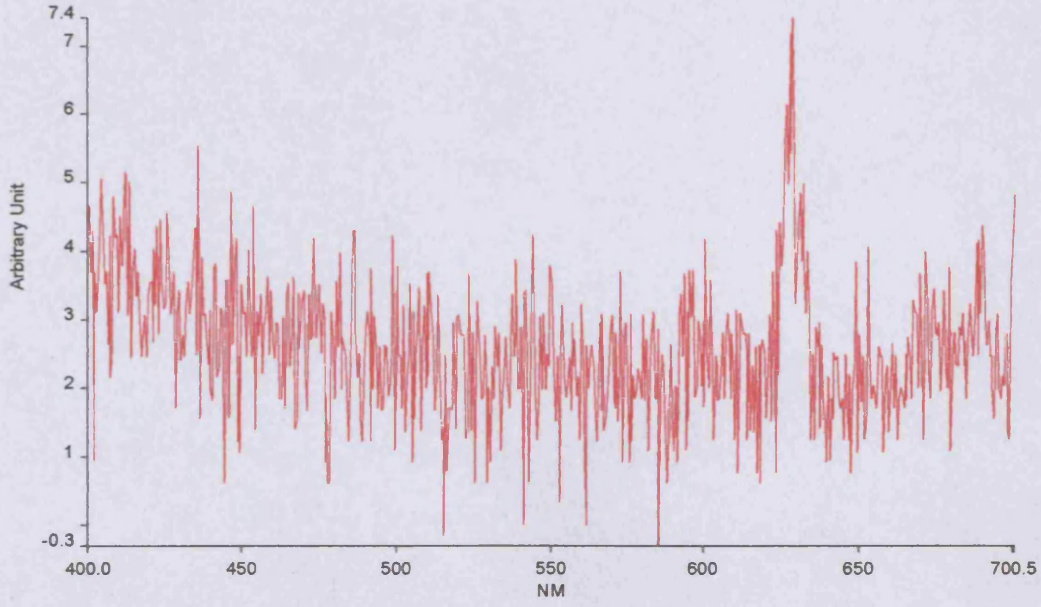

Fig.2.32: The emission spectrum of $[Tb(terpyO_2)_3][ClO_4]_3$ (λ_{exc} = 314nm, λ_{emis} = 544nm).

2.10.6 The Luminescence Properties of $[Eu(4\text{-}^{is}Pr\text{-}PhenylQuater)_2(H_2O)][ClO_4]_3$

The absorbance spectrum of the 4-^{is}Pr-PhQuater ligand recorded in DMF at room temperature showed a broad band at 275nm (ε = 62 188 $M^{-1}cm^{-1}$) with a shoulder appearing at 321nm (ε = 14 148 $M^{-1}cm^{-1}$) attributed to $\pi \rightarrow \pi^*$ transitions on the pyridine rings. The absorbance spectrum of the complex at dilute concentration (8µmol) in DMF gave the same absorbance spectrum as the ligand, with the same result if repeated in acetonitrile. This observation might be caused by de-complexation of the ligand at these dilute levels of concentration. The emission spectrum of the dilute sample, excited at 275nm, gave a broad ligand emission at 357nm (see fig.2.33), although very weak Eu emission can be observed at 615nm. To determine if the complexes were being de-complexed at dilute concentrations a concentrated sample was run.

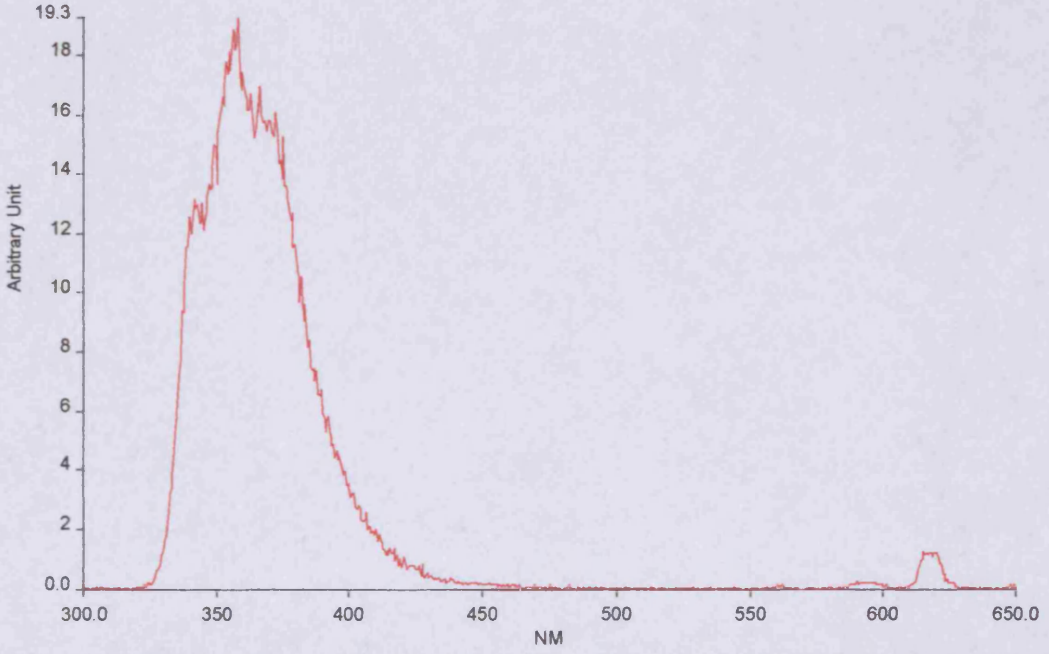

Fig.2.33: The emission spectrum of the dilute $[Eu(4\text{-}^{is}Pr\text{-}PhenylQuater)_2(H_2O)][ClO_4]_3$ complex (λ_{exc} = 275nm, λ_{emis} = 357nm).

The concentrated sample (400μmol) in acetonitrile at room temperature yielded an emission spectrum but was too concentrated to obtain an absorbance spectrum.

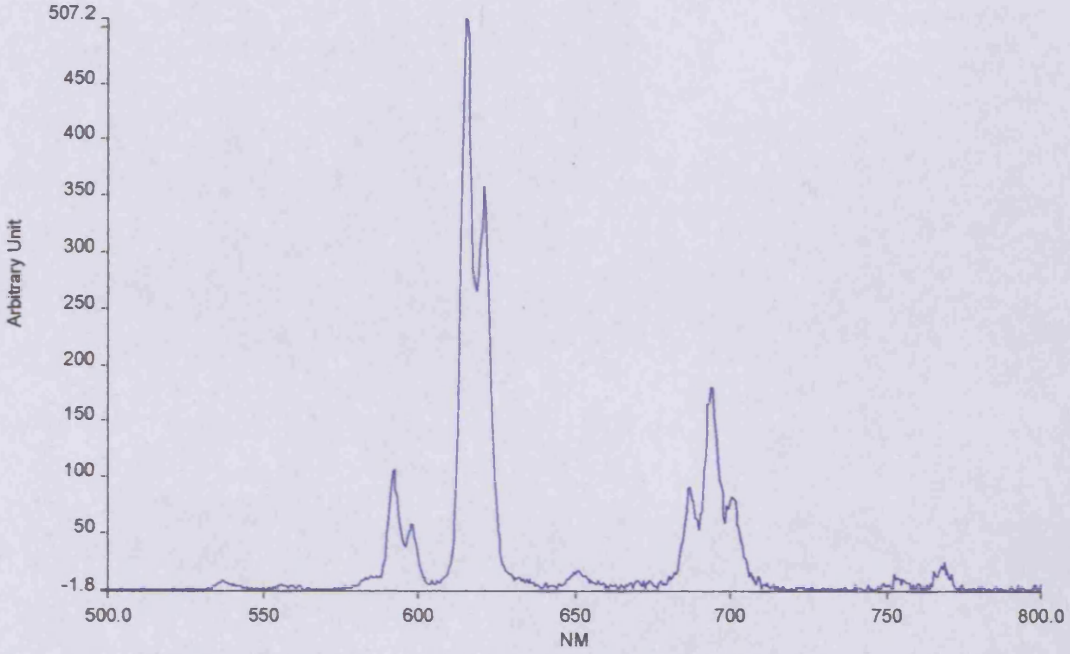

Fig.2.34: The emission spectrum of $[Eu(4\text{-}^{is}Pr\text{-}PhenylQuater)_2(H_2O)][ClO_4]_3$ (λ_{exc} = 382nm, λ_{emis} = 615nm).

The emission spectrum shows a typical emission spectrum for Eu(III) with the complex exhibiting the greatest amount of peak splitting in this series of complexes. This would imply that this complex has the lowest symmetry in solution. The forbidden $^5D_0 \rightarrow {}^7F_0$ transition is observed weakly, the $^5D_0 \rightarrow {}^7F_1$ transition is observed as a strong doublet as is the very strong $^5D_0 \rightarrow {}^7F_2$ transition, the $^5D_0 \rightarrow {}^7F_3$ transition is observed as a weak peak and the $^5D_0 \rightarrow {}^7F_4$ transition is observed as a strong triplet. The relative integrated areas of the $^5D_0 \rightarrow {}^7F_J$ transitions are 0.08, 1.0, 5.58, 0.12 and 2.47 for J=0, 1, 2, 3 and 4 respectively. At this concentration no ligand emission can be observed and so the intense ligand emission in the dilute sample must be attributed to de-complexation. This would indicate the ligand is a relatively weak binder of the lanthanides.

2.10.7 The Luminescence Properties of $[Tb(4\text{-}^{is}Pr\text{-}PhenylQuater)_2(H_2O)][ClO_4]_3$

Similar to the Eu complex, the Tb complex exhibits decomplexation at low concentrations and absorbance spectra of the complex could not be obtained. Metal luminescence could only be detected at high concentration (400μmol) and a sample analysed in acetonitrile at room temperature yielded the Tb(III) emission spectrum.

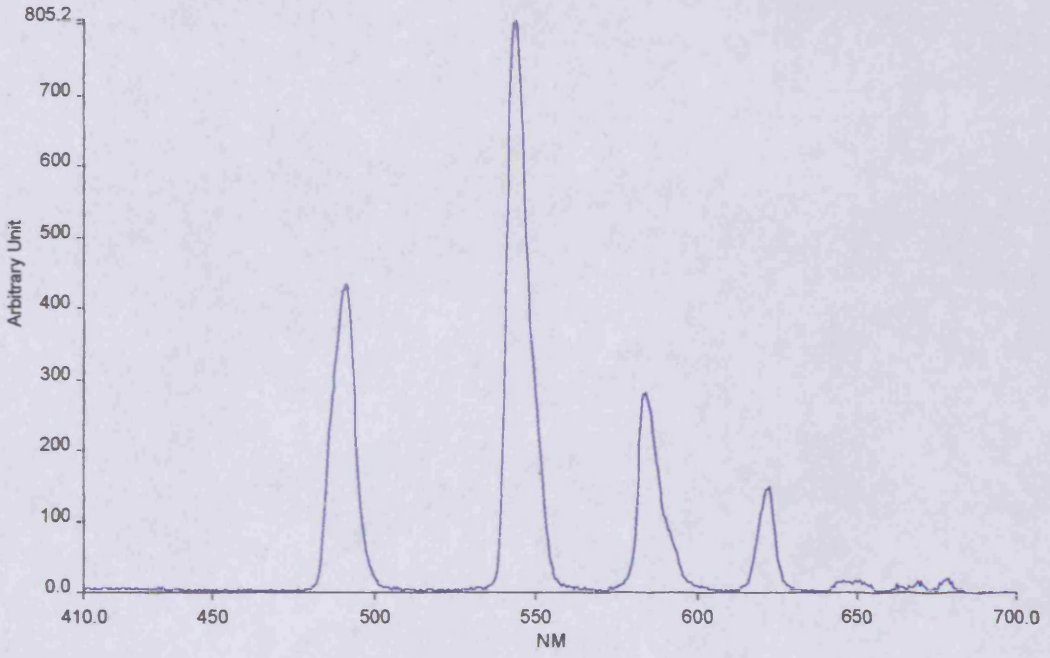

Fig.2.35: The emission spectrum of $[Tb(4\text{-}^{is}Pr\text{-}PhenylQuater)_2(H_2O)][ClO_4]_3$ (λ_{exc} = 382 nm, λ_{emis} = 543 nm).

The emission spectrum showed several sharp bands, typical of Tb(III) emission. The relative integrated areas of the $^5D_4 \rightarrow {}^7F_J$ transitions are 1.0, 1.75, 0.62, 0.25, 0.04, 0.014 and 0.013 for J=6, 5, 4, 3, 2, 1 and 0 respectively.

2.10.8 The Luminescence Properties of $[Eu(PhQuaterO_2)_2][ClO_4]_3$

The absorbance spectrum of the PhquaterpyridineO_2 ligand recorded in CH_3CN at room temperature shows a broad band at 268nm (ε = 59 010 $M^{-1}cm^{-1}$) with two shoulders at 288nm (ε = 41 502 $M^{-1}cm^{-1}$) and 326nm (ε = 11 128 $M^{-1}cm^{-1}$) attributed to $\pi \rightarrow \pi^*$ transitions on the pyridine rings. Upon complexation to the Eu(III) ion, the $\pi \rightarrow \pi^*$ transitions undergo drastic changes with a broadening of the spectrum showing two bands at 230nm (ε = 72 404 $M^{-1}cm^{-1}$) and 254nm (ε = 74 703 $M^{-1}cm^{-1}$) with a shoulder at 332nm (ε = 16 966 $M^{-1}cm^{-1}$)(see Fig.2.36).

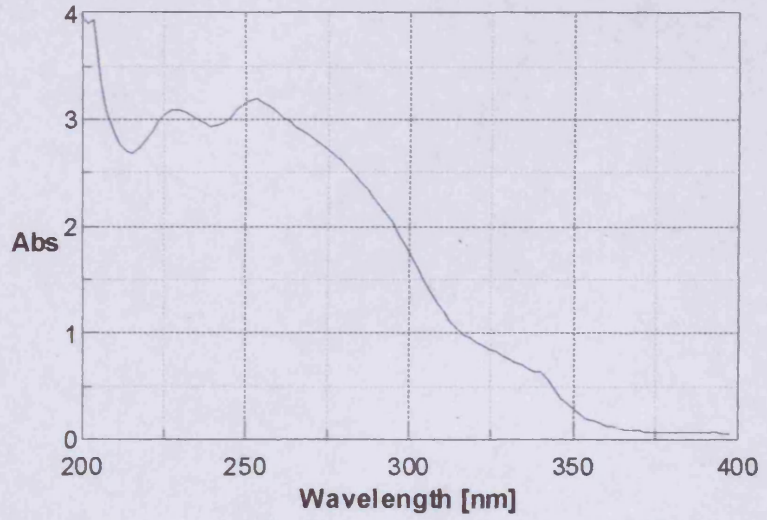

Fig.2.36: The absorbance spectrum of $[Eu(PhQuaterO_2)_2][ClO_4]_3$

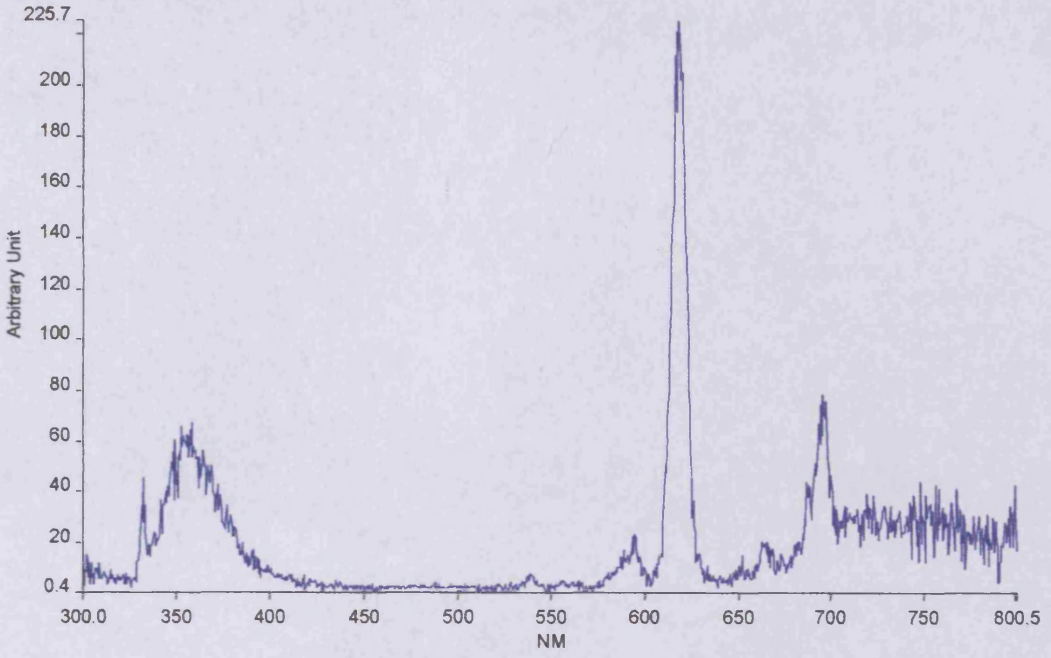

Fig.2.37: The emission spectrum of $[Eu(PhQuaterO_2)_2][ClO_4]_3$ in CH_3CN (λ_{exc} = 332nm, λ_{emis} = 618 nm).

The emission spectrum shows less splitting of the peaks compared to the parent complex with the $^5D_0 \rightarrow {}^7F_4$ transition being seen as a singlet with a shoulder. The relative integrated areas of the $^5D_0 \rightarrow {}^7F_J$ transitions are 1.0, 10.75, 0.42 and 2.16 for J=1, 2, 3 and 4 respectively. Of note is the broad peak observable at 356nm attributed to ligand emission. This unwanted ligand emission could be arising from de-complexation of the complex at this concentration in solution, uncoordinated ligand that is present in the solution or perhaps an unwanted energy loss pathway due to inefficient energy transfer from the ligand triplet state to the excited metal state.

2.10.9 The Luminescence Properties of $[Eu(PhQuaterO_4)_2][ClO_4]_3$

The absorbance spectrum of the Eu(III) complex in CH_3CN shows three broad peaks at 230nm (ε = 72 778 $M^{-1}cm^{-1}$), 268nm (ε = 61 762 $M^{-1}cm^{-1}$) and 312nm (ε = 45 832 $M^{-1}cm^{-1}$)(see Fig.2.38). The absorbance spectrum has a similar ε_{max} to that of the

PhquaterpyridineO$_2$ Eu(III) complex (ε_{max} = 72 404 $M^{-1}cm^{-1}$) but the shoulder at 332nm in the bis-oxide is not observed in the tetra-oxide. A shoulder instead appears at 312nm in the tetra-oxide which would suggest an increase in energy of the excited state of the ligand, taking it away from an ideal energy match for Eu(III) but making it a better energy match for Tb(III).

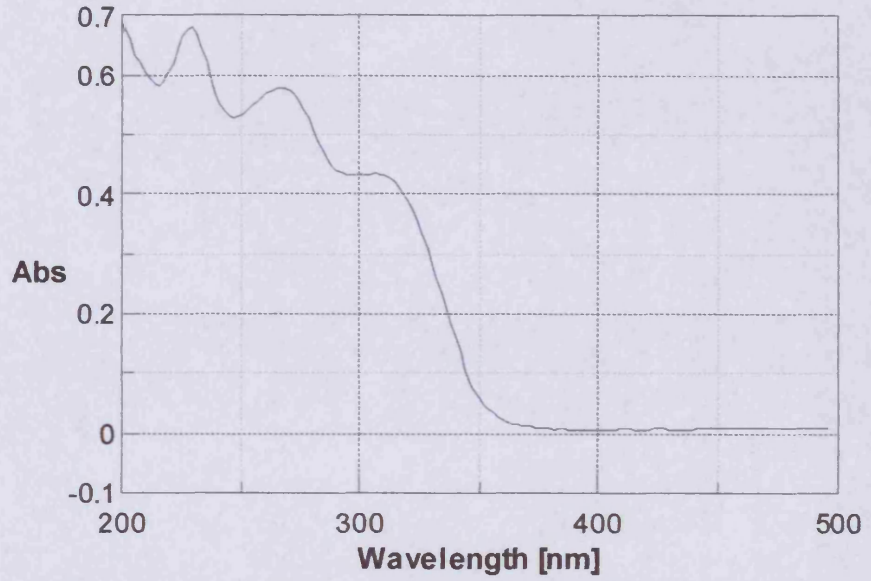

Fig.2.38: The absorbance spectrum of [Eu(PhQuaterO$_4$)$_2$][ClO$_4$]$_3$ in CH_3CN.

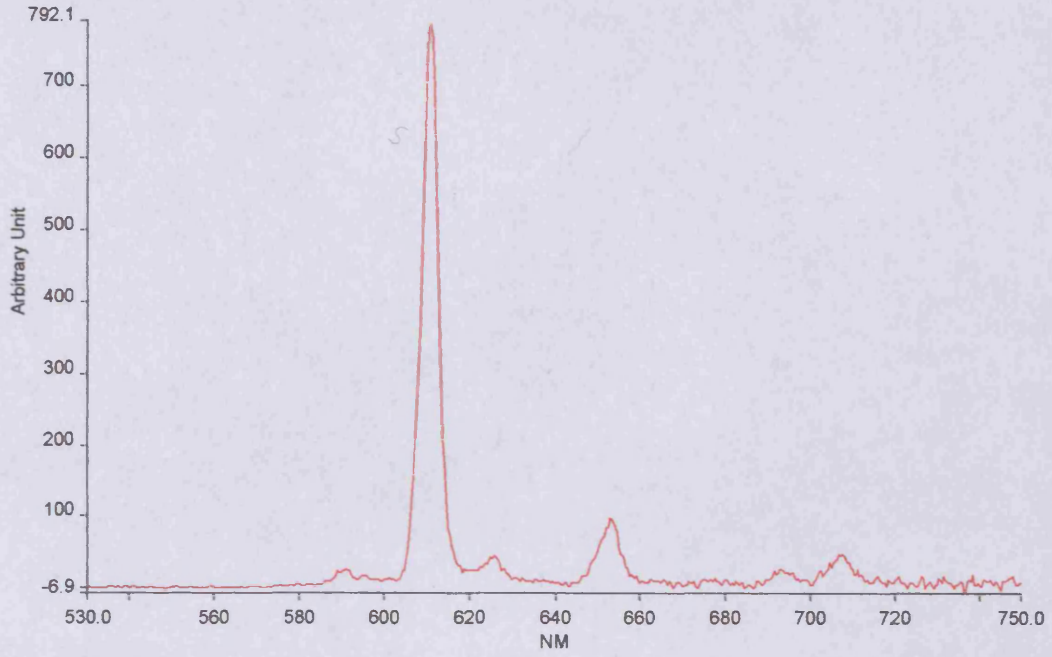

Fig.2.39: The emission spectrum of $[Eu(PhQuaterO_4)_2][ClO_4]_3$ in CH_3CN (λ_{exc} = 326nm, λ_{emis} = 611 nm).

The complex exhibits even less splitting of the peaks than the bis-oxide implying it is the most symmetrical in solution of the quaterpyridine complex series. The relative integrated areas of the $^5D_0 \rightarrow {}^7F_J$ transitions are 1.0. 37.6, 1.22, 1.39 and 2.4 for J=1, 2, 3, 4 and 5 respectively. The complex exhibits the greatest value of η in this series of complexes with an η value of 37.6. This would indicate the $PhquaterO_4$ ligand has the strongest donor properties of the series.

2.10.10 The Luminescence Properties of $[Eu(4\text{-}^{is}Pr\text{-}PhQuinque)_2][ClO_4]_3$

The absorbance spectrum of the 4-^{is}Pr-PhQuinque ligand recorded in DMF at room temperature shows a broad band at 272nm (ε = 51 725 $M^{-1}cm^{-1}$) with shoulders appearing at 281nm (ε = 49 541 $M^{-1}cm^{-1}$) and 317nm (ε = 18 246 $M^{-1}cm^{-1}$) attributed to $\pi \rightarrow \pi^*$ transitions on the pyridine rings. The absorbance spectrum of the complex at dilute concentration (8μmol) and concentrated levels (400μmol) in DMF gave the

same absorption spectrum as the ligand. Similar to the Quaterpyridine complexes this was attributed to de-complexation of the ligand at these levels of concentration. Excitation of a concentrated solution (400μmol) at 338nm revealed a broad ligand emission at 360nm (see fig.2.40) with no Eu(III) emission observed. This could be attributed to a number of reasons including decomplexation of the ligand in solution (which is suggested by the absorbance spectrum) or perhaps a mismatching of the ligand triplet state to the excited metal state causing a very inefficient energy transfer resulting in only ligand emission being observed.

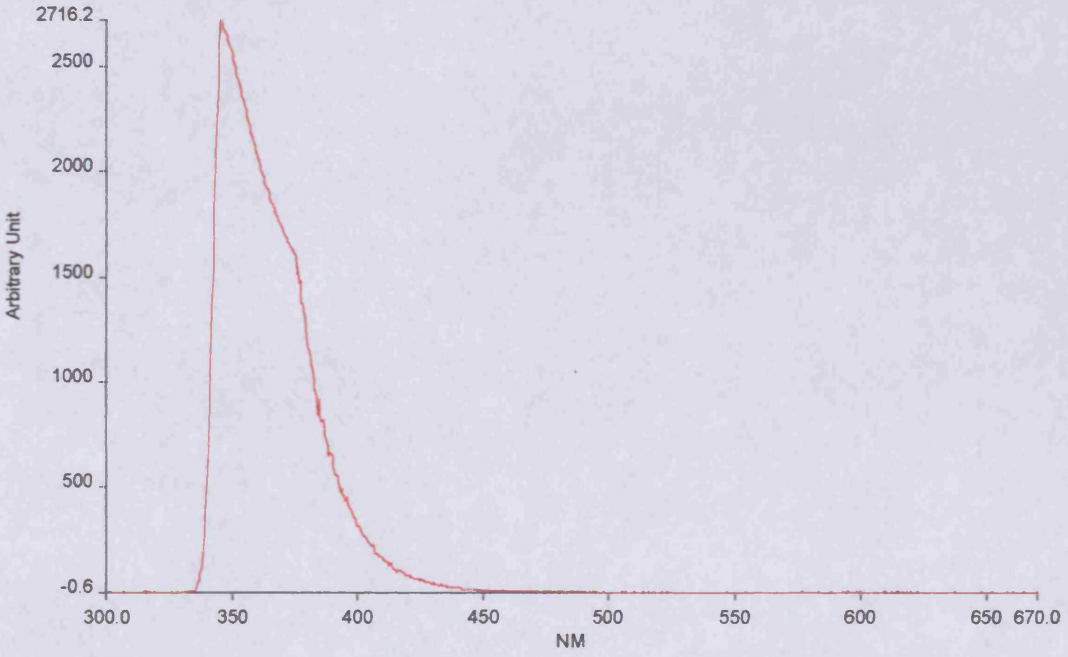

Fig.2.40: The emission spectrum of $[Eu(4\text{-}^{is}Pr\text{-}PhQuinque)_2][ClO_4]_3$ in CH_3CN (400μmol) (λ_{exc} =340nm, λ_{emis} =350nm).

2.10.11 The Luminescence Properties of $[Tb(4\text{-}^{is}Pr\text{-}PhQuinque)_2][ClO_4]_3$

Analogous to the Eu(III) complex, the absorbance spectrum of the complex at dilute (8μmol) and concentrated levels (400μmol) in DMF also gave the same absorption spectrum as the ligand. Excitation of the concentrated sample (400μmol) at 338nm in DMF showed a broad ligand emission which had two peaks at 356 and 371nm (see

fig.2.41). Unlike the Eu(III) complex a very weak lanthanide emission can de seen arising from the Tb(III) metal at 544nm. This could perhaps indicate a slightly better matching of the ligand and metal energy levels compared to the Eu(III) complex.

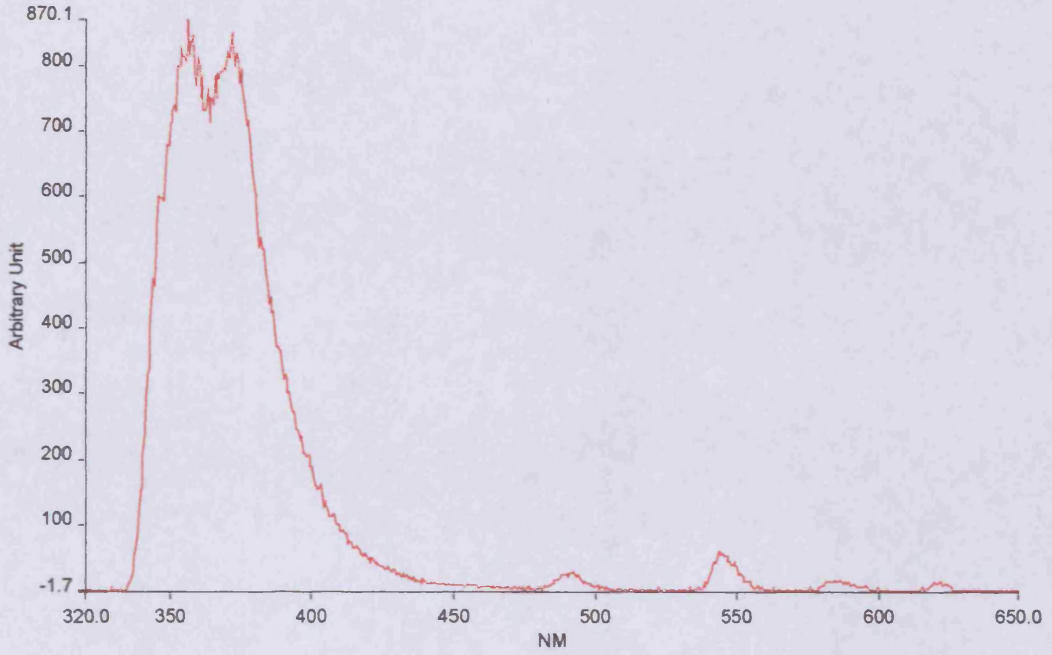

Fig.2.41: The emission spectrum of $[Tb(4\text{-}^{is}Pr\text{-}PhQuinque)_2][ClO_4]_3$ in CH_3CN (400μmol) (λ_{exc} =338nm, λ_{emis} =356nm).

The Tb(III) emission showed four bands with the relative integrated areas of the $^5D_4 \rightarrow {}^7F_J$ transitions being 1.0, 2.15, 0.72 and 0.38 for J= 6, 5, 4 and 3 respectively.

2.10.12 The Luminescence Properties of $[Eu(4\text{-}^{is}Pr\text{-}PhQuinqueO_2)_2][ClO_4]_3$

As has been seen before, at low concentrations only ligand emission was observed, therefore a concentrated sample (400μmol) in DMF at room temperature was analysed yielding the emission spectrum but the solution was too concentrated to obtain an absorbance spectrum.

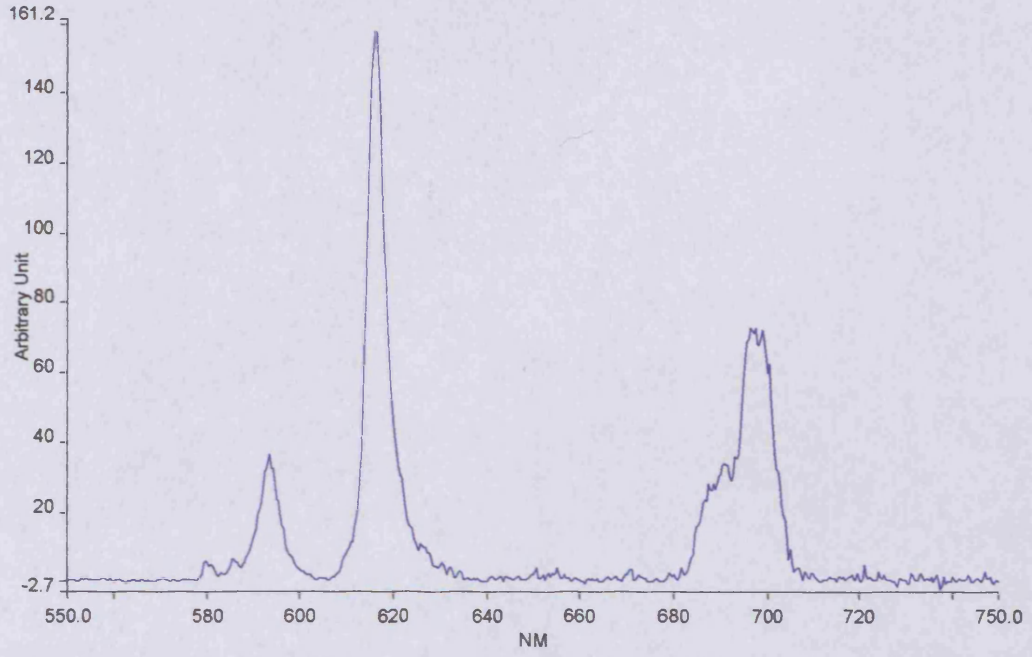

Fig.2.42: The emission spectrum of the concentrated sample of $[Eu(4\text{-}^{is}Pr\text{-}PhQuinqueO_2)_2][ClO_4]_3$ (λ_{exc} = 365nm, λ_{emis} = 615nm).

The emission spectrum is typical for Eu(III) with the relative integrated areas of the $^5D_0 \rightarrow {}^7F_J$ transitions being 0.1, 1.0, 4.5, 3.96 for J=0, 1, 2 and 4 respectively. The introduction of the N-oxides appears to have improved the lanthanide binding strength of the ligand as no lanthanide emission could be detected for the $[Eu(4\text{-}^{is}Pr\text{-}PhQuinque)_2][ClO_4]_3$ complex due to de-complexation in solution.

2.10.13 The Luminescence Properties of $[Tb(4\text{-}^{is}Pr\text{-}PhQuinqueO_2)_2][ClO_4]_3$

Analogous to the Eu(III) complex, at low concentrations only ligand emission was observed. Therefore, a concentrated sample (400μmol) in DMF at room temperature was analysed yielding the emission spectrum but which was too concentrated to obtain an absorbance spectrum. The concentrated sample (400μmol) gave an emission spectrum ten times weaker than that of the Eu(III) complex. As

well as Tb(III) emission, a broad ligand emission centred at 410nm can be seen in the emission spectrum.

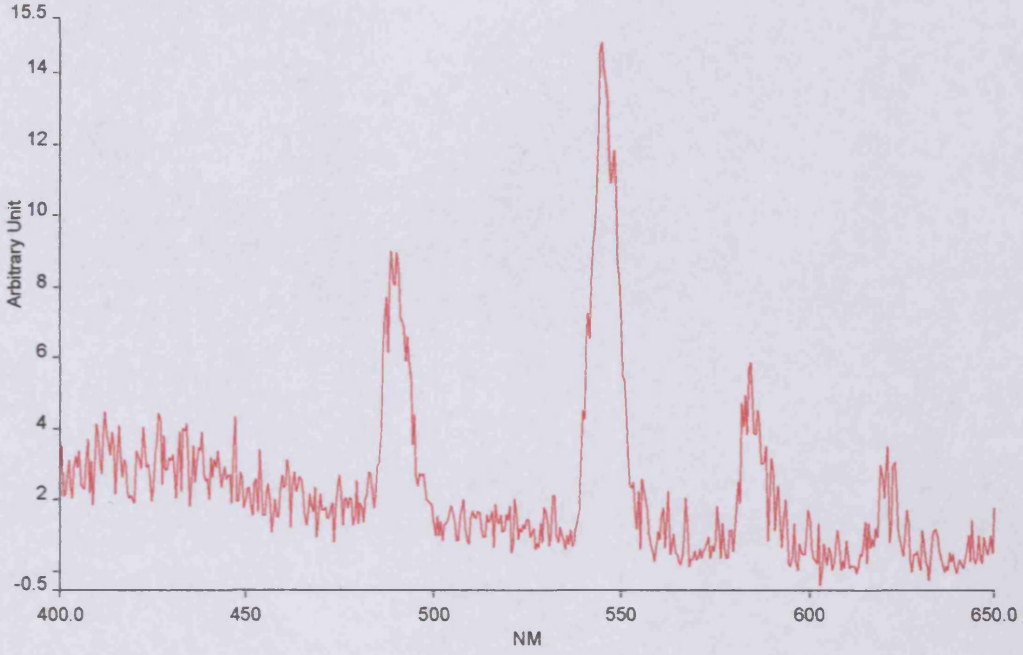

Fig.2.43: The emission spectrum of the concentrated sample of $[Tb(4\text{-}^{is}Pr\text{-}PhQuinqueO_2)_2][ClO_4]_3$ (λ_{exc} =367nm, λ_{emis} =544nm).

The relative integrated areas of the $^5D_4 \rightarrow {}^7F_J$ transitions are 1.0, 1.7, 0.55 and 0.16 for J=6, 5, 4 and 3 respectively.

2.11 Relative Quantum Yields and Discussion

The relative quantum yields (Φ) of the compounds were analysed using equation 1.2 and the method described therein. The compounds that exhibited decomplexation at low concentrations were unable to be measured due to the required low concentrations to obtain an absorbance of 1, therefore equimolar solutions of these complexes (400μmol) have been measured under the same excitation maximum to obtain a comparative value. All compounds in this study have been measured relative to $[Eu(PhTerpyAcid_2)(H_2O)_2][ClO_4]_2$ (to be discussed in chapter 3) which has been assigned the arbitrary value of 1. The photophysical properties of the previously characterised species $[Eu(terpy)_3][ClO_4]_3$ was also measured for comparative purposes. A summary of the results is given in table 2.9.

Compound	Solvent	ε_{max} ($M^{-1}cm^{-1}$)	η^a	Φ^b	Luminescence Intensity of equimolar solutions (400μmol)[b,e]
$Eu(Terpy)_3^{3+}$	CH_3CN	-	2.5	0.38[c]	-
$Eu(TerpyO)_3^{3+}$	CH_3CN	68 960 (204nm)	6.25	0.56[c]	-
$Eu(TerpyO_2)_3^{3+}$	CH_3CN	60 850 (232nm)	16.67	0.32[c]	0.25
$Eu(TerpyO_3)_3^{3+}$	CH_3CN	50 520 (220nm)	9.09	0.18[c]	-
$Eu(4\text{-}^{is}Pr\text{-}PhQuater)_2^{3+}$	CH_3CN	-	5.58	-	0.96
$Eu(PhQuaterO_2)_2^{3+}$	CH_3CN	74 703 (254nm)	10.75	0.50[d]	15.23
$Eu(PhQuaterO_4)_2^{3+}$	CH_3CN	72 778 (230nm)	37.6	1.18[d]	73.59
$Eu(4\text{-}^{is}Pr\text{-}PhQuinque)_2^{3+}$	CH_3CN	-	-	-	0
$Eu(4\text{-}^{is}Pr\text{-}PhQuinqueO_2)_2^{3+}$	CH_3CN	-	4.5	-	0.318
$Tb(Terpy)_3^{3+}$	CH_3CN	69 404 (204nm)	-	0.258[c]	-
$Tb(TerpyO)_3^{3+}$	CH_3CN	62 240 (204nm)	-	0.025[c]	-
$Tb(TerpyO_2)_3^{3+}$	CH_3CN	66 340 (230nm)	-	0[c]	-
$Tb(4\text{-}^{is}Pr\text{-}PhQuater)_2^{3+}$	CH_3CN	-	-	-	2.03
$Tb(4\text{-}^{is}Pr\text{-}Phquinque)_2^{3+}$	CH_3CN	-	-	-	0.17
$Tb(4\text{-}^{is}Pr\text{-}PhQuinqueO_2)_2^{3+}$	CH_3CN	-	-	-	0.034

Table 2.9: Absorption and emission characteristics. [a]η=J2/J1 [b](in relation to $[Eu(PhTerpyAcid_2)(H_2O)_2][ClO_4]_2$ =1) [c]excitation wavelength of 314nm [d]excitation wavelength of 332nm [e]excitation wavelength of $\lambda_{exc\ max}$

It should be mentioned first of all the high error involved in these relative quantum yield measurements. At least a 10% error can be assumed in the observed quantum yields and so only general observations have been made regarding the measured compound properties.

All of the complexes have shown adequate solubility in acetonitrile with the solubility decreasing from the terpyridines to the quinquepyridines. With regard to absorption properties, the quaterpyridines exhibit the highest extinction coefficients. The introduction of heterocyclic N-oxide groups improves the absorption maximum of these ligands with increases of up to 15 693$M^{-1}cm^{-1}$ making the ligands more efficient antennas. Since complexation gives rise to a red shift of the quaterpyridine N-oxide absorptions, the observed differences may be related to the amount of ligand-metal interaction in the complex. This fact can be used to help reinforce the idea of decomplexation occurring in the Eu(4-^{is}Pr-PhQuaterpyridine)$_2$ complex (whose absorption spectrum is identical to that of the free ligand at low concentration) as it is unlikely that the ligand-metal interaction is so minimal that no shifts are seen in the absorption spectrum. The absorption spectra of the terpyridine N-oxide complexes display a photochemical reaction that is also apparent in the free ligands. One possible explanation is the photochemical ring opening of the pyridine N-oxide which is a known reaction.[36] Attempts to carry out these photochemical reactions preparatively have resulted in complex mixtures of species that we were unable to separate or characterise by ^{1}H-NMR studies.

The relative luminescence yields are generally higher for Eu(III) than for Tb(III) chelates of the ligands. The complex with the lowest relative quantum yield is the Tb(terpyO)$_3$(ClO_4)$_3$ complex (Φ=0.025) and the complex with the highest relative quantum yield is Eu(PhQuaterO$_4$)$_2$(ClO_4)$_3$ (Φ=1.18). The Eu(PhQuaterO$_4$)$_2$(ClO_4)$_3$ is also the most luminescent complex when analysed as a concentrated solution with Tb(4-^{is}Pr-PhQuinque)$_2$(ClO_4)$_3$ being the least luminescent. The Eu(4-^{is}Pr-PhQuinque)$_2$(ClO_4)$_3$ complex did not appear to exhibit any appreciable metal-

centred luminescence at room temperature when the absorption bands of the ligand are excited. From the observations thus far it would appear that the quaterpyridines provide the best matching of the ligand triplet state to the excited lanthanide metal state for the LMCT process, though it is difficult to be certain due to the various factors which affect luminescence intensity. Also, it would seem from the data that Eu(III) provides a better matching of energy levels between the ligand and metal than Tb(III) with the $Eu(terpyO)_3^{3+}$ complex having a ~22 times greater Φ than $Tb(terpyO)_3^{3+}$.

Comparison of solutions of the terpy N-oxide series of complexes (using excitation 310nm) shows that as the number of N-oxide groups in a complex decrease, then the relative luminescence intensity increases. However, it should be noted that the total removal of all N-oxides donors, i.e. the parent $[Eu(terpy)_3][ClO_4]_3$ complex, results in a decrease in luminescence relative to the mono-oxide (although, the Φ value for $[Eu(terpy)_3][ClO_4]_3$ is not an accurate value as at the required 68μmol concentration a notable degree of ligand emission is observed, thus giving an inaccurate reading for the complex. This has been previously observed for the complex,[34] and is perhaps related to its low value of η signifying the poor donor property of the ligand. The approximate ratios of these relative quantum yields is 13:7:4:9 for mono-oxide:bis-oxide:tris-oxide:unsubstituted terpyridine. Comparison of solutions of the quaterpyridine N-oxide complexes (using excitation 326nm) shows a differing result with the luminescence intensity increasing with an increasing number of N-oxide donors. The quinquepyridines show a similar trend to the quaterpyridines with the luminescence intensity increasing with the introduction of N-oxide donors; very poor or no Eu(III) or Tb(III) emission is observed except when N-

oxides are present. While other groups have shown that the inclusion of an N-oxide group has increased the luminescent properties of their complexes[7, 37 and 38] as with the quaterpyridine and quinquepuridine complexes described here, our findings with the terpyridines are similar to those of Pietraszkiewicz,[32] who found no simple correlation between the luminescence intensity and the number of N-oxide groups.

The inclusion of the N-oxides, which although do not provide a simple correlation to an increase in luminescence intensity, do seem to increase the binding capabilities of the ligands to lanthanides. The ter- and quaterpyridine N-oxide complexes neither exhibit decomplexation of their complexes in solution at low concentration or ligand emission in their emission spectra indicating stronger lanthanide binding, whereas the un-oxidised ter- and quaterpyridine complexes show both decomplexation at low concentration and ligand emission in their absorbance and luminescence spectra. Analysis of the η values possibly reflects this observation with the ter- and quaterpyridine N-oxides having much higher values (lowest η=8.19) than the parent complexes (η=2.5 for $[Eu(terpy)_3][ClO_4]_3$). Also of interest is that the highest observed value of η (37.6) belongs to the most luminescent complex $Eu(PhQuaterO_4)_2$ whilst the least luminescent complex in the series, $Eu(terpyO_3)_3$, has one of the lowest measured η values of 9.09.

It should be remembered at this point that changes in luminescence intensity can be attributed to three factors. i) The energy matching of the ligand triplet level and the metal excited state ii) Changes in geometry and ligand field. iii) Changes in the number of solvent molecules coordinated to the lanthanide metal. An increasing number of N-oxide donors will affect all three factors to varying degrees and it is

difficult to determine which factor is being affected if not all. Using the Eu(4-^{is}Pr-PhQuinque)$_2$ and Eu(4-^{is}Pr-PhQuinqueO_2)$_2$ complexes as a case in point, the N-oxide has increased the luminescence of the complex compared to its parent complex but unlike the terpyridine and quaterpyridine N-oxides, it appears to exhibit a decomplexation of the ligand at low concentrations. It is difficult to believe that the complexes do not bond to the lanthanide ions as well as the quaterpyridines but actually forms a 1:1 complex with up to four solvent molecules coordinated thus reducing the luminescence intensity due to O-H vibrations. This however would be difficult to assess as the complexes are not luminescent in D_2O/H_2O due to dissociation and so the number of lanthanide-bound water molecules (q) cannot be determined by experimental lifetimes at 295K in H_2O and D_2O solutions (see chapter 1.6).

2.12 Conclusions

The ligands investigated appear to be good building blocks for designing extended ligands aimed at sensitising trivalent luminescent europium and terbium ions. The most intense luminescence is shown by the $Eu(PhQuaterO_4)_2$ complex. This conclusion is drawn from both the efficiency of absorption (ε =72 778 $M^{-1}cm^{-1}$) and the relative quantum yield (Φ=1.18, relative to $[Eu(PhTerpyAcid_2)(H_2O)_2][ClO_4]_2$=1). The complexes that had to be analysed at high concentrations gave an idea as to the order of complex luminescence intensities but had the problem that they were not absorbing an equal amount of UV light so not allowing a fair comparison.

One of the more prominent observations of this part of the investigation is the presence of a concentration effect, which must reflect on the chemical stability of the complexes. The non-oxidised complexes exhibited the greatest susceptibility to decomplexation at low concentration (<100μmol) with purely ligand emission being observed in the emission spectra. The inclusion of the N-oxides appeared to increase the chemical stability of the complexes with no or very little ligand emission being observed at low concentration (<100μmol), only Eu(III) or Tb(III) emission. Also of interest is the lack of a simple correlation between the luminescent intensity and the number of N-oxide donor groups. This shows how difficult it is to predict and assess how the luminescence properties of a complex will be affected by modification but it should also be considered that this complication can also be one of the advantages of these types of lanthanide complex systems. As the ligand is both the lanthanide sensitiser and lanthanide-shielding moiety, when one is altered so is the other.

Considering that the main application probably lies in the use of Eu(III) and Tb(III) complexes as luminescent labels in fluoroimmunoassays, it will also be necessary to take into account the possible effects that both the attachment of the label to the biological species and the serum medium may have on the luminescent intensity and on the chemical stability of the complexes. Obviously, the chemical stability of the complexes has been shown to be inadequate at this stage and further modifications are required. These modifications to increase binding strength are to be discussed in the next chapter.

2.13 References

1) M. Burrows, Synthesis and Coordination of Polypyridyl N-oxide Ligands, PhD Thesis, UWC, 2002.

2) F. Kröhnke, *Synthesis*, (1976), 1.

3) W. Zecher, F. Kröhnke, *Chem. Ber.*, **94**, (1961), 690 and 698 and 707.

4) G. W. V. Cave, C. L. Raston, *Chem. Commun.*, (2000), 2199-2200.

5) D. L. Jameson, L. E. Guise, *Inorg. Synth.*, **32**, 46.

6) D. L. Jameson, L. E. Guise, *Tetrahedron Lett.*, **32**, (1991), 1999.

7) J.M. Lehn, Christine O. Roth, *Helv. Chim Acta.*, 74 (1991), 572. L. Prodi, M. Maestri, V. Balzani, J.M. Lehn, C. Roth, *Chem. Phys. Lett.*, 180, (1991), 45.

8) Coord. Chem. Rev., 123, (1993), 201-228

9) C. O. Paul-Roth, J. M. Lehn, J. Guilhem, C. Pascard, *Helv. Chim Acta.*, 78, (1995), 1895.

10) A. R. Katrizky, J. M. Lagowski, *Chemistry of the Heterocyclic N-oxides*, academic press, (1971).

11) M. Nakajima, M. Saito, M. shiro, S. M. Hasimoto, *J. Am. Chem. Soc.*, **120**, (1998), 6419.

12) B. Q. Ma, S. Gao, H. L. Sun, G. Xian-Xu, *J. Chem Soc. Dalton Trans.*, **201**, 130.

13) E. Barmejo, R. Carbello, A. Castineiras, R. Dominguez, C. Maichle-Mossmer, J. Strahle, D.X. West, *Polyhedron*, (1995), 3695.

14) J. T. Hung, S. Kumaresan, L. C. Lin, Y. S. Wen, L. K. Liu, L. K. Lu, J. R. Hwu, *Organometallics*, **15**, (1996), 5605.

15) P. Brougham, M. S. Cooper, D. A. Cummerson, H. Heaney, N. Thompson, *Synthesis*, (1987), 1015-1017.

16) S. Daya, M. Kol, S. Rozen, *Synthesis*, (1999), 1427-1430.

17) C. Coperet, H. Adolfsson, V. T. A. Khuong, A. K. Yudin, K. B. Sharpless, *Tetrahedron Lett.*, **39**, (1998), 761.

18) S. Caron, N. M. Do, J. E. Sieser, *Tetrahedron Lett.*, (2000), 2299-2302.

19) F. H. Case, *J. Org. Chem.*, **27**, (1962), 640.

20) R. P. Thummel, Y. Jahng, *J. Org. Chem.*, **50**, (1985), 3635-3636.

21) S. Dayan, S. Rozen, *Angew. Chem. Int. Ed.*, **38**, (1999), 3471.

22) A. J. Amoroso, M. W. Burrows, R. Haigh, M. Hatcher, M. Jones, U. Kynast, K. M. A. Malik, D. Sendor, Paper to be published.

23) F. Renaud, C. Piguet, G. Bernardinelli, G. Hopfgartner, J.-C. G. Bünzli, *Chem. Commun.*, **1999**, 457.

24) F. Renaud, C. Piguet, G. Bernardinelli, G. Hopfgartner, J.-C. G. Bünzli, *J. Am. Chem. Soc.*, **121**, (1999), 9326.

25) D. A. Bardwell, J. C. Jeffery, P. L. Jones, J. A. McCleverty, E. Psillakis, Z. Reeves, M. D. Ward, *J. Chem. Soc., Dalton Trans*, (1997), 2079-2086.

26) C. O. Paul-Roth, J.-M. Lehn, J. Guilhem, C. Pascard, *Helv. Chim. Acta.*, **78**, (1995), 1895.

27) P. Gawryszewska, L. Jerzykiewicz, M. Legendziewicz, J. P. Riehl, *Inorg. Chem.*, **39**, (2000), 5365.

28) J. L. Toner, Eur. Pat. Appl. EP288, 256.

29) W. Dai, H. Hu, X. Wei, S. Zhu, D. Wang, K. Yu, N. Dalley, X. Kou, *Polyhedron*, **16**, 12, (1997), 2059-2065.

30) A. Seminara, A. Musemeci, *Inorg. Chim. Acta.*, **95**, (1984), 291-307.

31) (a) A. Musumeci, R. P. Bonomo, A. Seminara, *Inorg. Chim. Acta.*, **45**, (1980), L169-71. (b) A. Musumeci, R. P. Bonomo, V. Cucinotta, A. Seminara, *Inorg. Chim. Acta.*, **59**, (1982), 133.

32) M. Pietraszkiewicz, J. Karpiuk, O. Pietraszkiewicz, *J. Alloys Comp.*, **141**, (2000), 300-301.

33) D. A. Durham, G. H. Frost, F. A. Hart, *J. Inorg. Nucl. Chem.*, **31**, (1969), 833-838.

34) S. Petoud, J-C. Bünzli, K. J. Schenk, C. Piguet, *Inorg. Chem.*, **36**, (1997), 1345-1353.

35) V-M Mukkala, C. Sund, M. Kwiatkowski, P. Pasanen, M. Högberg, J. Kankare, H. Takalo, *Helv. Chim. Acta*, **75**, (1992), 1621-1632.

36) C. Lohse, L. Hagedorn, A. Albini, E. Fasani, *Tetrahedron*, **44**, (1998), 2591.

37) For example see: (a) G.F. de Sa, W. M. d Azevedo, A. S. L. Gomes, *J. Chem. Res.*, (1994), 234. (b) P. Gawryszewska, L. Jerzykiewicz, M. Pietraszkiewicz, J. Legendziewicz, J. P. Riehl, **39**, (2000), 5365.

38) C. De Mello Donega, S. A. Junior, G. F. de Sa, *chem. Comm.*, (1996), 1199.

Chapter 3

Oligopyridine Acid and Amide Lanthanide Complexes

3.1 Introduction

The Eu(III) and Tb(III) chelates of ter-, quater- and quinquepyridine were shown to be potential probe alternatives in fluoroimmunoassays. However, in evidence were two major problems involving a lack of chemical stability of the complexes in solution and also ligand instability, specifically a photochemical reaction that is occurring with irradiation of the terpyridine N-oxides. To overcome these problems it was decided to attach strong lanthanide binding groups to the 6 position of the external pyridines to not only increase stability of the complexes but also to stabilise the ligands themselves. The obvious choice was the inclusion of hard anionic carboxylate groups. Various groups have utilised this binder successfully and some of the strongest macrocyclic ligands reported are extended carboxylic acid system such as DOTA.[1] Therefore, the targeted ligands incorporating carboxylic acid binders are shown in fig 3.1.

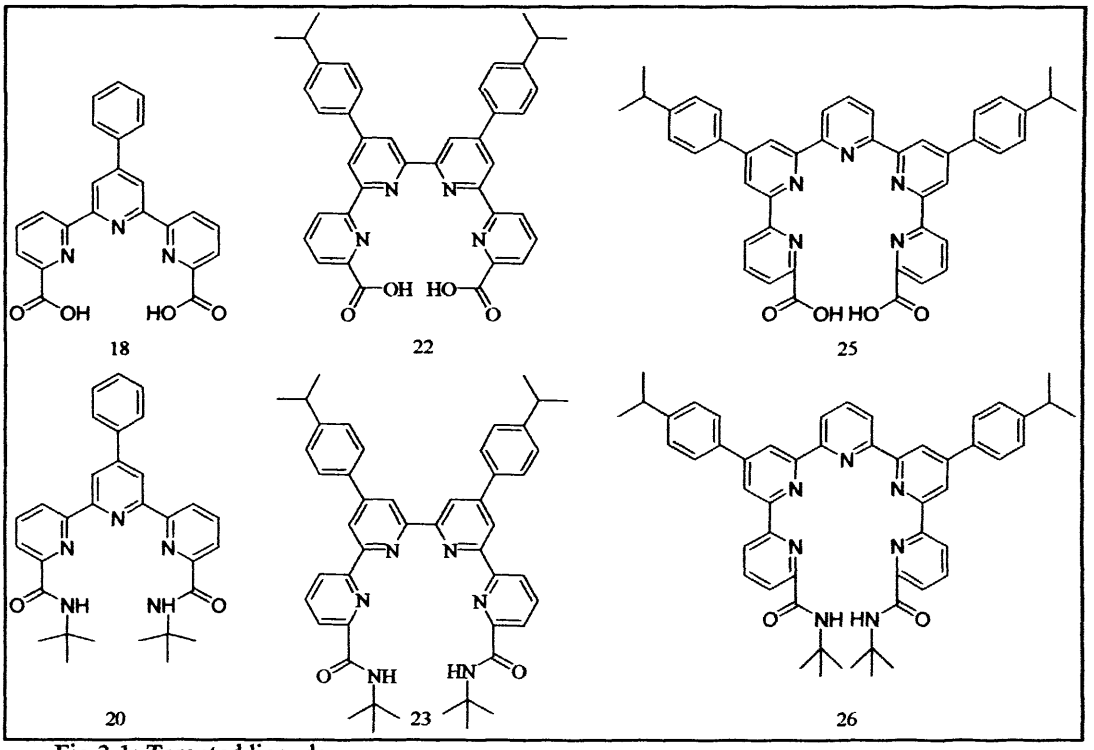

Fig.3.1: Targeted ligands

The inclusion of the phenyl groups on the backbone of the terpyridine sensitiser are to provide an extra light-absorbing moiety, previous studies have shown an increase in lanthanide complex quantum yields of 4-alkylated 2,2';6',2''-terpyridines.[2] The inclusion of the isopropyl groups shall become apparent upon reading the ligand synthesis section, they are merely present to increase the solubility properties of the ligand in required solvents such as DCM. Preliminary results of the acid bearing compounds **18**, **22** and **25** found the ligands to be strong coordinators of lanthanide(III) ions and able to transfer energy from the ligand triplet state to the excited metal state of the lanthanide with varying degrees of efficiency. However, the complexes were found to possess limited solubility being only soluble in DMF solutions with that solubility decreasing from the bipyridines to the quinquepyridines. They have shown only limited or no solubility in water, acetonitrile and alcohols. The replacement of the acid groups with *tert*-butyl amides to give ligands **20**, **23** and **26** was decided upon to increase the solubility of the oligopyridines. The introduction of the amides would also be of interest for the investigation of their properties in the energy transfer process and to determine if they assist effective coordination of the lanthanides. The N-oxides of **18** were also synthesised and coordinated with Eu(III) to determine any improvement in the luminescence characteristics. Also the ligand **29** was synthesised for comparative purposes. Its Eu(III) complex has previously been analysed by Bünzli and co-workers[3] who determined its absolute quantum yield in water. The relative quantum yields were determined of all the complexes and a comparison carried out across this series and the complexes from the previous chapter to determine any improvements of luminescent properties and the optimum lanthanide sensitizer.

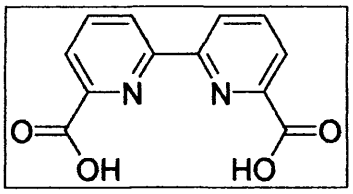

Fig.3.2: Ligand **29**

Toner and co-workers have previously reported compounds such as **18** and recommended it as a suitable lanthanide sensors in a past patent[4] but they did not study the influence of the chelating groups on the luminescent properties of lanthanide complexes or isolate and characterise the complexes. Also, very few quantum yields were measured. Similar ligands with an increased number of binding arms such as the carbonyliminodiacetic acid (see Fig. 3.3) are also described therein.

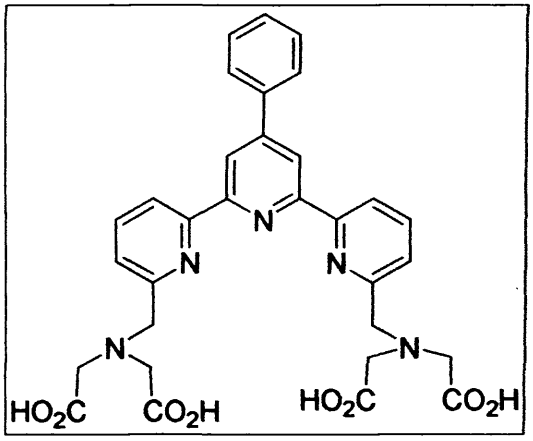

Fig.3.3: carbonyliminodiacetic acid example

The research groups of group of Mukkala *et al*, as discussed in chapter 1, have successfully synthesised and briefly reported similar compounds using the carbonyliminodiacetic acid arms instead of carboxylic acids.[5] Their study showed promising results and that the presence of carboxylic acid arms led to an enhancement of the overall stability of the complexes. Also, the group of Yuan has carried out similar work using polyacid derivatives of thienyl-substituted terpyridine analogues (see chapter 1).[6]

With regards to saturation of the coordination sites around the lanthanide ions (typically eight or nine) the group of Sammes and co-workers have carried out synergistic chelation investigations with ligands similar to **18**.[7 and 8] Due to the pentadentate coordination capabilities of **18**, if only one ligand is coordinated to the metal centre then theoretically there may be four sites free for coordination of solvent molecules, but if two ligands are coordinated to give a ten coordination geometry then it is obvious one site is going to be uncoordinated and the metal will be sterically very crowded. These spare coordination sites might cause the self-assembly of large supramolecular type structures, as previously observed in the mono-acid terpyridine-6-carboxylic acid.[9] In this compound a hexameric europium wheel is formed giving complicated spectroscopic and analytical results. To fill any empty coordination sites Sammes and co-workers studies have shown that provided the coordination sites around the ion are not over-occupied, a second ligand can also approach and coordinate. They went on to develop a luminescence trigger in which the sensitizer approaches the shielded cation to from a 1:1:1 complex that exhibits efficient luminescence. Their results were successful when utilising macrocyclic systems such as aza-crown derivatives but with regards to compound **18**, lifetime results indicated that the corresponding EuL and EuL_2 complexes were being formed, concluding that terpyridine diacids are not suitable for ternary assay systems.

The quaterpyridine and quinquepyridines **22** and **25** should pose less of a problem; with six and seven site coordination possible the formation of 1:1 complexes is more likely than 2:1 complexes. Although this still leaves a number of sites free for coordination of solvent molecules the ligands themselves might prevent the approach of these unwanted solvent molecules by the improved shielding configurations

adopted by these ligands. Dai and co-workers have found that the similar quinquepyridine ligands **27** and **28** (see Fig.3.4) can form mono helical and double helical configurations with copper and cadmium.[10] The double helical complex was obtained by **27** coordinating around two copper atoms with a hexa-coordination geometry via the nitrogen atoms (see Fig.3.5). The structure successfully prevents the approach of solvent molecules, wrapping up the copper atom. The monohelical complex is achieved by **28** coordinating around one cadmium atom (see fig.3.6). The Cd(II) ion is of the correct size (r = 1Å) for the cavity of the quinquepyridine in the all cis conformation (r = 1Å) easily forming the mononuclear complex, while the size of the copper ion is too small. Eu(III) has a ionic radius of 1.09Å and could easily fit into this cavity. The only drawback of the monohelical structure is that it still allows the approach of two solvent molecules, although the two extra acid arms could possibly block the area of approach for complexes of **25**.

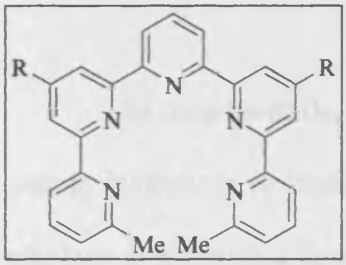

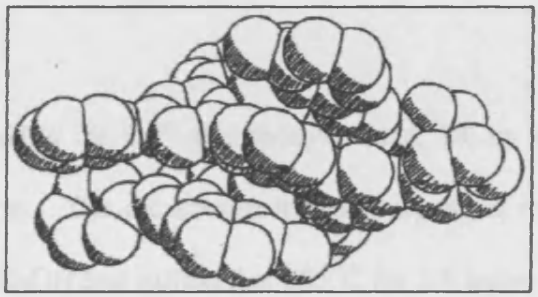

Fig.3.4: Ligand **27** (R=Phenyl) and Ligand **28** (R=H). Fig. 3.5: Double helical configuration of Cu[**27**]$_2$

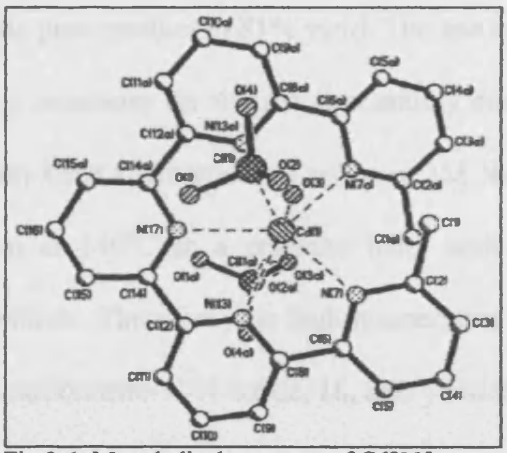

Fig.3.6: Monohelical structure of Cd[**28**]

3.2 Synthesis of 4'-phenyl-2,2':6',2''-terpyridine-6,6''-dicarboxylic acid 1,1',1''-trioxide and -6,6'''-dicarboxamide

The ligand 4'-phenyl-2,2':6',2''-terpyridine-6,6''-dicarboxylic acid 1,1',1''-trioxide, **19**, was synthesised following the four-step reaction shown in scheme 3.1. Synthesis of the bis- and tris-oxide ligands were in the same manner as described in chapter two and were followed by a modified *Reissert-Henze* reaction.[11] This involved treatment of the N-oxide with a ten-fold excess of trimethylsilanecarbonitrile and a four-fold excess of benzoyl chloride in dichloromethane at ambient temperature with stirring for 14 hours to yield the 6,6''-dicarbonitrile, **17**. After the addition of 10% sodium carbonate and filtering, a simple washing process with water yielded the pure product in 77% yield for the 6,6''-dicarbonitrile, **17**, and 41% yield for the 6,6''-dicarbonitrile-1'-N-oxide, **16**.

The dicarbonitrile, **17**, was converted to the 6,6''-dicarboxylic acid, **18**, by a simple hydrolysis in basic aqueous solution. The dicarbonitrile was suspended in ethylene glycol with a three-fold excess of NaOH and refluxed at 205°C for 2.5 hours. An extraction with ether-toluene followed by acidification to pH 5 of the aqueous solution precipitated the pure product in 81% yield. The use of ethylene glycol at such a high temperature was necessary for the reaction mainly due to solubility problems. The reaction had already been attempted by a reflux in 3M NaOH and also by a reflux in 5M NaOH solution at 140°C in a pressure tube, with starting material being obtained with both methods. Therefore, the high temperature forcing conditions were required. The 6,6''-dicarbonitrile-1'-N-oxide, **16**, also yielded the same reaction

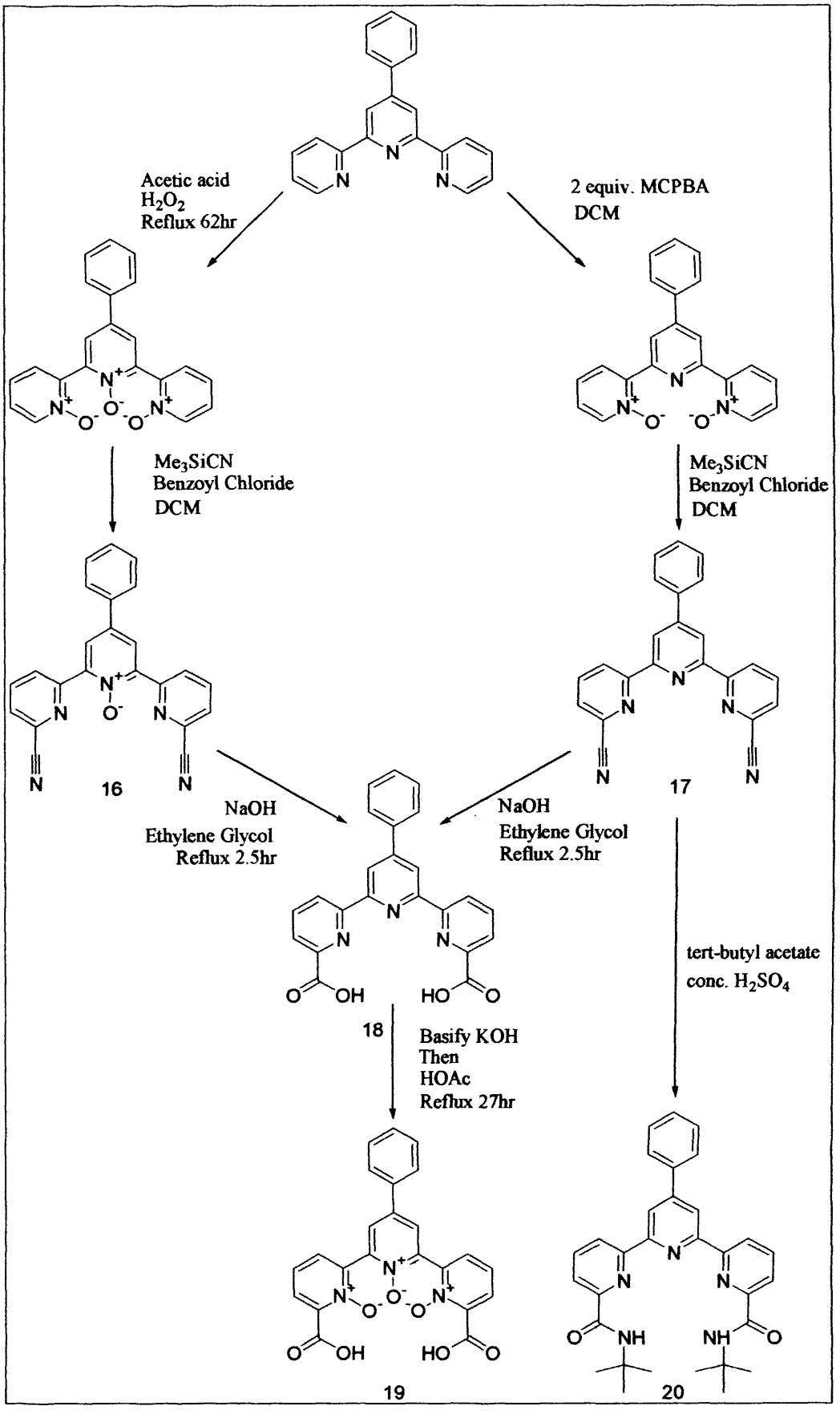

Scheme 3.1: Reaction scheme for the synthesis of 4'-phenyl-2,2':6',2''-terpyridine-6,6''-dicarboxylic acid 1,1',1''-trioxide and diamide

product, 6,6''-dicarboxylic acid, with complete removal of the N-oxide. It was hoped the reaction would maintain the N-oxide to yield the 6,6''-dicarboxylic acid-1'-N-oxide which might have been an interesting binding ligand.

Oxidation of the 6,6''-dicarboxylic acid, **18**, to yield N-oxides proved to be quite difficult. Selective oxidation by the use of mcpba to yield mono- or bis-oxides proved futile. This is probably due to the steric hindrance introduced by the carboxylic acid arms now in the 6 position of the external pyridine rings, preventing approach of the mcpba oxidiser. Non-selective oxidation, using H_2O_2 to synthesis the tris-oxide, **19**, proved successful although care has to be taken to fully oxidise the ligand. Mixtures can be obtained which we were unable to separate, even by column chromatography where the presence of the acid groups causes the compound to be retained by the solid phase. Synthesis of **19** first required basification of the ligand with KOH in MeOH to enable solubility of the ligand in the solvent. The ligand was then oxidised in glacial acetic acid with the addition 30% H_2O_2 and a 24-hour reflux, similarly to the method discussed in the previous chapter. Concentration of the solution in vacuo and adjustment of the solution to pH 5 precipitated the product in 61% yield.

Conversion of the nitrile to the *tert*-butyl amide, **20**, was achieved by the use of a modified Ritter reaction.[12] Slow addition of a catalytic amount of concentrated sulphuric acid to a stirred solution of **17** in *tert*-butyl acetate followed by stirring for 5 hours at 45°C yielded two layers with the bottom brown layer being collected and neutralised with 20% potassium carbonate to precipitate the product. Washing with methanol yielded the pure product in 36% yield.

Spectral and analytical data for all compounds synthesised are fully in accord with each of the proposed structures. IR studies for **16** and **17** both indicated the presence of the nitrile functionality with weak absorptions at 2233cm^{-1}. The characteristic bis-oxide peaks at 1259, 1227 and 1211cm^{-1} were absent for **17** and for **16** the tris-oxide peaks at 1273 and 1247cm^{-1} had been replaced by a single peak at 1244cm^{-1} indicative of the 1'-N-oxide. Similar to the precursor compounds the absorption bands characteristic of the pyridine moiety were present ($\nu_{C=C}$ and $\nu_{C=N}$ at 1591(w) and ν 1577(s)). IR studies of the 6,6''-dicarboxylic acid, **18**, showed the removal of the nitrile stretch and the introduction of the C=O stretch at 1705(s) cm^{-1}. The C-O stretch is apparent at 1296(w) cm^{-1} with the O-H stretch present at 3427cm^{-1}. The absorption bands characteristic of the pyridine moiety were present ($\nu_{C=C}$ and $\nu_{C=N}$) with a shift from 1591 and 1571cm^{-1} in the nitrile compound to 1601 and 1584cm^{-1}. IR studies of the 6,6''-dicarboxylic acid 1,1',1''-trioxide, **19**, showed a shift of the C=O stretch from 1705 to 1715cm^{-1} due to the presence of the polarised N-oxides. The characteristic N-O stretch appeared at 1261(m) cm^{-1} with a weaker peak at 1230cm^{-1}, lower than the tris-oxides N-O stretches (1273 and 1247cm^{-1}). The pyridine moiety absorptions had undergone a large shift from 1601 and 1584cm^{-1} to 1603 and 1490cm^{-1}. IR studies of the 6,6''-dicarboxamide, **20**, showed the removal of the nitrile stretch and the presence of C=O (1681(s) cm^{-1}) and N-H stretches (3381(m) cm^{-1}) characteristic of the amide group. N-H bending could also be observed at 1570 and 1553cm^{-1}. The typical pyridine absorption bands were also present at 1584 and 1517cm^{-1}.

Mass Spectrum studies of all ligands indicate unambiguously the described structures. The EI+ spectrum of the 6,6''-dicarbonitrile, **17**, shows an intense peak at

m/z=359 corresponding to the parent ion as well as fragmentation of the compound to m/z= 331 and 306, denoting the loss of one and two nitrile groups respectively. Accurate mass measurements using ES+ gave the correct value of $[M+H]^+$= 360.1253 (calculated mass = 360.1249). The EI+ spectrum of the dicarbonitrile-1'-mono oxide, **16**, shows an intense peak at m/z=376 corresponding to the parent ion. Extensive fragmentation is present in the spectrum with the more indicative fragmentation products being at m/z=332 (the loss of two nitrogen's from the nitrile groups and also the oxygen from the N-oxide), 320 and 308 (the loss of one and two carbons from what is left of the nitrile groups). The CI+ spectrum of the 6,6''-dicarboxylic acid, **18**, shows an intense peak at m/z=398 corresponding to the protonated parent ion, $[M+H]^+$. Fragmentations to m/z= 368 (loss of two oxygen's from the acid groups), 354 (loss of one acid group) and 310 (loss of the two acid groups) are all indicative of the proposed structure. The FAB spectrum of the 6,6''-dicarboxylic acid 1,1',1''-trioxide, **19**, showed the diprotonated parent ion peak present at m/z=445. Fragmentations to m/z= 401(loss of an acid group), and 353 (loss of the three N-oxide oxygens and an acid group) are both indicative of the proposed structure. Accurate mass measurements using ES+ gave the correct value of $[M+H]^+$= 446.0992 (calculated mass = 446.0988). The EI+ spectrum of the 6,6''-dicarboxamide, **20**, shows an intense peak at m/z=508 corresponding to the parent ion as well as fragmentation of the compound to m/z= 452, denoting the loss of one tert-butyl group. Accurate mass measurements using ES+ gave the correct value of $[M+H]^+$= 508.2706 (calculated mass = 508.2707).

The ^{1}H-NMR spectra, similar to the mass spectra, all indicate unambiguously the proposed structures for the discussed ligands. The NMR data is presented in table 3.1.

Compound	H3	H4	H5	H6	H3'	H_O	H_M	H_P	$H_{t\text{-butyl}}$
PhTerpy (**1b**)	8.62	7.85	7.31	8.69	8.69	7.82	7.45	7.43	-
PhTerpyO_2 (**3b**)	8.16	7.26	7.26	8.41	9.15	7.77	7.37	7.37	-
PhTerpyCN_2 (**17**)	8.81	7.96	7.86	-	8.76	7.70	7.72	7.46	-
PhTerpyCN_2O (**16**)	8.97	7.95	7.74	-	8.36	7.74	7.51	7.42	-
PhTerpyAcid$_2$ (**18**)	8.94	8.26	8.19	-	8.94	7.98	7.67	7.61	-
PhTerpyA_2O_3 (**19**)	8.48	7.92	8.28	-	8.45	7.90	7.57	7.49	-
PhTerpyAmide$_2$ (**20**)	8.73	7.99	8.22	-	8.61	7.80	7.54	7.47	1.5

Table 3.1: ^{1}H-NMR data for the ligands synthesised (ppm)

The ^{1}H-NMR in $CDCl_3$ of PhenylTerpyCN_2, **17**, displays seven peaks with the correct integrals and expected coupling patterns present. The loss of one peak from the spectrum points towards the formation of the nitrile compound from the 1,1''-bisoxide. With the removal of the N-oxides the proximity effect of the δ^- oxygen's is no longer felt by the H3' proton and thus is observed at a similar chemical shift as un-substituted 4'-phenyl-2,2':6',2''-terpyridine, **1b**. The H3 and H4 protons are now shifted 0.65 and 0.7 ppm respectively downfield, reminiscent of the parent ligand **1b**, with H5 experiencing a shift of 0.6 ppm downfield compared to the precursor 1,1''-bisoxide ligand, **3b**. The phenyl group does not experience any of the changes to any great degree and only small shifts are observed.

The ^{1}H-NMR in $CDCl_3$ of the oxidised PhenylTerpyCN$_2$O, **16**, displays seven peaks with the correct integrals and expected coupling patterns present. The presence of the N-oxide in the N2 position is highlighted by a 0.81 ppm downfield shift of the H3 proton combined with a small 0.48 ppm downfield shift of the H5 proton compared to the precursor ligand **3b**. The δ^- oxygen proximity causes a greater effect on the surrounding protons than the electron withdrawing nitrile groups in the H6 and 6'' positions, as can be seen by comparison of the 6,6''-dicarbonitrile and the dicarbonitrile-1'-mono oxide data.

The PhTerpyAcid$_2$ ligand, **18**, is very insoluble in its protonated form, being only soluble in heated DMSO (deprotonation yields the ligand soluble in alcohols). The ^{1}H-NMR in D_6-DMSO displays several peaks with correct integrals and expected coupling patterns present. The acid group OH proton is not observed. The conversion of the nitrile to the carboxylic acid produces further chemical shifts in the pyridyl ring protons to which they are attached. Due to the greater electron-withdrawing strength of the carboxylic acid over the nitrile group, H5 and H4 experience shifts of 0.33 ppm and 0.30 ppm respectively downfield and H3 undergoes a smaller shift of 0.13 ppm downfield compared to the precursor 6,6''-dicarbonitrile ligand, **17**. Once again the phenyl group does not experience any of the changes to any great degree and only small shifts are observed.

With the introduction of the N-oxides to the 4'-phenyl-2,2':6',2''-terpyridine-6,6''-dicarboxylic acid ligand, the ^{1}H-NMR of ligand **19** exhibits the effects produced by both the carboxylic acid and the tris-N-oxides. Similarly to 2,2':6',2''-terpyridine-1,1',1''-tri oxide, **4a** in chapter 2, it is predicted that the steric hindrance of the ligand

prevents the ligand lying in a planar manner. With this deviation of the conformation preventing the enhanced deshielding effect produced by the extended ring system, a drop in the chemical shift is observed in the ligand system protons with H3' and H3 undergoing the most drastic shifts occurring 0.49 ppm and 0.46 ppm upfield compared to the precursor 6,6''-dicarboxylic acid ligand, **18**.

The ^{1}H-NMR of the 6,6''-dicarboxamide, **20,** in $CDCl_3$ displays nine peaks with correct integrals and expected coupling patterns present. Effects similar to that of the 6,6''-dicarboxylic acid ligand **18** are observed with H5 experiencing the greatest shift being observed 0.36 ppm downfield and H3 and H4 being observed 0.08 and 0.03 ppm upfield and downfield respectively compared to the precursor 6,6''-dicarbonitrile ligand, **17**. The characteristic tert-butyl groups appear at 1.5 ppm as a singlet with the correct integration and the N-H proton appears at 8.12 as a broadened singlet. This peak broadening is a result of the restricted rotation that occurs along the C-N bond leading to non-equivalence of the two hydrogens on the nitrogens, quite common in amide ^{1}H-NMR spectra.

3.3 Synthesis of 4',4''-(4-isopropyphenyl)-2,2':6',2'':6'',2'''quaterpyridine-6,6'''-dicarboxylic acid and -6,6'''-dicarboxamide

The 4',4''-(4-isopropyphenyl)-2,2':6',2'':6'',2'''quaterpyridine-6,6'''-dicarboxylic acid and -6,6'''-dicarboxamide ligands were synthesised in an analogous fashion as that of the terpyridines with the three-step reaction shown in scheme 3.2. Synthesis of the bis-oxide was achieved in the same manner as discussed in chapter 2. The introduction of the isopropyl groups are a necessity to increase the solubility of the ligand in the required solvent, DCM , for the cyanation reaction. Reactions with 4',4''-bisphenyl-2,2':6',2'':6'',2'''quaterpyridine gave a mixture of products and starting material due to their lack of solubility in the DCM preventing the reaction from proceeding to completion. The 6,6'''-dicarbonitrile, **21**, was obtained by the addition of 10 stoichiometric amounts of trimethylsilanecarbonitrile and a four-fold excess of benzoyl chloride in dichloromethane to yield the pure product in 51% yield.

Initial attempts to convert the dicarbonitrile, **21**, to the 6,6'''-dicarboxylic acids, **22**, by hydrolysis in basic ethylene glycol solution were unsuccessful. The decreased solubility of the larger ligand hindered the reaction preventing the formation of the product with a 2.5-hour reaction time. Increased reaction times of up to 24 hours gave a black solid with the ^{1}H-NMR showing a spectrum with no peaks present, indicating the starting material is decomposing at the required high temperature of 205°C. Therefore, the more forcing method using acid hydrolysis with concentrated sulphuric acid in glacial acetic acid was utilised. Suspension of the dicarbonitrile, **21**, in glacial acetic acid followed by the addition of catalytic

concentrated sulphuric acid and a 24-hour reflux resulted in a green solution. Upon cooling a solid precipitated yielding the product in 50% yield.

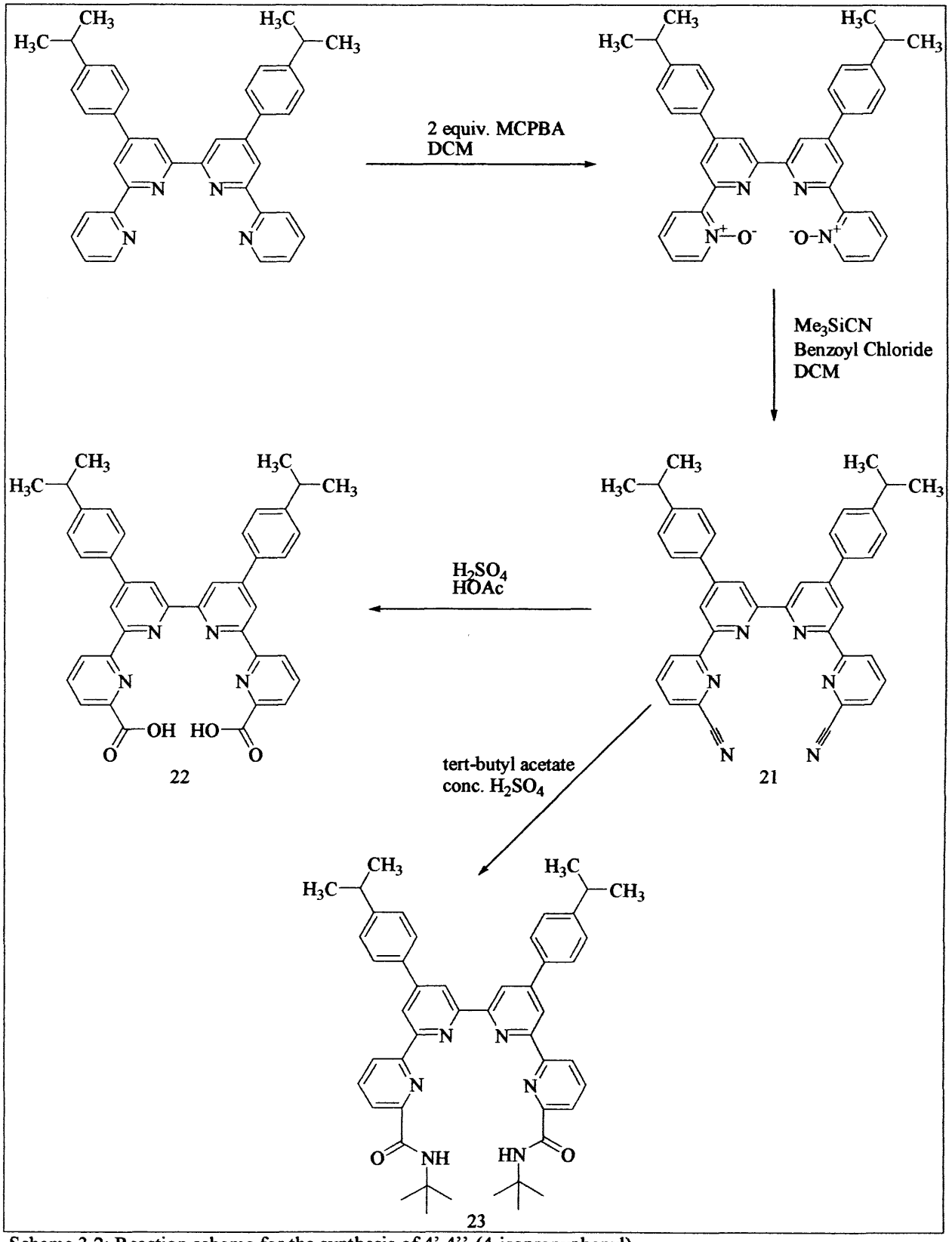

Scheme 3.2: Reaction scheme for the synthesis of 4',4''-(4-isopropyphenyl)-2,2':6',2'':6'',2'''quaterpyridine-6,6'''-dicarboxylic acid and -6,6'''-dicarboxamide

Oxidation of ligand **22** was not attempted for two reasons. Firstly, the terpyridine dicarboxylic acid proved quite difficult itself to oxidise and this combined with the difficulties encountered oxidising non-substituted quaterpyridine imply that oxidation of quaterpyridine dicarboxylic acid would be an extremely difficult reaction requiring extremely forcing conditions. Secondly, preliminary luminescence measurements which were taken of the 4'-phenyl-2,2':6',2''-terpyridine-6,6''-dicarboxylic acid 1,1',1''-trioxide Eu(III) complexes (to be discussed) gave disappointing results and it was decided to avoid the difficult oxidation of the ligand which at this time had the high probability of providing poor results.

Conversion of the nitrile to the tert-butyl amide, **23**, was achieved analogously to that of the terpyridines and proved a facile reaction. The pure product was obtained in 71% yield.

Spectral and analytical data for all compounds synthesised are fully in accord with each of the proposed structures but with the mass spectrum measurements giving some complex results. IR studies for the 6,6'''-dicarbonitrile, **21**, indicates the presence of the nitrile functionality with the characteristic absorption at 2228(w) cm^{-1}. The characteristic pyridine moiety absorption bands ($\nu_{C=C}$ and $\nu_{C=N}$) are present at 1593(s) and 1577(s) cm^{-1}. IR studies of the 6,6'''-dicarboxylic acid, **22**, showed the removal of the nitrile absorption and the presence of a C=O stretch at 1734(m) cm^{-1} and a O-H stretch at 3407(bm) cm^{-1}. The pyridine moiety absorptions have moved to the higher frequencies of 1624(s) and 1601(s) cm^{-1} due to the presence of the electron-withdrawing acid groups. IR studies of the 6,6'''-dicarboxamide, **23**, also indicate the loss of the nitrile peak with the introduction of C=O (1683(s) cm^{-1}) and N-H (3387(m)

cm^{-1}) stretches indicative of the amide group. The pyridine absorptions were present at frequencies similar to that of the nitrile (1597(m) and 1585(s) cm^{-1}).

Mass spectrum studies provided correct results for the described structures. The EI+ spectrum of the 6,6'''-dicarbonitrile, **21**, shows in intense peak at 596m/z corresponding to the parent ion with fragmentation of the isopropyl groups to 581 and 565 m/z. The EI+ spectrum of the 6,6'''-dicarboxylic acid ligand, **22**, shows the expected parent ion present at m/z 635 with a slight impurity from an additional Na+ ion present at m/z 657. The EI+ spectrum of the 6,6'''-dicarboxamide ligand, **23**, revealed some complex mixtures with the parent ion present at m/z 745 and unassigned peaks at m/z 797 and 853.

The ^{1}H-NMR spectra indicate unambiguously the proposed structures with the ligands showing trends analogous to the terpyridine ligands previously discussed. The NMR data is presented in table 3.2.

Compound	H3	H4	H5	H6	H3'	H5'	H_O	H_M	H_{iso}	H_{CH3}
4-^{is}Pr-PhQuater (**5b**)	8.64 - 8.70	7.81 - 7.86	7.30	8.64 - 8.70	8.87	8.64 - 8.70	7.81 - 7.86	7.37	2.96	1.28
4-^{is}Pr-PhQuaterO_2 (**6b**)	8.33	7.39	7.26	8.38	9.24	8.75	7.73	7.34	2.94	1.26
4-^{is}Pr-PhQuaterCN_2 (**21**)	8.95	8.29	8.10	-	8.67	8.92	7.91	7.51	n/o[a]	1.34
4-^{is}Pr-PhQuaterAcid$_2$ (**22**)	8.89 - 8.92	8.21	8.16	-	8.89 - 8.92	8.89 - 8.92	7.91	7.49	3.02	1.3
4-^{is}Pr-PhQuaterAmide$_2$ (**23**)	8.76	7.99	8.22	-	8.61	8.89	7.79	7.42	2.98	1.3

Table 3.2: ^{1}H-NMR data for the ligands synthesised (ppm). [a] n/o: not observed

The ^{1}H-NMR of 4-^{is}Pr-PhQuaterCN$_2$, **21**, was obtained in D$_6$-DMSO at 110°C due to the extremely poor solubility of the ligand. The spectrum displays 9 peaks with correct integrals and coupling patterns. Analogous to 4'-phenyl-2,2':6',2''-terpyridine-6,6''-dicarbonitrile, **17**, the loss of the 1,1'''-bisoxide and the introduction of the electron-withdrawing nitrile group to the H6 and H6''' position results in an enhanced deshielding effect in the ligand system producing shifts in the ligand protons similar to the parent ligand 4-^{is}Pr-PhQuater, **5b**. The H3, H4 and H5 protons shift by 0.62, 0.9 and 0.84 ppm respectively to a higher frequency compared to the precursor 1,1'''-bisoxide. The phenyl protons are relatively unaffected by the system changes.

The 4-^{is}Pr-PhQuaterAcid$_2$, **22**, ligand displays similar NMR and solubility trends to 4'-phenyl-2,2':6',2''-terpyridine-6,6''-dicarboxylic acid, **18**, with the protonated form being very insoluble but deprotonation increasing the solubility allowing the ligand to dissolve in alcohols and water. The ^{1}H-NMR spectrum in DMSO reveals six peaks and a multiplet of peaks present at the chemical shift of 8.89-8.92 preventing assignation of these protons. The integrals and coupling patterns are correct for the predicted structure. The multiplet of peaks at 8.89-8.92 ppm are indicative of the synthesis of the ligand with the remaining ligand protons occurring at similar chemical shifts to the precursor 6,6'''-dicarbonitrile, **21**. The phenyl and isopropyl groups do not experience any of the changes to any great degree and only small shifts are observed.

The ^{1}H-NMR of the more soluble 4-^{is}Pr-QuaterAmide$_2$, **23**, in CDCl$_3$ showed eleven peaks with correct integrals and coupling patterns. The characteristic *tert*-

butyl groups appear at 1.51 ppm as a singlet and the N-H proton appears as a broad singlet at 8.15 ppm. The ligand protons occur at analogous shifts to that of PhTerpyAmide$_2$, **20**, with the same discussion applied here. The chemical shifts are quite similar to the precursor 6,6'''-dicarbonitrile, **21**, with small shifts of 0.19, 0.3 and 0.12 ppm being observed for the H3, H4 and H5 protons. Therefore, the *tert*-butyl and N-H protons verify the synthesis of the 6,6''-dicarboxamide.

3.4 Synthesis of 4',4'''-(4-isopropyphenyl)-2,2':6',2'':6'',2''':6''',2'''':6'''',2''''-quinquepyridine-6,6''''-dicarboxylic acid and -6,6''''-dicarboxamide

The ligands were synthesised analogously to the ter- and quaterpyridines with the three-step reaction shown in scheme 3.3. Similarly to the ter and quaterpyridines the bis oxide was synthesised in the same manner as discussed in chapter 2 and was followed by the modified *Reissert-Henze* reaction. The increased solubility with the inclusion of isopropyl groups on the phenyl backbone allowed the dinitrile, **24**, to be obtained in 49% yield.

The conversion of the dinitrile to the dicarboxylic acid encountered the same problems as the quaterpyridines but was obtained using the acid hydrolysis method with concentrated sulphuric acid. The dicarboxylic acid, **25**, was obtained in 71% yield.

The conversion of the dinitrile to the tert-butyl amide, **26**, once again proved a facile reaction, using the same method used as that for the ter- and quaterpyridines. The pure product was obtained in 41% yield.

Spectral and anayltical data for the ligands synthesised are all in accord with the proposed structures. IR studies for the 6,6''''-dicarbonitrile, **24**, shows the expected characteristic nitrile absorption at 2236(w) cm^{-1}. The characteristic pyridine moiety absorptions ($\nu_{C=C}$ and $\nu_{C=N}$) are present at 1606(m) and 1580(s) cm^{-1}. IR studies of the 6,6''''-dicarboxylic acid, **25**, revealed the absence of the nitrile

absorptions and the introduction of a C=O stretch at 1717(m) cm^{-1} and a O-H stretch at 3430(bm) cm^{-1}. IR studies of the 6,6''''-dicarboxamide, **26**, also showed a loss of the nitrile peak and the presence of a C=O stretch at 1684(s) cm^{-1}. The characteristic amide N-H stretch was present at 3381cm^{-1} with the pyridine moiety absorptions present at 1608(m) and 1580(m) cm^{-1}.

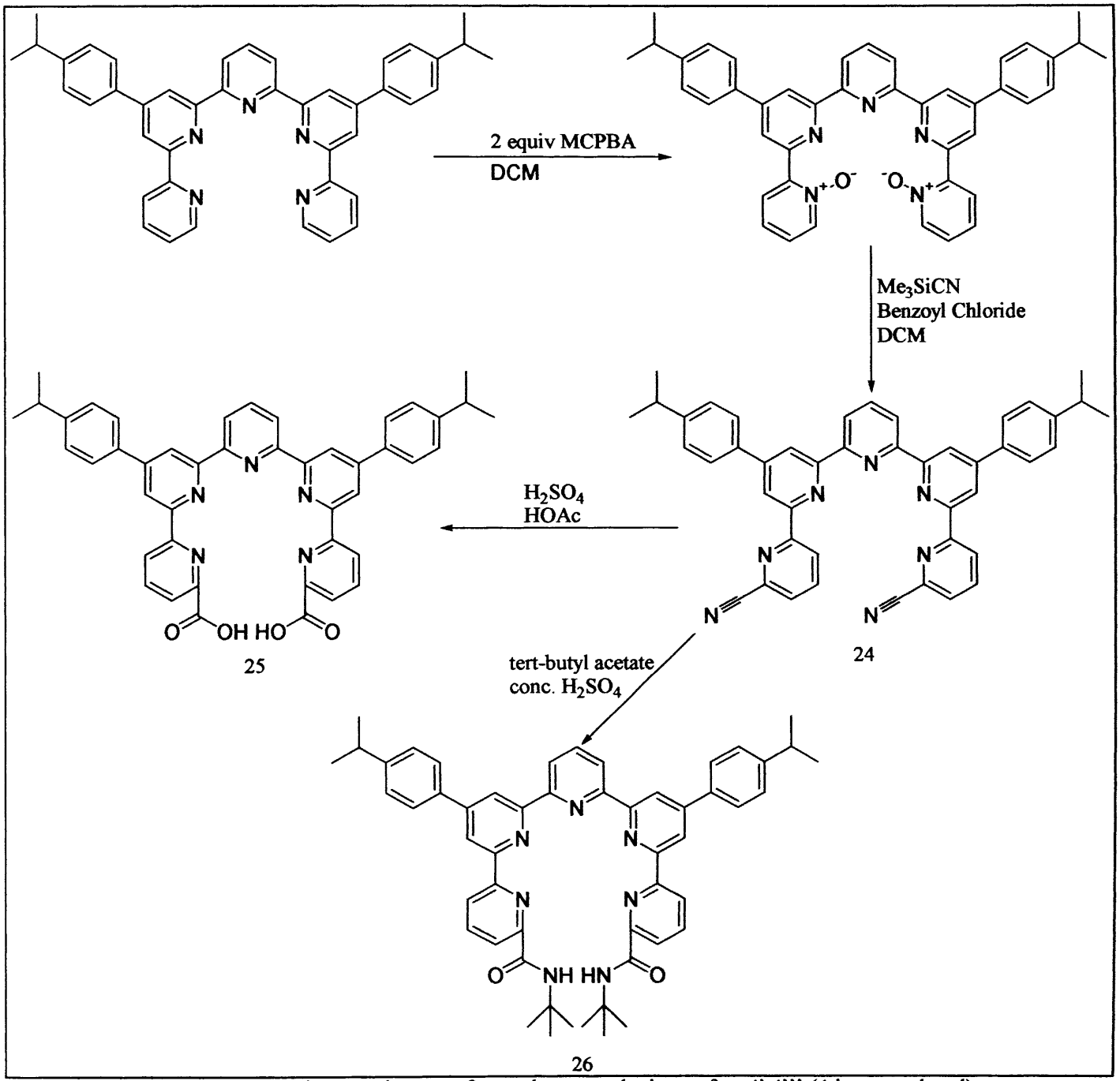

Scheme 3.3: Reaction scheme for the synthesis of 4',4'''-(4-isopropyphenyl)-2,2':6',2'':6'',2''':6''',2''''-quinquepyridine-6,6''''-dicarboxylic acid and -6,6''''-dicarboxamide

Mass spectrum studies of the ligands indicate the predicted structures with correct accurate mass measurements. Limited fragmentation of the ligands was observed throughout. The EI+ spectrum of the 6,6''''-dicarbonitrile, **24**, shows an intense peak at m/z 673 corresponding to the parent ion. Accurate mass measurements gave a ion mass of 673.2941 (calculated = 673.2948) and a $[M-H]^+$ of 372.2862 (calculated = 672.2870). The ES+ of the 6,6''''-dicarboxylic acid, **25**, shows an intense peak at m/z 712 corresponding to $[M+H]^+$ with higher fragments present at m/z 734 and 750 due to the presence of Na and K. The ES+ accurate mass of the ion gave a correct result 712.2928 (calculated mass = 712.2918). The ES+ of the 6,6''''-dicarboxamide **26** showed the parent $[M+H]^+$ at m/z 822 with a higher fragment containing Na present at m/z 844. The ES+ accurate mass gave the correct result of 822.4498 (calculated mass = 822.4490).

The ^{1}H-NMR spectra indicate the proposed structures, reinforcing the accurate mass spectrum results. The observed trends are once again similar to the terpyridine ligands and so a repeat of the full discussion shall be avoided. The NMR data is presented in table 3.3.

Compound	H3	H4	H5	H6	H3'	H_O	H_M	H5'	H3''	H4''	H_{iso}	H_{CH3}
4-^{is}Pr-Quinque (**8**)	8.69	7.86	7.31	8.95	8.69	7.86	7.36	8.69	8.65	8.01	2.96	1.28
4-^{is}Pr-QuinqueO_2 (**9**)	8.54	7.27	7.40	8.34	8.94	7.79	7.35	9.26	8.40	7.95	2.95	1.26
4-^{is}Pr-QuinqueCN_2 (**24**)	8.88	7.97	8.61	-	8.73	7.84	7.39	8.97	7.68	7.99	2.95	1.29
4-^{is}Pr-Quinque$Acid_2$ (**25**)	8.64	8.03	8.42	-	8.64	7.70	7.27	8.67	8.03	7.94	2.85	1.17
4-^{is}Pr-Quinque$Amide_2$ (**26**)	8.78	7.98 - 8.04	8.22	-	8.62	7.82	7.41	8.96	8.68	7.98 - 8.04	2.99	1.31

Table 3.3: ^{1}H-NMR data for the ligands synthesised (ppm)

The ^{1}H-NMR of 4-^{is}Pr-QuinqueCN$_2$, **24**, was obtained in $CDCl_3$, being more soluble than its quaterpyridine counterpart. The spectrum displays 11 peaks with correct integrals and coupling patterns. Analogous to the terpyridine and quaterpyridine dicarbonitriles, the introduction of the electron withdrawing nitrile groups to the 6 and 6'''' positions and the removal of the N-oxides allows the enhanced deshielding effect to occur producing shifts in the ligand system protons similar to the parent ligand 4-^{is}Pr-Quinque, **8**, with the exception of the H5 proton. The H3, H4 and H5 protons are shifted 0.4, 0.7 and 1.21 ppm downfield respectively. The peak corresponding to H6 is no longer present and the H3' and H5' protons that undergo the proximity deshielding effect from the N-oxides in the bis-oxide are now observed at the lower chemical shifts of 8.73 and 8.97, a lowering of 0.21 and 0.29 ppm respectively.

The ^{1}H-NMR of the 4-^{is}Pr-QuinqueAcid$_2$, **25**, was obtained in DMSO, showing the same solubility trends as the ter- and quaterpyridines. The spectrum displays eleven peaks with the O-H proton not being observed. The integrals and coupling patterns are all correct. Unlike the terpyridine and quaterpyridine dicarboxylic acid, in which their H3, H4 and H5 protons all undergo a downfield shift going from the dinitrile to the dicarboxylic acid, the 4-^{is}Pr-QuinqueAcid$_2$ H3 and H5 protons are shifted 0.24 and 0.19 ppm upfield respectively compared to the precursor dicarbonitrile, **24**. The rest of the ligand protons occur at similar chemical shifts as that of the unsubstituted parent ligand, **8**.

The ^{1}H-NMR of the more soluble 6,6''''-dicarboxamide, **26**, was obtained in $CDCl_3$ and showed 13 peaks with correct integrals and coupling patterns. The

characteristic N-H protons appear at 8.16 ppm as a broad singlet and the *tert*-butyl groups appear at 1.52 ppm as a singlet. Both peaks are at similar chemical shifts as the analogous ter- and quaterpryidine dicarboxamides. The rest of the ligand system protons are observed at similar chemical shifts as that of the 4-^{is}Pr-QuinqueAcid$_2$, **25**, with H3 and H5 being shifted 0.1 and 0.39 ppm upfield respectively compared to the precursor dinitrile, **24**.

3.5 Europium and Terbium Terpyridine Acid and Amide Complexes

The Europium (III) and Terbium (III) complexes obtained and discussed here illustrate the differing solubilities, binding strengths and coordination capabilities between the acids and amide ligands. The acid complexes produce analyses suggestive of their proposed structures whilst the amides allow the formation of the 1:1 complexes due to the presence of the protective t-butyl amide groups. To allow a proposal of the molecular formulas of the complexes we have made use of the work of de Silva and co-workers analysis of Ln(III) complexes with ligand **29** (see Fig. 3.7).[13] The ligand **29** is pentadentate and is identical to the terpyridine dicarboxylic acid and dicarboxamide ligands synthesised here which therefore leaves four sites free for coordination, assuming a coordination number of nine as discussed in the introduction. By comparison of the luminescence lifetimes of the Ln(III) complex in MeOH and MeOD, De Silva determined that the average number of lanthanide-bound MeOH molecules was two, suggesting the remaining coordination sphere is made up of two counterions. Using these analysis and assumptions we have assigned our proposed structures as having two lanthanide-bound water molecules and two counterions.

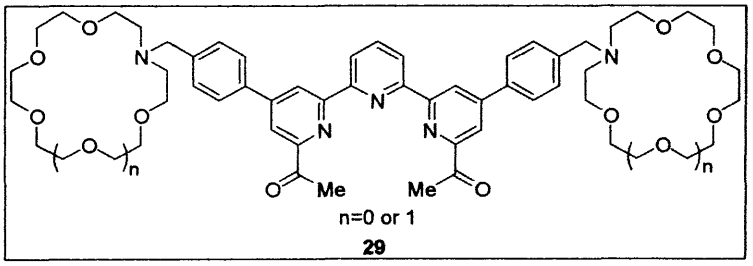

Fig.3.7: Ligand **29**.

$[Eu(PhTerpyAcid_2)(H_2O)_2][ClO_4]_2$, $[Tb(PhTerpyAcid_2)(H_2O)_2][ClO_4]_2$ and 4'-phenyl-2,2':6',2''-terpyridine-6,6''-dicarboxylic acid 2:1 with $Eu(ClO_4)_3$

The complexes were synthesised using both 1:1 and 2:1 ligand to metal stoichiometries. The method for synthesis involved the addition of either Eu(III) or $Tb(III)(ClO_4)_3$ to either a twofold or an equal molar amount of deprotonated ligand in ethanol (deprotonation was achieved with two equivalents of KOH in ethanol). After stirring for one hour a white precipitate was obtained which was filtered off and dried. The compounds were found to be insoluble in solvents such as acetonitrile, DCM, THF and alcohols, sparingly soluble in water and soluble in DMF and DMSO.

IR spectra of the three metal complexes are very similar, showing the presence of absorption bands characteristic of the pyridine moiety ($\nu_{C=C}$ and $\nu_{C=N}$ around 1591 and 1570cm^{-1}) and of the carboxylate groups. The absorption band characteristic of the C=O absorption was observed at the lower frequency of 1610cm^{-1}, 95cm^{-1} lower than in the free ligand and typical of a carboxy anion, which would indicate coordination of the metal via the carboxylate groups. This is in agreement with the results of Bünzli and co-workers[3] for the analysis of Ln(III) complexes of 2,2'-bipyridine-6,6'-dicarboxylic acid (**29**). The C=O absorption of the [Eu(2,2'-bipyridine-6,6'-dicarboxylic acid)$_2$](Et_3NH) complex undergoes a 91cm^{-1} shift in comparison to the free ligand, comparable to the shifts observed in this study. The 2:1 Eu(III) complex also exhibits the 1610cm^{-1} C=O absorption. The strong absorption at 1090cm^{-1} indicates the presence of the perchlorate counterion.

The ^{1}H-NMR spectrum of the 1:1 europium complex in D_6-DMSO displays six peaks with correct coupling patterns and integrations for the complex. One peak is absent and presumed to be concealed behind the DMSO peak in the spectrum. As the complex is only soluble in DMSO the spectrum cannot be attained in differing solvents so as to obtain this missing peak. The phenyl protons are deshielded by the presence of the paramagnetic metal with the ortho proton being shifted by 1.14ppm to 8.96ppm, the meta proton shifting 0.6ppm to 8.17ppm and the para proton shifting 0.48ppm to 7.97ppm. The pyridine protons experience a greater shielding effect, attributed to their closer proximity to the paramagnetic Eu(III) ion, with the H3' and 5' protons being observed at 7.63 and the H3 and either the H4 or H5 protons being observed at 3.12 and –0.71ppm respectively. As the pyridine protons do not undergo as great a shift as in the amide complexes (see below) it may be postulated that the approach of the Eu(III) ion is not as close to the pyridines as in the amides. The ^{1}H-NMR spectrum of the 2:1 europium complex in D_6-DMSO displays the exact same spectrum as the 1:1 complex indicating the preference of the complex to form similar complexes as the 1:1 complexes in solution or that the same compound has been formed. Interestingly there is no evidence of free ligand in the ^{1}H-NMR spectrum.

The NOBA/Matrix FAB MS of the 1:1 Eu(III) complex showed intense peaks at m/z 332 attributed to the ligand with a loss of four oxygens, m/z 714 attributed to EuL(NOBAcid), m/z 844 attributed to $[EuL(NOBA)_2]$ and m/z 998 attributed to $Eu_2L(NOBA)_2$-H. The ES- spectrum showed an intense peak at 99 attributed to the perchlorate counterion, $[ClO_4]^-$. As was discussed in the introduction, the complex might be present in an extended ligand:metal system in the solid-state involving many metal and ligand mixtures.

The intended 2:1 complexes results strongly indicate the formation of a 1:1 complex with the ES+ MS showing intense peaks at m/z 548 (corresponding to a 1:1 EuL complex), 566 (corresponding to EuL(O^-)), 612 (corresponding to EuL-2O+(ClO_4), loss of O from the ligand), and m/z 628 (corresponding to EuL-O+(ClO_4), loss of O from the ligand). The ES- revealed the presence of $(ClO_4)^-$ at m/z 99. The expected parent ion should occur at m/z 941. The ES+ MS of the Tb(III) 1:1 complex showed the presence of the [TbL] ion at m/z 554 and provided better evidence than the Eu(III) complex suggesting the formation of the 1:1 complex. Intense peaks were observed at m/z 554 $[M-3ClO_4]^+$ and 851$[M]^+$. The ES- revealed the presence of $(ClO_4)^-$ at m/z 99. The FAB MS of the complex revealed the 1:1 [TbL] ion at m/z 554.

It can be seen from the data presented that there is strong evidence for the formation of 1:1 complexes. ^{1}H-NMR studies indicate the coordination of the lanthanide ions by the lanthanide-induced shifts produced in the ligand protons with the IR studies showing characteristic shifts of 95cm^{-1} in the C=O absorption bands. The MS studies give strong indications of the formation of the complexes.

4'-phenyl-2,2':6',2''-terpyridine-6,6''-dicarboxylic acid 1,1',1''-trioxide 2:1 with $Eu(ClO_4)_3$

The N-oxide acid complex was synthesised in the same manner as the previous complexes, with the $Eu(III)(ClO_4)_3$ being added to a solution of the deprotonated ligand in ethanol. The white precipitate obtained was stirred for one hour and filtered. The complex is more insoluble than the previous non-oxidised $PhterpyAcid_2$ Ln(III) complexes, being soluble only in DMF and DMSO. The IR spectrum showed the characteristic pyridine absorptions at 1604cm^{-1} and the C=O absorption was present at 1634cm^{-1}, not as low as the previous complexes but still 69cm^{-1} lower than the free ligand indicating stronger coordination through the carboxylic acids. The N-oxide absorptions were also observed, appearing at 1214cm^{-1}, 47cm^{-1} lower than in the free ligand, also indicating coordination through the N-oxides.

The NOBA matrix MS of the 2:1 complex revealed numerous peaks present at m/z 413 (corresponding to [L-2O]), 429 (corresponding to [L-O]), 689 (corresponding to $[Eu_2L\text{-}2CO]$) and 792 (corresponding to $[EuL(ClO_4)_2]$). There were additional higher fragments which could indicate the presence of extended ligand-metal frameworks.

The ^{1}H-NMR obtained in D_6-DMSO yielded a very weak spectrum, probably due to the reduced solubility of the complex in the DMSO, with seven peaks observed. Broadening of the peaks had occurred and assigning of the peaks proved difficult. The proton peaks were shifted with respect to the free ligand and occur at

2.52 to 7.58ppm, indicating the presence of the paramagnetic Eu(III) ion in the compound.

$[Eu(PhTerpyAmide_2)(H_2O)_2][ClO_4]_3$ and $[Tb(PhTerpyAmide_2)(H_2O)_2][ClO_4]_3$

Synthesis of the complexes involved the suspension of the ligands in ethanol and the addition of either Eu(III) or $Tb(III)(ClO_4)_3$ with stirring. After a 24-hour stirring period the mixture yielded a yellow solution to which diethyl-ether was added to precipitate the complex. The complex is soluble in alcohols, DCM and acetonitrile but insoluble in water. The IR spectra of the two complexes are similar with the characteristic pyridine absorptions occurring at 1597 and 1557cm^{-1}. The C=O absorption of the amide is observed at 1632cm^{-1}, 49cm^{-1} lower than the free ligand indicating coordination to the lanthanide metal through the amide group. A strong perchlorate absorption is present at 1092cm^{-1}.

The ES+ MS of the Eu(III) complex shows intense peaks at m/z 858 corresponding to the parent ion with the loss of a perchlorate, $[EuL-H][ClO_4]_2$ and m/z 758 corresponding to the parent ion with the loss of two perchlorates, $[EuL-H][ClO_4]$. Fragmentation also shows a peak at m/z 508 corresponding to the [ligand+H]. The ES+ MS of the Tb(III) complex is similar showing intense peaks at 864 and 764 corresponding to the parent ion with the loss of one and two perchlorates. Fragmentation reveals the [ligand+H] at m/z 508.

The ^{1}H-NMR of the Eu(III) complex in CD_3CN displays nine broad signals ranging from –3 to 7.5ppm with integrals corresponding to one ligand coordinated to

one Eu(III) metal. The spectrum indicates coordination of the Eu(III) metal to the cavity of the ligand as the pyridine protons surrounding the cavity undergo large chemical shifts due to the through space interactions of the paramagnetic centre. The H3 and H5 protons experience the greatest shifts appearing at –3 and –1.56ppm, 2.3ppm lower than the acid complexes. The phenyl and amide CH_3 groups are relatively unaffected by the paramagnetic Eu(III) metal, appearing at similar chemical shifts as observed for free ligand, indicating their greater distance from the metal centre and further reinforcing the presence of the Eu(III) metal in the cavity of the ligand.

The IR, NMR and MS data presented unambiguously point towards the formation of the 1:1 complexes.

3.6 Europium and Terbium Quaterpyridine Acid and Amide Complexes

The europium and terbium complexes obtained once again illustrate the differing solubilities and coordination capabilities between the acids and amides. The acid complexes produce analyses suggestive of oligomeric mixtures whilst the amide complexes provide unambiguous evidence for the formation of 1:1 complexes due to the presence of the protective t-butyl amide groups. The proposed structures have been assigned using the assumption of two lanthanide-bound water molecules as discussed for the terpyridine complexes. This leaves one site free for the coordination of one perchlorate counterion due to the hexadentate nature of these quaterpyridine ligands.

$[Eu(4\text{-}^{is}Pr\text{-}PhQuaterAcid_2)(H_2O)_2][ClO_4]$ and

$[Tb(4\text{-}^{is}Pr\text{-}PhQuaterAcid_2)(H_2O)_2][ClO_4]$

The complexes were synthesised in an analogous fashion to the $PhTerpyAcid_2$ Eu(III) and Tb(III) complexes. The compounds were found to have similar solubilities as the terpyridine dicarboxylic acid complexes. IR spectra of the two complexes are very similar, showing the characteristic pyridine moiety absorptions at 1609 and 1575cm^{-1}. The C=O absorption underwent a 93cm^{-1} shift, analogous to the shift observed in the $PhTerpyAcid_2$ complexes, being observed at the lower frequency of 1641cm^{-1} indicating coordination of the lanthanide ion via the carboxylate groups. A strong absorption at 1091cm^{-1} indicated the presence of the perchlorate counterion.

The ES+ MS of the Eu(III) complex indicated the 1:1 complex showing intense peaks at m/z 632 (corresponding to $[L+H]^+$), 835 (corresponding to [EuL-3O+(ClO_4)) and m/z 853 (corresponding to $[EuL-2O+(ClO_4)]^+$). The ES- spectrum showed an intense peak at 99 attributed to the perchlorate counterion, $[ClO_4]^-$. The ES+ MS of the Tb(III) complex also indicates the formation of the 1:1 complex showing numerous peaks at m/z 653 (corresponding to $[L+Na^+]^+$), 790 (corresponding to $[TbL]^+$), 823 (corresponding to $[TbL+2O]^+$) and m/z 988 (corresponding to $[TbL+2(ClO_4)]^+$). The ES- spectrum showed an intense peak at *m/z* 99 attributed to the perchlorate counterion, $[ClO_4]^-$.

The ^{1}H-NMR of the Eu(III) complex in D_6-DMSO revealed two different ligand environments in an equal ratio. The first ligand environment was determined to be uncomplexed ligand with the other being the complexed ligand. The complexed ligand revealed shifted ligand proton peaks occurring in the range of 0.96-7.07ppm. This lanthanide induced shift indicated the coordination of the Eu(III) ion to the ligand.

$[Eu(4\text{-}^{is}Pr\text{-}PhQuaterAmide_2)(H_2O)_2][ClO_4]_3$ and

$[Tb(4\text{-}^{is}Pr\text{-}PhQuaterAmide_2)(H_2O)_2][ClO_4]_3$

The complexes were synthesised by the addition of either Eu or $Tb(ClO_4)_3$ to an equal molar amount of ligand suspended in hot ethanol. After 15 minutes stirring a solution was obtained and the mixture stirred for a further hour. Addition of diethyl-ether precipitated a white solid which was filtered and dried. The solubilities of the complexes were similar to that of the corresponding terpyridine complexes possessing

greater solubility in organic solvents than the complexes of the dicarboxylic acid counterparts. The IR spectra of the two complexes were similar with the characteristic pyridine moiety absorption's present at 1596 and 1575cm^{-1}. The C=O absorption of the amide group now occurs at 1652cm^{-1}, a lowering of 31cm^{-1} (18cm^{-1} less than the terpyridine dicarboxamide complexes) indicating coordination of the Eu(III) ion through the amide groups. A strong absorption at 1089cm^{-1} is indicative of the presence of the perchlorate counterion.

The ES+ MS of the Eu(III) complex shows intense peaks at m/z 1095 and 995 corresponding to the parent ion with a loss of one and two perchlorate counterions respectively. A fragmentation peak at m/z 745 corresponds to the ligand fragment, [L+H]. The ES+ MS of the Tb(III) complex shows similar patterns with peaks at m/z 1101 and 1001 present again corresponding to the parent ion with a loss of one and two perchlorates respectively. A peak at m/z 745 corresponds to the ligand fragment, [L+H].

The ^{1}H-NMR spectrum of the Eu(III) complex in CD_3CN displays twelve peaks with correct integrations, however broadening of the peaks has eliminated most of the coupling patterns. All of the protons on the ligand have undergone a downfield shift due to the presence of the paramagnetic Eu(III) ion with the protons closest to the metal cavity undergoing the greatest shifts. The NH protons of the amide feel the greatest effect of the Eu(III) ion appearing at –5.47 and –2.79ppm, the Eu(III) ion causing non-equivalence of their chemical environments so as to appear as separate peaks with integrals of one. The isopropyl protons and *tert*-butyl groups undergo minor downfield shifts from their positions in the free ligand (2.08 and 2.47ppm

downfield shifts respectively) due to their distance from the metal ion. The phenyl ortho and meta protons undergo upfield shifts of 1.91 and 0.65ppm respectively in comparison to their positions in the free ligand ^{1}H-NMR. The cavity pyridine protons all undergo upfield shifts occurring at chemical shifts between 4.83 and –1.57ppm. All of the data indicates the presence of a single species in solution, with a 1:1 metal:ligand stoichiometry.

3.7 Europium and Terbium Quinquepyridine Acid and Amide Complexes

The Eu(III) and Tb(III) complexes of the quinquepyridine carboxylic acid and amides all provide clear evidence for the formation of 1:1 metal:ligand complexes providing simpler spectroscopic and analytical data than the ter- and quaterpyridine analogues. This would suggest the quinquepyridines are better designed to envelop the lanthanide ions, perhaps forming the helical structures as discussed in the introduction. A proposal of the molecular formulae of the quinquepyridine carboxylic acid and amide complexes has made use of the structure of Cd[**28**] (discussed in section 3.1) and also of the work of de Silva as discussed in section 3.5. The Cd(II) ion shares an ionic radius similar to Eu(III), (Cd(II) r =1Å, Eu(III) r =1.09Å) and so it could be thought that the monohelical structure of Cd[**28**] could be adopted by the Eu(III) complexes. However the monohelical structure of Cd[**28**] allows the approach of two solvent molecules. This combined with de Silva's findings of Ln(III) complexes of **29** have an average number of lanthanide-bound MeOH molecules of two and the heptadentate nature of the quinquepyridine ligands has lead to the assumptions that the 4-^{is}Pr-PhQuinqueAcid$_2$ Eu(II) and Tb(III) complexes have two lanthanide-bound water molecules and one perchlorate counterion. The 4-^{is}Pr-PhQuinqueAmide$_2$ Eu(III) and Tb(III) complexes have the proposed molecular formulas of two lanthanide-bound water molecules and three perchlorate counterions to balance the Ln(III) ion charge.

[Eu(4-^{is}Pr-PhQuinqueAcid$_2$)(H$_2$O)$_2$][ClO$_4$] and

[Tb(4-^{is}Pr-PhQuinqueAcid$_2$)(H$_2$O)$_2$][ClO$_4$]

The complexes were synthesised in an analogous fashion to the terpyridine and quaterpyridine carboxylic acid complexes. The compounds were found to have similar solubilities as the previous acid complexes. IR spectra of the two complexes are similar, showing similar characteristics as the ter and quaterpyridine carboxylic acid complexes. The characteristic pyridine moiety absorptions were observed at 1573 and 1542cm^{-1} and the characteristic strong C=O absorption was observed at a lower frequency than observed in the ter- and quaterpyridine counterparts pointing towards a somewhat weakened C=O bond appearing at 1607cm^{-1}. This larger shift of 110cm^{-1} from the free ligand reveals a greater displacement of the electronic density of the carboxylate functions towards the metal binding oxygen atoms. A medium absorption at 1089cm^{-1} indicates the presence of the perchlorate counterion.

The ES+ MS of the Eu(III) and Tb(III) complexes showed unambiguous evidence towards the formation of 1:1 ligand:metal stoichiometries, unlike the ter- and quaterpyridine analogues. The Eu(III) complex showed an intense peak at m/z 860 corresponding to the parent ion $[Eu+L]^+$. The ES+ MS of the Tb(III) complex gave the same result with the parent $[Tb+L]^+$ ion being observed at m/z 868. Higher fragments were not observed in either spectrum indicating the presence of only the 1:1 complexes. The ES- spectra of both complexes had a peak at m/z 99 indicating the presence of perchlorate.

The ^{1}H-NMR of the Eu(III) complex in D_6-DMSO displayed eleven peaks with the correct integration but broadening of the peaks eliminating all coupling patterns. The coordination of the paramagnetic Eu(III) ion to the ligand is in evidence with all of the surrounding pyridine cavity protons undergoing large chemical shifts occurring between 14.7 and 0.16ppm. Determination of the individual protons has not yet been achieved due the loss of all coupling patterns. The MS and NMR data both verify the presence of a single species in solution and the formation of 1:1 metal:ligand complexes.

$[Eu(4\text{-}^{is}Pr\text{-}PhQuinqueAmide_2)(H_2O)_2][ClO_4]_3$ and

$[Tb(4\text{-}^{is}Pr\text{-}PhQuinqueAmide_2)(H_2O)_2][ClO_4]_3$

Once again the complexes were synthesised in an analogous fashion as the ter- and quaterpyridine analogues. The solubilities of the complexes were also similar to the corresponding ter- and quaterpyridine complexes. The IR spectra of the two complexes were similar with the characteristic pyridine moiety absorption's present at 1606 and 1575cm^{-1}. The C=O absorption of the amide group now occurs at 1643cm^{-1}, a lowering of 41cm^{-1} (8cm^{-1} less than the terpyridine dicarboxamide complexes but 10cm^{-1} greater than the quaterpyridine dicarboxamide complexes) indicating coordination of the Ln(III) ions through the amide groups. A strong absorption at 1090cm^{-1} is indicative of the presence of the perchlorate counterion.

The ES+ MS of the Eu(III) complex shows intense peaks at m/z 1170 and 1070 corresponding to the $[EuL(ClO_4)_2]^+$ and $[EuL(ClO_4)\text{-}H]^+$ fragments respectively. The ES+ MS of the Tb(III) complex gave the same result with peaks at m/z 1178 and

1078 present again corresponding to the $[TbL(ClO_4)_2]^+$ and $[TbL(ClO_4)\text{-}H]^+$ fragments respectively.

The ^{1}H-NMR of the Eu(III) complex in CD_3CN displayed nine clear peaks with at least three peaks (including the t-butyl groups) obscured behind a broadened peak at 3-4.5ppm. Thirteen peaks would be expected in the ^{1}H-NMR for this complex. The pyridyl protons occur in the range 8.7 to –2.4ppm, with the external backbone phenyl protons and the attached isopropyl groups being observed close to their free ligand positions, feeling a minimal effect from the Eu(III) ion. As with all of the amide complexes discussed in this chapter, the data confirms the presence of a single species in solution and the formation of 1:1 metal:ligand complexes.

3.8 Luminescence Studies

The emission spectra of all complexes were measured along with the absorbance spectra where possible. No luminescence has been observed in aqueous solution for any of the complexes, with the acid complexes being partially soluble in water and the amides being even less soluble. The emission spectra were obtained in the same manner that the complexes in the previous chapter were obtained. Similar to the unsubstituted precursor complexes in the previous chapter, the amides display decomplexation at low solution concentrations, with ligand emission being observed at these low concentrations. This shall be discussed in more detail when encountered. Where ligand luminescence was observed in the lanthanide complex emission spectra, the emission spectra of the ligands were also carried out to verify this.

In all of the Eu(III) complexes the $^5D_0 \rightarrow {}^7F_2$ emission dominates the spectrum indicating that the Eu(III) ion is in a non-centrosymmetric ligand field which allows not only magnetic-dipole but also electric-dipole transitions,[14] analogously to the complexes discussed in chapter 2. The $^5D_0 \rightarrow {}^7F_2/{}^5D_0 \rightarrow {}^7F_1$ ratios (η) range from 7.94 to 5.3, much lower than the maximum result observed for the Eu(quaterO$_4$) complex (37.6) seen in the last chapter. In fact the highest ratio seen here is lower than most of the lowest ratios seen from the N-oxides in the last chapter (8.19 for terpyO). This would falsely insinuate that the acid and amide ligands are weaker donors to the lanthanides than the N-oxides discussed previously. Despite the lower η ratios the acid and amide

complexes display superior luminescent properties than the N-oxides, in part at least, due to the inclusion of the stronger binding groups.

The emission spectra of the Eu(III) complexes are reported in Table 3.4 and Figs 3.9-3.24 with the Tb(III) complexes reported in Table 3.5 and Figs. 3.10-3.25.

Complex	$^5D_0 \rightarrow {}^7F_0$	$^5D_0 \rightarrow {}^7F_1$	$^5D_0 \rightarrow {}^7F_2$	$^5D_0 \rightarrow {}^7F_3$	$^5D_0 \rightarrow {}^7F_4$
$Eu(BipyAcid_2)_2^{3+}$	572(0.52)	590(1.0) 595	612(13.2)	649(0.16)	698(0.67) 707
$Eu(BipyA_2O_2)^{3+}$	-	-	-	-	-
$Eu(PhTerpyAcid_2)^{3+}$	574(0.1)	591(1.0) 597	615(8.65) 620	650(0.28)	684(3.13) 695 698 704
$Eu(PhTerpyA_2O_3)^{3+}$	-	-	-	-	-
$Eu(PhTerpyAmide_2)^{3+}$	579(0.1)	587(1.0) 592 596	616(5.83) 620	650(0.09)	690(1.72) 695 699
$Eu(4\text{-}^{is}Pr\text{-}PhQuaterAcid_2)^{3+}$	575(0.05)	590(1.0) 595	614(7.94) 620	650(0.3)	690(0.2)
$Eu(4\text{-}^{is}Pr\text{-}PhquaterAmide_2)^{3+}$	578(0.33)	585(1.0) 595	614(6.1)	650(0.17) 654	684(2.25) 695 701
$Eu(4\text{-}^{is}Pr\text{-}PhQuinqueAcid_2)^{3+}$	575(0.009)	587(1.0) 594 597	615(4.77)	650(0.3)	686(0.75) 694 701
$Eu(4\text{-}^{is}Pr\text{-}PhQuinqueAmide_2)^{3+}$	575(0.006)	586(1.0) 595	615(5.3)	646(0.27)	685(1.57) 694 703

Table 3.4: Peak positions and relative integrals in the emission spectra of Eu(III) complexes (nm).

Complex	$^5D_4\rightarrow$ $^7F_6$	$^5D_4\rightarrow$ $^7F_5$	$^5D_4\rightarrow$ $^7F_4$	$^5D_4\rightarrow$ $^7F_3$	$^5D_4\rightarrow$ $^7F_2$	$^5D_4\rightarrow$ $^7F_1$	$^5D_4\rightarrow$ $^7F_0$
$Tb(PhTerpyAcid_2)^{3+}$	491	545	587	620	640	670	-
	(1.0)	(2.2)	(0.7)	(0.3)	(0.15)	(0.05)	
$Tb(PhTerpyAmide_2)^{3+}$	490	545	582	623	649	670	678
	(1.0)	(2.0)	(0.7)	(0.28)	(0.04)	(0.016)	(0.016)
$Tb(4\text{-}^{is}Pr\text{-}PhQuaterAcid_2)^{3+}$	490	543	583	623	649	-	-
	(1.0)	(2.3)	(0.7)	(0.4)	(0.46)		
$Tb(4\text{-}^{is}Pr\text{-}PhquaterAmide_2)^{3+}$	490	543	583	622	651	669	681
	(1.0)	(1.9)	(0.6)	(0.27)	(0.05)	(0.01)	(0.017)
$Tb(4\text{-}^{is}Pr\text{-}PhQuinqueAcid_2)^{3+}$	485	544	583	622	-	-	-
	(1.0)	(1.5)	(0.3)	(0.78)			
$Tb(4\text{-}^{is}Pr\text{-}PhQuinqueAmide_2)^{3+}$	485(1.0)	543	583(0.6)	621	649	670	682
	492	(1.9)	594	(0.25)	(0.05)	(0.02)	(0.01)

Table 3.5: Peak positions and relative integrals in the emission spectra of Tb(III) complexes (nm).

3.8.1 The Luminescence Properties of $[Eu(PhTerpyAcid_2)(H_2O)_2][ClO_4]_2$ and $[Tb(PhTerpyAcid_2)(H_2O)_2][ClO_4]_2$

The absorbance spectrum of the protonated 4'-phenyl-2,2':6',2''-terpyridine-6,6''-dicarboxylic acid ligand recorded in DMF at room temperature shows a broad band at 272nm (ε = 27 210 $M^{-1}cm^{-1}$) with two shoulders at 284nm (ε = 25 428 $M^{-1}cm^{-1}$) and 321nm (ε = 7401 $M^{-1}cm^{-1}$) attributed to $\pi\rightarrow\pi^*$ transitions on the pyridine rings. Upon complexation to Eu(III) or Tb(III), the $\pi\rightarrow\pi^*$ transitions are shifted to lower energy, as often observed during the complexation of heteroaromatic systems with lanthanide ions.[15] The absorbance spectra of the Eu(III) and Tb(III) complexes are alike showing two separate bands with the red shifted, lower energy band having two maxima at 334nm

(Eu(III) ε = 10 488 $M^{-1}cm^{-1}$, Tb(III) ε = 11 778 $M^{-1}cm^{-1}$) and 342nm (Eu(III) ε = 10 256 $M^{-1}cm^{-1}$, Tb(III) ε = 11 464 $M^{-1}cm^{-1}$) and the higher energy band having a maxima at 294nm (Eu(III) ε = 30 123 $M^{-1}cm^{-1}$, Tb(III) ε = 34 182 $M^{-1}cm^{-1}$) with shoulders at 284nm (Eu(III) ε = 26 904 $M^{-1}cm^{-1}$, Tb(III) ε = 29 298 $M^{-1}cm^{-1}$) and 266nm (Eu(III) ε = 22 384 $M^{-1}cm^{-1}$, Tb(III) ε = 23 524 $M^{-1}cm^{-1}$) (see Fig.3.8).

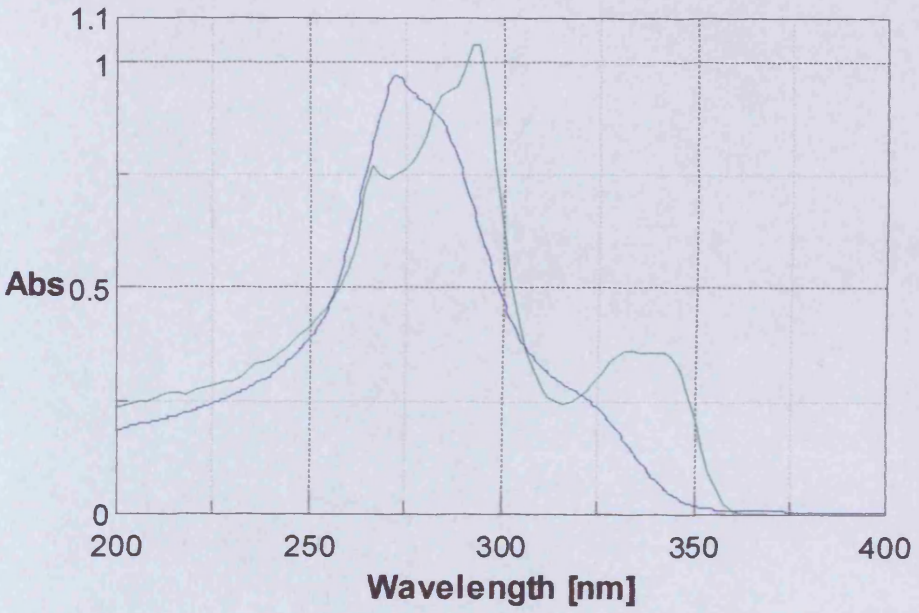

Fig. 3.8: The absorbance spectrum of $PhTerpyAcid_2$ (——) $[Eu(PhTerpyAcid_2)(H_2O)_2][ClO_4]_2$ and $[Tb(PhTerpyAcid_2)(H_2O)_2][ClO_4]_2$ (——) in DMF

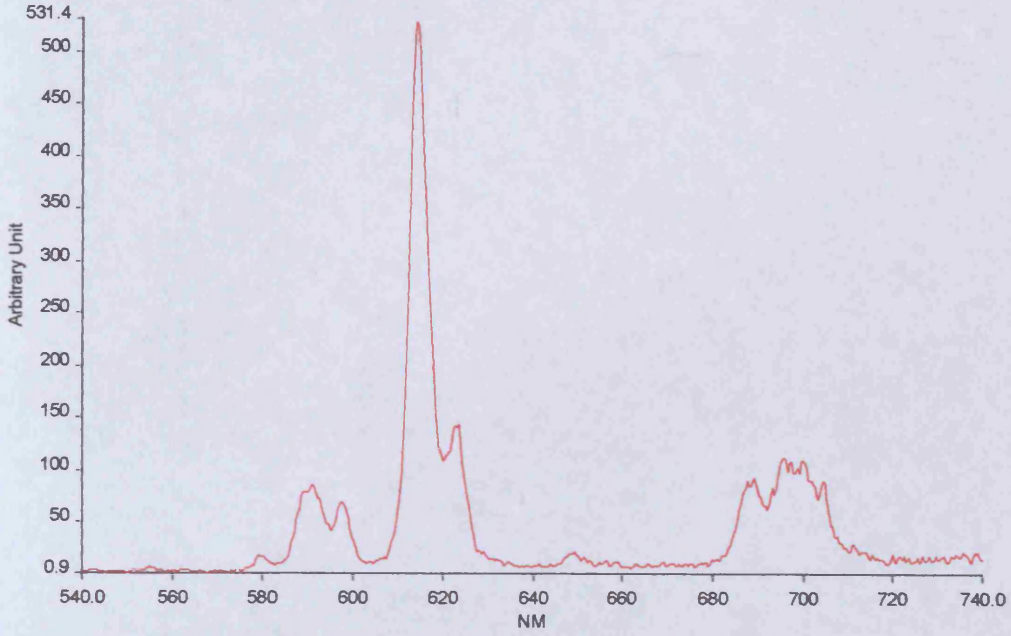

Fig. 3.9: The emission spectrum $[Eu(PhTerpyAcid_2)(H_2O)_2][ClO_4]_2$ in DMF (λ_{exc} = 354nm, λ_{emis} = 615nm).

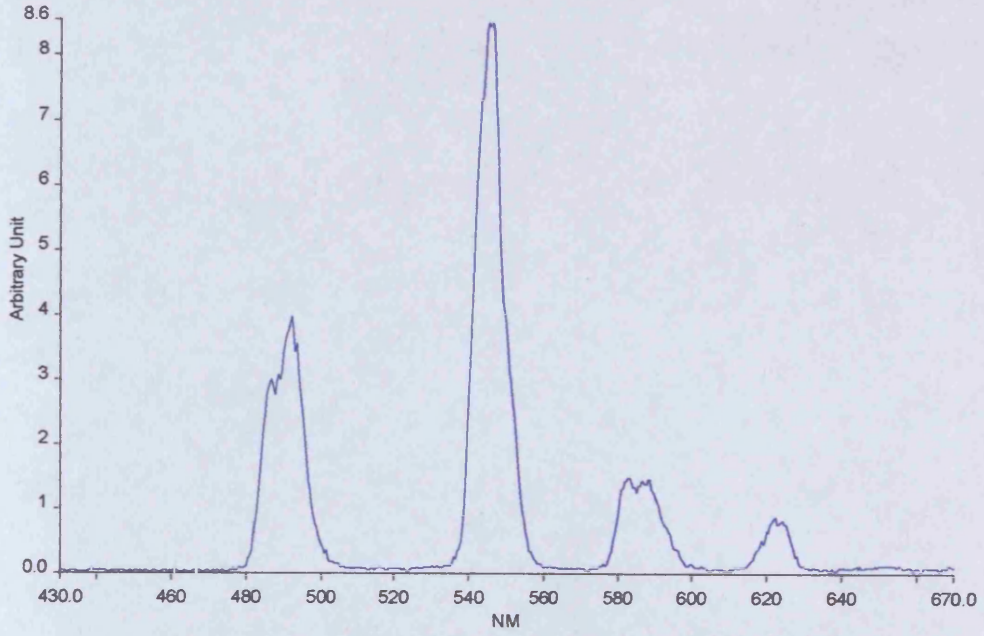

Fig. 3.10: The emission spectrum of $[[Tb(PhTerpyAcid_2)(H_2O)_2][ClO_4]_2$ in DMF (λ_{exc} = 355nm, λ_{emis} = 545nm).

The emission spectrum of the Eu(III) complex showed nine sharp bands (see Fig.3.9) typical of Eu(III) complexes and the bands are assigned in Table 3.4. A predominant peak occurring at 615nm is observed and the increased line splitting of the peaks would indicate that the complex has a much lower symmetry than its precursor terpyridine N-oxides in solution, understandable from both the mass spectrum results and comparison of the structures. The relative integrated areas of the $^5D_0 \rightarrow {}^7F_J$ transitions are 0.1, 1.0, 8.65, 0.28 and 3.13 for J=0, 1, 2, 3 and 4 respectively.

The emission spectrum of the Tb(III) complex shows four sharp bands (see Fig.3.10), typical of Tb(III) emission and the bands are assigned in Table 3.5. The very weak $^5D_4 \rightarrow {}^7F_1$, $^7F_0$ transitions are too weak to analyse. The relative integrated areas of the $^5D_4 \rightarrow {}^7F_J$ transitions are 1.0, 2.2, 0.66, 0.33, 0.15 and 0.05 for J=6, 5, 4, 3 and 2 respectively.

3.8.2 The Luminescence Properties of $[Eu(PhTerpyAmide_2)(H_2O)_2][ClO_4]_3$ and $[Tb(PhTerpyAmide_2)(H_2O)_2][ClO_4]_3$

The absorbance spectrum of the N,N'-(di-*tert*-butyl)-4'-phenyl-2,2':6',2''-terpyridine-6,6''-dicarboxamide ligand recorded in DMF at room temperature shows a broad band with a maxima present at 268nm (ε = 37 168 $M^{-1}cm^{-1}$) and a shoulder on the peak at 298nm (ε = 29 174 $M^{-1}cm^{-1}$). A shoulder can also be observed at 322nm (ε = 8304 $M^{-1}cm^{-1}$). The absorbance spectra of the Eu(III) and Tb(III) complexes at dilute concentration (45μmol) in DMF gave the same absorption spectrum as the ligand.

Excitation of the dilute solutions at 295nm in DMF and CH_3CN yielded a broad ligand emission at 355nm (see fig.3.11) and the excitation spectrum was acquired using this wavelength. There was no Eu(III) or Tb(III) emission present in the spectrum. Similar to the parent unsubstituted ligand complexes, it appears that decomplexation of the amide complex is occurring.

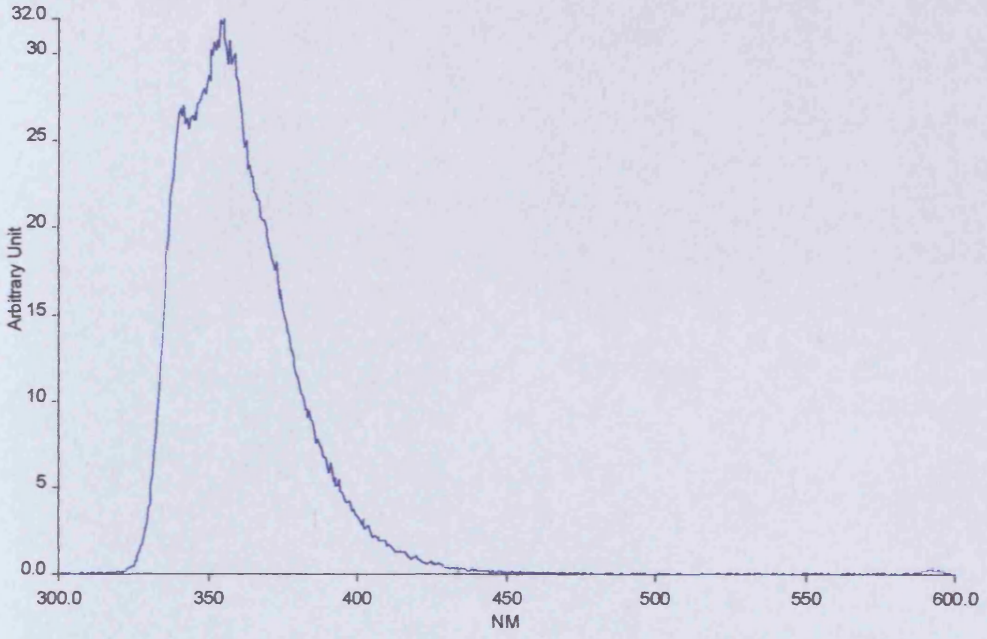

Fig. 3.11: The emission spectrum of dilute $[Eu(PhTerpyAmide_2)(H_2O)_2][ClO_4]_3$ in DMF (λ_{exc} = 295nm, λ_{emis} = 355nm).

The absorption spectra of concentrated samples of the Eu(III) and Tb(III) complexes in CH_3CN (350μmol) were analogous but too intense and off the scale of the spectrometer, although the weaker absorptions could be analysed (See Fig. 3.12). The spectra reveal that upon complexation a shifting of the shoulder at 282nm by 16nm to

298nm occurs. The weaker shoulders are also red shifted appearing at 326nm and 350nm.

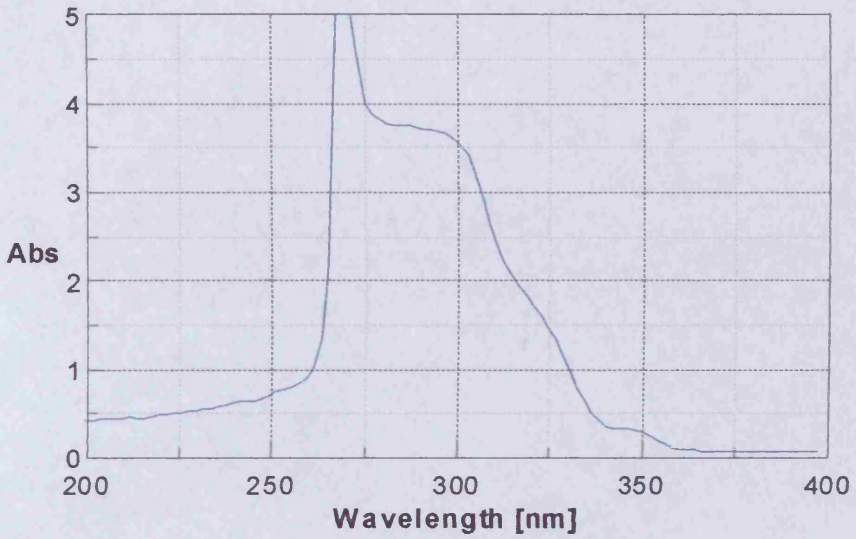

Fig. 3.12: Absorbance spectrum of the concentrated $[Eu(PhTerpyAmide_2)(H_2O)_2][ClO_4]_3$ and $[Tb(PhTerpyAmide_2)(H_2O)_2][ClO_4]_3$ in CH_3CN.

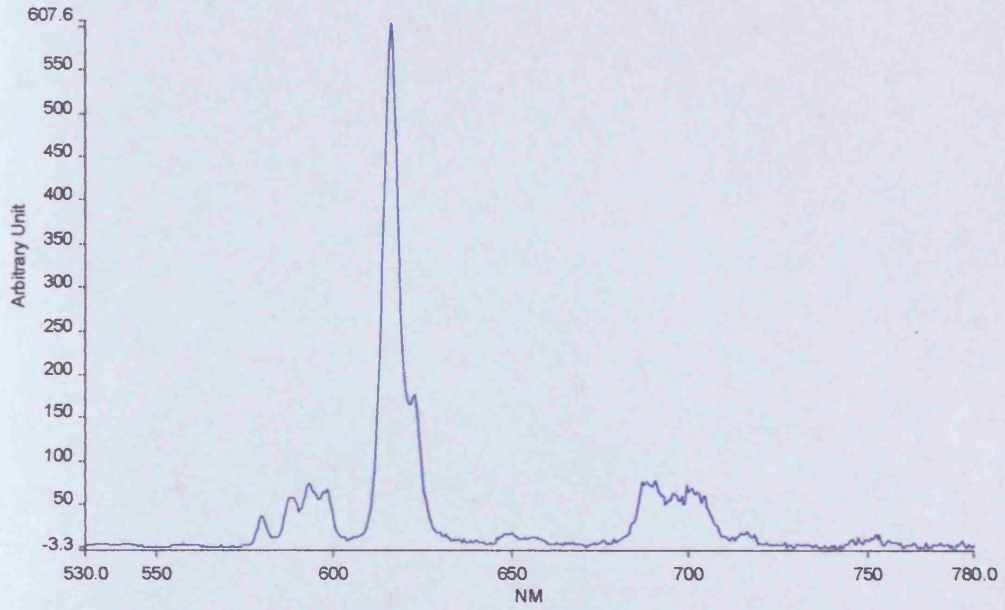

Fig. 3.13: The emission spectrum $[Eu(PhTerpyAmide_2)(H_2O)_2][ClO_4]_3$ in CH_3CN (λ_{exc} = 357nm, λ_{emis} = 615nm).

The emission spectrum showed ten sharp bands typical of Eu(III) emission (see Fig.3.13) with a predominant peak occurring at 615nm. The single peak observed at 579nm corresponding to the $^5D_0 \rightarrow {}^7F_0$ transition is suggestive of a single complex species in solution. The complex exhibits the greatest amount of peak splitting in the terpyridine series suggesting that, if it is a single species, the amide substituted complexes are the least symmetrical in solution, not surprising considering the bulky tert-butyl amide arms that are present. The relative integrated areas of the $^5D_0 \rightarrow {}^7F_J$ transitions are 0.12, 1.0, 5.83, 0.09 and 1.72 for J=0, 1, 2, 3 and 4 respectively.

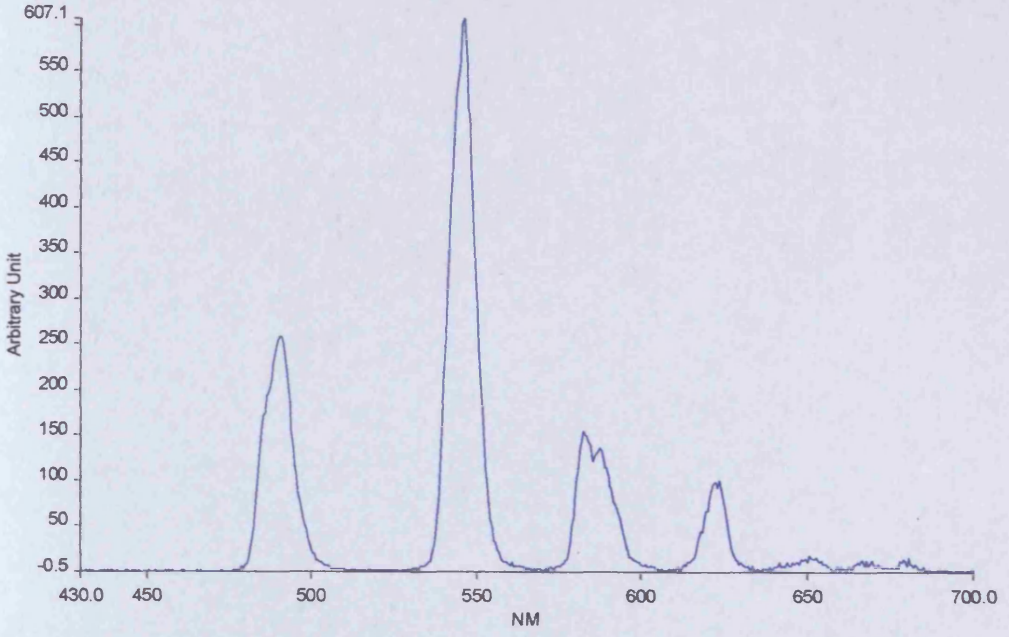

Fig. 3.14: The emission spectrum of $[Tb(PhTerpyAmide_2)(H_2O)_2][ClO_4]_3$ in CH_3CN (λ_{exc} = 357nm, λ_{emis} = 544nm).

The emission spectrum of $[Tb(PhTerpyAmide_2)(H_2O)_2][ClO_4]_3$ shows four sharp bands (see Fig.3.14) with three less intense peaks present, typical of Tb(III) emission.. The relative integrated areas of the $^5D_4 \rightarrow {}^7F_J$ transitions are 1.0, 2.0, 0.66, 0.28, 0.04, 0.016 and 0.016 for J=6, 5, 4, 3, 2 and 1 respectively. Of note is a weak, broad peak observable at 355nm perhaps suggestive of small amounts of uncomplexed ligand.

The presence of Eu(III) and Tb(III) emission in the concentrated complex samples would seem to indicate that a decomplexation of the complexes is occurring in the dilute sample. This would suggest that the poor lanthanide emission at low concentration is not due to a poor matching of the energy levels but that the diamide ligands must be considered weak co-ordinators of Eu(III) and Tb(III) ions.

3.8.3 The Luminescence Properties of $[Eu(4\text{-}^{is}Pr\text{-}PhQuaterAcid_2)(H_2O)_2][ClO_4]$ and $[Tb(4\text{-}^{is}Pr\text{-}PhQuaterAcid_2)(H_2O)_2][ClO_4]$

The absorbance spectrum of the protonated 4-^{is}Pr-quaterpyridine-6,6'''-dicarboxylic acid ligand recorded in DMF at room temperature shows a broad band at 275nm (ε = 19 303 $M^{-1}cm^{-1}$) with two shoulders at 286nm (ε = 17 097 $M^{-1}cm^{-1}$) and 323nm (ε = 4794 $M^{-1}cm^{-1}$) attributed to $\pi \rightarrow \pi^*$ transitions on the pyridine rings. Upon complexation to Eu(III) or Tb(III), the $\pi \rightarrow \pi^*$ transitions are shifted to lower energy, as observed in the complexation of the other ligand systems used in this study. The spectrum reveals two maxima appearing at 268nm (Eu(III) ε = 54 311 $M^{-1}cm^{-1}$, Tb(III) ε = 55 311 $M^{-1}cm^{-1}$) and 288nm (Eu(III) ε = 56 738 $M^{-1}cm^{-1}$, Tb(III) ε = 57 123 $M^{-1}cm^{-1}$).

The $\pi \rightarrow \pi^*$ shoulders that appeared in the ligand spectrum have undergone red shifts of 30nm to 316nm (Eu(III) ε = 39 228 $M^{-1}cm^{-1}$, Tb(III) ε = 38 904 $M^{-1}cm^{-1}$) and 29nm to 352nm (Eu(III) ε = 10 442 $M^{-1}cm^{-1}$, Tb(III) ε = 10 529 $M^{-1}cm^{-1}$) (see Fig. 3.15). These red shifts are ~10nm greater than in the terpyridine dicarboxylic acid complexes. The complex extinction coefficients are also similar to the terpyridine dicarboxylic acid complexes at the long wavelength part of the spectrum (ε ~ 10 529 $M^{-1}cm^{-1}$ at ~350nm) but are much greater at the short wavelength (ε ~ 25 000 $M^{-1}cm^{-1}$ higher for the quaterpyridines than the terpyridine counterpart) making the quaterpyridines better chromophores for the absorption of energy for the complexes.

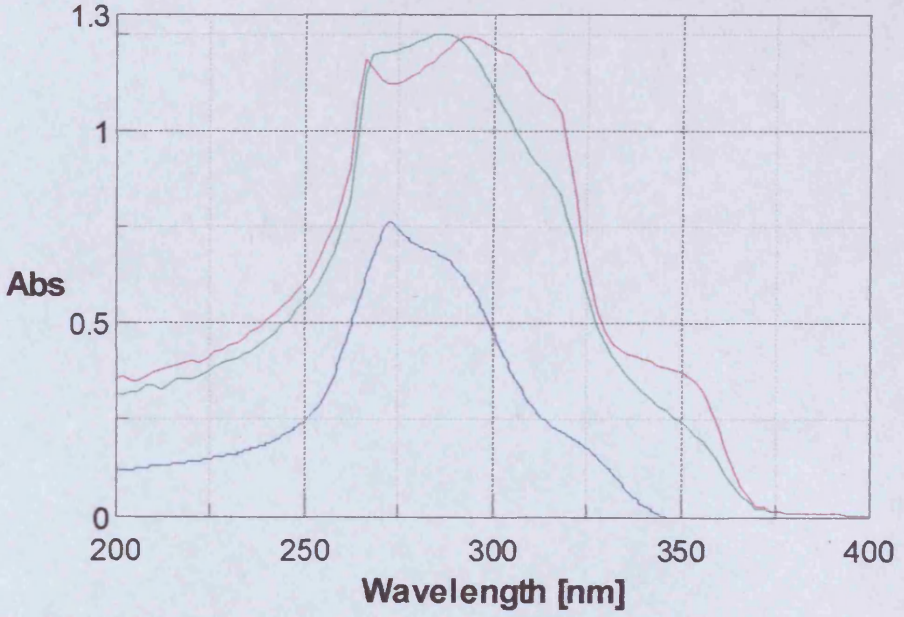

Fig. 3.15: The absorbance spectrum of 4-^{iso}Pr-PhQuaterAcid$_2$(——), [Eu(4-^{iso}Pr-PhQuaterAcid$_2$)$(H_2O)_2$][ClO_4](——) and [Tb(4-^{iso}Pr-PhQuaterAcid$_2$)$(H_2O)_2$][ClO_4](——) in DMF.

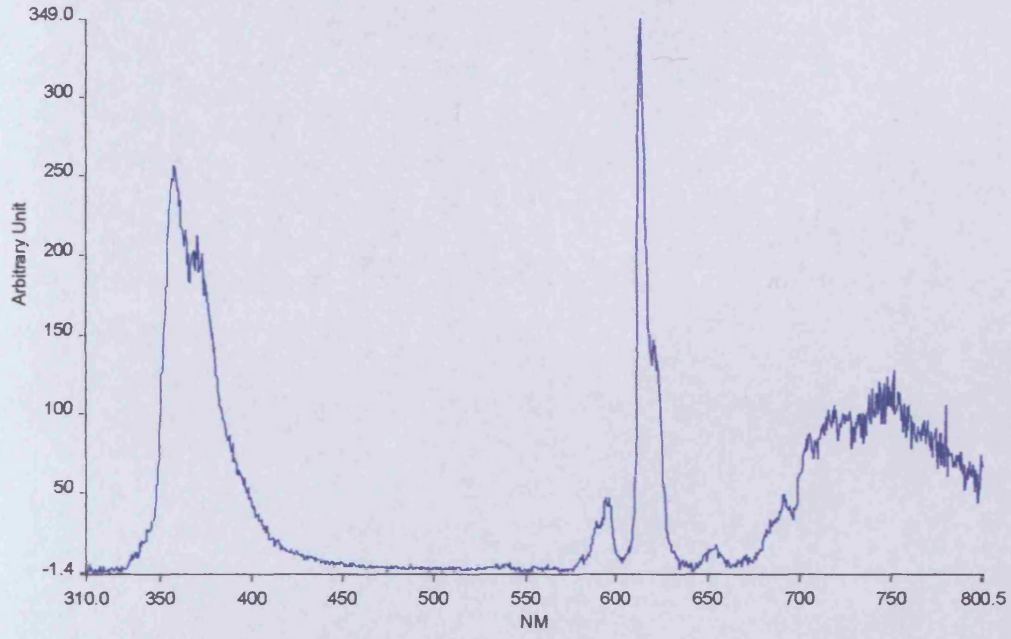

Fig. 3.16: The emission spectrum of $[Eu(4\text{-}^{iso}Pr\text{-}PhQuaterAcid_2)(H_2O)_2][ClO_4]$ in DMF (λ_{exc} = 319nm, λ_{emis} = 615nm).

The emission spectrum of the Eu(III) complex showed several bands (see Fig. 3.16) typical of Eu(III) emission with a predominant peak occurring at 615nm. The spectrum displayed a greater amount of peak splitting than the quaterpyridine N-oxides but less than the parent quaterpyridine complex. This would indicate the complex has a lower symmetry in solution than the N-oxides but higher than the unsubstituted quaterpyridine complex. The relative integrated areas of the $^5D_0 \rightarrow {}^7F_J$ transitions are 0.05, 1.0, 7.94, 0.3 and 0.2 for J=0, 1, 2, 3 and 4 respectively. Unfortunately, all of the $^5D_0 \rightarrow {}^7F_4$ cannot be seen as it is concealed behind the harmonic emission of the intense ligand emission occurring at 358nm. The very strong ligand emission is one of the most prominent features of the spectrum, which would either indicate poor energy transfer efficiency or decomplexation of the ligand occurring in the solution.

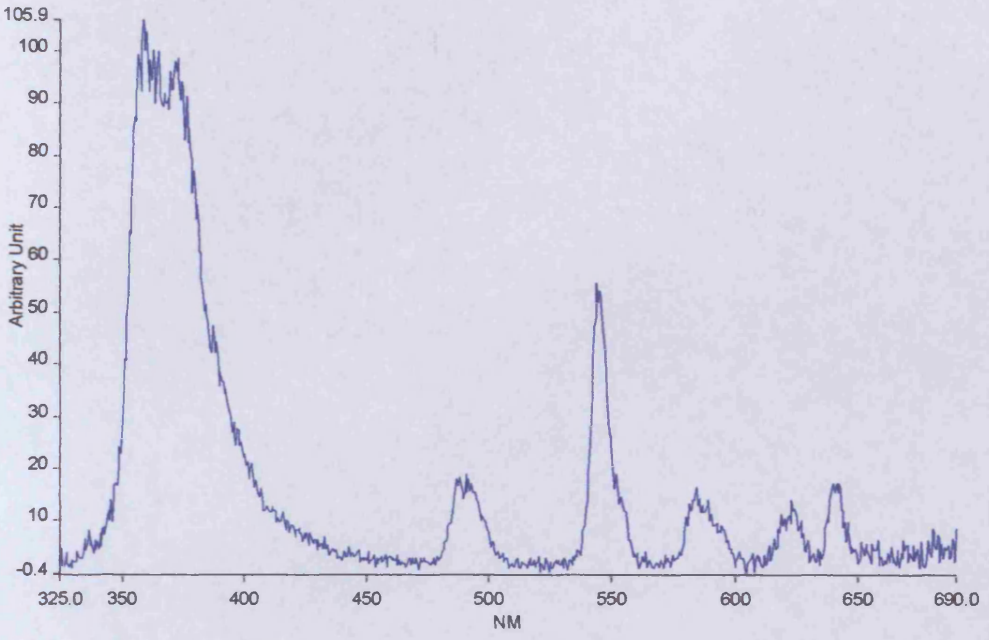

Fig. 3.17: The emission spectrum of $[Tb(4\text{-}^{iso}Pr\text{-}PhQuaterAcid_2)(H_2O)_2][ClO_4]$ in DMF (λ_{exc} = 322nm, λ_{emis} = 543nm).

The emission spectrum of the Tb(III) complex showed four sharp bands (see Fig.3.17), typical of Tb(III) emission. The $^5D_4 \rightarrow {}^7F_2$ transition and the very weak $^5D_4 \rightarrow {}^7F_1$, $^7F_0$ transitions are not observable. The relative integrated areas of the $^5D_4 \rightarrow {}^7F_J$ transitions are 1.0, 2.32, 0.73, 0.41 for J=6, 5, 4 and 3 respectively. As with the Eu(III) analogue, the very strong ligand emission at 358nm is one of the most prominent features of the spectrum, which would either indicate very poor energy transfer efficiency or decomplexation of the ligand occurring in the solution.

3.8.4 The Luminescence Properties of $[Eu(4\text{-}^{is}Pr\text{-}PhQuaterAmide_2)(H_2O)][ClO_4]_3$ and $[Tb(4\text{-}^{is}Pr\text{-}PhQuaterAmide_2)(H_2O)][ClO_4]_3$

The absorbance spectrum of the 4-^{is}Pr-PhQuinqueAmide$_2$ ligand recorded in DMF at room temperature showed a broad band with a maxima at 268nm (ε = 72 443 $M^{-1}cm^{-1}$) and shoulders at 292nm (ε = 58 884 $M^{-1}cm^{-1}$) and 322nm (ε = 22 387 $M^{-1}cm^{-1}$).

The absorbance spectra of the complexes in CH_3CN, similar to the other amide bearing ligands in this series, could not be obtained. At concentrations low enough to yield an absorbance spectrum, the complex underwent decomplexation resulting in a ligand spectrum. This was confirmed by luminescence spectroscopy showing ligand fluorescence similarly to other systems. Concentrated samples of the Eu(III) and Tb(III) complexes (400μmol) in acetonitrile at room temperature yielded emission spectra upon analysis.

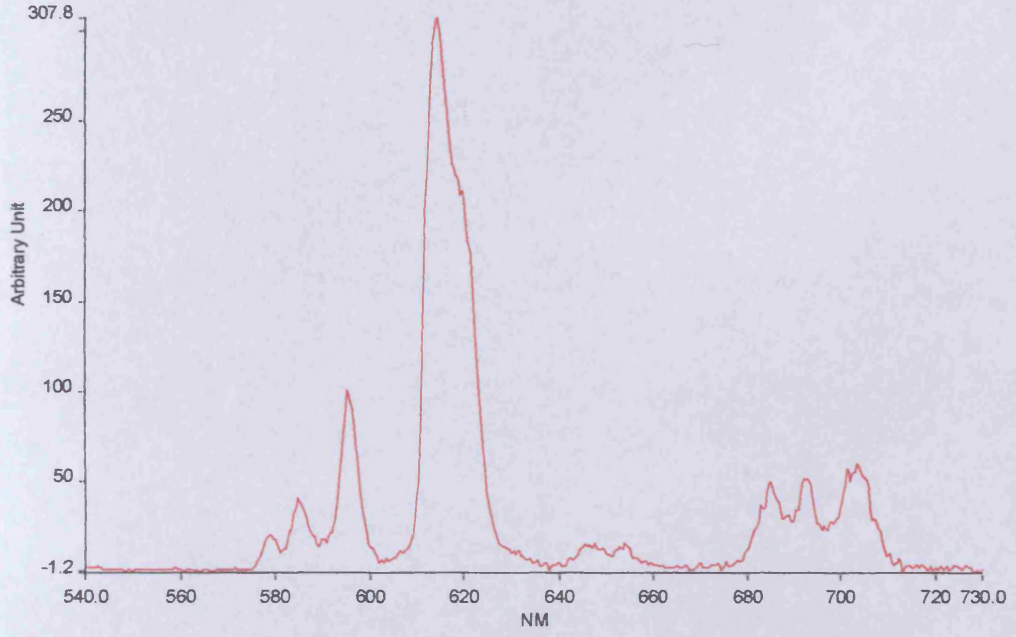

Fig. 3.18: The emission spectrum of $[Eu(4\text{-}^{iS}Pr\text{-}PhQuaterAmide_2)(H_2O)][ClO_4]_3$ in CH_3CN (λ_{exc} = 371nm, λ_{emis} = 615nm).

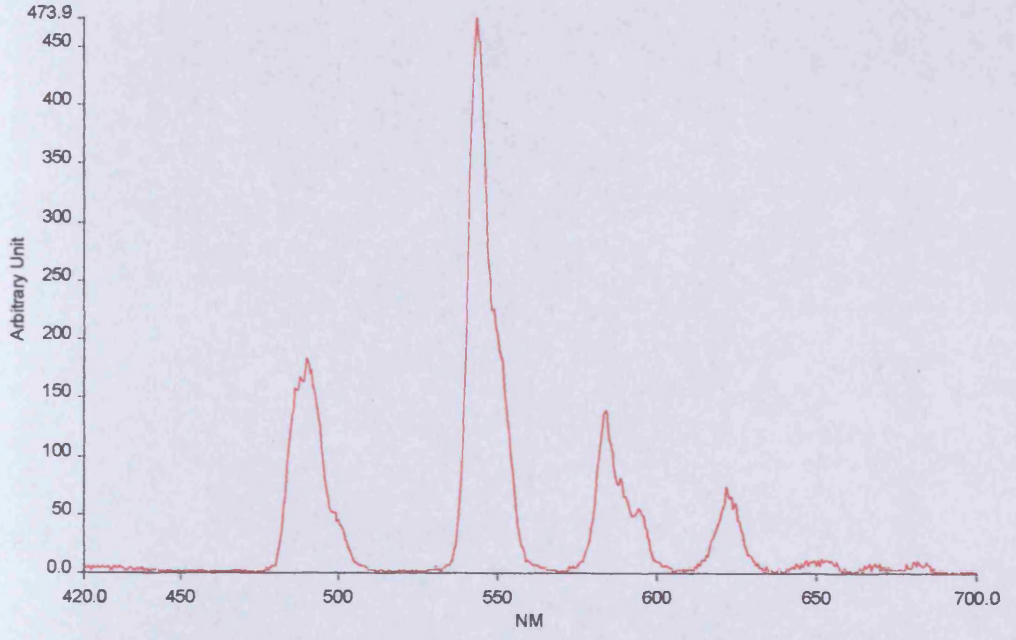

Fig. 3.19: The emission spectrum of $[Tb(4\text{-}^{iS}Pr\text{-}PhQuaterAmide_2)(H_2O)][ClO_4]_3$ in CH_3CN (λ_{exc} = 372nm, λ_{emis} = 543nm).

The emission spectrum of the Eu(III) complex is typical for Eu(III) showing nine peaks. The spectrum displayed a greater amount of peak splitting than its acid bearing counterpart indicating a lower symmetry. The relative integrated areas of the $^5D_0 \rightarrow {}^7F_J$ transitions are 0.33, 1.0, 6.1, 0.17 and 2.25 for J=0, 1, 2, 3 and 4 respectively. At this concentration no ligand emission can be observed. The emission spectrum of the Tb(III) complex showed several sharp bands, typical of Tb(III) emission. The relative integrated areas of the $^5D_4 \rightarrow {}^7F_J$ transitions are 1.0, 1.97, 0.63, 0.27, 0.05, 0.01 and 0.017 for J=6, 5, 4, 3, 2, 1 and 0 respectively.

3.8.5 The Luminescence Properties of [Eu(4-^{is}Pr-PhQuinqueAcid$_2$)(H$_2$O)$_2$][ClO$_4$] and [Tb(4-^{is}Pr-PhQuinqueAcid$_2$)(H$_2$O)$_2$][ClO$_4$]

The absorbance spectrum of the protonated 4',4'''-(4-isopropyphenyl)-2,2':6',2'':6'',2''':6''',2'''':6'''',2''''-quinquepyridine-6,6''''-dicarboxylic acid ligand recorded in DMF at room temperature shows a broad band at 268nm (ε = 70 968 $M^{-1}cm^{-1}$) with shoulders appearing at 288nm (ε = 55 213 $M^{-1}cm^{-1}$) and 322nm (ε = 23 136 $M^{-1}cm^{-1}$) attributed to $\pi \rightarrow \pi^*$ transitions on the pyridine rings. Upon complexation the Eu(III) and Tb(III) complexes show very different absorption spectra and the reasons for this are attributed to ligand to metal charge transfer of the Eu(III) metal. The Eu(III) complex shows two maxima with the most absorbing peak at a similar position to the ligand at 268nm (ε = 74 220 $M^{-1}cm^{-1}$) and the shoulder in the ligand spectrum now appearing as a maxima being red shifted 14nm to a lower energy appearing at 302nm (ε = 76 590 $M^{-1}cm^{-1}$). Two shoulders can also be observed at 328nm (ε = 57 480 $M^{-1}cm^{-1}$) and 358nm (ε

= 28 810 $M^{-1}cm^{-1}$). The Tb(III) complex absorption spectrum shows two separate bands with greatly differing extinction coefficients to that of the Eu(III) complex. The maxima that was observed at 302nm in the Eu(III) complex has shifted an extra 10nm appearing at 312nm with a weaker extinction coefficient (ε = 57 698 $M^{-1}cm^{-1}$). The maxima at 268nm remains at the same position as in the Eu(III) complex but with an extinction coefficient nearly twice as intense (ε = 135 653 $M^{-1}cm^{-1}$) (See Fig. 3.20). Compared to the terpyridine and quaterpyridine dicarboxylic acid complexes the quinquepyridine dicarboxylic acid complexes offer the highest extinction coefficients with ε increasing through the series due the increasing conjugation contained in the ligands. The [Eu(4-^{iso}Pr-PhQuinqueAcid$_2$)(H_2O)$_2$] [ClO_4] complex also displays the longest maximum wavelength (358nm) of the series being 6nm longer than the quaterpyridine analogue making it the most desirable for bioassays.

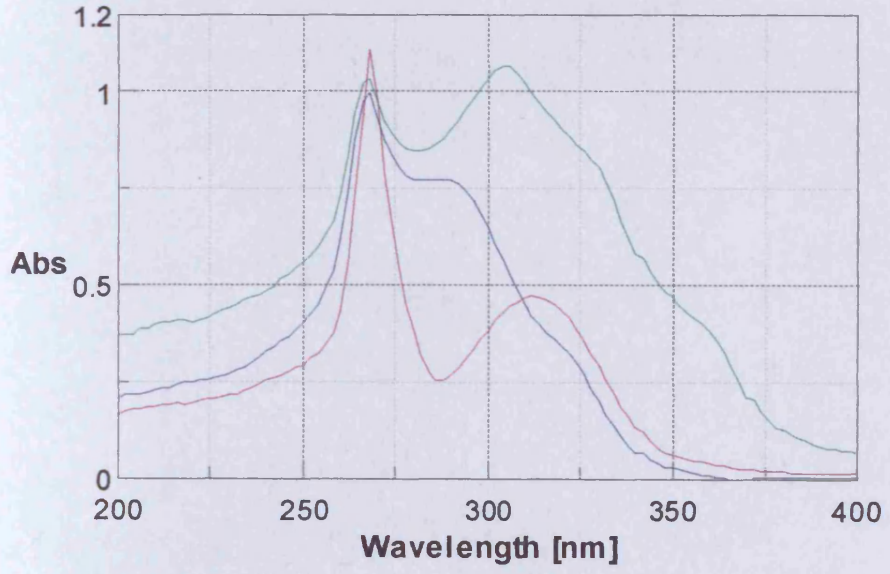

Fig. 3.20: The absorbance spectrum of 4-^{iso}Pr-PhQuinqueAcid$_2$ (——), [Eu(4-^{iso}Pr-PhQuinqueAcid$_2$)(H_2O)$_2$][ClO_4] (——) and [Tb(4-^{iso}Pr-PhQuinqueAcid$_2$)(H_2O)$_2$][ClO_4] (——) in DMF

The emission spectra of the two complexes were very different with the Tb(III) complex only displaying ligand emission in its emission spectrum.

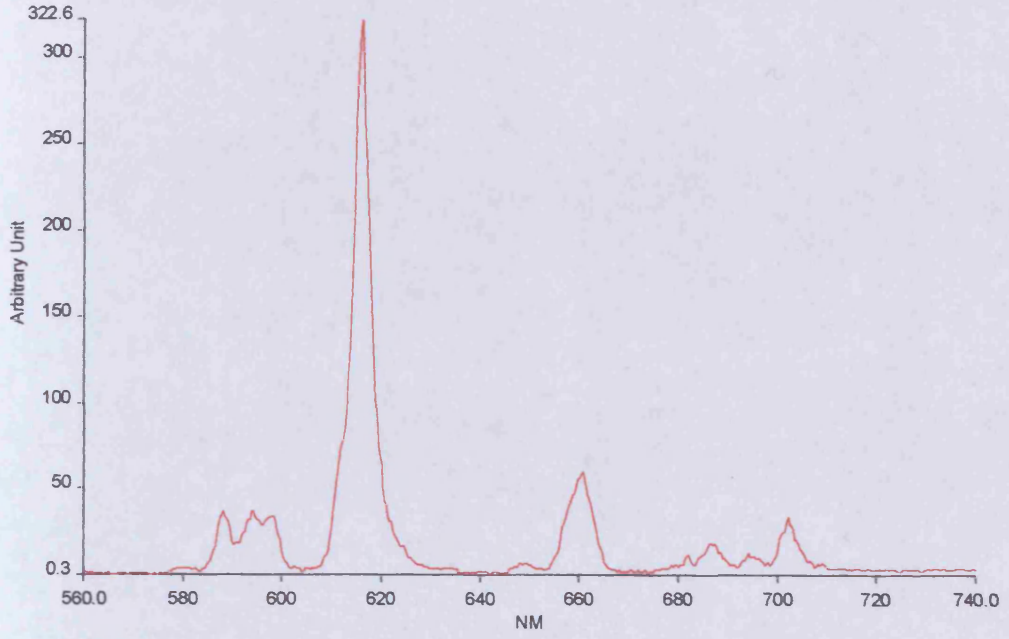

Fig. 3.21: The emission spectrum of $[Eu(4\text{-}^{iso}Pr\text{-}PhQuinqueAcid_2)(H_2O)_2][ClO_4]$ in DMF (λ_{exc} = 330nm, λ_{emis} = 615nm).

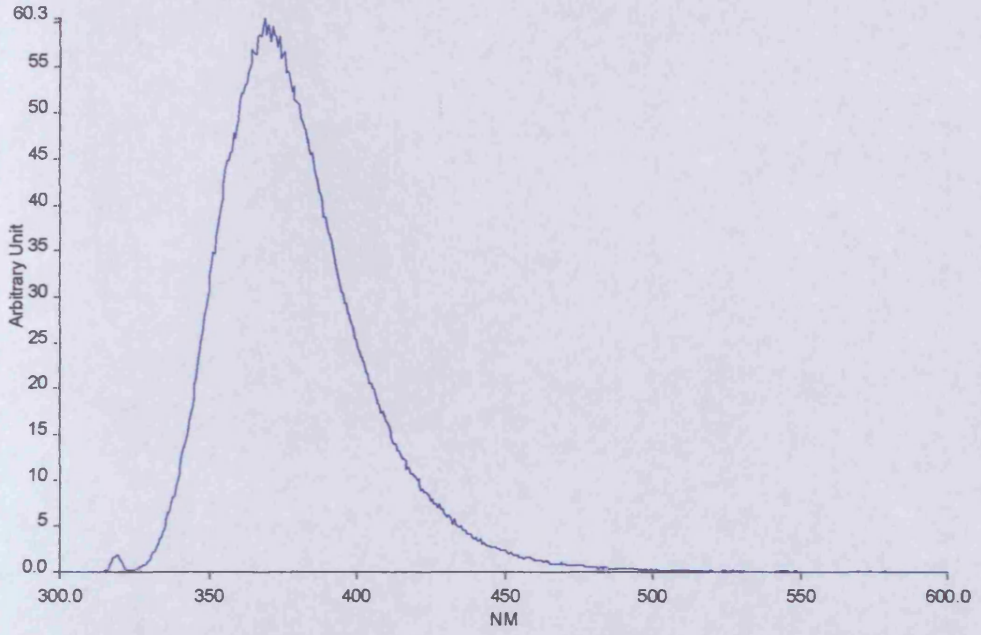

Fig. 3.22: The emission spectrum $[Tb(4\text{-}^{iso}Pr\text{-}PhQuinqueAcid_2)(H_2O)_2][ClO_4]$ in DMF (λ_{exc} = 274nm, λ_{emis} = 368nm).

The emission spectrum of the Eu(III) complex showed eight sharp bands (see Fig.3.21) typical of Eu(III) emission with a predominant peak occurring at 615nm. The spectrum shows a greater amount of peak splitting than any of the previous quinquepyridine complexes, suggesting a less symmetrical structure in solution which would agree with the proposed helical geometries. The relative integrated areas of the $^5D_0 \rightarrow {}^7F_J$ transitions are 0.009, 1.0, 4.77, 0.03 and 0.75 for J= 1, 2, 3 and 4 respectively. The peak at 660nm should be ignored, as this is merely a harmonic of the excitation frequency of 330nm.

The emission spectrum of the Tb(III) complex is dominated by a broad ligand emission appearing at 368nm with no Tb(III) emission present (see Fig. 3.22). As shown,

the mass spectrum and other spectroscopic measurements indicate the proposed complex has been formed. Therefore, by considering the nature of the europium complex, this broad ligand emission and lack of Tb(III) emission suggests a very poor matching of the energy levels, such that the Tb(III) emission is unattainable.

3.8.6 The Luminescence Properties of $[Eu(4\text{-}^{iS}Pr\text{-}PhQuinqueAmide_2)(H_2O)_2][ClO_4]_3$ and $[Tb(4\text{-}^{iS}Pr\text{-}PhQuinqueAmide_2)(H_2O)_2][ClO_4]_3$

As has become expected for the amide bearing ligand series the $[Eu(4\text{-}^{iS}Pr\text{-}PhQuinqueAmide_2)(H_2O)_2][ClO_4]_3$ and $[Tb(4\text{-}^{iS}Pr\text{-}PhQuinqueAmide_2)(H_2O)_2][ClO_4]_3$ complexes show decomplexation of the complexes at low solution concentrations suggesting relatively low stability constants. The absorption spectra of the complexes in CH_3CN and DMF at low concentration (16μmol) show the same spectra as the ligand and the emission spectra for the dilute samples (16μmol) in CH_3CN at room temperature show purely ligand emission (see Fig. 3.23). Excitation at 298nm produces a broad ligand emission appearing at 357nm.

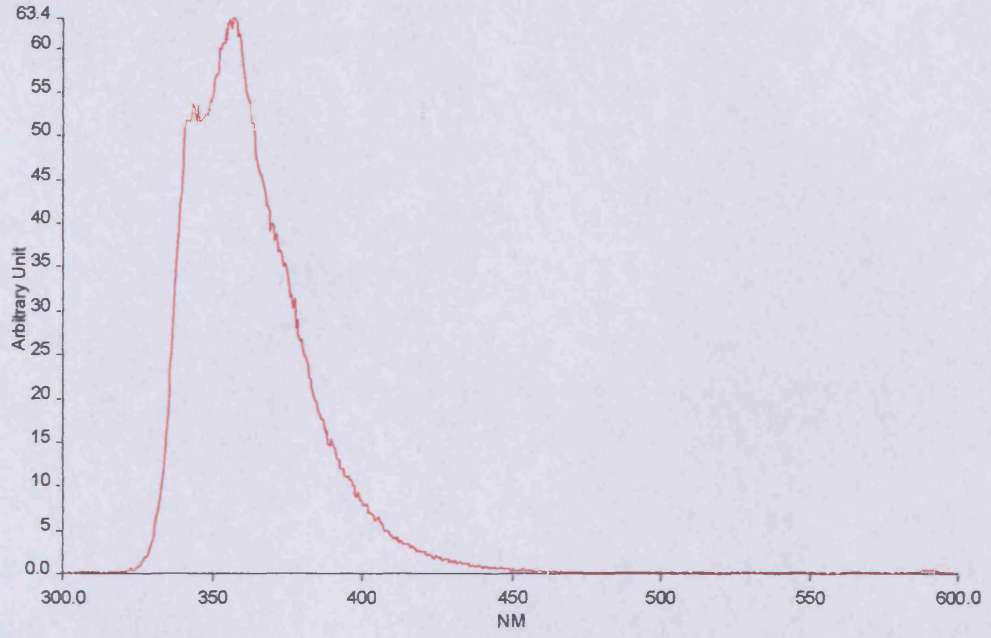

Fig. 3.23: Emission spectrum of dilute (16μmol) $[Eu(4\text{-}^{tS}Pr\text{-}PhQuinqueAmide_2)(H_2O)_2][ClO_4]_3$ and $[Tb(4\text{-}^{tS}Pr\text{-}PhQuinqueAmide_2)(H_2O)_2][ClO_4]_3$ in CH_3CN (λ_{exc} = 298nm, λ_{emis} = 357nm).

Concentrated samples (400μmol) of the Eu(III) and Tb(III) complexes in CH_3CN were analysed. The absorption spectra could not be obtained due to the concentration levels being too high for the spectrometer but emission spectra could be obtained. At these increased concentrations decomplexation does not appear to be taking place. Excitation at 375nm produced the emission spectra.

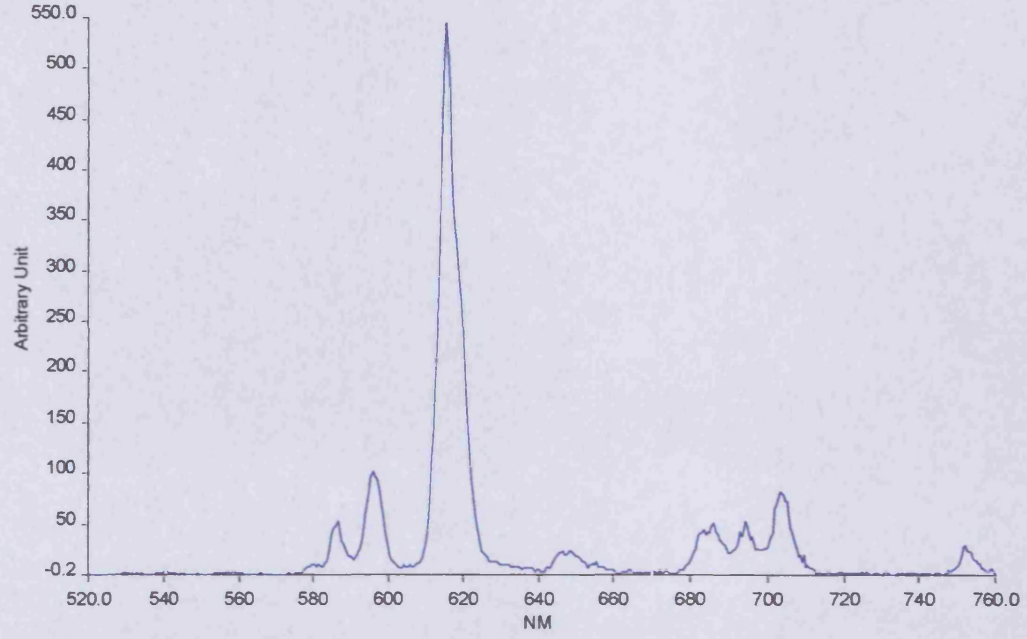

Fig. 3.24: The emission spectrum of $[Eu(4\text{-}^{iso}Pr\text{-}PhQuinqueAmide_2)(H_2O)_2][ClO_4]_3$ in CH_3CN (λ_{exc} = 375nm, λ_{emis} = 615nm).

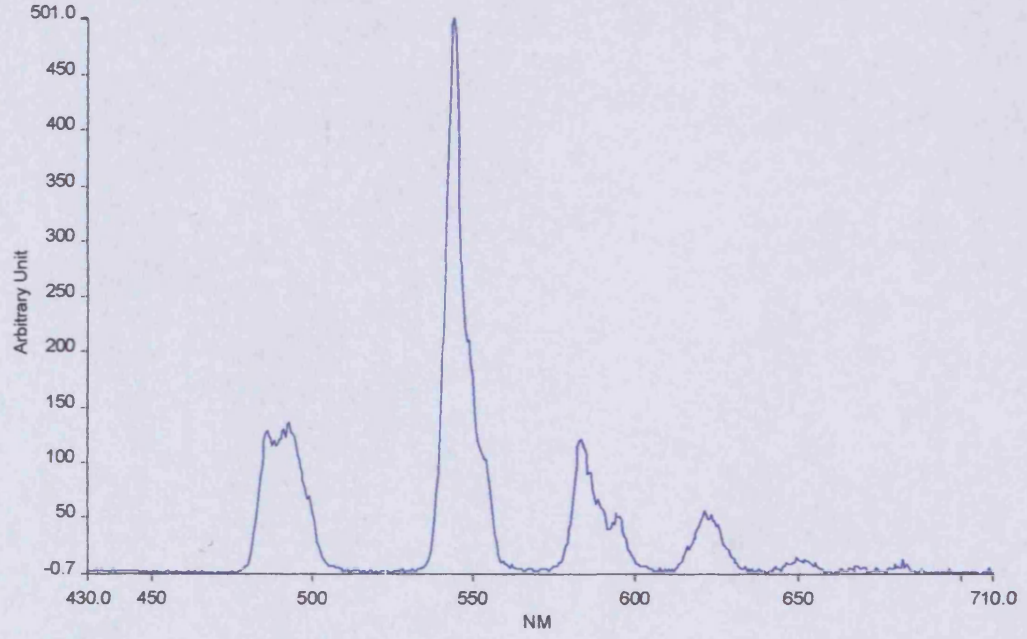

Fig. 3.25: The emission spectrum of $[Tb(4\text{-}^{iso}Pr\text{-}PhQuinqueAmide_2)(H_2O)_2][ClO_4]_3$ in CH_3CN (λ_{exc} = 375 nm, λ_{emis} = 544 nm).

The emission spectrum of the Eu(III) complex showed eight sharp bands (see Fig. 3.24), typical of the Eu(III) emission seen in this study with a predominant peak occurring at 615 nm. The complex undergoes an even greater amount of peak splitting than its acid counterpart so suggesting it is the least symmetrical complex of the quinquepyridine series of complexes. The relative integrated areas of the $^5D_0 \rightarrow {}^7F_J$ transitions are 0.006, 1.0, 5.3, 0.27, 1.57 for J=0, 1, 2, 3 and 4 respectively. The emission spectrum of the Tb(III) complex showed several sharp bands (see Fig.3.25), typical of Tb(III) emission. The relative integrated areas of the $^5D_4 \rightarrow {}^7F_J$ transitions are 1.0, 1.99, 0.63, 0.25, 0.05, 0.002 and 0.001 for J=6, 5, 4, 3, 2 and 1 respectively.

3.9 Relative quantum Yields and Discussion

The relative quantum yields (Φ) were measured in an analogous fashion to the compounds in the last chapter (section 2.11). All compounds have been measured relative to $[Eu(PhTerpyAcid_2)(H_2O)_2][ClO_4]_2$ which has been assigned the arbitrary value of 1. The compound Eu(2,2'-bipyridine-6,6'-dicarboxylic acid)$_2$(Et_3NH) which has previously been synthesised by Mukkala *et al*[5] and further studied by Bünzli *et al*[3] has been synthesised and contrasted to the compounds analysed in this study.

Compound	Solvent	ε_{max} ($M^{-1}cm^{-1}$)	η^a	Φ^b	Luminescence Intensity of equimolar solutions (400μmol)[b,f]
$Eu(BipyAcid_2)_2^{3+}$	DMF	18 886 (nm)	13.17	3.24[c]	-
$Eu(PhTerpyAcid_2)^{3+}$	DMF	30 123 (294nm)	8.65	1.0[c]	1.0
$Eu(PhTerpyAmide_2)^{3+}$	CH_3CN	-	5.83	-	0.895
$Eu(PhTerpyAcid_2O_3)^{3+}$	DMF	-	-	0[d]	0
$Eu(4\text{-}^{is}Pr\text{-}PhQuaterAcid_2)^{3+}$	DMF	56 738 (288nm)	7.94	0.57[d]	-
$Eu(4\text{-}^{is}Pr\text{-}PhQuaterAmide_2)^{3+}$	CH_3CN	-	6.10	-	0.68
$Eu(4\text{-}^{is}Pr\text{-}PhQuinqueAcid_2)^{3+}$	DMF	76 590 (302nm)	4.77	0.78[c]	-
$Eu(4\text{-}^{is}Pr\text{-}PhQuinqueAmide_2)^{3+}$	CH_3CN	-	5.30	-	0.85
$Tb(PhTerpyAcid_2)^{3+}$	DMF	34 182 (294nm)	-	0.4[e]	-
$Tb(PhTerpyAmide_2)^{3+}$	CH_3CN	-	-	-	1.67
$Tb(4\text{-}^{is}Pr\text{-}PhQuaterAcid_2)^{3+}$	DMF	57 123 (288nm)	-	0.172[e]	-
$Tb(4\text{-}^{is}Pr\text{-}PhQuaterAmide_2)^{3+}$	CH_3CN	-	-	-	1.34
$Tb(4\text{-}^{is}Pr\text{-}PhQuinqueAcid_2)^{3+}$	DMF	135 653 (268nm)	-	0.019[e]	-
$Tb(4\text{-}^{is}Pr\text{-}PhQuinqueAmide_2)^{3+}$	CH_3CN	-	-	-	1.2

Table 3.6: Absorption and emission characteristics. [a]η=J2/J1 [b]in relation to $[Eu(PhTerpyAcid_2)(H_2O)_2][ClO_4]_2$ =1 [c]excitation wavelength of 286nm [d]excitation wavelength of 306nm [e]excitation wavelength of 320nm [f]excitation wavelength of $\lambda_{exc\ max}$

It should be mentioned first of all the high error involved in these relative quantum yield measurements. At least a 10% error can be assumed in the observed quantum yields and so only general observations have been made regarding the measured compound properties.

Concerning the absorption properties, complexation of the ligands to Eu(III) and Tb(III) produces increases in the extinction coefficients of the ligands making them more efficient antennas. The Eu(III) and Tb(III) complexes of PhTerpyAcid$_2$ have shown an increase of 2900 $M^{-1}cm^{-1}$ over the free ligand, the Eu(III) and Tb(III) complexes of 4-^{is}Pr-PhQuaterAcid$_2$ have shown the vast increase of 37435 $M^{-1}cm^{-1}$ over the free ligand and the Eu(III) and Tb(III) complexes of 4-^{is}Pr-PhQuinqueAcid$_2$ have shown an increase of 5622 $M^{-1}cm^{-1}$ over the free ligand.

The carboxylic acid bearing ligands display no concentration dependence behaviour unlike the amide bearing ligand complexes which display decomplexation at concentrations lower than 400μmol in CH_3CN and DMF. This is not reflected in the measured η ratios with all of the complexes falling in the range of 4.77-8.65, showing that the η ratio is a very crude indicator of the donor ability of the ligand. The binding strength of the acids can therefore be regarded as adequate whist the amides can be considered as poor binders of the lanthanides. The inclusion of the strongly binding carboxylic acid groups has decreased the solubility of the ligands being only soluble in DMF and DMSO. The inclusion of the amide groups however, although not as strongly binding as the acids, has increased the solubility of the complexes making them soluble in organic solvents in which they should be less likely to dissociate.

The highest quantum yield was observed for the Eu(BipyAcid$_2$)$_2$(Et_3NH) complex. The absolute quantum yield of this complex has been determined to be 11.5% by Bünzli *et al*[3] and has a relative quantum yield 3.24 times that of the Eu(III)

complex of $PhTerpyAcid_2$. The $[Eu(PhTerpyAcid_2)(H_2O)_2][ClO_4]_2$ complex has in turn a 1.24 and 1.75 times higher Φ than $[Eu(4\text{-}^{is}Pr\text{-}PhQuinqueAcid_2)(H_2O)_2][ClO_4]$ and $[Eu(4\text{-}^{is}Pr\text{-}PhQuaterAcid_2)(H_2O)_2][ClO_4]$ respectively. This possibly suggests that the $Eu(BipyAcid_2)_2(Et_3NH)$ complex provides the best matching of the ligand triplet level to the excited metal state (υ ~17300cm^{-1}) with the ligand triplet level decreasing in energy from the bipyridine to the quinquepyridine carboxylic acid ligands. This lowering of the triplet level with the introduction of the carboxylic acid binders in the 6 position of the external pyridine rings and with the increasing number of pyridine rings in the ligand would also explain the results found for the Tb(III) complexes. As the ligand triplet level and metal excited state appears to be such a good match for the bipyridine ligand and the ligand triplet level is decreasing through the terpyridine to quinquepyridine ligands then the energy match to the Tb(III) ion for these ligands should be even worse for the ter- to the quinquepyridine ligands as the excitation is needed to be at the higher υ of ~20400cm^{-1}. This trend is indeed seen for the Tb(III) complexes with the $PhTerpyAcid_2$ complex having a Φ = 0.4, the 4-^{is}Pr-$PhQuaterAcid_2$ complex having a Φ = 0.172 and the 4-^{is}Pr-$PhQuinqueAcid_2$ complex having the lowest relative quantum yield observed for the Tb(III) complexes with Φ = 0.019. The analytical and spectroscopic data for $[Tb(4\text{-}^{is}Pr\text{-}PhQuinqueAcid_2)(H_2O)_2][ClO_4]$ indicates formation of the 1:1 complex and so poor luminescence data can therefore quite possibly be attributed to the very poor energy transfer mechanism.

Surprisingly, the amide bearing ligand complexes show an opposite result to the carboxylic acid bearing ligand complexes. The Tb(III) complexes of the amides, whose relative quantum yields could not be determined due to decomplexation of the

complexes at low concentration, exhibit much brighter luminescence than their Eu(III) complex counterparts. This would indicate that the amide ligand triplet levels are at a more suitable level for the Tb(III) excited metal state than that of Eu(III) and the substitution of the amide binders at the 6 position of the external pyridine ligands have the affect of raising the ligand triplet level unlike the carboxylic acids which appear to lower the ligand triplet level. The trend of a decrease in luminescence intensity going from the terpyridine to the quinquepyridine ligands that was seen for the carboxylic acid bearing ligands is also seen for the amide ligands, $[Tb(PhTerpyAmide_2)(H_2O)_2][ClO_4]_3$ having the highest Tb(III) luminescence intensity of the series of complexes with a measured intensity of 1.67.

To show the intensity of the luminescence displayed by these Eu(III) and Tb(III) complexes, photographs of 400μmol solutions in DMF exposed to 365nm UV light were taken. The results are displayed in Figs. 3.26 - 3.31.

Fig. 3.26: Appearance of samples when not exposed to UV light

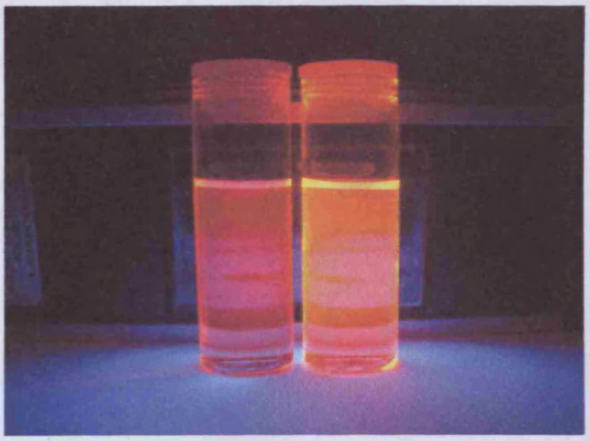

Fig. 3.27: Eu(III) complexes of $BipyAcid_2$ (left) and $PhTerpyAcid_2$ (right)

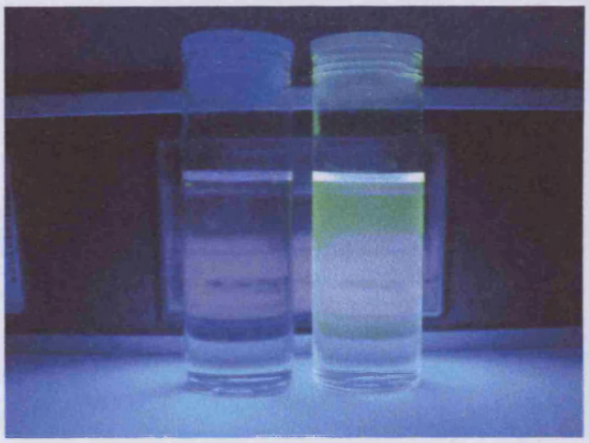

Fig. 3.28: Tb(III) complexes of $BipyAcid_2$ (left) and $PhTerpyAcid_2$ (right)

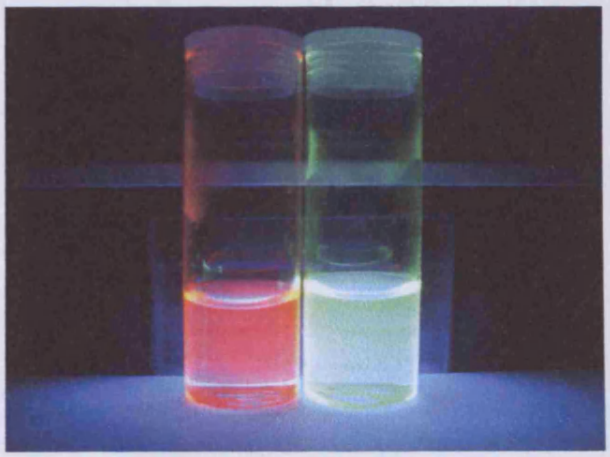

Fig. 3.29: Eu(III) and Tb(III) complexes of $PhTerpyAmide_2$

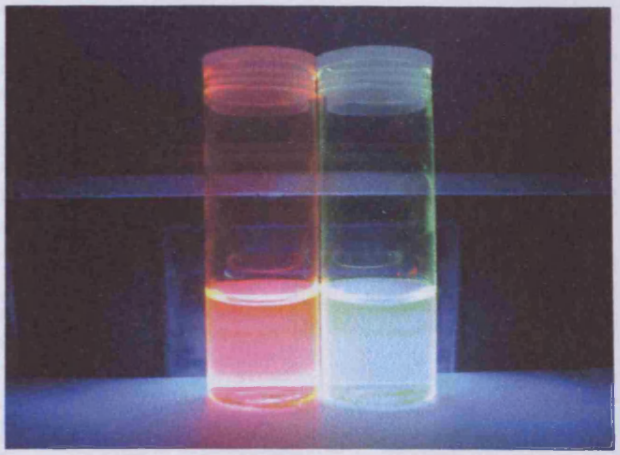

Fig. 3.30: Eu(III) and Tb(III) complexes of 4-^{is}Pr-PhQuaterAmide$_2$

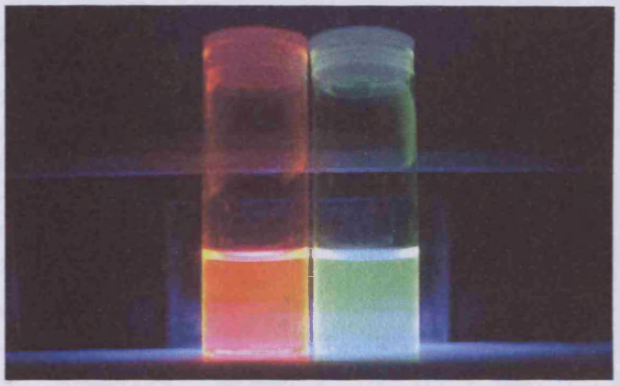

Fig. 3.31: Eu(III) and Tb(III) complexes of 4-^{is}Pr-PhQuinqueAmide$_2$

The first point that can be mentioned from these photographs is how much brighter the $[Eu(PhTerpyAcid_2)(H_2O)_2][ClO_4]_2$ complex appears than the $Eu(BipyAcid_2)_2(Et_3NH)$ complex in Fig.3.27. This is probably due to the UV excitation at 365nm being an excellent match for excitation of $[Eu(PhTerpyAcid_2)(H_2O)_2][ClO_4]_2$ ($\lambda_{exc\ max}$ 355nm) but not so good for excitation of $Eu(BipyAcid_2)_2(Et_3NH)$ ($\lambda_{exc\ max}$ 320nm). The other fact that is highlighted by these photographs is how the amide bearing ligand complexes appear more suitable for the Tb(III) ion rather than the Eu(III) ion, reinforcing the results obtained from the quantum yield measurements. Interestingly, the 4-^{is}Pr-PhQuinqueAmide$_2$ displays bright luminescence when complexed to both Eu(III) and Tb(III) ions.

3.10 Conclusions

All of the ligands discussed in this study with the exception of 4'-phenyl-2,2':6',2''-terpyridine-6,6''-dicarboxylic acid 1,1',1''-trioxide are capable of sensitising trivalent lanthanide europium and terbium ions. The inclusion of the carboxylic acid binding groups has increased the stability of the lanthanide complexes in solution with no decomplexation being observed at concentrations less than 400μmol, unlike the parent ligands and their N-oxides. The amides, although increasing solubility, do not appear to bind the lanthanides as efficiently as the oligopyridine carboxylic acid ligands and display decomplexation at concentrations less than 400μmol. The introduction of the carboxylic acid and amide groups has appeared to decrease and increase the ligand triplet levels respectively. This has had the affect of making the carboxylic acid containing ligands more suitable for Eu(III) sensitisation and less suitable for Tb(III) emission and vice-versa for the amide ligands.

With regards to the coordination behaviour of the carboxylic acid ligands, the bipyridine and 4-^{is}Pr-PhQuinquepyridines are the most efficient providing unambiguous analysis to the formation of the 2:1 and 1:1 complexes respectively. The carboxylic acid terpyridine and quaterpyridines appear to form the desired 1:1 ligand:metal stoichiometries but complex mass spectra are obtained perhaps suggesting extended metal ligand systems in solution. This has been attributed to the unsuitable number of free coordination sites available in the terpyridine and quaterpyridine ligands resulting in an insufficient number of free sites for 2:1 ligand:metal coordination and too many free sites for solvent molecule lanthanide-

binding in 1:1 metal:ligand ratios. The bipyridine and quinquepyridine carboxylic acid ligands on the other hands can form stable 2:1 and 1:1 ligand:metal ratios with the bipyridine ligand having no coordination sites free for the 2:1 complex and the quinquepyridine ligand being able to form a protective helical structure around the lanthanide ion.

To fully determine the coordination numbers of the complexes and therefore shielding capabilities of the ligands, lifetime measurements of the complexes need to be acquired. At this time a lifetime spectrometer was not available for the study and so the dysprosium induced shift method, as described in chapter 1, was attempted. Unfortunately, the necessary concentrations of 100-10mmol could not be attained due to the poor solubilities of the complexes.

A luminescence overview of all of the complexes analysed in this study is given in graph 3.1 (excluding the Eu(III) complexes of $PhQuaterO_2$ and $PhQuaterO_4$). Among the complexes examined the most intense luminescence is shown by the $Eu(BipyAcid_2)_2(Et_3NH)$ complex and the $[Tb(PhTerpyAcid_2)(H_2O)_2][ClO_4]_2$ complex with this conclusion being drawn from the relative quantum yields. The most luminescent complexes from the equimolar solution luminescence measurements are the $[Eu(PhQuaterO_4)_2][ClO_4]_3$ (73.59) and $[Tb(4\text{-}^{is}Pr\text{-}PhQuater)_2(H_2O)][ClO_4]_2$ complexes. The poor performance of the $[Eu(4\text{-}^{is}Pr\text{-}PhQuaterAcid_2)(H_2O)_2][ClO_4]$ and $[Tb(4\text{-}^{is}Pr\text{-}PhQuaterAcid_2)(H_2O)_2][ClO_4]$ complexes highlight the difficulties faced in this area of research. The quaterpyridines and their N-oxides provided the most intense luminescence in concentrated solution luminescence analysis but upon modification to the 6,6'''- disubstituted dicarboxylic acid ligands the lanthanide

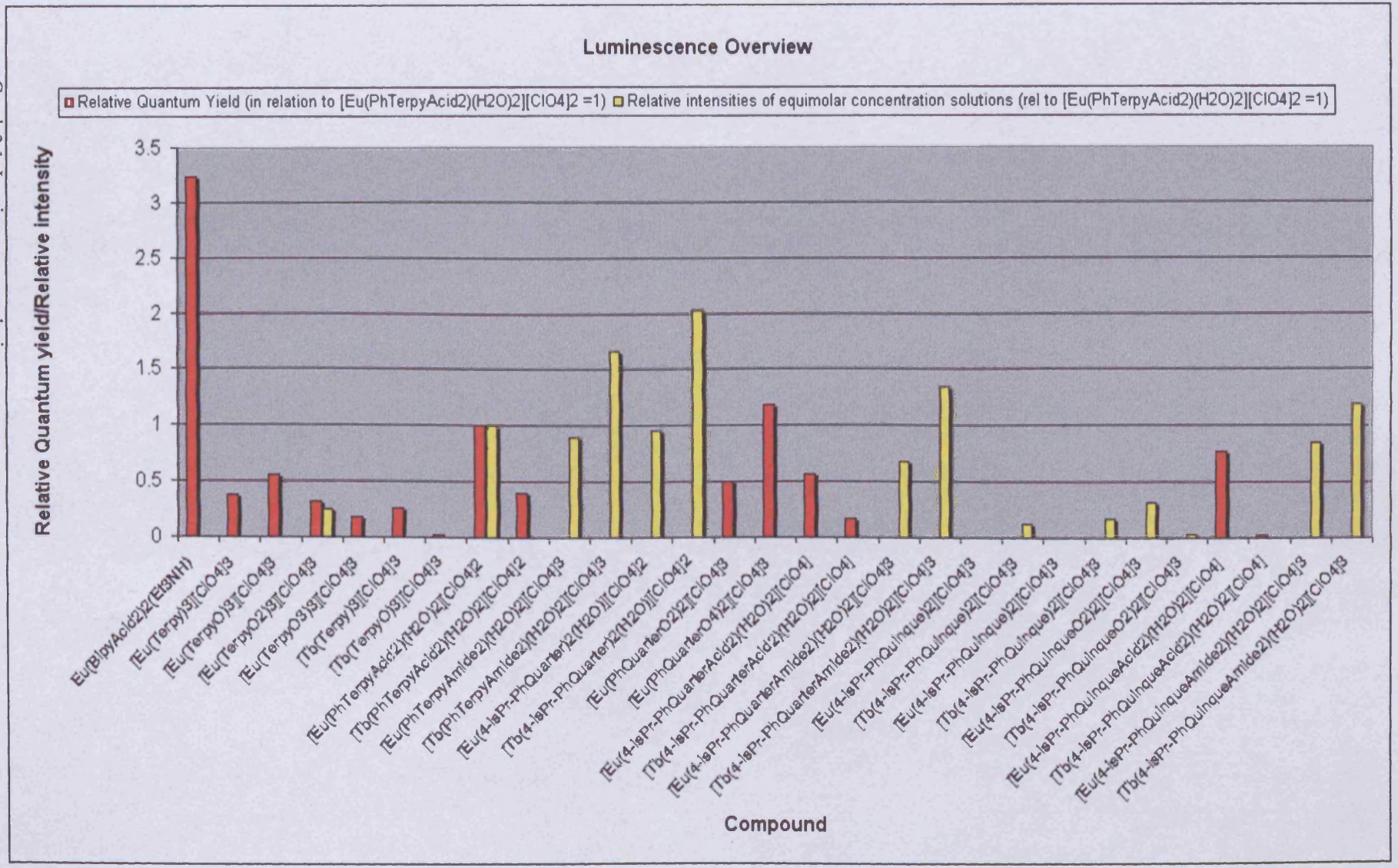

Graph 3.1: Luminescence analysis summary

complexes provide poorer results with regard to relative quantum yields and coordination.

This study has shown that these sets of ligands have the potential to be developed into highly luminescent Eu(III) and Tb(III) chelates and the inclusion of carboxylic acid binding groups increases stability of the complexes in solution notably over complexes containing ligands without binding carboxylic acids groups. Further studies are currently being undertaken to determine the ability of these ligands to sensitise luminescence from other lanthanide metals as well as computational studies to try to explain the trends we have observed in terms of the orbital energies of our ligands. This may allow us to determine which ligand from a series of substituted pyridine-based donors will be the best sensitizer when oxidised or substituted with carboxylic acid or amide groups and thus allow the rapid and facile synthesis of new improved antennae.

3.11 References

1) D. Parker, G. J. A. Williams, *J. Chem. Soc., Dalton Trans.*, (1996), 3613-3628.

2) H.-R. Mürner, E. Chassat, R. P. Thummel, J.-C G. Bünzli, *J. Chem. Soc., Dalton Trans.*, (2000), 2809-2816.

3) J.-C. G. Bünzli, L. J. Charbonnière, R. F. Ziessel, *J. Chem. Soc., Dalton Trans.*, (2000), 1917-1923.

4) J. L. Toner, Eur. Pat. Appl. EP288, 256.

5) V-M. Mukkala, C. Sund, M. Kwiatkowski, P. Pasanen, M. Högberg, J. J. Kankare, H. Takalo, *Helv. Chim. Acta*, **75**, (1992), 1621. V-M. Mukkala, J. J. Kankare, *Helv. Chim. Acta*, **75**, (1992), 1578; V-M. Mukkala, M. Kwiatkowski, J. J. Kankare, H. Takalo, *Helv. Chim. Acta*, **76**, (1993), 893. V-M. Mukkala, M. Helenius, I. Hemmilä, J. Kankare, H. Takalo, *Helv. Chim. Acta*, **76**, (1993), 1361.

6) J. Yuan, M. Tan, G. Wang, *J. Luminesc.*, **106**, 2, (2004), 91-101.

7) J. Coates, P. G. Sammes, R. M. West, *J. Am. Chem. Soc., Perkin Trans.*, **2**, (1996), 1275-1282.

8) J. Coates, P. G. Sammes, R. M. West, *J. Am. Chem. Soc., Perkin Trans.*, **2**, (1996), 1283-1287.

9) Y. Bretonnière, M. Mazzanti, J. Pècaut, M. M. Olmstead, *J. Am. Chem. Soc.*, **124**, (2002), 9012-9013.

10) W. Dai, H. Hu, X. Wei, S. Zhu, D. Wang, K. Yu, N. Dalley, X. Kou, *Polyhedron*, **16**, 12, (1997), 2059-2065.

11) W. K. Fife, *J. Org. Chem.*, **48**, (1983), 1375-1377.

12) K. L. Reddy, *Tet. Lett.*, **44**, (2003), 1453-1455.

13) A. P. de Silva, H. Q. N. Gunaratne, T. E. Rice, S. Stewart, *Chem. Commun.*, (1997), 1891-1892.

14) C. Piguet, J-C. G. Bűnzli, G. Bernardinelli, G. Hopfgartner, A. F. Williams, *J. Am. Chem. Soc.*, **115**, (1993), 8197.

15) C. Piguet, J-C. G. Bűnzli, G. Bernardinelli, G. Hopfgartner, A. F. Williams, *J. Am. Chem. Soc.*, **115**, (1993), 8197.

Chapter 4

The Synthesis of Chiral Oxazoline Ligands

4.1 Introduction

When the ligand environment about either Eu^{3+} or Tb^{3+} is chiral or contains chiral centres, the $^5D_J \rightarrow {}^7F_J$ transitions each exhibit some partial circular polarisation in their luminescence. This phenomenon is generally referred to as either emission optical activity or circularly polarised luminescence (CPL).[1] CPL is the emission analogue of circular dichroism, and it probes the chirality and natural optical activity of the emitting system. The largest degree of circular polarisation is invariably observed in the $^5D_0 \rightarrow {}^7F_1$ transitions of Eu^{3+} and the $^5D_4 \rightarrow {}^7F_5$ and $^7F_3$ transition regions of Tb^{3+}, reflecting the relatively strong magnetic dipole nature of these transitions. Eu^{3+} and Tb^{3+} CPL spectra exhibit an extraordinary sensitivity to the stereochemical characteristics of the ligand environment. Since nearly all systems of biological interest have some degree of chirality CPL is an especially attractive probe for investigating Eu^{3+} and Tb^{3+} biomolecular interactions.

To investigate the possible properties of chiral lanthanide complexes it was decided to utilise the chemistry of the nitrile function. A quick, one-step process was required and the oxazoline functionality was decided upon.

The oxazoline cycle was first prepared in 1884[2] and has been extensively applied in the last two decades, principally in asymmetric catalytic processes and there are more than 200 papers analysing the co-ordination compounds of these ligands. They are among the most frequently studied chiral nitrogen containing ligands due to the high enantioselectivities achieved in a range of processes. Oxazolines have also been widely used in many areas of chemistry[3] proving how

versatile the ring can be. It can act as a co-ordinating ligand, protector group and activating moiety.

Such a widespread use of these ligands in a great variety of organic transformations is basically due to the ease with which they can be prepared from aminoacids and synthetic aminoalcohols, and also the stability of the oxazoline ring once formed. Usually, oxazoline ligands are synthesised from aminoalcohols and a nitrile containing moiety or a carboxylic acid derivative,[4] although there are in addition, a variety of different procedures for differing sensitive precursors.[5]

The oxazoline fragment is potentially a versatile Lewis base and as described before, lanthanides are hard Lewis acids, which prefer to co-ordinate to hard bases with complexes primarily held together by electrostatic interactions. This therefore may in theory make the oxazoline moiety a good candidate for co-ordinating lanthanides. It is nearly a planar molecule (the torsion angles 5-1-2-3 and 4-3-2-1 are 4.21 and 2.48°) in spite of the two C_{sp3} at positions 4 and 5 and its structure has a small contribution from the charged resonance structure of the double bond (see Fig.4.1).[6+7]

Fig.4.1: Charged resonance structure of the double bond

Also, similarly to the N-donors in the poly-pyridine ligands described, the N atom has a sp^2 orbital with potential for binding to lanthanides. No complexes have been reported in which the oxygen of the oxazoline moiety acts as the donor atom.

Structural data for oxazolines co-ordinated to lanthanides are not available, although some complexes of benzoxazoles with the actinides $U^{(VI)}$ and $Th^{(IV)}$ ions have been described.[8]

4.1.1 Routes to Oxazolines

There are 4 general routes to the preparation of oxazolines as described in Scheme 4.1.[9] Although all routes are viable for our ligand types we are only interested in utilising the nitrile methodology. This procedure for the preparation of mono- and bis-(2-oxazolines) was first reported in 1974 by Witte and Seeliger[10] and involved the direct reaction of nitriles with amino alcohols in the presence of catalytic amounts of metal salts. The procedure was carefully reinvestigated by Bolm *et al* [11] and slightly modified to give the procedure used in this work. The procedure entails refluxing a solution of an appropriate dinitrile and an excess of the appropriate amino alcohol in chlorobenzene in the presence of a catalytic amount of zinc dichloride. Aqueous workup followed by column chromatography should yield the bis(2-oxazoline). The bis(2-oxazoline) ligands synthesised by Bolm *et al* were obtained in moderate to good yields.

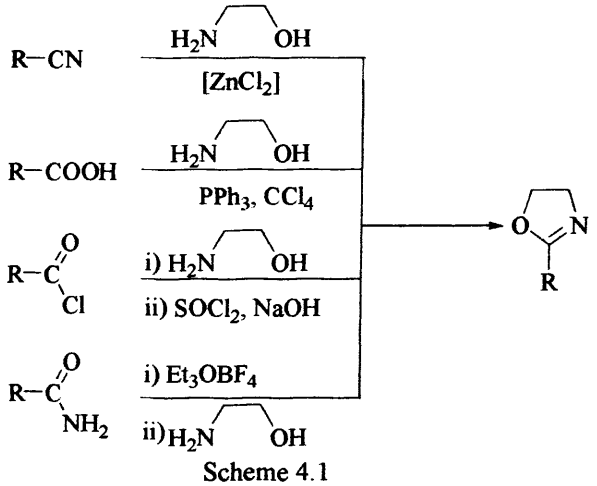

Scheme 4.1

To utilise the other three methodologies require numerous reaction steps and the use of the nitrile functionality as a precursor. While it is a viable alternative, unfortunately this went against our time constraints for this research. Also, the syntheses of poly-pyridyl bis-nitrile compounds are limited in their reaction scale to ~1.5g due the use of volatile cyanides and the safety procedures for their use in this laboratory. Thus, the numerous reaction steps required would be detrimental to the overall yield and hamper our efforts. Therefore, only reactions utilising the nitrile starting material were attempted.

Ligands **31** and **32** were targeted as a starting point as described in scheme 4.2. The ligand **33**, bis(oxazolinyl)bipyridine (Bipymox) has previously been synthesised[12] but not via reaction of the nitrile moiety. It was readily synthesised from 2,2'bipyridine-6,6'-dicarboxylic acid in several steps and was found to be a rigid bidentate bipyridine ligand with two free oxazoline rings when co-ordinated to Rhodium(III) trichloride. This was determined by ^{1}H-NMR experiments in which the proton signals of the pyridine and oxazoline rings are affected by coordination of the rhodium(III) centre, but no dynamic character due to the coordination of the oxazoline rings in the range of –50° to 50°C could be found. ^{1}H-NMR studies also indicated the complex to have a C_2-symmetric structure. Crystals suitable for structure determination could not be obtained.

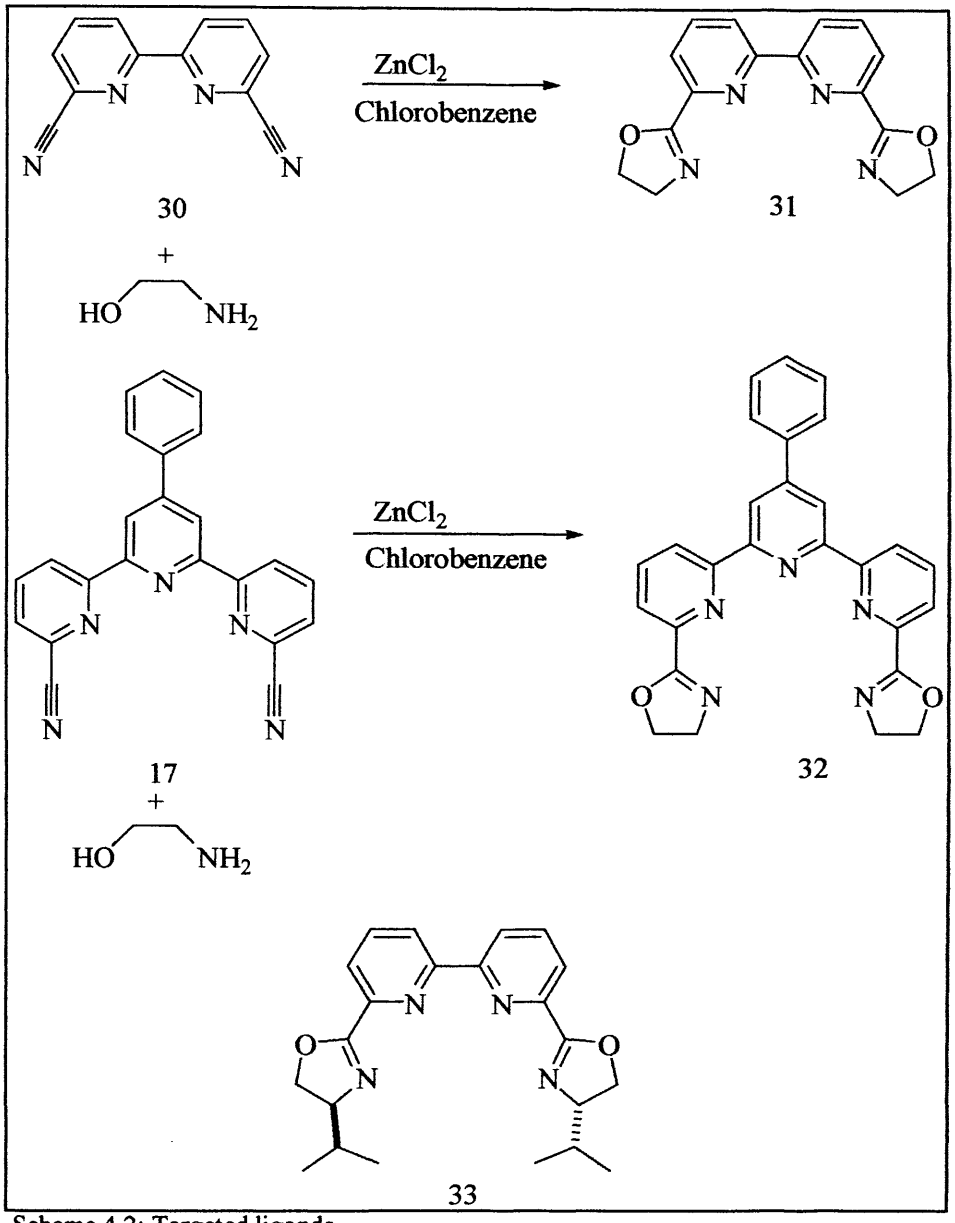

Scheme 4.2: Targeted ligands

4.2 Results/Discussion

As a test of the reaction conditions, 4-cyanopyridine, **34,** was refluxed with ethanolamine (see scheme 4.2) in dry chlorobenzene with the $ZnCl_2$ catalyst (5mol%) for 48hr. By removal of the solvent in vacuo a white solid was obtained which was dissolved in DCM. After extraction with water, followed by an extraction of the aqueous phase, the combined organic phases were removed in vacuo to yield a white

crystalline solid in 81% yield. After extraction, analysis of the water layer shows that it contains none of the product and is true to all of the reactions carried out throughout the chapter. Spectroscopic analysis of the product showed ligand **35** had been successfully synthesised. The IR analysis revealed a loss of the nitrile band at 2233cm^{-1} and ^{1}H-NMR in $CDCl_3$ revealed two new peaks were now present at δ4.07 and δ4.4 assigned to the oxazoline ring protons H_3 and H_4 respectively.

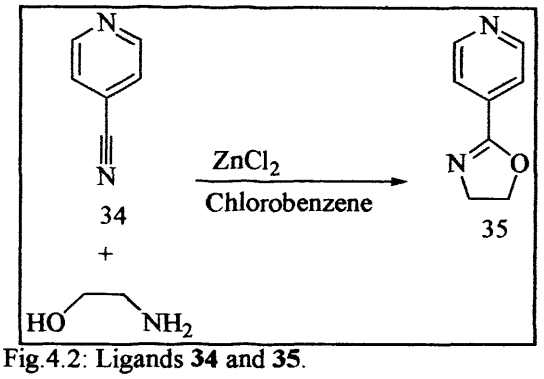

Fig.4.2: Ligands **34** and **35**.

With the reaction procedure proven to work for cyano-pyridines it was applied to the synthesis of the bipyridine ligand **31**. Refluxing the 2,2'-bipyridine-6,6'-dicarbonitrile, **30**, with ethanolamine in dry chlorobenzene with the $ZnCl_2$ catalyst (5mol%) for 48hr and by removal of the solvent in vacuo a white solid was obtained. This solid was dissolved in DCM and extraction with water followed by removal of the organic phase in vacuo yielded a white solid. The IR analysis revealed a weak peak at 2233cm^{-1} characteristic of the nitrile functionality and ^{1}H-NMR analysis confirmed the compound to be the starting material, **30**, with the characteristic shifts of $H_5 + H_{5'}$ present as a double doublet at δ7.72, $H_4 + H_{4'}$ present as a triplet at δ7.96 and $H_3 + H_{3'}$ present as a doublet at δ8.67.

The experiment was repeated with longer reaction times of 94hrs. A white solid was obtained and spectroscopic analysis revealed the compound to be the starting material **30**.

With the attempted synthesis of ligand **31** in mind, the reaction procedure was utilised for the synthesis of the terpyridine ligand **32**. Similarly, refluxing the starting material 4'-phenyl-2,2':6',2''-terpyridine-6,6''-dicarbonitrile, **17**, with ethanolamine in dry chlorobenzene with the $ZnCl_2$ catalyst for 48hr and by removal of the solvent in vacuo a white solid was obtained. This solid was dissolved in DCM and extraction with water followed by removal of the organic phase in vacuo yielded a white solid. The IR analysis revealed a weak peak at 2233cm^{-1}, characteristic of the nitrile functionality and ^{1}H-NMR analysis confirmed the compound to be the starting material **17** (^{1}H-NMR as discussed in chapter 3) with the characteristic shifts observed. A series of small multiplets were present at δ4.1, 4.5, 7.25, 8.01, 9.6 and 9.9 which, although too weak to assign, were thought to be small amounts of the terpyridine ligand **32** synthesised in the ratio of 90:10 of starting material to compound **32**, respectively.

The experiment was also repeated with longer reaction times of 94hrs. A white solid was obtained and spectroscopic analysis showed the compound to once again be the starting material **17**.

An explanation for the synthesis of ligands **31** and **32** not proceeding as anticipated had to be considered. The mechanism of the reaction is thought to involve a polarisation of the nitrile functionality by the $ZnCl_2$ catalyst. The polarised nitrile

then undergoes nucleophillic attack of the nitrogen lone pair of the ethanolamine followed by a ring closure (see Fig. 4.3). Therefore, the reaction cannot proceed without the $ZnCl_2$ catalyst being able to co-ordinate to the nitrile functionality. As has been shown in previous chapters, terpyridine and bipyridine are excellent coordinators of the lanthanides and similarly for transition metals.[13] If the $ZnCl_2$ is being coordinated to the ligand centre instead of polarising the nitrile this would halt the reaction. To investigate this possibility 4'-phenyl-2,2':6',2''-terpyridine-6,6''-dicarbonitrile, **17**, was coordinated to $Cu(ClO_4)_2$ to see if the metal complexes to the ligand centre and also to investigate if the copper complex once synthesised can then undergo an oxazoline synthesis reaction.

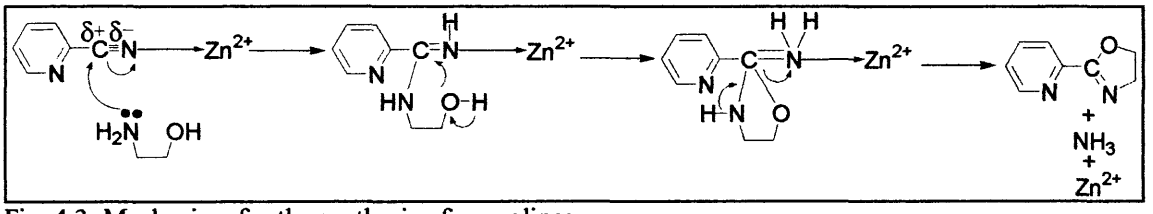

Fig. 4.3: Mechanism for the synthesis of oxazolines

For the complexation reaction, 1 molar equivalent of $Cu(ClO_4)_2$ was added to 2 molar equivalents of 4'-phenyl-2,2':6',2''-terpyridine-6,6''-dicarbonitrile, **17**, in EtOH. The mixture was stirred for 1h and the precipitate that formed collected by filtration under gravity. The green solid was washed with Et_2O and dried under vacuum giving a yield of 85%. The IR spectrum revealed no movement of the characteristic nitrile band that was still present at 2238cm^{-1}. This indicated that the nitrile groups had no involvement in the bonding upon coordination. The aromatic peaks of the terpyridine fragment had all shifted varying amounts, providing evidence for the involvement of the terpyridine fragments coordination to the $Cu(ClO_4)_3$. The strong C=C band had shifted 22cm^{-1} to 1591cm^{-1} and the medium C=N band had

shifted 5cm^{-1} to 1577cm^{-1}. The aromatic bands had undergone shifts of ~20cm^{-1}. A strong perchlorate band was now present at 1086cm^{-1}, giving further evidence of complexation. The C-H bands had also undergone frequency shifts of up to 28cm^{-1}. The mass spectrum of the $[Cu(L17)_2].(ClO_4)_2$ complex exhibits the parent ion minus the two perchlorate ions at 781 (40%) with the correct isotope pattern for the copper ligand system present.

4.2.1 Single crystal X-ray Structure of $[Cu(L17)_2][ClO_4]_2$

Slow diffusion of Et_2O into a CH_3CN solution of $[Cu(L17)_2].(ClO_4)_2$ afforded green/yellow plates suitable for X-ray diffraction. Single crystal X-ray determination revealed a six coordinate copper centre bound meridonally by two 4'-phenyl-2,2':6',2''-terpyridine-6,6''-dicarbonitrile ligands with two ClO_4 and two CH_3CN solvent / anion molecules present, as shown in Fig. 4.4 (ClO_4 and CH_3CN omitted from figure for clarity). Relevant bond lengths and angles are listed in table 4.1. On close inspection, the Cu-N3/N8 bond lengths (1.952(3)- 1.970(3)) are notably shorter than the axial Cu-N1/4/6/9 donor bond lengths (2.233(3)- 2.276(3)), which would suggest a pseudo Jahn-Teller compression and from the work of Folgado and Reinen[12] it is likely that the observed structure is the result of a dynamic pseudo Jahn-Teller tetragonal distortion. That is, this observed compression may be caused by the crystal lattice in the system being flexible enough to allow fluxionality between the two tetragonal distortions predicted by Jahn-Teller theory and only the averaging of these positions in the structure at 298K has been observed. A comparison to the study of Folgado and Reinen's unsubstituted terpyridine ligand systems [14] reveals similar results, in which a series of Cu(II)terpyridine complexes were prepared and

the geometrical structure investigated by X-ray crystallography and variable temperature EPR. All of their bis terpyridyl copper complexes were found to bind meridonally with the predominant strain component of the rigid ligand corresponding to a pseudo compression along the molecular z axis of the MN_6 octahedral polyhedron with typical Cu-N bond lengths of 1.955(3)-1.984(3) for Cu-N3/N8 and 2.150(3)-2.201(3) donor bond lengths for the axial Cu-N1/4/6/9, similar to $[Cu(L17)_2][ClO_4]_2$. It is of interest to note that that it has previously been found that placing alkyl or aryl substituents in both of the 6- and 6''- positions of a 2,2':6',2''-terpyridine prevents coordination to an iron(II) centre on steric grounds,[15 & 16] though coordination to a ruthenium centre can be achieved.[15 & 17] No such steric hindrance was observed with L17, with the reaction occurring over a matter of seconds at room temperature.

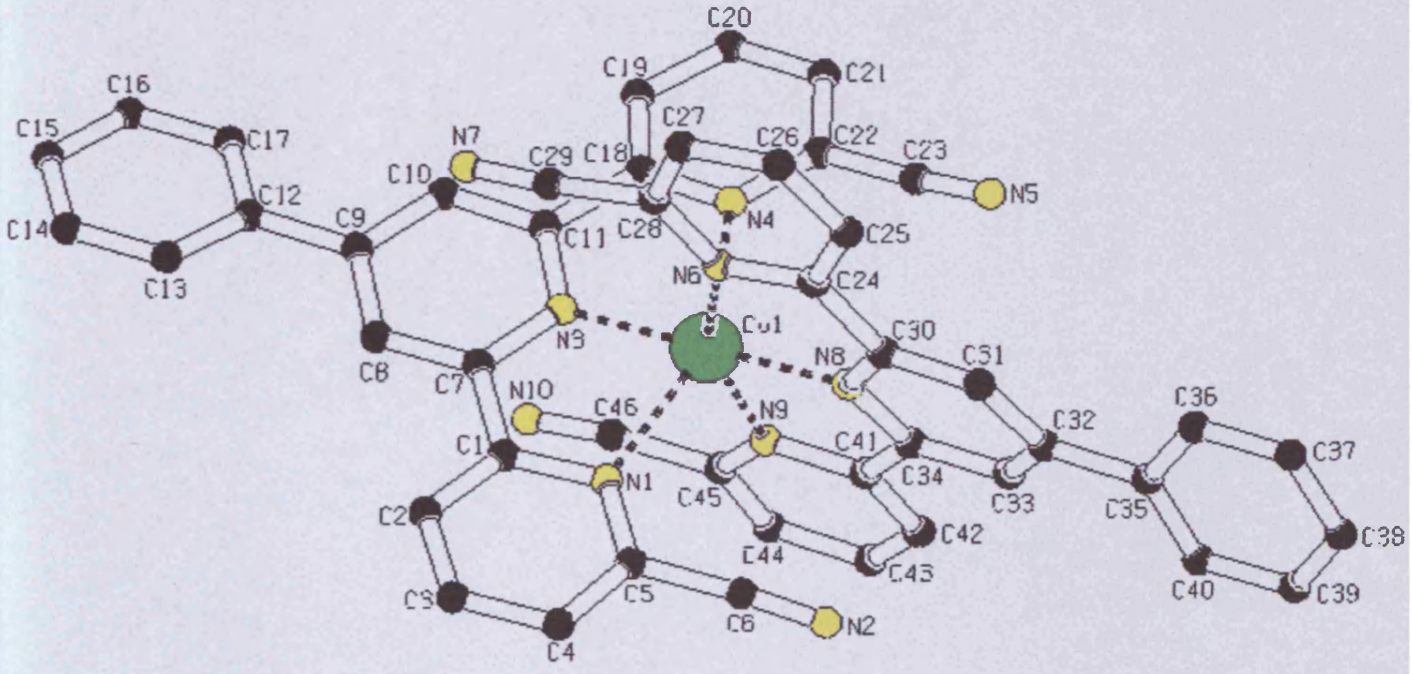

Fig. 4.4: Ortep plot of $[Cu(L17)_2].(ClO_4)_2$

Table 4.1: Selected bond lengths (Å) and bond angles (°) for $[Cu(L17)_2].(ClO_4)_2$.

N1-Cu1	2.276(3)	N3-Cu1	1.970(3)
N4-Cu1	2.255(3)	N6-Cu1	2.240(3)
N8-Cu1	1.952(3)	N9-Cu1	2.233(3)
N3-Cu1-N9	178.34(12)	N8-Cu1-N9	77.44(11)
N3-Cu1-N9	104.17(11)	N8-Cu1-N6	78.12(11)
N3-Cu1-N6	100.29(11)	N9-Cu1-N6	155.35(10)
N8-Cu1-N4	103.39(10)	N3-Cu1-N4	77.04(11)
N9-Cu1-N4	92.01(10)	N6-Cu1-N4	90.52(10)
N8-Cu1-N1	102.83(10)	N3-Cu1-N1	91.58(10)
N6-Cu1-N1	96.92(10)	N4-Cu1-N1	153.70(10)

Table 4.2: Crystal data and structure refinement for $[Cu(L17)_2].(ClO_4)_2$.

Empirical formula	$C_{48.50}H_{29}Cl_2CuN_{11.50}O_8$	
Formula weight	1035.27	
Temperature	120(2) K	
Wavelength	0.71073 Å	
Crystal system	Monoclinic	
Space group	*C2/c*	
Unit cell dimensions	$a = 18.6046(4)$ Å	$\alpha = 90°$
	$b = 14.8764(3)$ Å	$\beta = 96.7030(10)°$
	$c = 32.9036(7)$ Å	$\gamma = 90°$
Volume	9044.5(3) Å^3	
Z	8	
Density (calculated)	1.521 Mg / m^3	
Absorption coefficient	0.672 mm^{-1}	
F(000)	4220	
Crystal	Plate; green/yellow	
Crystal size	0.20 x 0.16 x 0.06 mm^3	
θ range for data collection	3.01 – 27.50°	
Index ranges	$-23 \le h \le 24$, $-19 \le k \le 19$, $-42 \le l \le 42$	
Reflections collected	31692	
Independent reflections	9985 [$R_{int} = 0.0803$]	
Completeness to $\theta = 27.50°$	95.9 %	
Absorption correction	Semi–empirical from equivalents	
Max. and min. transmission	0.9608 and 0.8773	
Refinement method	Full-matrix least-squares on F^2	
Data / restraints / parameters	9985 / 0 / 696	
Goodness-of-fit on F^2	1.023	
Final *R* indices [$F^2 > 2\sigma(F^2)$]	$R1 = 0.0623$, $wR2 = 0.1560$	
R indices (all data)	$R1 = 0.1003$, $wR2 = 0.1785$	
Extinction coefficient	0.00000(12)	
Largest diff. peak and hole	1.244 and –0.897 e Å^{-3}	

Ligand **17** successfully complexed to $Cu(ClO_4)_2$, showing that the transition metal catalysts are in fact coordinating to the ligand instead of polarising the nitrile group. Attempts to synthesis oxazolines using $[Cu(L17)_2].(ClO_4)_2$ proved unsuccessful yielding unreacted $[Cu(L17)_2].(ClO_4)_2$. Therefore, a means of

preventing the co-ordination of the metal catalyst to the ligand and instead produce a polarisation of the nitrile group was required and two routes were considered. The first route involved using a metal catalyst with a larger radius to try to decrease the probability of coordination before polarisation of the nitrile. The alternative route involves utilising the PhterpyCN$_2$-mono oxide ligand **16** to block the coordination site.

- **4.2.2 Route 1 – Increased Catalyst Radius**

P. Zhou *et al* have found that 2-amino-2-methylpropoxide complexed with a 5-10% molar equivalent of anhydrous lanthanide chloride suspension in toluene and reacted with different carboxylic esters to produce 2-oxazolines.[18] Therefore by using the larger cation $LaCl_3$ as the metal catalyst it should allow the reaction to proceed. The 4'-phenyl-2,2':6',2''-terpyridine-6,6''-dicarbonitrile, **17**, was refluxed with ethanolamine in dry chlorobenzene with the $LaCl_3$ (5mol%, flame dried under vacuum) catalyst for 48hr. Removal of the solvent and extraction of the solid into DCM was followed by an extraction with water. Removal of the DCM layer in vacuo yielded a white solid in 80% yield. Spectroscopic analysis of the product showed the material to be the starting material **17**.

- **4.2.3 Route 2 – Blocking the Coordination Site using PhterpyCN$_2$-mono oxide**

The 4'-phenyl-2,2':6',2''-terpyridine-6,6''-dicarbonitrile-1'-N-oxide, **16**, that was synthesised in chapter 3 could be utilised to block the coordination site. The N-oxide points towards the coordination site core, thus filling the site within which any metals would sit for coordination. To test if the ligand could be used in this fashion it was complexed with $Cu(ClO_4)_2$.

For the complexation reaction, 1 molar equivalent of $Cu(ClO_4)_2$ was added to 2 molar equivalents of PhterpyCN$_2$-mono oxide, **16**, in EtOH and the mixture was stirred for 1h. No precipitate had formed so diethyl ether was added and the precipitate collected by filtration under gravity. Spectroscopic analysis revealed that the compound was the starting material **16**. The ligand **16** was shown not to coordinate $Cu(ClO_4)_2$ so the N-oxide could potentially stop coordination of the metal catalyst allowing the reaction scheme to proceed. With this established it was utilised in the attempted synthesis of ligand **36**.

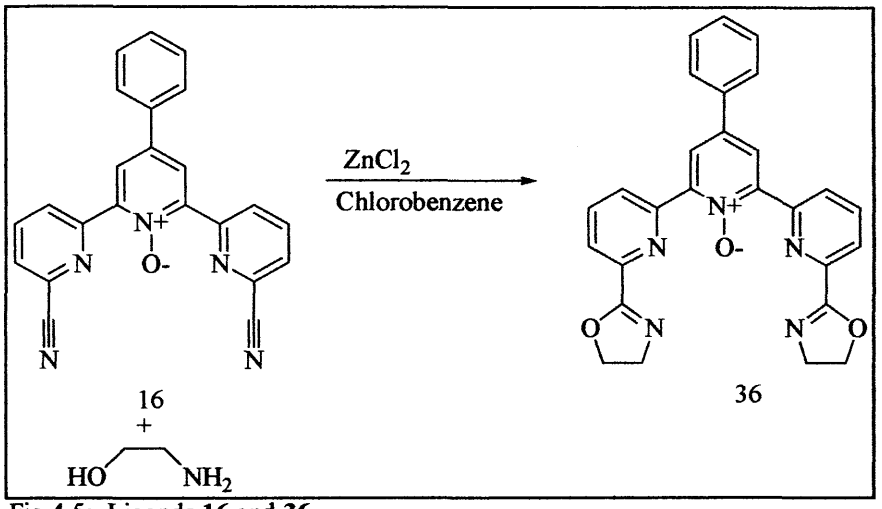

Fig.4.5: Ligands **16** and **36**.

The PhTerpyCN$_2$-mono oxide **16** was refluxed with ethanolamine in dry chlorobenzene with the $ZnCl_2$ catalyst (5mol%). The reaction was followed by TLC (95% chloroform/5% methanol) and after 48h it was shown that starting material was still present. The reaction was allowed to continue for 10 days and was followed by TLC analysis which showed that the starting material **16** was present but another compound was being synthesised in small quantities. Despite attempts to isolate the product using chromatography, no product was isolated and the identity of this trace product remains unclear. Even though the ligand is unable to co-ordinate metals strongly it must still be weakly interacting with the metal salt catalyst in solution preventing the reaction pathway.

4.3 Conclusion

The syntheses of oxazolines from the nitrile functionality in our proposed reaction schemes have so far been unsuccessful. It is believed that the metal catalyst, which is vital to the reaction proceeding, is being coordinated to the ligand core instead of polarising the nitrile functionality. Two methods were adopted to try to prevent this event from occurring. Increasing the metal catalyst radius proved unsuccessful whist utilising the 1'-N-oxide **16** stopped coordination of the transition metal perchlorate $Cu(ClO_4)_2$ and looked the more promising method. Unfortunately, during the attempted synthesis of ligand **36** it would appear that the metal catalyst must still be being weakly coordinated to the ligand core in solution instead of polarising the nitrile functionality.

Obviously, the use of these strongly coordinating ligands has hindered our proposed reaction schemes. If the research group were to continue attempting the synthesis of chiral oxazolines it would require synthesis from an alternative route. The route that would have the highest probability of success would be from the dicarboxylic acid. This route has been proven, as discussed in the introduction, for the synthesis of bipymox and similarly should work for the terpyridine fragment. This route was not investigated in this study for numerous reasons. The oligopyridine dicarboxylic acids were some of our target ligands as discussed in chapter 3. The overall yields to get these ligands were quite poor so to use them as a precursor would have been quite time consuming in synthesising adequate amounts for these reaction purposes. The dicarboxylic acids that were synthesised were used for the preparation of lanthanide complexes, as was the initial purpose of this luminescence investigation.

4.4 References

1) Frederick S. Richardson, *Chem. Rev.*, **82**, (1982), 541-552.

2) R. Andreasch, *Monatsh. Chem.*, **5**, (1884), 33.

3) J. A. Frump, *Chem. Rev.*, **71**, (1971), 483.

4) M. Reuman, A.I. Meyers, *Tetrahedron*, **41**, (1985), 837.

5) T.G. Gant, A.I. Meyers, *Tetrahedron*, **50**, (1994), 2297.

6) D.L. Eng-Wilmot, D.van der Helm, *J. Am. Chem. Soc.*, **102**, (1980), 7719.

7) M. Gomez, G. Muller, M. Rocamora, *Coor. Chem. Rev.*, **193-195**, (1999), 769-835.

8) *Chem. Abstr.*, **125**, (1996), 47583w.

9) M. Reuman, A. I. Meyers, *Tetrahedron*, **41**, (1985), 837. (b) T. G. Grant, A. I. Meyers, *Tetrahedron*, **50**, (1994), 2297. (c) D. J. Ager, I. Prakash, D. R. Schaad, *Chem. Rev.*, **96**, (1996), 835. (d) M. Peer, J.C. de Jong, M. Keifer, T. Langer, H. Rieck, H. Schell, P. Sennhenn, J. Springz, H. Steinhagen, B. Wiese, G. Helmchen, *Tetrahedron*, **52**, (1996), 7547 and references therein.

10) H. Witte, W. Seeliger, *Liebigs Ann. Chem.*, (1974), 996.

11) C. Bolm, K. Weickhardt, M. Zehnder, T. Ranff, *Chem. Ber.*, **124**, (1991), 1173-1180.

12) H. Nishiyama, S. Yamaguchi, S. Park, K. Itoh, *Tetrahedron: Asymmetry*, **4**, (1993), 143-150.

13) M. Burrows, Synthesis and Coordination of Polypyridyl N-oxide Ligands, PhD Thesis, UWC, 2002.

14) J-V Folgado, W. Henke, R. Allman, H. Stratemeier, D. Beltrán-Porter, T. Rojo, D. Reinen, *Inorg. Chem.*, **29**, (1990), 2035-2042.

15) A. M. W. C. Thompson, *Coord. Chem. Rev.*, **160**, (1997), 1-52.

16) A. A. Schilt, G. F. Smith, *Anal. Chim. Acta*, **15**, (1956), 567.

17) J. R. Kirchhoff, D. R. Mcmillin, P. A. Marnot, J.-P. Sauvage, *J. Am. Chem. Soc.*, **107**, (1985), 1138.

18) P. Zhou, J. E. Blubaum, C. T. Burns, N. R. Natale, *Tet. Lett.*, **38**, 40, (1997), 7019-7020

Chapter 5

Experimental

5.1 Experimental

All NMR spectra were recorded on a Bruker DPX400 or a Jeol Oxford 300 spectrometer. Infrared spectra (pressed KBr disc) were recorded on a Perkin-Elmer 1600 or a Jasco FT/IR-660 Plus. Ultraviolet absorption spectra were recorded on a Jasco V-570 UV/VIS/NIR Spectrophotometer. Emission and excitation spectra were recorded on a LS-50B instrument (Perkin-Elmer Instruments) equipped with a Hamamatsu R928 red-sensitive photomultiplier tube. Emission spectra were corrected from the wavelength dependence of the photomultiplier tube, according to the instrument guidebook. Mass spectra were performed by the EPSRC national mass spectromety service centre (Swansea). X-Ray crystallography was performed by the EPSRC National Crystallography Service (Southampton) or Dr. Li Ling Ooi at Cardiff University.

5.2 Synthesis of 2,2':6',2''-terpyridine Ligands

Synthesis of 2,2':6',2''-terpyridine (1a) [1] 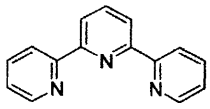

A flame dried 1L 2-neck flask was purged with argon. Anhydrous THF (400ml) and potassium t-butoxide (20g, 0.179mol) was added followed by 2-acetylpyridine (10.34g, 85.4mmol). The solution was stirred at room temperature for two hours whereupon a white solid formed. The β-(dimethyl-amino)vinyl 2-pyridyl ketone (15.03g, 85.4mmol) was added in a single portion and the solution , which gradually turns a very deep red, was stirred at room temperature for 40-60 hours. The reaction mixture was cooled in ice and a solution of ammonium acetate (64.1g, 0.833mol) in acetic acid (200ml) was added with stirring. Methanol (40ml) was added, the flask fitted with a distillation head, the mixture heated to reflux and the THF gradually removed by distillation over a five-hour period. The distillation continued until the head temperature reached 115°C. The mixture was poured onto water (400ml) and the acetic acid neutralised with sodium carbonate (~300g). Toluene (120ml) and celite (20g) was added and the mixture stirred and heated at 80°C. The mixture was cooled to room temperature and filtered through a pad of celite. The solid was broken up into a powder and washed with toluene (3x75ml). The organic layer of the filtrate was separated and the aqueous layer extracted with 2x100ml of toluene. The combined organic layers were stirred with 25g of alumina(II) and filtered. The powder was evaporated down to give a brown oil which was dissolved in 80ml of chloroform and 40g of alumina(II) was added. The powder was added to the top of alumina(II) column and eluted with 20:1 cyclohexane/ethyl acetate. A light yellow fraction was collected and evaporated down to yield the pure product. Yield: 57%

^{1}H-NMR ($CDCl_3$): 7.30(2H, ddd, *J* 7.3, 4.8, 1.3Hz, $H_{5+5''}$), 7.82(2H, m, $H_{4+4''}$), 7.93(1H, t, *J* 7.43Hz, $H_{4'}$), 8.41(2H, d, *J* 7.74Hz, $H_{3'+5'}$), 8.58(2H, d, *J* 7.94Hz, $H_{3+3''}$), 8.65(2H, ddd, *J* 4.7, 2.0, 0.9Hz, $H_{6+6''}$).

Synthesis of 2,2':6',2''-terpyridine-1-mono oxide (2a) [2+3]

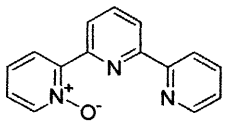

3-chloroperbenzoic acid (0.55g, 2mmol) was added to a solution of 2,2':6',2''-terpyridine (0.5g, 2.15mmol) in DCM (30ml). After stirring at room temperature for 12 hours the solution was neutralised with 10% Na_2CO_3 solution and the solvent removed in vacuo to yield a white solid. Chromatography on alumina, eluting with $CHCl_3$ then EtOAc, yielded the mono-oxide in the CHCl3 fraction with the EtOAc fraction containing 2,2':6',2''-terpyridine-1,1''-bis oxide. After removal of solvent the pure product was isolated. Yield: 35%

^{1}H-NMR ($CDCl_3$): 7.32(3H, m, *J* 7.81Hz, $H_{5''+5+4}$), 7.81(1H, m, *J* 7.67Hz, $H_{4''}$), 7.95(1H, t, *J* 7.90Hz, $H_{4'}$), 8.34(2H, m, *J* 8.41Hz, H_3), 8.47(2H, m, *J* 9.68Hz, $H_{5+3''}$), 8.68(1H, d, *J* 3.94Hz, $H_{6''}$), 9.00(1H, d, *J* 7.93Hz, $H_{3'}$); IR KBr/cm^{-1}: 1424(s), 1395(s), 1326(w), 1302(w), 1261(s), 1235(w), 1207(s), 1173(w), 1148(w), 1101(s), 1080(s), 1031(s), 987(w), 855(w), 804(s), 775(s), 744(s); MS *m/z* EI+: 249[M] (48%), 233[M-O] (12%).

Synthesis of 2,2':6',2''-terpyridine-1,1'-bis oxide (3a) [2+3]

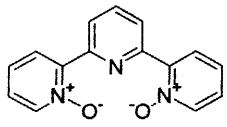

3-chloroperbenzoic acid (1.1g, 4mmol) was added to a solution of 2,2':6',2''-terpyridine (0.5g, 2.15mmol) in DCM (30ml). After stirring at room temperature for 12 hours acetone was added to precipitate the product. After standing for 1 hour the pure product was collected by filtration. Yield: 83%

^{1}H-NMR ($CDCl_3$): 7.28(2H, td, *J* 2.1, 6.8Hz, $H_{4+4''/5+5''}$), 7.36(2H, td, *J* 0.9, 7.6Hz, $H_{4+4''/5+5''}$), 7.92(1H, t, *J* 8.0Hz, $H_{4'}$), 8.13(2H, dd, *J* 2.1, 8.0Hz, $H_{3+3''}$), 8.29(2H, dd, *J* 0.8, 6.4Hz, $H_{6+6''}$), 8.85(2H, d, *J* 8.0Hz, $H_{3'+5'}$); IR KBr/cm^{-1}: 1484(s), 1437(s), 1418(s), 1381(s), 1318(w), 1302(w), 1259(s), 1227(s), 1211(s), 1153(w), 1097(w), 1079(s), 1031(s), 839(s), 821(s), 771(s), 749(s), 721(s); MS *m/z* EI+: 266[M](100%), 250[M-O] (22%), 234[M-2O] (2%).

Synthesis of 2,2':6',2''-terpyridine-1,1',1''-tri oxide (4a) [2+3]

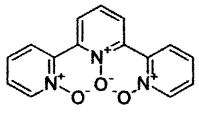

A solution of 2,2':6',2''-terpyridine (0.4g, 1.7mmol) in glacial acetic acid (2ml) and hydrogen peroxide (1.5ml, 30% aq. Soln.) was refluxed for 2hr at 80°C. After addition of a further portion of hydrogen peroxide (1.5ml, 30% aq. Soln.) the temperature was raised to 90°C and the reaction refluxed for a further 18hrs. The solution was cooled to room temperature and acetone (30ml) added to precipitate the pure product which was collected by filtration. Yield: 80%.

^{1}H-NMR ($CDCl_3$): 7.28(4H, m, *J* 18.7Hz, $H_{4+4''+5+5''}$), 7.37(1H, t, *J* 8.0Hz, $H_{4'}$), 7.67(2H, m, *J* 13.91Hz, $H_{3+3''}$), 7.72(2H, d, *J* 7.96Hz, $H_{3'}$), 8.27(2H, m, *J* 7.7Hz, $H_{6+6''}$); IR KBr/cm^{-1}: 1467(s), 1420(s), 1418(s), 1381(s), 1273(s), 1247(s), 1122(s), 1026(w), 961(w), 861(s), 775(s), 746(s); MS *m/z* EI+: 281[M] (50%), 249[M-2O] (12%).

5.3 Synthesis of 4'-phenyl-2,2':6',2''-terpyridine Ligands

Synthesis of 4'-phenyl-2,2':6',2''-terpyridine (1b)[4]

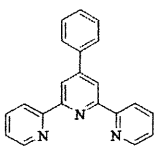

Ammonium acetate (100g, 1.3mol) was added to a mixture of 3-phenyl-1,5-dipyridin-2-ylpentane-1,5-dione (15g, 45.5mmol) and EtOH (200ml). After refluxing

overnight, the mixture was concentrated in vacuo and put in a refrigerator overnight. The precipitate was filtered and washed with EtOH (5ml). Yield: 67%.

^{1}H-NMR ($CDCl_3$): 7.31(2H, t, *J* 3.6Hz, $H_{5+5'}$), 7.43(1H, t, *J* 7.71Hz, H_p), 7.45(2H, t, *J* 7.72Hz, H_m), 7.82(2H, d, *J* 1.77Hz, H_o), 7.85(2H, t, *J* 7.8Hz, $H_{4+4''}$), 8.62(2H, d, *J* 7.07Hz, $H_3 + H_{3''}$), 8.69(4H, s and d, $H_{6+6''} + H_{3'+5'}$); IR KBr/cm^{-1}: 3049(w), 1583(s), 1564(s), 1559(m), 1502(w), 1464(m), 1408(w), 1384(m), 1261(w), 1124(w), 1081(w), 1043(w), 986(w), 896(w), 797(m), 764(s), 674(m), 617(m); UV (DMF) λ: 272 (log ε 4.62), shoulder 318 (log ε 3.97).

Synthesis of 4'-phenyl-2,2':6',2''-terpyridine 1,1''-bisoxide (3b)

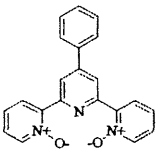

The 3-chloroperbenzoic acid (9.3g, 54mmol, 60% pure) was added to a mixture of 4'-phenyl-2,2':6',2''-terpyridine (5g, 16.2mmol) and CH_2Cl_2 (50ml). After stirring overnight, the mixture was washed with 10% Na_2CO_3 solution (2x30ml) and water (30ml), dried (Mg_2SO_4) and evaporated. Yield: 69%.

^{1}H-NMR ($CDCl_3$): 7.26-7.28(2H, m, $H_{4+4''}$), 7.33-7.42(5H, m, $H_{5+5''}+H_m+H_p$), 7.78(2H, d, *J* 7Hz, H_o), 8.17(2H, dd, *J* 2, 8Hz, $H_{3+3''}$), 8.32(2H, d, *J* 6.49Hz, $H_{6+6''}$), 9.51(2H, s, $H_{3'+5'}$); IR KBr/cm^{-1}: 3115(w), 3054(w), 1616(m), 1587(m), 1545(m), 1488(m), 1431(m), 1488(m), 1431(m), 1393(s), 1279(m), 1247(s), 1223(s), 1152(w), 1034(m), 873(m), 849(s), 769(s), 702(m), 613(w), 589(w), 523(w); UV (DMF) λ: 268 (log ε 4.54), shoulder 286 (log ε 4.39), 354 (log ε 3.76).

Synthesis of 4'-phenyl-2,2':6',2''-terpyridine 1,1',1''-trioxide (3b)

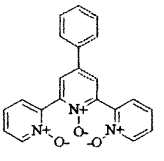

A solution of 4'-phenyl-2,2':6',2''-terpyridine (3g, 9.7mmol) in glacial acetic acid (30ml) and hydrogen peroxide (15ml, 30% aq. Soln.) was refluxed for 2hr at 80°C. After addition of a further portion of hydrogen peroxide (15ml, 30% aq.

Soln.) the temperature was raised to 90°C and the reaction refluxed for a further 63hrs. The mixture was then concentrated in vacuo and 10% Na_2CO_3 (50ml) added and extracted into chloroform (50ml). The solvent was removed in vacuo and the yellow oil dissolved in EtOH with diethyl ether added to precipitate out product. Yield: 40%.

^{1}H-NMR (D_2O): 7.27-7.32(4H, m, $H_{4+4''}$+$H_{5+5''}$), 7.35-7.42(3H, m, H_m+H_p), 7.60(2H, d, *J* 7Hz, H_o), 7.73(2H, d, *J* 7.1Hz, $H_{3+3''}$), 7.96(2H, s, $H_{3'+5'}$), 8.29(2H, d, *J* 7.2Hz, $H_{6+6''}$); IR KBr/cm^{-1}: 3115(w), 3063(w), 1670(w), 1623(w), 1547(w), 1486(s), 1420(s), 1349(m), 1292(s), 1245(s), 1207(m), 1150, 1032(w), 905(w), 872(s), 850(m), 810(m), 759(s), 697(m), 607(m), 565(w), 480(w); UV (DMF) λ: 268 (log ε 4.54), 314 (log ε 4.35).

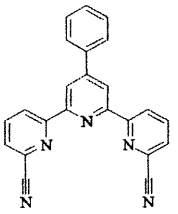

Synthesis of 4'-phenyl-2,2':6',2''-terpyridine-6,6''-dicarbonitrile (17)

Me_3SiCN (4.356g, 44mmol) was added to 4'-phenyl-2,2':6',2''-terpyridine 1,1''-bisoxide (1.5g, 4.4mmol) in CH_2Cl_2 (50ml). After 5 minutes and within 20 minutes, benzoyl chloride (2.464g, 18mmol) was added. After stirring overnight, the mixture was evaporated down to half volume, 10% K_2CO_3 solution (128ml) added, the mixture stirred for 15min, and the precipitate filtered and washed with H_2O and CH_2Cl_2. Yield: 77%.

^{1}H-NMR ($CDCl_3$): 7.46(1H, t, *J* 7.24Hz, H_p), 7.52(2H, t, *J* 7.72Hz, H_m), 7.7(2H, dd, *J* 2.1, 7.26Hz, H_o), 7.86(2H, d, *J* 7.26Hz, $H_{5+5''}$), 7.96(2H, t, *J* 7.93Hz, $H_{4+4''}$), 8.76(2H, s, $H_{3'+5'}$), 8.81(2H, dd, *J* 2.1, 7.34Hz, $H_{3+3''}$); IR KBr/cm^{-1}: 3078(w), 2960(w),

2233(w), 1700(w), 1591(w), 1577(s), 1565(m), 1532(m), 1461(m), 1449(m), 1393(s), 1260(w), 1075(m), 983(w), 886(w), 814(s), 753(s), 737(m), 668(m), 615(m);

MS *m/z* EI: 359[M](100%); Cl+(NH_3): 360[M+H](100%); Accurate Mass ES+: [M+H] calculated 360.1249 , measured 360.1253

Synthesis of 4'-phenyl-2,2':6',2''-terpyridine-6,6''- dicarbonitrile-1'-mono oxide (16)

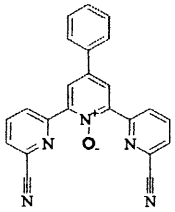

Me_3SiCN (2.772g, 28mmol) was added to 4'-phenyl-2,2':6',2''-terpyridine 1,1',1''-trioxide (1g, 2.8mmol) in CH_2Cl_2 (40ml). After 5 minutes and within 20 minutes, benzoyl chloride (1.568g, 11mmol) was added. After stirring overnight, the mixture was evaporated down to half volume, 10% K_2CO_3 soln. (80ml) added, the mixture stirred for 15min, and the precipitate filtered and washed with H_2O and CH_2Cl_2. Yield: 50%.

^{1}H-NMR ($CDCl_3$): 7.42(1H, t, *J* 6.8Hz, H_p), 7.51(2H, t, *J* 7.78Hz, H_m), 7.74(4H d, *J* 7.88Hz, $H_{5+5''}+H_o$), 7.95(2H, t, *J* 7.88Hz, $H_{4+4''}$), 8.36(2H, s, $H_{3'+5'}$), 8.97(2H, d, *J* 8.21Hz, $H_{3+3''}$); IR KBr/cm^{-1}: 3078(m), 2238(m), 1685(m), 1582(s), 1577(s), 1461(m), 1449(m), 1429(s), 1401(m), 1398(s), 1332(m), 1244(s), 1240(s), 1198(m), 1091(m), 1075(m), 988(m), 886(m), 809(s), 753(s), 737(m), 668(w), 615(m).

Synthesis of 4'-phenyl-2,2':6',2''-terpyridine-6,6''-dicarboxylic acid (18)

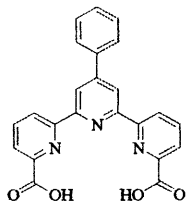

4'-phenyl-2,2':6',2''-terpyridine-6,6''-dicarbonitrile (0.5g, 1.4mmol) and NaOH (0.168g, 4.2mmol) were suspended in ethylene glycol (18ml). The mixture was refluxed at 205°C for 2.5hr. H_2O (15ml) was added and the mixture extracted with

50:50 ether-toluene (30ml). The aqueous phase was collected and evaporated to half volume and acidified with 5M HCl. The precipitate was filtered and washed with water (5ml). Yield: 81%.

^{1}H-NMR (D_6-DMSO): 7.61(1H, t, *J* 6.91Hz, H_p), 7.67(2H, t, *J* 7.31Hz, H_m), 7.98(2H, d, *J* 7.71Hz, H_o), 8.19(2H, d, *J* 7.64Hz, $H_{5+5''}$), 8.26(2H, t, *J* 7.86Hz, $H_{4+4''}$), 8.94(4H, s+d, $H_{3'+5'}$+ $H_{3+3''}$); IR KBr/cm^{-1}: 1705(s), 1601(s), 1584(s), 1547(m), 1508(w), 1450(m), 1383(m), 1320(w), 1296(w), 1261(m), 1084(w), 1002(w), 879(w), 838(w), 763(m), 725(w), 659(w); MS *m/z* EI: 397[M](20%), 353[M+H-COOH](30%), 309[M+H-2COOH](100%); Cl+(NH_3): 398[M+H](20%), 354[M+H-COOH](20%), 310[M+H-2COOH](35%); UV (DMF) λ: 272.5 (log ε 4.43), shoulders 284 (log ε 4.40), 321 (log ε 3.87).

Synthesis of 4'-phenyl-2,2':6',2''-terpyridine-6,6''-dicarboxylic acid 1,1',1''-trioxide (19)

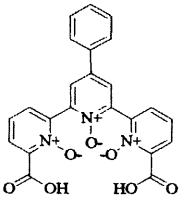

To an ice-cooled solution of 4'-phenyl-2,2':6',2''-terpyridine-6,6''-dicarboxylic acid (0.15g, 0.38mmol) in MeOH (40ml) was added KOH (0.022g, 0.38mmol). The solvent was removed in vacuo and the remaining solid was dissolved in glacial acetic acid (10ml). H_2O_2 (5ml, 30% aq. Soln.) was added and the mixture was refluxed at 80°C for 3 hr. Additional H_2O_2 (4ml, 30% aq. Soln.) was added and the mixture refluxed at 90°C for a further 24hr. The solution was concentrated down in vacuo and acidified with 5M HCl. The precipitate was filtered and washed with water (5ml). Yield: 61%.

^{1}H-NMR (D_6-DMSO): 7.49(1H, t, *J* 7.6Hz, H_p), 7.57(2H, t, *J* 7.56Hz, H_m), 7.9(2H, d, *J* 7.82Hz, H_o), 8.05(2H, t, *J* 7.92Hz, $H_{4+4''}$), 8.28(2H, dd, *J* 5.96, 1.99Hz, $H_{5+5''}$), 8.45(2H, s, $H_{3'+5'}$), 8.48(2H, dd, *J* 5.96, 2.03Hz, $H_{3+3''}$); IR KBr/cm^{-1}: 3087(w),

1715(s), 1473(m), 1426(s), 1384(s), 1263(m), 1165(w), 1076(w), 885(w), 764(s), 798(w), 572(m), 493(w); MS *m/z* FAB: 446[M+H](10%), 384[M-COOH-O](50%); Accurate Mass ES+: [M+H] calculated 446.0988, measured 446.0992; UV (DMF) λ: 271.5 (log ε 4.58), shoulder 314 (log ε 4.34).

Synthesis of N,N'-(di-*tert*-butyl)-4'-phenyl-2,2':6',2''-terpyridine-6,6''-dicarboxamide (20)

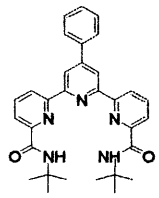

To a stirred solution of 4'-phenyl-2,2':6',2''-terpyridine-6,6''-dicarbonitrile (0.1g, 0.277mmol) in *tert*-butyl acetate (10ml) was added conc. sulphuric acid (0.7ml, 0.05mmol), slowly at room temperature over 5 min. The resulting solution was stirred at 45°C for 5h and cooled. The mixture was separated and the bottom brown layer collected. This was slowly poured onto cold aqueous 20% $KHCO_3$ (50ml) to neutralise the acid and precipitate the product. The product was filtered, washed with cold water and washed with methanol (3 x 10ml). Yield: 36%.

^{1}H-NMR ($CDCl_3$): 1.5(18H, s, $H_{t\text{-}butyl}$), 7.47(1H, t, *J* 7.436Hz, H_p), 7.54(2H, t, *J* 7.714Hz, H_m), 7.8(2H, d, *J* 7.106Hz, H_o), 7.99(2H, t, *J* 7.806Hz, $H_{4+4''}$), 8.12(2H, bs, H_{NH}), 8.22(2H, dd, *J* 7.601, 0.768Hz, $H_{5+5''}$), 8.61(2H, s, $H_{3'+5'}$), 8.73(2H, dd, *J* 7.947, 0.857Hz, $H_{3+3''}$); IR KBr/cm^{-1}: 3381(m), 3066(w), 2964(m), 2865(w), 1681(s), 1606(w), 1584(s), 1553(m), 1517(s), 1461(m), 1393(m), 1364(m), 1262(s), 1226(m), 1101(bm), 1080(m), 1020(bm), 851(w), 830(m), 801,(m), 762(m), 735(w), 699(m); MS *m/z* ES+: 510$[M+3H]^+$(5%), 509$[M+2H]^+$(30%), 508$[M+H]^+$(100%); Accurate Mass ES+: $[M+H]^+$ calculated 508.2707, measured 508.2706; UV (DMF) λ: 268 (log ε 4.57), shoulder 284 (log ε 4.46).

5.4 Synthesis of 4',4''-(4-isopropyphenyl)-2,2':6',2'':6'',2'''-quaterpyridine Ligands

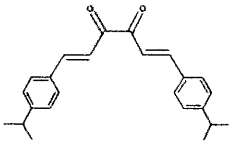

Synthesis of 1,6-Bis(4-isopropyphenyl)hexa-1,5-diene-3,4-dione (14b)

Piperidine (0.3ml, 3mmol) and glacial acetic acid (0.18ml, 3mmol) were added to a stirred solution of 4-isopropylbenzaldehyde (9.6g, 0.06mmol) and diacetyl (1.32g, 15mmol) in MeOH (9ml). The mixture was refluxed for 2hrs and concentrated in vacuo before cooling. The precipitate was filtered and washed with MeOH (3ml). Yield: 9%. **Note: For the synthesis of the 4',4''-bisphenyl-2,2':6',2'':6'',2'''quaterpyridine ligand (5a) substitute benzaldehyde for 4-isopropylbenzaldehyde.**

^{1}H-NMR ($CDCl_3$): 1.21(12H, d, *J* 6.95Hz, H_{CH3}), 2.88(2H, septet, *J* 6.91Hz, H_{Iso}), 7.26(4H, d, *J* 6.19Hz, H_m), 7.38(2H, d, *J* 16.14Hz, H_4), 7.56(4H, d, *J* 8.3Hz, H_o), 7.79(2H, d, *J* 16.17Hz, H_3); IR KBr/cm^{-1}: 2960(m), 2922(w), 1669(s), 1598(s), 1563(m), 1509(m), 1462(m), 1418(m), 1381(w), 1361(w), 1342(w), 1322(m), 1293(m), 1203(m), 1181(m), 1116(w), 1097(w), 1057(w), 1017(m), 991(s), 839(m), 818(s), 762(m), 733(w), 663(m), 566(m), 533(w).

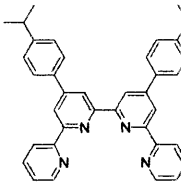

Synthesis of 4',4''-(4-isopropyphenyl)-2,2':6',2'':6'',2'''-quaterpyridine (5b)[4]

1,6-Bis(4-isopropyphenyl)hexa-1,5-diene-3,4-dione (0.3g, 0.87mmol) was added to a solution of N-[1-oxo-2-(2-pyridyl)ethyl]-pyridinium iodide (PPI) (0.569g, 1.8mmol) and ammonium acetate (0.67g, 8.7mmol) in EtOH (20ml). The mixture was refluxed for 4 hrs and concentrated in vacuo to give a precipitate. The precipitate was filtered and washed with EtOH (5ml). Yield: 48%.

^{1}H-NMR ($CDCl_3$): 1.28(12H, d, *J* 6.95Hz, H_{CH3}), 2.96(2H, septet, *J* 6.9Hz, H_{iso}), 7.30(2H, t, *J* 6.1Hz, $H_{5+5'''}$), 7.37(4H, d, *J* 8.11Hz, H_m), 7.81-7.86(6H, m, H_o+$H_{4+4'''}$), 8.64-8.70(6H, m, $H_{5'+3'''}$+$H_{6+6'''}$+$H_{3+3'''}$), 8.87(2H, s, $H_{3'+5''}$); IR KBr/cm^{-1}: 2960(m), 2919(w), 1595(m), 1582(s), 1550(m), 1536(m), 1502(m), 1465(m), 1383(m), 1260(w), 1096(w), 1034(w), 830(m), 794(m), 737(w), 661(w), 615(w); MS *m/z* EI: 546[M](50%); Cl+(NH_3): 547[M+H](100%); UV (DMF) λ: 275.5 (log ε 4.79), shoulder 321 (log ε 4.15), 451 (log ε 3.84)

Synthesis of 4',4''-(4-isopropyphenyl)-2,2':6',2'':6'',2'''-quaterpyridine-1,1'''-bisoxide (6b)

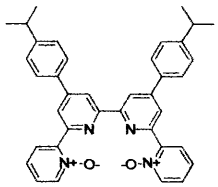

The 3-chloroperbenzoic acid (0.45g, 2.6mmol, 60% pure) was added to a mixture of 4',4''-(4-isopropyphenyl)-2,2':6',2'':6'',2'''quaterpyridine (0.265g, 0.485mmol) in DCM (30ml). After stirring for 90hrs, the solvent was removed in vacuo and the solid stirred in acetone for 30min. The precipitate was filtered and washed with acetone (10ml). Yield: 57%.

^{1}H-NMR ($CDCl_3$): 1.26(12H, d, *J* 6.89Hz, H_{CH3}), 2.94(2H, septet, *J* 6.92Hz, H_{iso}), 7.26(2H, t, *J* 7.43Hz, $H_{5+5'''}$), 7.34(4H, d, *J* 8.09Hz, H_m), 7.39(2H, t, *J* 7.67Hz, $H_{4+4'''}$), 7.73(4H, d, *J* 8.07Hz, H_o), 8.33(2H, d, *J* 6.44Hz, $H_{6+6'''}$), 8.38(2H, dd, *J* 1.94, 5.91Hz, $H_{3+3'''}$), 8.75(2H, s, $H_{5'+3''}$), 9.24(2H, s, $H_{3'+5''}$); IR KBr/cm^{-1}: 2960(s), 2924(w), 2858(w), 1608(m), 1582(s), 1536(m), 1503(w), 1485(m), 1442(w), 1434(m), 1383(s), 1275(m), 1270(m), 1240(m), 1214(m), 1203(m), 1152(w), 1024(m), 896(w), 855(m), 830(m), 764(s), 697(m), 640(w), 620(w), 568(w); MS *m/z* EI+: 580[M+2H](20%), 579[M+H] (50%), 578[M](100%), 546[M-2O](30%); Cl+(NH_3): 581[M+3H](10%), 580[M+2H](40%), 579[M+H](100%), 563[M-O](55%), 547[M-2O](60%); UV (DMF) λ: 268 (log ε 4.77), shoulder 288 (log ε 4.62), 326 (log ε 4.05).

Synthesis of 4',4''-bisphenyl-2,2':6',2'':6'',2'''-quaterpyridine-1,,1':1'',1'''-quateroxide (7)

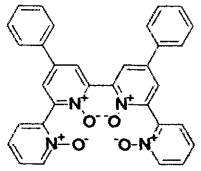

Trifluoracetic acid anhydride (8.4g, 40mmol) in acetonitrile (10ml) was added drop wise over 10 minutes at 0°C to a stirring suspension of urea hydrogen peroxide (4.7g, 50mmol) in acetonitrile (25ml). Stirring was continued at 0°C for 30 minutes after which time a suspension of 4',4''-bisphenyl-2,2':6',2'':6'',2'''quaterpyridine (1g, 2.16mmol) in acetonitrile (10ml) was added drop wise. The suspension was allowed to rise to room temperature then refluxed at 50°C for 48 hours. The reaction mixture was evacuated at reduced pressure {do not heat} to yield a yellow oil which was washed with distilled water (3x50ml). The remaining oil was refluxed in ethanol (50ml) with stirring for 1 hour and allowed to cool. The white precipitate was collected by filtration. Yield: 35%

^{1}H-NMR($CDCl_3$): 7.26(2H, m, $H_{5+5''}$), 7.34-7.39(8H, m, $H_{4+4''}$+ H_{m+p}), 7.69(4H, dd, *J* 1.4, 7.1Hz, H_o), 7.69(2H, m, $H_{3+3''}$), 7.9(2H, d, *J* 2.7Hz, $H_{5'+3''}$), 8.05(2H, d, *J* 2.9Hz, $H_{3'+5''}$), 8.29(2H, m, $H_{6+6''}$); IR KBr/cm^{-1}: 1558(s), 1493(s), 1423(s), 1360(s), 1261(s), 1096(s), 1021(s), 892(s), 874(s), 800(s), 765(s), 697(s); MS *m/z* APCI: 527[M+H](75%), 511[M+H-O](22%), 496[M+H-2O](19%), 465[M+H-3O](11%).

Synthesis of 4',4''-(4-isopropyphenyl)-2,2':6',2'':6'',2'''-quaterpyridine-6,6'''-dicarbonitrile (21)

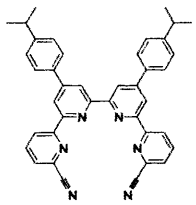

Me_3SiCN (0.475g, 4.8mmol) was added to 2,2':6',2'':6'',2'''quaterpyridine-1,1'''-bisoxide (0.28g, 0.48mmol) in CH_2Cl_2 (10ml). After 5 minutes and within 20 minutes, benzoyl chloride (0.269g, 1.92mmol) was added. After stirring overnight, the mixture was evaporated down to half volume, 10% K_2CO_3 soln. (15ml) added, the

mixture stirred for 15min, and the precipitate filtered and washed with H_2O and CH_2Cl_2. Yield: 51%.

^{1}H-NMR (D_6-DMSO)110°C: 1.34(12H, d, *J* 9.16Hz, H_{CH3}), 7.51(4H, d, *J* 10.64Hz, H_m), 7.91(4H, d, *J* 10.8Hz, H_o), 8.1(2H, d, *J* 10.08Hz, $H_{5+5'''}$), 8.29(2H, t, *J* 10.44Hz, $H_{4+4'''}$), 8.67(2H, s, $H_{3'+5''}$), 8.92(2H, s, $H_{5'+3''}$), 8.95(2H, d, *J* 10.8Hz, $H_{3+3'''}$); IR KBr/cm^{-1}: 2960(m), 2873(w), 2228(w), 1593(s), 1577(s), 1541(s), 1500(m), 1449(m), 1388(m), 1269(w), 1260(w), 1081(m), 1045(m), 891(w), 819(s), 666(m); MS *m/z* EI+: 596[M](100%); Cl+(NH3): 597[M+H](80%), 572[M-CN](20%).

Synthesis of 4',4''-(4-isopropyphenyl)-2,2':6',2'':6'',2'''-quaterpyridine-6,6'''-dicarboxylic acid (22)

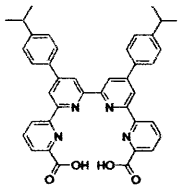

Concentrated H_2SO_4 (5ml) was added to 2,2':6',2'':6'',2'''quaterpyridine-6,6'''-dicarbonitrile (164mg, 258μmol) in 25ml of glacial acetic acid. The mixture was refluxed under Ar for 24hrs and then filtered. Diethyl-ether was added to the filtrate and the product filtered off and dried on the line. Yield: 50%

^{1}H-NMR (D_6-DMSO): 1.3(12H, d, *J* 6.84Hz, H_{CH3}), 3.02(2H, septet, *J* 6.96Hz, H_{iso}), 7.49(4H, d, *J* 7.96Hz, H_m), 7.91(4H, d, *J* 7.72Hz, H_o), 8.16(2H, d, *J* 7.52Hz, $H_{5+5'''}$), 8.21(2H, t, *J* 7.6Hz, $H_{4+4'''}$), 8.89-8.92(6H, m, $H_{3+3'''}$+ $H_{3'+5'}$ + $H_{3''+5''}$); IR KBr/cm^{-1}: 3407(bm), 2962(m), 1734(m), 1624(s), 1601(s), 1514(w), 1508(w), 1458(w), 1433(w), 1396(m), 1244(s), 1175(s), 1096(w), 1056(m), 1014(m), 886(m), 851(m), 830(m), 770(w), 675(w) MS *m/z* ES+: 635[M+H](90%); UV (DMF) λ: 272.5 (log ε 4.29), shoulder 286.5 (log ε 4.23), 323.5 (log ε 3.68).

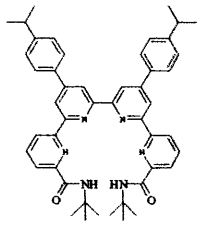

Synthesis of N,N'-(di-*tert*-butyl)-4',4''-(4-isopropyphenyl)-2,2':6',2'':6'',2'''-quaterpyridine-6,6'''-dicarboxamide (23)

To a stirred solution of 2,2':6',2'':6'',2'''quaterpyridine-6,6'''-dicarbonitrile (0.1g, 0.167 mmol) in *tert*-butyl acetate (10ml) was added conc. sulphuric acid (0.7ml, 0.05mmol) slowly at room temperature in 5 min. The resulting solution was stirred at 45°C for 5h and cooled. The mixture was separated and the bottom brown layer collected. This was slowly poured onto cold aqueous 20% $KHCO_3$ (50ml) to neutralise the acid and precipitate the product. The product was filtered and washed with cold water and methanol (3 x 10ml). Yield: 71%.

^{1}H-NMR ($CDCl_3$): 1.3 (12H, d, *J* 6.94Hz, $H_{iso\text{-}CH3}$), 1.51(18H, s, $H_{butyl\text{-}CH3}$) 2.98(2H, septet, *J* 6.95Hz, H_{iso}), 7.42(4H, d, *J* 7.9Hz, H_m), 7.79(4H, d, *J* 8.25Hz, H_o), 7.99(2H, t, *J* 7.84Hz, $H_{4+4''}$), 8.15(2H, bs, H_{NH}), 8.22(2H, d, *J* 7.24Hz, $H_{5+5'''}$), 8.61(2H, d, *J* 1.69Hz, $H_{3'+3''\text{ or }5'+5''}$), 8.76(2H, dd, *J* 6.93, 0.733Hz, $H_{3+3'''}$), 8.89(2H, d, *J* 1.50Hz, $H_{3'+3''\text{ or }5'+5''}$); IR KBr/cm^{-1}: 3461(bm), 3387(m), 2961(s), 2926(m), 2869(w), 1683(s), 1597(m), 1585(s), 1543(m), 1517(s), 1457(m), 1419(w), 1387(s), 1363(m), 1322(w), 1303(w), 1267(w), 1240(w), 1227(w), 1128(w), 1112(w), 1077(w), 1049(w), 1019(w), 997(w), 926(w), 889(w), 829(s), 774(m), 746(w), 706(w), 687(m), 637(w), 559(bw); MS *m/z* ES+: 853[M+K^++CH_3COOH](100%), 745[M+H](10%); UV (CH_3CN) λ: 264 (log ε 4.54), shoulder 284 (log ε 4.46), 324 (log ε 3.86).

5.5 Synthesis of 4',4'''-(4-isopropyphenyl)-2,2':6',2'':6'',2''':6''',2'''':6'''',2'''''-quinquepyridine Ligands

Synthesis of 2,6-pyridine dicarboxylic acid chloride

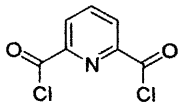

2,6-pyridine dicarboxylic acid (60mmol, 10g) was added to Thionyl chloride (463mmol, 33.3ml) and refluxed for 3 days. The Thionyl chloride was removed in vacuo yielding the product. Yield: 98%

^{1}H-NMR ($CDCl_3$): 8.17(1H, t, *J* 7.8Hz, H_4), 8.36(2H, d, *J* 7.8Hz, H_{3+5}); IR KBr/cm^{-1}: 1752(s), 1575(w), 1423(w), 1259(s), 1244(s), 1198(m), 1157(w), 995(m), 954(m), 868(bs), 829(s), 734(m), 705(w).

Synthesis of 2,6-diacetylpyridine

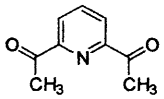

MeLi in ether (103ml, 166mmol) was added over 1h into the cooled (-78°C) suspension of CuI (30.27g, 159mmol) in ether (65ml) and THF (200ml). The resulting yellow suspension was slowly warmed up to –20°C over 1h, then cooled to –78°C again. 2,6-pyridine dicarboxylic acid chloride (12.216g, 60mmol) in THF (65ml) was added over 30mins. The resulting orange-yellow suspension was stirred at lower than –30°C for 2.5h and then hydrolysed with saturated NH_4Cl solution. After warming to room temperature, the colour of the aqueous phase changed from light orange to blue. The mixture was filtered through celite and the celite washed consecutively with ether (30ml) and DCM (30ml). The organic phase was separated off. The aqueous phase was extracted with ether (2x50ml) and DCM (2x50ml). The combined organic solutions were combined and dried over Na_2SO_4. Removal of the solvent yielded the product. Yield: 83%

^{1}H-NMR ($CDCl_3$): 2.76(6H, s, H_{CH3}), 7.96(1H, dd, *J* 2, 7.3Hz, H_4), 8.18(2H, d, *J* 7.7Hz, H_{3+5}); IR KBr/cm^{-1}: 1706(s), 1579(m), 1411(m), 1361(s), 1302(s), 1232(s), 1142(w), 1112(m), 1091(m), 1066(m), 1011(w), 996(m), 946(m), 820(s), 735(m).

Synthesis of 15

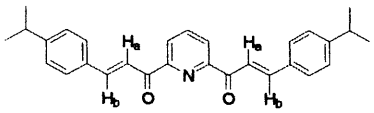

2,6-diacetylpyridine (2g, 12mmol), 4-tert-isopropyl-benzaldehyde (4.44g, 30mmol) and diethylamine (5ml) were heated to reflux in propan-1-ol (30ml) for 24h. The mixture was cooled to –30^{0}C for 5hrs and the precipitate filtered. Yield: 39%

^{1}H-NMR ($CDCl_3$): 1.25(12H, d, *J* 6.88Hz, H_{CH3}), 2.92(2H, septet, *J* 6.9Hz, $H_{isopropyl}$), 7.27(4H, d, *J* 8.11Hz, H_o), 7.66(4H, d, *J* 8.14Hz, H_m), 7.97(2H, d, *J* 16.08Hz, H_b), 8.01(1H, t, *J* 7.76Hz, H_4), 8.31(2H, d, *J* 7.39Hz, H_{3+5}), 8.37(2H, d, *J* 16.06Hz, H_a); IR KBr/cm^{-1}: 3057(w), 2960(m), 2925(w), 2867(w), 1668(s), 1616(s), 1604(s), 1574(m), 1510(w), 1461(w), 1420(m), 1382(w), 1330(m), 1208(w), 1032(m), 984(m), 813(s), 746(w), 668(w), 641(m).

Synthesis of 4',4'''-(4-isopropyphenyl)-2,2':6',2'':6'',2''':6''',2''''-quinquepyridine (8)[4]

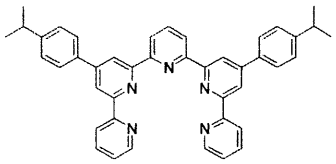

15 (1g, 2.4mmol), PPI (1.56g, 4.8mmol) and ammonium acetate (9.24g, 120mmol) were refluxed in MeOH (30ml) for 24h. The mixture was put in the freezer and the precipitate filtered and washed with cold MeOH (5ml). Yield: 92%

^{1}H-NMR ($CDCl_3$): 1.28(12H, d, *J* 6.93Hz, H_{CH3}), 2.96(2H, septet, *J* 6.92Hz, $H_{isopropyl}$), 7.31(2H, m, $H_{5+5''''}$), 7.36(4H, d, *J* 8.22Hz, H_m), 7.86(4H, d, *J* 8.16Hz, H_o), 7.86(2H, m, $H_{4+4''''}$), 8.01(1H, t, *J* 7.81Hz, $H_{4''}$), 8.65(2H, dd, *J* 2.33, 7.71Hz, $H_{3''+5''}$), 8.69(6H, m, $H_{3+3'+3'''+3''''+5'+5''''}$), 8.95(2H, d, *J* 1.67Hz, $H_{6+6''''}$); IR KBr/cm^{-1}: 3190(bs), 3053 (w), 2960(m), 2927(w), 2868(w), 1605(m), 1580(s), 1565(s), 1546(s), 1514(m),

1473(m), 1415(m), 1388(s), 1273(w), 1120(w), 1094(w), 1079(w), 1039(w), 1015(w), 990(w), 897(w), 833(w), 821(m), 795(m), 744(m), 672(m), 661(m), 637(w), 617(w); MS *m/z* APCI: 624[M+H](100%); UV (DMF) λ: 272.5 (log ε 4.71), shoulder 281 (log ε 4.69), 317 (log ε 4.26).

Synthesis of 4',4'''-(4-isopropyphenyl)-2,2':6',2'':6'',2''':6''',2''''-quinquepyridine-1,1''''-bisoxide (9)

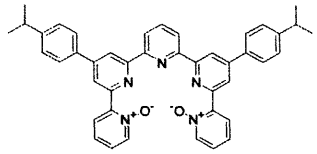

The 3-chloroperbenzoic acid (0.46g, 1.6mmol, 60% pure) was added to a mixture of 4',4'''-(4-isopropyphenyl)-2,2':6',2'':6'',2''':6''',2''''-quinquepyridine (0.5g, 0.8mmol) and CH_2Cl_2 (20ml). The mixture was stirred for 24h and the precipitate filtered. The DCM was removed in vacuo and acetone added (50ml). The mixture was stirred for 30mins and put in the freezer overnight. The precipitate was filtered and washed with cold acetone (3ml) yielding the product. Yield: 42%.

^{1}H-NMR ($CDCl_3$): 1.26(12H, d, *J* 6.93Hz, H_{CH3}), 2.95(2H, septet, *J* 6.91Hz, H_{iso}), 7.27(2H, td, *J* 1, 7.426Hz, $H_{4+4''''}$), 7.35(4H, d, *J* 8.224Hz, H_m), 7.40(2H, td, *J* 1, 7.74Hz, $H_{5+5''''}$), 7.79(4H, d, *J* 8.91Hz, H_o), 7.95(1H, t, *J* 7.748Hz, $H_{4''}$), 8.34(2H, d, *J* 5.91Hz, $H_{6+6''''}$), 8.40(2H, dd, *J* 2.06, 8.06Hz, $H_{3''+5''}$), 8.54(2H, d, *J* 7.86Hz, $H_{3+3''''}$), 8.94(2H, s, $H_{3'+5''''}$), 9.26(2H, s, $H_{5'+3''''}$); IR KBr/cm^{-1}: 3109(w), 2960(m), 2926(w), 2862(w), 1610(m), 1580(s), 1569(s), 1543(s), 1515(m), 1479(w), 1429(w), 1386(s), 1271(m), 1193(w), 1078(w), 1034(m), 897(w), 860(m), 818(s), 767(m), 668(s), 647(w); MS *m/z* APCI: 656[M+H](10%), 640[M-O](70%), 624[M-2O](30%); UV (DMF) λ: 268 (log ε 4.86), shoulder 290 (log ε 4.68), 322 (log ε 4.30).

Synthesis of 4',4'''-(4-isopropyphenyl)-2,2':6',2'':6'',2''':6''',2''''-quinquepyridine-6,6''''-dicarbonitrile (24)

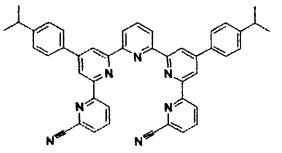

Me_3SiCN (0.39g, 3.95mmol) was added to 4',4'''-(4-isopropyphenyl)-2,2':6',2'':6'',2''':6''',2''''-quinquepyridine-1,1''''-bisoxide (0.259g, 0.395mmol) in 2,2':6',2'':6'',2''':6''',2''''-quinquepyridine-1,1''''-bisoxide (0.259g, 0.395mmol) in CH_2Cl_2 (25ml). After 5 minutes and within 20 minutes, benzoyl chloride (0.18ml, 1.58mmol) was added. After stirring overnight, the mixture was evaporated down to half volume, 10% K_2CO_3 soln. (15ml) added, the mixture stirred for 15min, and the precipitate filtered and washed with H_2O and CH_2Cl_2. Yield: 49%.

^{1}H-NMR ($CDCl_3$): 1.29(12H, d, *J* 6.92Hz, H_{CH3}), 2.98(2H, septet, *J* 6.86Hz, H_{iso}), 7.39(4H, d, *J* 8.147Hz, H_m), 7.68(2H, dd, *J* 0.71, 6.76Hz, $H_{3''+5''}$), 7.84(4H, d, *J* 8.15Hz, H_o), 7.97(2H, t, *J* 7.92Hz, $H_{4+4''''}$), 7.99(1H, t, *J* 7.74Hz, $H_{4''}$), 8.61(2H, d, *J* 7.79Hz, $H_{5+5''''}$), 8.73(2H, d, *J* 1.5Hz, $H_{3'+5'''}$), 8.88(2H, d, *J* 7.9Hz, $H_{3+3''''}$), 8.97(2H, d, *J* 1.7Hz, $H_{5'+3'''}$); IR KBr/cm^{-1}: 3072(w), 3026(w), 2960(m), 2926(w), 2873(w), 2236(w), 1606(m), 1580(s), 1543(s), 1517(m), 1453(m), 1416(w), 1390(s), 1367(w), 1304(w), 1277(m), 1198(w), 1151(w), 1118(w), 1081(w), 1050(m), 1016(w), 989(m), 900(m), 816(s), 746(w), 681(w), 656(m), 648(m), 581(w); MS *m/z* EI: 673[M](100%); Accurate Mass EI+: $[M-H]^+$ calculated 672.2870, measured 672.2862, [M] calculated 673.2948, measured 673.2941.

Synthesis of 4',4'''-(4-isopropyphenyl)-2,2':6',2'':6'',2''':6''',2''''-quinquepyridine-6,6''''-dicarboxylic acid (25)

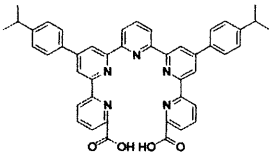

Concentrated H_2SO_4 (0.1ml) was added to 4',4'''-(4-isopropyphenyl)-2,2':6',2'':6'',2''':6''',2''''-quinquepyridine-6,6''''-dicarbonitrile (0.06g, 0.08mmol) in 25ml of glacial acetic acid. The mixture was refluxed under Ar for 24hrs and then

filtered. Diethyl-ether was added to the filtrate and the product filtered off and dried in vacuo. Yield: 71%

^{1}H-NMR (D_6-DMSO): 1.17(12H, d, *J* 6.72Hz, H_{CH3}), 2.85(2H, septet, *J* 6.15Hz, H_{iso}), 7.27(4H, d, *J* 7.818Hz, H_m), 7.7(4H, d, *J* 7.77Hz, H_o), 7.94(1H, t, *J* 7.34Hz, $H_{4''}$), 7.27(4H, d, *J* 7.818Hz, H_m), 7.7(4H, d, *J* 7.77Hz, H_o), 7.94(1H, t, *J* 7.34Hz, $H_{4''}$), 8.03(4H, m, $H_{4+4''''+3''+5''}$), 8.42(2H, d, *J* 7.5Hz, $H_{5+5''''}$), 8.64(2H, d, *J* 7.2Hz, $H_{3+3''''}$), 8.67(2H, s, $H_{5'+3'''}$), 8.72(2H, s, $H_{3'+5'''}$); IR KBr/cm^{-1}: 3430(bm), 3171(m), 3088(m), 2960(s), 2926(m), 2867(w), 1717(bm), 1603(s), 1583(s), 1569(s), 1544(m), 1517(m), 1460(m), 1418(w), 1388(m), 1363(m), 1340(m), 1259(m), 1227(m), 1163(bm), 1086(m), 1048(m), 1015(m), 991(m), 889(w), 819(s), 774(m), 745(w), 669(m), 644(w), 578(m), 539(w); MS *m/z* ES+: 712[M+H]$^+$(40%); Accurate Mass ES+: [M-H]$^+$ calculated 712.2918, measured 712.2928; UV (DMF) λ: 268 (log ε 4.85), shoulder 288 (log ε 4.74), 322 (log ε = 4.36).

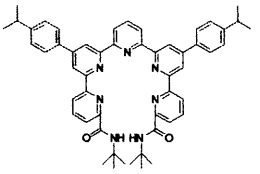

Synthesis of N,N'-(di-*tert*-butyl)-4',4'''-(4-isopropyphenyl)-2,2':6',2'':6'',2''':6''',2''''-quinquepyridine-6,6''''-dicarboxamide (26)

To a stirred solution of 4',4'''-(4-isopropyphenyl)-2,2':6',2'':6'',2''':6''',2''''-quinquepyridine-6,6''''-dicarbonitrile (0.1g, 0.148mmol) in *tert*-butyl acetate (10ml) was added conc. sulphuric acid (0.7ml, 0.05mmol) slowly at room temperature in 5 min. The resulting solution was stirred at 45°C for 5h and cooled. The mixture was separated and the bottom brown layer collected. This was slowly poured onto cold aqueous 20% $KHCO_3$ (50ml) to neutralise the acid and precipitate the product. The product was filtered, washed with cold water and washed with methanol (3 x 10ml). Yield 41%.

^{1}H-NMR ($CDCl_3$): 1.307(12H, d, *J* 6.94Hz, $H_{iso\text{-}CH3}$), 1.517(18H, s, $H_{butyl\text{-}CH3}$) 2.99(2H, septet, *J* 6.95Hz, H_{iso}), 7.41(4H, d, *J* 8.153Hz, H_m), 7.82(4H, d, *J* 8.122Hz,

H_o), 8.04-7.98(3H, m, $H_{4+4'',4''''}$), 8.16(2H, s, H_{NH}), 8.22(2H, d, *J* 7.493Hz, $H_{5+5''''}$), 8.62(2H, d, *J* 1.495Hz, $H_{3',3''' \text{ or } 5',5''}$), 8.68(2H, d, *J* 7.783Hz, $H_{3'',5''}$), 8.78(2H, d, *J* 7.672Hz, $H_{3+3''''}$), 8.96(2H, d, *J* 1.483Hz, $H_{3',3''' \text{ or } 5',5''}$); IR KBr/$cm^{-1}$: 3381(m), 2961(s), 2915(m), 2865(m), 1684(s), 1608(m), 1580(m), 1563(m), 1544(m), 1516(s), 1458(m), 1416(w), 1389(s), 1363(m), 1302(w), 1261(s), 1222(w), 1096(bm), 1046(bm), 1017(bm), 891(w), 816(s), 773(m), 745(w), 700(w), 677(w), 650(w); Ms *m/z* ES+: 844$[M+Na]^+$(100%), 822$[M+H]^+$(60%); Accurate Mass ES+: $[M+H]^+$ calculated 822.4490, measured 822.4498; UV (DMF) λ: 268 (log ε 4.86), shoulder 292 (log ε 4.77), 322 (log ε 4.35).

5.6 Synthesis and Attempted Synthesis of Oxazoline Ligands

Synthesis of Ligand 35

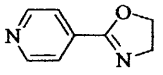

Zinc chloride (68mg, 0.5mmol) was melted under vacuum and cooled under nitrogen. At room temperature dry chlorobenzene (30ml) was added followed by the 4-cyanopyridine, **34**, (1.04g, 10mmol) and the ethanolamine (30mmol). The mixture was refluxed for 48hrs. The solvent was removed in vacuo and the solid dissolved in DCM (30ml). The solution was extracted with water (3x 20ml) and the aqueous Phase with DCM (30ml). The combined organic phases were dried with Mg_2SO_4 and the solvent removed in vacuo to yield the product.

^{1}H-NMR($CDCl_3$): 4.07(2H, d, J=11.57Hz, H_3), 4.4(2H, d, J=9.37Hz, H_4), 7.72(2H, d, J=3.2Hz, H_m), 9.11(2H, d, J=3Hz, H_o).

Attempted Synthesis of Ligand 31

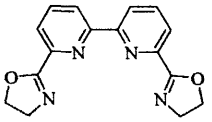

Zinc chloride (10mg, 1.6μmol) was melted under vacuum and cooled under nitrogen. At room temperature dry chlorobenzene (15ml) was added followed by the 2,2'-bipyridine-6,6'-dicarbonitrile, **30,** (0.15g, 721μmol) and the ethanolamine (0.088g, 1.44mmol). The mixture was refluxed for 48hrs (and 94hrs). The solvent was removed in vacuo and the solid dissolved in DCM (20ml). The solution was extracted with water (3x 15ml) and the aqueous Phase with DCM (20ml). The combined organic phases were dried with Mg_2SO_4 and the solvent removed in vacuo to yield a white solid.

Attempted Synthesis of Ligand 32

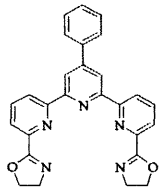

Zinc chloride (10mg, 1.6μmol) was melted under vacuum and cooled under nitrogen. At room temperature dry chlorobenzene (20ml) was added followed by the 4'-phenyl-2,2':6',2''-terpyridine-6,6''-dicarbonitrile, **17**, (0.15g, 721μmol) and the ethanolamine (88mg, 1.44mmol). The mixture was refluxed for 48hrs (and 94hrs). The solvent was removed in vacuo and the solid dissolved in DCM (20ml). The solution was extracted with water (3x 15ml) and the aqueous Phase with DCM (20ml). The combined organic phases were dried with Mg_2SO_4 and the solvent removed in vacuo to yield a white solid.

Attempted Synthesis of Ligand 32 via the larger catalyst $LaCl_3$

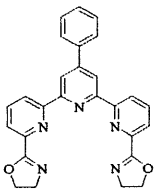

Lanthanide Chloride (0.0148g, 40μmol) was melted under vacuum and cooled under nitrogen. At room temperature dry chlorobenzene (20ml) was added followed by the 4'-phenyl-2,2':6',2''-terpyridine-6,6''-dicarbonitrile, **17**, (0.212g, 587μmol) and the ethanolamine (0.11g, 40μmol). The mixture was refluxed for 48hrs. The solvent was

removed in vacuo and the solid dissolved in DCM (20ml). The solution was extracted with water (3x 15ml) and the aqueous Phase with DCM (20ml). The combined organic phases were dried with Mg_2SO_4 and the solvent removed in vacuo to yield a white solid.

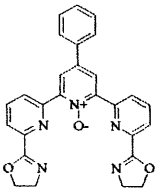

Attempted Synthesis of Ligand 36

Zinc chloride (5mg, 0.8μmol) was melted under vacuum and cooled under nitrogen. At room temperature dry chlorobenzene (10ml) was added followed by the 4'-phenyl-2,2':6',2''-terpyridine-6,6''-dicarbonitrile-1'-N-oxide, **16**, (0.065g, 172μmol) and the ethanolamine (0.032g, 516μmol). The mixture was refluxed for 48hrs and a TLC (95% chloroform/5% methanol) carried out. The TLC showed starting material was still present so the reaction was continued for a further 10 days being tested daily by TLC. After this time the TLC analysis showed another material was being synthesised. More of the ethanolamine was added (30mg) and the reaction continued for a further 48hrs. The solvent was removed in vacuo and the solid dissolved in DCM (20ml). The solution was extracted with water (3x 10ml) and the aq. Phase with DCM (20ml). The combined organic phases were dried with Mg_2SO_4 and the solvent removed in vacuo to yield a white solid.

5.7 Preparation of Lanthanide Metal Complexes

5.7.1 2,2':6',2''-terpyridine Complexes

General procedure for the synthesis of 2,2':6',2''-terpyridine metal complexes: The ligands were dissolved in the minimum amount of hot ethanol. The metal perchlorate salt (0.33mol. equivalent) was also dissolved in ethanol and added to the ligand solution. A white occluded precipitate was formed almost immediately which was collected by filtration.

$[Eu(TerpyO)_3][ClO_4]_3$

Yield: 60%; ^{1}H-NMR (CD_3CN): -11.22(1H,s), -10.27(1H, s), 0.98(1H, s), 1.54(1H, d, *J* 7.35Hz), 3.90-3.76(2H, m), 4.80(1H, s), 5.27(1H, s), 5.45(1H, t, *J* 7.35Hz), 5.57(2H, d, *J* 7.35Hz), 5.79(2H, t, *J* 7.3Hz), 6.00(1H, d, *J* 7.3Hz), 6.71-6.63(2H, m), 6.87(1H, d, *J* 7.35Hz), 7.04(1H, t, *J* 7.3Hz), 7.38(1H, t, *J* 7.3Hz), 8.13(1H, s), 8.33(1H, t, *J* 7.35Hz), 8.41(1H, t, *J* 7.35Hz), 8.86-8.76(2H, m), 9.07-8.97(2H, m), 10.23(1H, d, *J* 7.35Hz), 10.48(1H, d, *J* 7.35Hz), 10.55(1H, d, *J* 7.35Hz), 10.70(1H, d, *J* 7.35Hz), 11.00(1H, d, *J* 11.1Hz), 12.15(1H, s), 12.97(1H, s); IR KBr/cm^{-1}: 1597(s), 1575(s), 1486(w), 1446(s), 1396(w), 1300(w), 1286(w), 1261(w), 1235(s), 1216(s), 1144(s), 1089(s), 1009(s), 853(s), 813(s), 779(s), 637(s), 666(s); MS *m/z* FAB-MS (NOBA Matrix): 1199[M+H](8%), 750[M-L-2ClO_4](22%); Anal. Found (%): C, 45.56; H, 2.90; N, 10.76. Calc. for $C_{45}H_{33}Cl_3N_9O_{15}Eu$ (%): C, 45.11; H, 2.78; N, 10.52.

$[Eu(TerpyO_2)_3][ClO_4]_3$

Yield: 69%; ^{1}H-NMR (CD_3CN): 5.81(2H, bs), 7.06(2H, bs), 7.18(2H, d, *J* 7.9Hz), 7.73(1H, t, *J* 7.5Hz), 9.25(2H, m), 9.54(2H, d, *J* 7.4Hz); IR KBr/cm^{-1}: 1589(w),

1569(w), 1446(s), 1394(w), 1276(w), 1230(s), 1215(sh), 1146(s), 1108(s), 1088(s), 996(w), 855(s), 842(s), 822(w), 772(s), 750(w), 726(w), 637(s), 626(s), 577(s), 557(w), 527(w); MS *m/z* FAB-MS (NOBA Matrix): 948[M-3ClO_4](29%), 782[M-L-2ClO_4](42%); Anal. Found (%): C, 43.86; H, 2.74; N, 10.40. Calc. for $C_{45}H_{33}Cl_3N_9O_{18}Eu$ (%): C, 43.37; H, 2.67; N, 10.12.

[Eu(TerpyO$_3$)$_3$][ClO_4]$_3$

Yield: 96%; IR KBr/cm^{-1}: 1623(s), 1506(w), 1470(s), 1446(s), 1435(s), 1397(s), 1278(s), 1233(s), 1211(sh), 1139(s), 1110(vs), 1088(vs), 852(s), 837(s), 804(s), 776(s), 625(s), 603(s), 590(s), 517(s); MS *m/z* FAB-MS (NOBA Matrix): 1095[M-2ClO_4](5%), 814[M-L-2ClO_4](26%); Anal. Found (%): C, 42.07; H, 2.72; N, 9.21. Calc. for $C_{45}H_{33}Cl_3N_9O_{21}Eu$ (%): C, 41.76; H, 2.57; N, 9.74.

[Tb(TerpyO)$_3$][ClO_4]$_3$

Yield: 80%; IR KBr/cm^{-1}: 1598(s), 1575(s), 1489(w), 1446(s), 1396(w), 1305(w), 1286(w), 1262(w), 1235(s), 1216(s), 1145(s), 1089(s), 1009(s), 856(s), 813(s), 779(s), 633(s), 664(s); MS *m/z* FAB-MS (NOBA Matrix): 250$[L+H]^+$(70%), 1203$[M+H]^+$(8%); Anal. Found (%): C, 45.56; H, 2.90; N, 10.76. Calc. for $C_{45}H_{33}Cl_3N_9O_{15}Tb$ (%): C, 44.85; H, 2.76; N, 10.46;

[Tb(TerpyO$_2$)$_3$][ClO_4]$_3$

Yield: 67%; IR KBr/cm^{-1}: 1592(w), 1569(w), 1443(s), 1395(w), 1275(w), 1230(s), 1215(sh), 1146(s), 1101(s), 1088(s), 989(w), 855(s), 840(s), 822(w), 777(s), 753(w), 726(w), 637(s), 626(s), 572(s), 557(w), 522(w); MS *m/z* FAB-MS (NOBA Matrix):

1151[M-ClO_4](10%); Anal. Found (%): C, 43.56; H, 2.70; N, 10.36. Calc. for $C_{45}H_{33}Cl_3N_9O_{18}Tb$ (%): C, 43.13; H, 2.65; N, 10.06.

5.7.2 4'-phenyl-2,2':6',2''-terpyridine Complexes

$[Eu(PhTerpyAcid_2)(H_2O)_2][ClO_4]_2$

4'-phenyl-2,2':6',2''-terpyridine-6,6''-dicarboxylic acid (0.03g, 75.2μmol) was dissolved in the minimum amount of ethanol with KOH (0.004g, 150.4μmol). $Eu(ClO_4)_3$ (0.0846g (40% H_2O solution), 75.2μmol) in ethanol (1ml) was added with stirring to the ligand solution and left to stir for 1 hour. The white precipitate was filtered. Yield: 70%

^{1}H-NMR (D_6-DMSO): -0.71(2H, d, J=7.1Hz), 3.12(2H, t, J=7.3Hz), 7.63(2H, s, $H_{3',5'}$), 7.97(1H, t, J=7.4Hz, H_p), 8.17(2H, t, J=7.2Hz, H_m), 8.96(2H, d, J=7Hz, H_o); IR KBr/cm^{-1}: 1611(s), 1590(s), 1563(s), 1546(w), 1457(m), 1416(m), 1383(m), 1267(w), 1142(m), 1101(s), 1081(s), 1011(s), 886(w), 785(w), 765(w), 725(w); MS *m/z* FAB: 332[L-O_4](30%), 714[EuL(NOBAcid)](10%), 844[EuL(NOBA)$_2$](10%) 998[Eu_2L(NOBA)$_2$-H](5%); *m/z* ES-: 99[ClO_4]$^-$(100%); UV (DMF) λ: 268 (log ε 4.35), 284 (log ε 4.43), 294 (log ε 4.48), 334 (log ε 4.02), 342 (log ε 4.01); Luminescence (DMF, λ_{exc}=354nm): 574(0.1), 597(1.0), 615(8.65), 650(0.28), 684(3.13); Anal. Found (%): C, 37.52; H, 2.45; N, 5.72. Calc. for $C_{23}H_{19}ClEuN_3O_{11}$ (%): C, 39.42; H, 2.73; N, 6.00.

4'-phenyl-2,2':6',2''-terpyridine-6,6''-dicarboxylic acid 2:1 with $Eu(ClO_4)_3$

4'-phenyl-2,2':6',2''-terpyridine-6,6''-dicarboxylic acid (0.05g, 125μmol) was dissolved in the minimum amount of ethanol with KOH (0.014g, 250μmol).

$Eu(ClO_4)_3$ (0.07g (40% H_2O solution), 63μmol) in ethanol (1ml) was added with stirring to the ligand solution and left to stir for 1 hour. The white precipitate was filtered. Yield: 58%

^{1}H-NMR (D_6-DMSO): 7.33(1H, t, J=7.44Hz, H_p), 7.41(2H, t, J=7.99Hz, H_m), 7.74(2H, d, J=7.39Hz, H_o), 7.94(2H, d, J=6.31Hz), 8.01(2H, t, J=7.38Hz, $H_{4+4''}$), 8.69(4H, d+s, $H_{3'+5'}$ + H_7); IR KBr/cm^{-1}: 1612(s), 1591(s), 1559(s), 1548(m), 1456(w), 1416(m), 1382(m), 1272(w), 1262(w), 1142(m), 1121(s), 1088(s), 1018(w), 886(w), 845(w), 791(w), 767(m), 726(w); MS *m/z* ES+: 546[EuL](60%), 566[EuL(O^-)](30%), 580[EuL(Cl)](35%), 600(40%), 612[EuL-2O+(ClO_4)](90%), 619(60%), 628[EuL-O+(ClO_4)](20%), 632(20%); MS *m/z* ES-: 99[ClO_4]$^-$(100%).

4'-phenyl-2,2':6',2''-terpyridine-6,6''-dicarboxylic acid 1,1',1''-trioxide 2:1 with $Eu(ClO_4)_3$

4'-phenyl-2,2':6',2''-terpyridine-6,6''-dicarboxylic acid 1,1',1''-trioxide (0.04g, 90μmol) was dissolved in the minimum amount of ethanol with KOH (0.01g, 180μmol). $Eu(ClO_4)_3$ (0.051g (40% H_2O solution), 45μmol) in ethanol (1ml) was added with stirring to the ligand solution and left to stir for 1 hour. The white precipitate was filtered. Yield: 55%

^{1}H-NMR (D_6-DMSO): 2.52(bs), 6.52(bs), 7.26(bs), 7.38(bs), 7.45(bs), 7.58(bs); IR KBr/cm^{-1}: 3074(m), 2914(m), 1640(s), 1604(m), 1432(w), 1393(s), 1349(m), 1265(shoulder), 1234(shoulder), 1214(m), 1088(s), 936(w), 896(w), 855(w), 768(m), 710(w), 623(s), 598(w); MS *m/z* LSIMS/NOBA matrix: 413[L-2O](70%), 429[L-O](20%), 523(10%), 661(5%), 689[Eu_2L-2CO](2%), 792[EuL(ClO_4)$_2$](2%), 803(2%), 1001(4%); UV (DMF) λ: 268 (log ε 4.38), shoulder 321 (log ε 4.05).

$[Tb(PhTerpyAcid_2)(H_2O)_2][ClO_4]_2$

4'-phenyl-2,2':6',2''-terpyridine-6,6''-dicarboxylic acid (0.05g, 125μmol) was dissolved in the minimum amount of ethanol with KOH (0.014g, 250.4μmol). $Tb(ClO_4)_3$ (0.143g (40% H_2O solution), 125μmol) in ethanol (1ml) was added with stirring to the ligand solution and left to stir for 1 hour. The white precipitate was filtered. Yield: 82%

IR KBr/cm^{-1}: 2962(w), 1613(s), 1594(s), 1568(s), 1546(w), 1457(m), 1441(m), 1418(m), 1383(m), 1261(w), 1192(w), 1094(s), 1019(s), 878(w), 844(w), 791(m), 766(m), 727(m), 623(m); MS *m/z* ES+: 554$[M-3ClO_4]^+$(90%), 586(40%), 618(60%), 851$[M]^+$(5%); *m/z* FAB-MS (NOBA matrix): 554$[M-3ClO_4]^+$(15%); UV (DMF) λ: 266 (log ε 4.37), 284 (log ε 4.47), 294 (log ε 4.53), 334 (log ε 4.07), 342 (log ε = 4.06)l; Luminescence (DMF, λ_{exc}=344nm): 491(1.0), 545(2.2), 587(0.66), 620(0.33), 640(0.15), 670(0.05); Anal. Found (%): C, 37.42; H, 2.51; N, 5.68. Calc. for $C_{23}H_{19}ClTbN_3O_{11}$ (%): C, 39.03; H, 2.71; N, 5.94.

$[Eu(PhTerpyAmide_2)(H_2O)_2][ClO_4]_3$

4'-phenyl-2,2':6',2''-terpyridine-6,6''-diamide (0.04g, 78.9μmol) was suspended in the ethanol (5ml). $Eu(ClO_4)_3$ (0.071g (50% H_2O solution), 78.9μmol) in ethanol (1ml) was added with stirring to the ligand suspension and left to stir for 24 hour. After this time a solution was obtained. Diethyl ether was added and the white precipitate was filtered. Yield: 74%

^{1}H-NMR (CD_3CN): -2.99(2H, s), -1.56(2H, d, J=8.782Hz), 0.29(2H, s), 1.56(18H, s, H_{CH3}), 2.16(2H, t, J=7.63), 2.89(2H, s), 7.28(2H, d, J= 7.356, H_o), 7.42(2H, t, J=7.324Hz, H_p), 7.52(2H, t, J=8.029Hz, H_m); IR KBr/cm^{-1}: 3374(bs), 3096(m), 2977(m), 2935(w), 1632(s), 1611(s), 1597(s), 1557(s), 1503(w), 1477(m), 1450(m),

1398(w), 1369(m), 1340(w), 1274(w), 1252(w), 1213(m), 1090(bs), 1014(s), 926(w), 907(w), 829(w), 766(m), 697(w); MS *m/z* ES+: 670[EuL+2H]$^{+}$(100%), 758[M-(ClO_4)+H]$^{+}$(20%), 858[M]$^{+}$(50%); MS *m/z* ES-: 99[ClO_4]$^{-}$(100%); Luminescence (CH_3CN, λ_{exc}=357nm): 579(0.12), 596(1.0), 616(5.83), 650(0.09), 690 (1.72).

[Tb(PhTerpyAmide$_2$)(H_2O)$_2$][ClO_4]$_3$

4'-phenyl-2,2':6',2''-terpyridine-6,6''-diamide (0.045g, 88.76μmol) was suspended in the ethanol (5ml). Tb(ClO_4)$_3$ (0.101g (40% H_2O solution), 88.76μmol) in ethanol (1ml) was added with stirring to the ligand suspension and left to stir for 24 hour. After this time a solution was obtained. Diethyl ether was added and the white precipitate was filtered. Yield: 92%

IR KBr/cm^{-1}: 3385(bs), 3102(m), 2977(w), 2932(w), 1633(s), 1612(s), 1598(s), 1557(s), 1501(w), 1477(m), 1450(m), 1398(w), 1369(m), 1340(w), 1275(w), 1252(w), 1213(m), 1090(bs), 1015(s), 929(w), 907(w), 830(w), 766(m), 697(w); MS *m/z* ES+: 764[M-(ClO_4)]$^{+}$(40%), 796(100%), 864[M+H)]$^{+}$(60%); MS *m/z* ES-: 99[ClO_4]$^{-}$ (100%); Luminescence (DMF, λ_{exc}=347nm): 490(1.0), 545(2.0), 587(0.66), 620(0.28), 640(0.04), 670(0.016).

5.7.3 4',4''-(4-isopropyphenyl)-2,2':6',2'':6'',2'''quaterpyridine Complexes

[Eu(4-^{is}Pr-PhQuater)$_2$(H_2O)][ClO_4]$_2$

4',4''-(4-isopropyphenyl)-2,2':6',2'':6'',2'''quaterpyridine (0.05g, 91.6μmol) was suspended in EtOH. Eu(ClO_4)$_3$ (0.051g, (40% H_2O solution), 45.8μmol) in EtOH

(1ml) was added with stirring to the ligand suspension and the mixture stirred overnight. The resulting precipitate was filtered. Yield: 52%

^{1}H-NMR (CD_3CN): 1.27(24H, d, J= 7.06Hz, H_{CH3}), 3.05(4H, septet, J= 6.8Hz, H_{iso}), 3.45(4H, bs, $H_{3'+5''}$ or $H_{5'+3''}$), 3.58(4H, d, J= 6.85Hz, $H_{3'+5''}$ or $H_{5'+3''}$), 3.82(4H, bs), 5.12(4H, bs), 5.34(4H, d, J=7.625Hz), 5.49(4H, bs), 7.45(16H, bs, H_o + H_m); IR KBr/cm^{-1}: 2960(m), 2855(w), 1607(s), 1574(w), 1541(s), 1487(m), 1457(m), 1423(w), 1396(m), 1292(w), 1257(w), 1242(m), 1197(w), 1167(w), 1091(s), 1010(m), 883(w), 835(m), 793(m), 737(w), 707(w), 674(m); MS *m/z* ES+: 547$[L+H]^+$(40%), 578(50%), 609(100%), 710(10%), 1157(5%), 1256(5%), 1320 $[\sim EuL_2+ClO_4]^+$(5%); MS *m/z* ES-: 99$[ClO_4]^-$(100%); Luminescence (CH_3CN, λ_{exc}=382nm): 578(0.08), 592(1.0), 615(5.58), 651 (0.12), 686(2.47); Anal. Found (%): C, 62.89; H, 4.95; N, 7.69. Calc. for $C_{76}H_{70}Cl_2EuN_8O_9$ (%): C, 62.42; H, 4.83; N, 7.66.

[Tb(4-^{is}Pr-PhQuater)$_2$(H_2O)][ClO_4]$_2$

4',4''-(4-isopropyphenyl)-2,2':6',2'':6'',2'''quaterpyridine (0.05g, 91.6μmol) was suspended in EtOH (5ml). $Tb(ClO_4)_3$ (0.053g, (40% H_2O solution), 45.8 μmol) in EtOH (1ml) was added with stirring to the ligand suspension and the mixture stirred overnight. The resultant precipitate was filtered. Yield: 52%

IR KBr/cm^{-1}: 2960(m), 2867(w), 1608(s), 1573(w), 1541(s), 1488(m), 1453(m), 1424(w), 1397(m), 1297(w), 1257(w), 1242(m), 1197(w), 1167(w)(s), 1089(s), 1011(m), 881(w), 834(m), 794(m), 735(w), 700(w), 668(m); MS *m/z* ES+: 547$[L+H]^+$(100%), 705$[TbL]^+$(20%), 904[M](10%), 1093$[2Lig+H]^+$(10%), 1259$[Tb_2Lig]^+$(5%), 1317$[TbL_2+ClO_2]$(5%); MS *m/z* ES-: 99$[ClO_4]^-$(100%); Luminescence (CH_3CN, λ_{exc}=382nm): 491(1.0), 543(1.75), 583(0.62), 622(0.25),

649(0.04), 670(0.014), 678(0.013) ; Anal. Found (%): C, 62.54; H, 4.85; N, 7.86. Calc. for $C_{76}H_{70}Cl_2TbN_8O_9$ (%):C, 62.13; H, 4.80; N, 7.63.

$[Eu(PhQuaterO_2)_2][ClO_4]_3$

4',4''-(4-isopropyphenyl)-2,2':6',2'':6'',2'''quaterpyridine-1,1'''-bisoxide (0.04g, 80.9μmol) was suspended in EtOH. $Eu(ClO_4)_3$ (0.036g, (40% H_2O solution), 40.4μmol) in EtOH (1ml) was added with stirring to the ligand suspension and the mixture stirred overnight. The resulting precipitate was filtered. Yield: 95%

IR KBr/cm-1: 1605(s), 1548(s), 1494(s), 1457(m), 1444(w), 1425(w), 1393(s), 1278(w), 1238(s), 1144(vs), 1108(vs), 1089(vs), 1008(m), 941(w), 881(w), 861(m), 813(w), 766(s), 727(w), 696(m), 625(s), 575(w), 495(w); MS *m/z* ES+: 495$[L+H]^+$(100%), 989$[L_2]^+$(10%), 1382$[EuL_2+2(ClO_4)+ 2(O^-)]$(5%); MS *m/z* ES-: 99$[ClO_4]^-$(100%); UV (DMF) λ: 230 (log ε 4.86), 254 (log ε 4.87), 332sh (log ε 4.23).

$[Eu(PhQuaterO_4)_2][ClO_4]_3$

4',4''-(4-isopropyphenyl)-2,2':6',2'':6'',2'''quaterpyridine-1,1,',1''',1'''-tetraoxide (0.03g, 57μmol) was suspended in EtOH. $Eu(ClO_4)_3$ (0.025g, (40% H_2O solution), 28μmol) in EtOH (1ml) was added with stirring to the ligand suspension and the mixture stirred overnight. The resulting precipitate was filtered. Yield: 60%

IR KBr/cm-1: 1626(s), 1569(m), 1497(s), 1447(s), 1429(m), 1415(s), 1378(w), 1325(w), 1281(w), 1239(s), 1223(s), 1140(s), 1090(Vs), 999(w), 889(w), 869(m), 835(m), 770(s), 719(w), 695(w), 636(m), 625(s), 600(m), 590(w), 569(m), 557(w), 509(w), 447(w); MS *m/z* ES+: 527$[L+H]^+$(90%), 1123(15%), 1249(10%), 1419$[TbL_2+(ClO_4)_2+O^-]$(5%); MS *m/z* ES-: 99$[ClO_4]^-$(100%); UV (DMF) λ: 230 (log ε 4.86), 268 (log ε 4.79), 312 (log ε 4.66).

[Eu(4-^{is}Pr-PhQuaterAcid$_2$)(H$_2$O)$_2$][ClO$_4$]

4',4''-(4-isopropyphenyl)-2,2':6',2'':6'',2'''quaterpyridine-6,6'''-dicarboxylic acid (0.04g, 63μmol) was suspended in water and the pH of the suspension adjusted to 5 with 5M HCl and 3M KOH. $Eu(ClO_4)_3$ (0.071g, (40% H_2O solution), 63μmol) in water (1ml) was added with stirring to the ligand suspension and the mixture stirred for 1 hour. The pH was adjusted to ~9 with 3M KOH and the mixture filtered. Yield: 51%

^{1}H-NMR (D_6-DMSO): 0.96(5H, bs), 1.05(1H, s), 1.12(3H, d, J=6.99Hz), 1.34(3H, bs), 2.7(1H, broad undefined septet, H_{iso}), 2.88(1H, quintet, J=7Hz, H_{iso}), 4.85(bs), 4.97(bs), 5.36(bs), 6.36(~1H, bs), 6.72(1H, bs), 7.07(~3H, bs), 7.35(1H, d, J=7.98Hz), 7.98(2H, d, J=7.79Hz), 8.63(s); IR KBr/cm^{-1}: 2959(m), 2923(w), 2870(w), 1641 (m), 1609(s), 1575(s), 1543(s), 1517(m), 1469(m), 1444(m), 1411(m), 1383(s), 1276(w), 1256(w), 1240(w), 1181(m), 1121(m), 1095(m), 1053(m), 1015(m), 832(m), 786(m), 706(m), 651(w), 624(w); MS *m/z* ES+: 632[L+H]$^+$(40%), 835[EuL-3O+(ClO_4)]$^+$(40%), 853[EuL-2O+(ClO_4)]$^+$(40%); MS *m/z* ES-: 99[ClO_4]$^-$(100%); UV (DMF) λ: 268 (log ε 4.73), 288 (log ε 4.75), 316sh (log ε 4.59), 352sh (log ε 4.02); Luminescence (DMF, λ_{exc}=362nm): 575(0.05), 590(1.0), 614(7.94), 650(0.3), 690(0.2).

[Tb(4-^{is}Pr-PhQuaterAcid$_2$)(H$_2$O)$_2$][ClO$_4$]

4',4''-(4-isopropyphenyl)-2,2':6',2'':6'',2'''quaterpyridine-6,6'''-dicarboxylic acid (0.05g, 78μmol) was suspended in water and the pH of the suspension adjusted to 5 with 5M HCl and 3M NaOH. $Tb(ClO_4)_3$ (0.09g, (40% H_2O solution), 78μmol) in water (1ml) was added with stirring to the ligand suspension and the mixture stirred

for 1 hour. The pH was adjusted to ~9 with 3M NaOH and the mixture filtered. Yield: 64%

IR KBr/cm^{-1}: 2959(m), 2933(w), 2875(w), 1652 (s), 1611(s), 1575(s), 15447(s), 1519(m), 1473(m), 1446(m), 1417(m), 1383(s), 1348 (m), 1329(w), 1273(m), 1262(m), 1240(w), 1180(m), 1121(m), 1108(m), 1089(m), 1015(m), 868(w), 836(m), 787(m), 707(m), 653(w), 625(w); MS *m/z* ES+: 653[L+Na$^+$]$^+$(50%), 790[TbL]$^+$(60%), 823[TbL+2O]$^+$(80%), 988[TbL+2(ClO_4)]$^+$(10%); MS *m/z* ES-: 99[ClO_4](100%); UV (DMF) λ: 266 (log ε 4.73), 294 (log ε 4.76), 316sh (log ε 4.61), 352sh (log ε 4.02); Luminescence (DMF, λ_{exc}=320nm): 490(1.0), 543(2.32), 583(0.73), 623(0.41).

[Eu(4-^{is}Pr-PhQuaterAmide$_2$)(H_2O)$_2$][ClO_4]$_3$

N,N'-(di-*tert*-butyl)-4',4''-(4-isopropyphenyl)-2,2':6',2'':6'',2'''quaterpyridine-6,6'''-dicarboxamide (0.041g, 55μmol) was suspended in hot EtOH (5ml). Eu(ClO_4)$_3$ (0.049g, (50% H_2O solution), 55μmol) in EtOH (1ml) was added with stirring to the ligand suspension. After 15min stirring a solution was obtained and the mixture stirred for 24h. Diethyl ether was added and the white precipitate was filtered. Yield: 98%

^{1}H-NMR (CD_3CN): -5.47(1H, bs, H_{NH}), -2.79(1H, bs, H_{NH}), -1.57(2H, bs), -0.96(18H, bs, $H_{CH3\text{-}amide}$), -0.57(2H, bs), 0.9(12H, d, *J* 7Hz, $H_{CH3\text{-}iso}$), 2.24(2H, bs), 2.63(2H, septet, *J* 7Hz, H_{iso}), 3.04(2H, bs), 4.83(2H, bs), 5.88(4H, bs, H_o), 6.77(4H, d, *J* 8Hz, H_m); IR KBr/cm^{-1}: 3101(w), 2962(m), 2926(w), 2867(w), 1652(s), 1631(s), 1596(s), 1557(m), 1543(m), 1519(w), 1472(m), 1436(m), 1397(w), 1385 (w), 1370(w), 1344(w), 1277(w), 1262(m), 1241(w), 1212(m), 1141(m), 1121(s), 1089(m), 1012(m), 928(w), 904(w), 880(w), 828(m), 768(m), 747(w), 700(w), 652(w), 624(m); MS *m/z* ES+: 745[L+H]$^+$(10%), 820(10%), 925(20%), 939(20%), 955(15%),

1027(30%), 1095$[M]^+$(15%); MS *m/z* ES-: 99$[ClO_4]^-$(100%); Luminescence (CH_3CN, λ_{exc}=371nm): 578(0.33), 585, 595(1.0), 614(6.1), 650, 654(0.17), 684, 695, 701(2.25).

$[Tb(4\text{-}^{is}Pr\text{-}PhQuaterAmide_2)(H_2O)_2][ClO_4]_3$

N,N'-(di-*tert*-butyl)-4',4''-(4-isopropyphenyl)-2,2':6',2'':6'',2'''quaterpyridine-6,6'''-dicarboxamide (0.04g, 53μmol) was suspended in hot EtOH (5ml). $Tb(ClO_4)_3$ (0.061g, (40% H_2O solution), 53μmol) in EtOH (1ml) was added with stirring to the ligand suspension. After 15min stirring a solution was obtained and the mixture stirred for 24h. Diethyl ether was added and the white precipitate was filtered. Yield: 98%

IR KBr/cm^{-1}: 3100(w), 2962(m), 2936(w), 2870(w), 1652 (s), 1634(s), 1600(s), 1575(m), 1543(m), 1515(w), 1473(m), 1437(m), 1397(w), 1385 (w), 1370(w), 1344(w), 1277(w), 1262(m), 1241(w), 1212(m), 1141(m), 1121(s), 1089(m), 1012(m), 928(w), 904(w), 880(w), 828(m), 768(m), 747(w), 700(w), 652(w), 624(m); MS *m/z* ES+: $[L+H]^+$ 745(30%), 877(25%), 933(50%), 947(60%), 1001$[M-(ClO_4)-H]^+$(55%), 1033(100%), 1047(60%), 1101$[M]^+$(50%); MS *m/z* ES-: 99$[ClO_4]^-$(100%); Luminescence (CH_3CN, λ_{exc}=372nm): 490(1.0), 543(1.97), 583(0.63), 622(0.27), 651(0.05), 669(0.01), 681(0.017).

5.7.4 4',4'''-(4-isopropyphenyl)-2,2':6',2'':6'',2''':6''',2''''-quinquepyridine complexes

$[Eu(4\text{-}^{is}Pr\text{-}PhQuinque)_2][ClO_4]_3$

4',4'''-(4-isopropyphenyl)-2,2':6',2'':6'',2''':6''',2''''-quinquepyridine (0.05g, 80μmol) was suspended in acetonitrile (5ml). $Eu(ClO_4)_3$ (0.045g (40% H_2O solution),

40μmol) in acetonitrile (1ml) was added with stirring to the ligand suspension. After 15min stirring a solution was obtained and the mixture stirred for 1h. Diethyl ether was added and the yellow precipitate was filtered. Yield: 47%

IR KBr/cm^{-1}: 3199(bm), 2960(m), 2873(w), 1610(s), 1578(m), 1542(m), 1482(m), 1450(m), 1400(m), 1305(w), 1243(m), 1143(s), 1110(s), 1085(s), 1013(m), 936(w), 887(w), 838(m), 823(m), 794(m), 749(w), 693(m), 672(m), 649(w), 636(m), 626(m), 582(w); MS *m/z* ES+: 624$[L]^+$(15%), $[EuL]^+$777(3%), 865(15%), 892$[EuL+(ClO_4)+O]^+$(100%), 934[~Eu_2L](25%); MS *m/z* ES-: 99$[ClO_4]$(100%).

[Tb(4-^{is}Pr-PhQuinque)$_2$][ClO_4]$_3$

4',4'''-(4-isopropyphenyl)-2,2':6',2'':6'',2''':6''',2'''':6'''',2''''-quinquepyridine (0.05g, 80μmol) was suspended in acetonitrile (5ml). $Tb(ClO_4)_3$ (0.045g (40% H_2O solution), 40μmol) in acetonitrile (1ml) was added with stirring to the ligand suspension. After 15min stirring a solution was obtained and the mixture stirred for 1h. Diethyl ether was added and the yellow precipitate was filtered. Yield: 47%

IR KBr/cm^{-1}: 3144(bm), 2958(w), 1607(s), 1572(m), 1542(m), 1481(m), 1449(m), 1400(m), 1297(w), 1245(m), 1143(s), 1114(s), 1086(s), 1013(m), 936(w), 881(w), 824(m), 794(m), 749(w), 693(m), 672(m); MS *m/z* ES+: 624[L](5%), 872(20%), 900[TbL+(ClO_4)+O](90%), 940[Tb_2L](20%); MS *m/z* ES-: 99$[ClO_4]$(100%).

[Eu(4-^{is}Pr-PhQuinqueO_2)$_2$][ClO_4]$_3$

4',4'''-(4-isopropyphenyl)-2,2':6',2'':6'',2''':6''',2'''':6'''',2''''-quinquepyridine-1,1''''-bisoxide (0.05g, 76μmol) was suspended in acetonitrile (5ml). $Eu(ClO_4)_3$ (0.043g (40% H_2O solution), 38μmol) in acetonitrile (1ml) was added with stirring to the ligand suspension. After 15min stirring a solution was obtained and the mixture

stirred for 1h. Diethyl ether was added and the yellow precipitate was filtered. Yield: 58%

IR KBr/cm^{-1}: 3098(bm), 2960(m), 2869(w), 1602(s), 1573(m), 1542(m), 1517(w), 1494(m), 1479(m), 1459(m), 1394(m), 1274(w), 1243(m), 1222(m), 1189(w), 1145(s), 1114(s), 1085(s), 1014(m), 929(w), 894(w), 860(w), 838(m), 776(m), 685(m), 651(w), 624(m), 582(w) 539(w); MS *m/z* ES+: 656$[L+H]^+$(40%), 938[EuL+(ClO_4)+2O](85%), 1006$[EuL+(ClO_4)_2]^+$(80%); Luminescence (CH_3CN, λ_{exc}=365nm): 591(0.1), 593(1.0), 615(4.5), 690(3.96).

$[Tb(4\text{-}^{is}Pr\text{-}PhQuinqueO_2)_2][ClO_4]_3$

4',4'''-(4-isopropyphenyl)-2,2':6',2'':6'',2''':6''',2'''':6'''',2''''-quinquepyridine-1,1''''-bisoxide (0.05g, 76μmol) was suspended in acetonitrile (5ml). $Tb(ClO_4)_3$ (0.043g (40% H_2O solution), 38μmol) in acetonitrile (1ml) was added with stirring to the ligand suspension. After 15min stirring a solution was obtained and the mixture stirred for 1h. Diethyl ether was added and the yellow precipitate was filtered. Yield: 60%

IR KBr/cm^{-1}: 3079(bm), 2960(m), 2873(w), 1604(s), 1574(m), 1542(m), 1496(m), 1481(m), 1461(m), 1395(m), 1274(w), 1244(m), 1222(m), 1187(w), 1142(s), 1112(s), 1088(s), 1015(m), 932(w), 893(w), 861(m), 820(m), 776(m), 685(m); MS *m/z* ES+: 656$[L+H]^+$(20%), 944$[TbL+2(ClO_4)+2O]^+$(100%), 1012 $[TbL+(ClO_4)_2]^+$(50%); Luminescence (CH_3CN, λ_{exc}=544nm): 490(1.0), 544(1.7), 584(0.55), 622(0.16).

$[Eu(4\text{-}^{is}Pr\text{-}PhQuinqueAcid_2)(H_2O)_2][ClO_4]$

4',4'''-(4-isopropyphenyl)-2,2':6',2'':6'',2''':6''',2'''':6'''',2''''-quinquepyridine-6,6''''-dicarboxylic acid (0.036g, 50.6μmol) was dissolved in the minimum amount of

ethanol and the pH adjusted to 5.5 with NaOH and HCl. $Tb(ClO_4)_3$ (0.057g (40% H_2O solution), 50.6μmol) in ethanol (1ml) was added with stirring to the ligand solution and the mixture refluxed overnight. The pH was adjusted to 8.5 and the white precipitate was filtered. Yield: 84%

^{1}H-NMR (D_6-DMSO): 0.16(2H, bs), 0.97(2H, bs), 1.15(1H, bs), 1.96(12H, bs, H_{CH3}), 3.86(2H, bs, H_{iso}), 6.04(2H, bs), 7.15(2H, bs), 8.8(4H, bs, $H_{o/m}$), 9.85(2H, bs), 10.67(4H, bs, $H_{o/m}$), 14.7(2H, bs); IR KBr/cm^{-1}: 1607(s), 1573(s), 1542(s), 1479(w), 1450(m), 1426(w), 1413(w), 1383(m), 1267(m), 1254(m), 1188(w), 1174(w), 1121(s), 1089(s), 1015(m), 876(w), 837(m), 820(w), 782(m), 747(w), 732(w), 707(m), 651(w), 622(w), 575(vw); MS *m/z* ES+: 288(100%), 860[EuL]$^+$(30%); MS *m/z* ES-: 99[ClO_4](100%); UV (DMF) λ: 268 (log ε 4.87), 302 (log ε 4.88), 328 (log ε 4.76), 358 (log ε 4.46); Luminescence (DMF, λ_{exc}=354nm): 575(0.009), 587(1.0), 615(4.77), 650(0.03), 685(0.75).

[Tb(4-^{is}Pr-PhQuinqueAcid$_2$)(H_2O)$_2$][ClO_4]

4',4'''-(4-isopropyphenyl)-2,2':6',2'':6'',2''':6''',2'''':quinquepyridine-6,6''''-dicarboxylic acid (0.04g, 56.3μmol) was dissolved in the minimum amount of ethanol and the pH adjusted to 5.5 with 3M NaOH and 3M HCl. $Tb(ClO_4)_3$ (0.0643g (40% H_2O solution), 56.3μmol) in ethanol (1ml) was added with stirring to the ligand solution and the mixture refluxed overnight. The pH was adjusted to 8.5 and the white precipitate was filtered. Yield: 95%

IR KBr/cm^{-1}: 3093(bw), 2963(w), 2929(w), 2870(w), 1607(s), 1573(s), 1543(s), 1483(w), 1452(m), 1426(w), 1414(w), 1385(m), 1267(m), 1256(m), 1191(w), 1171(w), 1121(s), 1087(s), 1016(m), 928(w), 879(w), 837(m), 823(w), 783(m), 749(w), 731(w), 707(m), 651(w), 622(w), 575(vw); MS *m/z* ES+: 868[TbL]$^+$(100%),

884[TbL+O]$^+$(20%), 900[TbL+2O]$^+$(30%), 916[TbL+3O](10%), 932[TbL+4O]$^+$(10%); MS *m/z* ES-: 99[ClO_4](100%); UV (DMF) λ: 268 (log ε 5.13), 312 (log ε 4.76).

[Eu(4-^{is}Pr-PhQuinqueAmide$_2$)(H_2O)$_2$][ClO_4]$_3$

N,N'-(di-*tert*-butyl)-4',4'''-(4-isopropyphenyl)-2,2':6',2'':6'',2''':6''',2''''-quinquepyridine-6,6''''-dicarboxamide (0.041g, 49.4μmol) was suspended in ethanol (5ml). Eu(ClO_4)$_3$ (0.045g (50% H_2O solution), 49.4μmol) in ethanol (1ml) was added with stirring to the ligand suspension. After 15min stirring a solution was obtained and the mixture stirred for 24h. Diethyl ether was added and the white precipitate was filtered. Yield: 47%

^{1}H-NMR (CD_3CN): -2.4(2H, bs), -1.87(2H, bs), -1.28(2H, bs), 1.2(2H), 1.63(12H, d, J=6.428Hz, $H_{CH3\text{-}iso}$), 2.67(4H, bs) 3-4.5(bs), 6.73(2H, bs), 8.11(4H, d, J=7.88Hz, $H_{o/m}$), 8.73(4H, s, $H_{o/m}$); IR KBr/cm^{-1}: 3096(w), 2963(m), 2915(w), 2865(w), 1643(s), 1606(s), 1575(s), 1557(s), 1483(w), 1457(m), 1338(w), ν 1369(m), 1337(w), 1257(w), 1212(w), 1090(s), 1012(m), 926(w), 908(w), 891(w), 826(m), 768(w), 747(w), 704(w), 650(w); MS *m/z* ES+: 972[EuL]$^+$(10%), 1072[M-(ClO_4)-H]$^+$(100%), 1172[M]$^+$(50%); MS *m/z* ES-: 99[ClO_4]$^-$(100%); Luminescence (CH_3CN, λ_{exc}=375nm): 575(0.006), 586(1.0), 615(5.3), 646(0.27), 685(1.57).

[Tb(4-^{is}Pr-PhQuinqueAmide$_2$)(H_2O)$_2$)][ClO_4]$_3$

N,N'-(di-*tert*-butyl)-4',4'''-(4-isopropyphenyl)-2,2':6',2'':6'',2''':6''',2''''-quinquepyridine-6,6''''-dicarboxamide (0.04g, 48.7μmol) was suspended in ethanol (5ml). Tb(ClO_4)$_3$ (0.056g (40% H_2O solution), 48.7μmol) in ethanol (1ml) was added with stirring to the ligand suspension. After 15min stirring a solution was obtained

and the mixture stirred for 24h. Diethyl ether was added and the white precipitate was filtered. Yield: 98%

IR KBr/cm^{-1}: 3086(w), 2961(m), 2925(w), 2865(w), 1640(s), 1606(s), 1575(s), 1553(s), 1483(w), 1457(m), 1338(w), 1369(m), 1337(w), 1272(w), 1253(w), 1212(w), 1090(bs), 1013(m), 929(w), 906(w), 886(w), 819(m), 768(w), 747(w), 704(w), 650(w); MS *m/z* ES+: 978$[TbL-H]^+$(10%), 1078$[M-(ClO_4)]^+$(100%), 1178$[M]^+$(45%); MS *m/z* ES-: 99$[ClO_4]^-$(100%); Luminescence (CH_3CN, λ_{exc}=374nm): 485(1.0), 543(1.99), 583(0.63), 621(0.25), 649(0.05), 665(0.002), 682(0.001).

5.8 Preparation of Transition Metal Complex

Synthesis of $[Cu(PhTerpyCN_2)_2][ClO_4]_2$

4'-phenyl-2,2':6',2''-terpyridine-6,6''-dicarbonitrile, **17,** (0.04g, 111μmol) was dissolved in the minimum amount of methanol and the $Cu(ClO_4)_2$ (0.021g, 55μmol) in methanol was added with stirring. The mixture was stirred for 1h and the precipitate filtered. The green solid was washed with Diethyl ether. Yield: 85%

IR (KBr)/cm^{-1}: $\nu_{C\equiv N}$ 2238(w), $\nu_{C=C}$ 1613(s), $\nu_{C=N}$ 1582(m), $\nu_{aromatic}$ 1546(m), 1480(w), 1449(m), 1383(w), ν 1260(m), ν_{ClO} 1086(s), 1011(s), ν_{CH} (aromatic) 819(m), 764(m), 653(w), 640(w), 620(m); MS m/z LSIMS: 360(35%), 388(50%), 422(75%), 463(100%), 541(30%), 616(30%), [M] cluster at 781(40%), good isotope for copper.

5.9 References

1) D. L. Jameson, L. E. Guise, *Inorg. Synth.*, **32**, 46.

2) R. P. Thummel, Y. Jahng, *J. Org. Chem.*, **27**, (1962), 640.

3) M. Burrows, Synthesis and Coordination of Polypyridyl N-oxide Ligands, PhD Thesis, UWC, 2002.

4) E.C. Constable, P. Harverson, D. R. Smith, L. A. Whall, *Tetrahedron*, **50**, (1994), 7799.

Appendix 1 – Crystal data and Refinement

Crystal Data and Refinement for 2.7.2 – $[Tb(terpyO)_3][ClO_4]_3$

Empirical formula	C97 H75.50 Cl6 N21.50 O30.50 Tb2	
Formula weight	2560.83	
Temperature	150(2) K	
Wavelength	0.71073 Å	
Crystal system	Triclinic	
Space group	P -1	
Unit cell dimensions	a = 14.02200(10) Å	α= 74.4470(10)°.
	b = 18.0070(2) Å	β= 81.2370(10)°.
	c = 21.5830(2) Å	γ = 77.0540(10)°.
Volume	5091.82(8) $Å^3$	
Z	2	
Density (calculated)	1.670 Mg/m^3	
Absorption coefficient	1.628 mm^{-1}	
F(000)	2568	
Crystal size	0.15 x 0.10 x 0.10 mm^3	
Theta range for data collection	2.93 to 27.48°.	
Index ranges	-17<=h<=17, -22<=k<=23, -27<=l<=28	
Reflections collected	77015	
Independent reflections	22878 [R(int) = 0.0712]	
Completeness to theta = 27.48°	97.9 %	
Absorption correction	Semi-empirical from equivalents	
Max. and min. transmission	0.8541 and 0.7923	
Refinement method	Full-matrix least-squares on F^2	
Data / restraints / parameters	22878 / 0 / 1406	
Goodness-of-fit on F^2	1.021	
Final R indices [I>2sigma(I)]	R1 = 0.0486, wR2 = 0.0976	
R indices (all data)	R1 = 0.0765, wR2 = 0.1088	
Largest diff. peak and hole	1.621 and -1.106 $e.Å^{-3}$	

Crystal Data and Refinement for 2.7.2 – $[Tb(terpyO_2)_3][ClO_4]_3$

Empirical formula	C49 H41 Cl3 N11 O18.50 Tb	
Formula weight	1345.20	
Temperature	150(2) K	
Wavelength	0.71073 Å	
Crystal system	Monoclinic	
Space group	C 2/c	
Unit cell dimensions	a = 23.6696(3) Å	α= 90°.
	b = 16.9864(2) Å	β= 100.4330(10)°.
	c = 26.1037(4) Å	γ = 90°.
Volume	10321.8(2) $Å^3$	
Z	8	
Density (calculated)	1.731 Mg/m^3	
Absorption coefficient	1.615 mm^{-1}	
F(000)	5408	
Crystal size	0.20 x 0.10 x 0.05 mm^3	
Theta range for data collection	2.94 to 27.44°.	
Index ranges	-27<=h<=30, -18<=k<=21, -33<=l<=33	
Reflections collected	50459	
Independent reflections	11591 [R(int) = 0.1143]	
Completeness to theta = 27.44°	98.3 %	
Absorption correction	Semi-empirical from equivalents	
Max. and min. transmission	0.9236 and 0.7383	
Refinement method	Full-matrix least-squares on F^2	
Data / restraints / parameters	11591 / 24 / 721	
Goodness-of-fit on F^2	1.180	
Final R indices [I>2sigma(I)]	R1 = 0.1545, wR2 = 0.3728	
R indices (all data)	R1 = 0.1798, wR2 = 0.3832	
Largest diff. peak and hole	7.051 and -4.258 $e.Å^{-3}$	

Crystal Data and Refinement for 2.8.1 – [Eu(4-^{is}PrPhenylQuaterpyridine)$_2$ (H_2O)][ClO_4]$_3$

Empirical formula	C83 H76.50 Cl4 Eu N9 O19	
Formula weight	1797.79	
Temperature	150(2) K	
Wavelength	0.71069 Å	
Crystal system	Orthorhombic	
Space group	C c m b	
Unit cell dimensions	a = 22.170(5) Å	α= 90°.
	b = 33.156(5) Å	β= 90°.
	c = 24.144(5) Å	γ = 90°.
Volume	17747(6) Å^3	
Z	8	
Density (calculated)	1.346 Mg/m^3	
Absorption coefficient	0.897 mm^{-1}	
F(000)	7364	
Crystal size	0.25 x 0.20 x 0.10 mm^3	
Theta range for data collection	3.55 to 25.02°.	
Index ranges	-26<=h<=26, -38<=k<=39, -28<=l<=28	
Reflections collected	55143	
Independent reflections	7963 [R(int) = 0.1075]	
Completeness to theta = 25.02°	99.6 %	
Absorption correction	Semi-empirical from equivalents	
Max. and min. transmission	0.9156 and 0.8068	
Refinement method	Full-matrix least-squares on F^2	
Data / restraints / parameters	7963 / 96 / 556	
Goodness-of-fit on F^2	1.103	
Final R indices [I>2sigma(I)]	R1 = 0.0926, wR2 = 0.2303	
R indices (all data)	R1 = 0.1342, wR2 = 0.2510	
Largest diff. peak and hole	2.254 and -1.131 e.Å^{-3}